Biological responses induced by aluminum-based vaccine adjuvants

Sietske Kooijman

ISBN:978-90-393-7019-3

The research of this thesis was performed at Intravacc

Printed by: Ipskamp printing, Enschede

Design: Rob van der Zwaard

Cover is een foto van de quilt gemaakt door Grace Kooijman en Karlijne van Weert welke geïnspireerd is op een quilt van Beverly St. Clair genaamd Double Helix I https://genomequilts.com/double-helix-i/

Biological responses induced by aluminum-based vaccine adjuvants

De biologische effecten veroorzaakt
door aluminium-bevattende vaccinadjuvantia
(met een samenvatting in het Nederlands)

Proefschrift

ter verkrijging van de graad van doctor aan de Universiteit Utrecht
op gezag van de rector magnificus, prof.dr. H.R.B.M. Kummeling, ingevolge
het besluit van het college voor promoties in het openbaar te verdedigen
op woensdag 26 september 2018 des ochtends te 10.30 uur door

Sietske Kooijman

geboren op 29 november 1988
te Arnhem

Promotoren:
Prof.dr. A.J.R. Heck
Prof.dr. G.F.A. Kersten

Copromotor:
Dr. H.D. Meiring

Dit proefschrift werd mede mogelijk gemaakt met financiële steun van het Ministerie van Volksgezondheid, Welzijn en Sport (IS200107). Dit proefschrift is ook gedeeltelijk mogelijk gemaakt door Proteins@work, een programma van het Netherlands Proteomics Centre, gefinancierd door de Nederlandse organisatie voor wetenschappelijk onderzoek als onderdeel van *"National Roadmap Large-scale Research Facilities of the Netherland"* (project nummer: 184.032.201).

Chapter 1

General introduction

General introduction

Vaccination belongs with sanitation and clean drinking water to the largest contributors in the control of infectious diseases. The introduction of vaccines has increased life expectancy and increased the chance that children survived the first 5 years of their lives. It has been estimated that, due to vaccination, 103 million cases of childhood diseases and 2.5 million deaths are prevented per year[1].

In the 18th century, Variola (smallpox) was a lethal disease. Edward Jenner, a general physician, was intrigued by the fact that people who had been infected with cowpox, a non-lethal variant of the smallpox disease, were immune to smallpox. In 1796, he inoculated a young boy with fresh material from cowpox lesions. Nine days later, he exposed the boy to smallpox; the boy did not become ill, thus indeed proved to be immune for smallpox. The treatment introduced by Edward Jenner was called *inoculation with vaccinia*, which later became *vaccination*[2]. From this point on, the science of vaccination was driven by new discoveries, for example the observation that microorganisms are the cause of infectious diseases, discovered by Robert Koch in 1876. Another important development/discovery was the use of adjuvants in inactivated vaccines. Ramon discovered that combining foreign substances with a toxoid injection resulted in a higher antitoxin production in horses[3]. In 1926, Glenny *et al*. discovered that the addition of aluminum salts to toxoid vaccines improved the immunogenicity and efficacy of these toxoid vaccines compared to non-adjuvanted vaccines[4-5].

In Latin, *adjuvare* means *to help*[3], hence the name 'adjuvant' refers to all components that are included in vaccine formulations to increase the immunogenicity of the co-inoculated antigen. In general, adjuvants are used to achieve one or more of the following effects:

1. increasing the immunogenicity of weak antigens[6];
2. enhancing the duration of the immune response[3, 7-8];
3. modulating antibody avidity, specificity, isotypes or subclasses[9];
4. stimulating cell-mediated responses[6];
5. enhancing the immune response in immature or senescent antigen presenting cells[7-8];
6. reducing the required dose of the antigen needed (cost reduction)[6];
7. prevent immunological interfering problems in combination vaccines.

Adjuvants are used to elicit an immune response towards less immunogenic, purified antigens. Life-attenuated and whole-inactivated vaccines which consist of complete microorganisms, usually contain intrinsic adjuvants, like LPS and pathogen-specific nucleic acids and are capable of eliciting a strong immune response without additional exogenous adjuvant[7-8, 10-11], even though the immunogenicity of these whole cell vaccines might be decreased upon inactivation[11]. Many vaccines however, are recombi-

nant or otherwise highly purified subunits. Immunization with these antigens results in modest humoral/antibody-based immune responses with little to no cellular immunity, making the inclusion of an adjuvant vital for its efficacy[11]. Despite the long history of their use, there is still some ambiguity remaining for some adjuvants about the molecular mechanism underlying the adjuvant activity, making it difficult to improve vaccines on a rational basis. For determining the most suitable adjuvant in a vaccine and determine the underlying mechanism of action of the adjuvant, characterization of the molecular mechanism involved is evident. Currently, only a few adjuvants are approved in human vaccines: aluminum salts, oil-in-water emulsion (*e.g.* MF59), synthetic monophosphoryl lipid A (MPL) and saponin (*e.g.* Quillaja Saponin QS21). For determining the ideal adjuvant-antigen combination for a vaccine against a specific pathogen, information about the mechanism of action of both the adjuvant and the pathogen is essential. In addition, it is important to know what the desired vaccine-induced immune response would look like.

Vaccine responses

Vaccine adjuvants are there to 'activate the innate immune response'. A required vaccine response would be a protective pathogen-specific, lasting response. This response is achieved by immunizing the host with antigens from the causative pathogen, either in an inactivated, life-attenuated, incomplete or synthetic form. This immunization of the host, with the causative pathogen is meant to induce a protective response, either cellular ($CD8^+$ T cells and $CD4^+$ T cells) or humoral ($CD4^+$ T cells and B cell-mediated antibodies)[12] depending on the localization of the causative pathogen during natural infection. *Cellular* responses are related to *intracellular* pathogens, while the *humoral* response is associated with *extracellular* pathogens. Cellular and humoral immune responses are part of the adaptive immune system which, upon activation, result in the clearance of the pathogen (utilizing pathogen-specific antibodies) or the clearance of cells infected by the pathogen (utilizing $CD8^+$ T-cells). This adaptive immune response is specific to the antigens in a vaccine and is initiated and shaped by the innate immune response (Figure 1), often related to vaccine adjuvants.

The 'innate' immune response is triggered when an Antigen Presenting Cell (APC), for example a monocyte, recognizes a Danger-Associated Molecular Pattern (DAMP) or Pathogen-Associated Molecular Pattern (PAMP). Examples of DAMPs are host cell DNA and uric acid, released by dying or damaged cells[13-15]. PAMPs can be bacterial lipopolysaccharides (LPS), viral RNA, bacterial DNA or other conserved microbial structures[16-17]. Both DAMPs and PAMPs or synthetic products mimicking these, can activate the innate immune system and could therefore be considered adjuvants. In addition, components that induce the release of DAMPs can also be a vaccine adjuvant, *e.g.* aluminum hydroxide ($Al(OH)_3$, which causes the release of DAMPs from cells of the innate immune system. PAMPs and DAMPs activate the innate immune system by ligating Pattern Recognition Receptors (PRRs)[16-17]. These receptors are mainly present on the cell surface of innate immune cells even though some are also present intracellularly, in other cells besides innate immune cells. Examples of receptors expressed by innate immune cells are: Toll Like Receptors (TLR), NOD like receptors and C-Type Lectin receptors. When a DAMP or PAMP ligates a PRR, the antigen presenting cell becomes activated and various innate immune mechanisms are initiated:

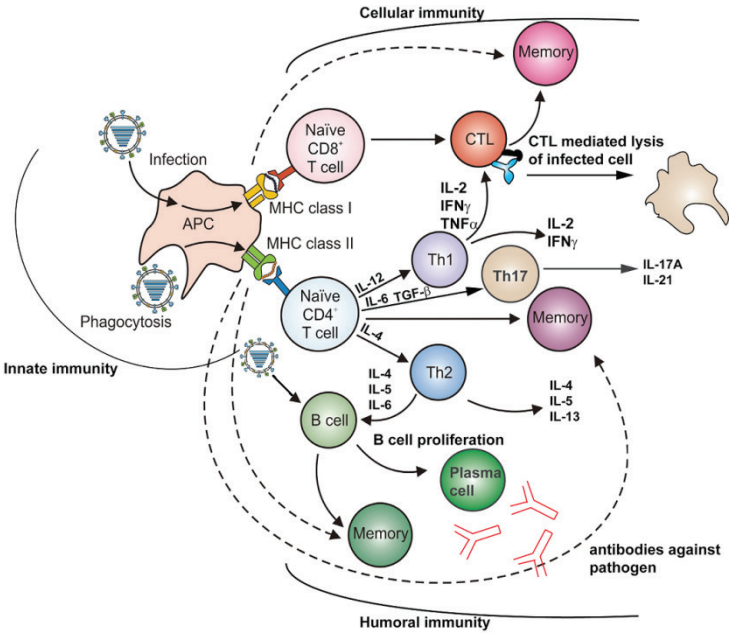

Figure 1. ***Humoral and cellular immunity.***
Activation of cellular and humoral immunity by the innate immune system. Adapted from C.E. van de Sandt et al.[12]. IL-2 is essential for T cell survival, while IL-6, IL-17A and TNFα are pro-inflammatory cytokines. IFNγ has antiviral properties and is associated with a Th1 response, IL-4 is Th2 polarizing cytokine IL-5 is involved in B cell development and a Th2-associated cytokine. IL-13 is an anti-inflammatory. IL-12 is aTh1 inducing cytokine TGFβ, is a growth factor inducing Th17 cells and IL-21 regulates proliferation of mature T and B cells upon stimulus.

1. influx of innate and adaptive immune cells populations at the site of injection as a result of chemotaxis (*in vivo*)[18];

2. pro-inflammatory cytokines are secreted[18];

3. expression of co-stimulatory molecules on the cell surface is upregulated[18];

4. HLA molecules are upregulated on the cell surface[18]

5. Immune cell maturation and enhanced phagocytotic capacity

The upregulation of co-stimulatory molecules and HLA class I and class II molecules on the cell surface, as well as the secretion of cytokines allow for effective antigen presentation by the activated APCs to T cells[19]. APCs can present antigen epitopes to two types of T cells: naïve $CD4^+$ T helper (Th) or naïve $CD8^+$ T cells. $CD8^+$ T cells recognize antigens presented by HLA class I molecules through their T cell receptor. Naïve $CD4^+$ Th cells recognize antigens presented in HLA class II through the T cell receptor. Depending on the cytokines secreted, the naïve $CD4^+$ Th cells differentiate towards a Th

type 1 (Th1), Th type 2 (Th2) or Th type 17 (Th17) cell type (Figure 1). The polarization of a naïve $CD4^+$ Th cell towards a Th1 cell results in cellular immunity and the clearance of intracellular pathogens, like viruses. The differentiation of a naïve $CD4^+$ Th cell towards a Th2 cell is associated with the induction of B cell proliferation, a humoral immune response and the clearance of extracellular parasites[12, 20-21]. The differentiation of naïve $CD4^+$ T cells towards Th17 cells result in the clearance of fungi and extracellular bacteria and in the induction of cell-mediated immunity[20-21]. Antigen presentation to $CD8^+$ T cells will result in the induction of a cellular immune response (Figure 1)[12]. Intact antigens can also directly bind to B cells which will result in a humoral immune response (Figure 1).

Vaccine adjuvantation

In view of the important function of adjuvants in modern vaccine concepts, a wide variety of potential agents has been tested to serve as safe and efficient additives to improve the immunogenicity and steer the immune response of vaccines. Although many adjuvants have been clinically tested[22], only a few have been approved and applied in human vaccines.

Aluminum salts

In 1926, Glenny *et al.* discovered that aluminum salts had adjuvant features. Diphtheria toxoid adsorbed to aluminum salts induced a significantly higher antibody titer against the toxoid compared to toxoid alone[4]. In the years to follow, aluminum salts were incorporated in many human vaccines, *e.g.* the combination vaccine containing diphtheria, tetanus and acellular pertussis antigens (DTaP), and hepatitis A and B vaccines, even though the mechanism of action was still largely unknown. Shortly after Glenny *et al*. discovered the potential of the aluminum salts, the *depot theory* was hypothesized. It was observed that the clearance of aluminum salt-adsorbed toxoids was delayed compared to non-adsorbed toxoids[5], thus the assumption was made that antigen aluminum salts aggregate at the site of injection forming a slow release depot. However, this theory is often challenged[23-25].

Different forms of aluminum-based adjuvants are available for human vaccines. Although chemically incorrect, they are identified as $Al(OH)_3$ and $AlPO_4$ (Figure 2). $Al(OH)_3$ is in fact aluminum oxyhydroxide, AlO(OH) and $AlPO_4$ is actually aluminum hydroxyphosphate, $Al(OH)(PO_4)$. They are commercially available or are made *in situ* by vaccine manufacturers, possibly resulting in different composition and characteristics. They differ in charge, form and adsorption capacity. $Al(OH)_3$ is positively charged at physiological pH, while $AlPO_4$ is negatively charged at physiological pH[6, 26]. The positive charge of $Al(OH)_3$ might allow for stronger interactions with negatively charged cell membranes than $AlPO_4$. In addition, $Al(OH)_3$ is crystalline while $AlPO_4$ is amorphous. In literature the term 'alum' is often used without qualifying which form is used.

Aluminum-based adjuvants stimulate the humoral immune response and are poor inducers of the cellular immune response. Potential mechanisms of action were discovered more recently:

1. the differentiation from monocytes/macrophages to mature antigen-presenting dendritic cells by $Al(OH)_3$ and $AlPO_4$, capable of eliciting a specific immune response[27-29];

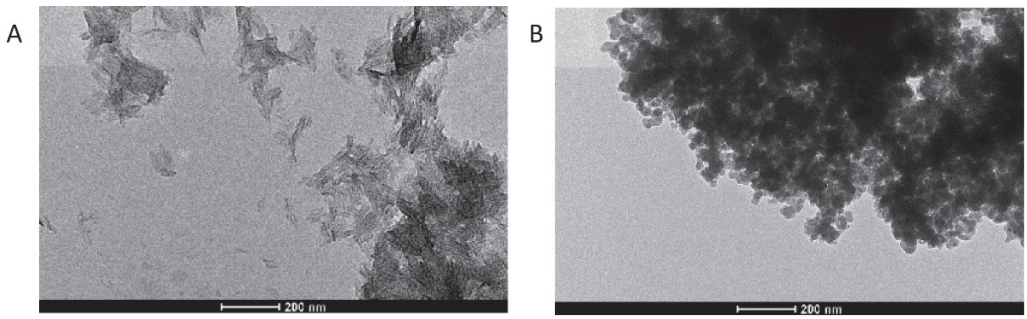

Figure 2. ***Transmission electron microscopy images.***
Images of aluminum hydroxide (Alhydrogel®) (A) and aluminum phosphate (Adju-Phos®) (B).

2. increase antigen presentation by HLA class II by both $Al(OH)_3$ and $AlPO_4$[28-31];

3. activation of the inflammasome by $Al(OH)_3$, which facilitates the secretion of IL-1β, a pro-inflammatory cytokine and inducer of Th2 polarization[13, 32-34];

4. complement activation by $Al(OH)_3$[35];

5. the induction of cell death and cell stress by $Al(OH)_3$, leading to the release of DAMPs[13, 15, 36].

By inducing cell death, $Al(OH)_3$ stimulation causes the release of uric acid and endogenous DNA. This endogenous DNA enhances HLA class II antigen presentation and prolonged $CD4^+$ T cell interactions with dendritic cells[15, 36]. In addition, the release of host cell DNA can also result in the secretion of IFNβ and IL-1β[15, 36]. Uric acid can activate the inflammasome *in vitro* and has a role in the recruitment of inflammatory monocytes to the site of injection, T cell priming and the humoral immune response towards $Al(OH)_3$[13, 32, 37].

LPS derivatives

Microbiota or microbial products, such as lipopolysaccharide (LPS) are also adjuvants. LPS is an important surface structure of Gram-negative bacteria, thus a naturally produced adjuvant. It resides in the outer leaflet of the outer membrane and is composed of various sugars and lipids with the following structure:

1. the O-antigen, maintaining the hydrophilicity of the molecule (Figure 3);

2. the inner and outer core classifying the LPS type;

3. lipid A, being the part that activates the innate immune system and is responsible for the pro-inflammatory responses induced by LPS[38-40](Figure 3).

Wild-type LPS is very potent stimulator of the innate immune response but also too toxic to be used directly as an adjuvant[40-44]. For vaccine applications, monophosphoryl

lipid A (MPLA), a detoxified derivative of LPS, is used in vaccines. MPLA is derived from LPS by removing one or more acyl chains, one or more polysaccharide side groups and by removing at least 2 phosphates[45]. MPLA is a TLR4 ligand, which induces similar cytokines compared to LPS but is at least a 100-fold less toxic. MPLA is used as an adjuvant, combined with $Al(OH)_3$, in human vaccines against HPV vaccine (Cervarix).

LPS interacts with TLR4 and has very strong effects on the CD4 T cell response[42]. When LPS is taken up by APCs, they start to produce various cytokines and effector molecules, including IL-1, IL-6, IL-8, IL-12, TNFα, IFNγ and platelet-activating factor[46-48]. LPS also induces the migration of APCs to the draining lymph nodes, specifically the T cell area, antigen processing and presentation and activation of the complement system. In addition, LPS induces the activation of antigen presentation and the production of cytokines. Moreover, in the presence of IFNγ LPS induces the formation of IgG2a, which is a Th1-related antibody[49]. So, LPS and derivatives allow for an effective priming of the adaptive immune response towards a Th1 immune response.

Emulsions

Emulsion adjuvants date back to the 1930s and are a two-phase adjuvant system, comprising of a hydrophilic and a hydrophobic phase. Simple emulsions are classified as either *oil-in-water* or *water-in-oil* emulsion[6]. The most successful emulsion adjuvant is MF59, a squalene-based *oil-in-water* emulsion, licensed in 1997 as adjuvant to overcome immunosenescence in an influenza vaccine, formulated for elderly[30, 50]. MF59 has proved to be safe and efficacious and is now licensed more broadly[50]. The benefit of MF59 as an adjuvant in flu vaccines is that it protects against more heterologous strains[50]. *In vitro* studies revealed that MF59 activates human monocytes and macrophages, to release chemokines that attract monocytes and granulocytes, like IL-8[29]. In addition, cytokines secreted upon MF59 stimulation attract activated T cells, *e.g.* CCL2. Besides these chemoattractant properties, it was identified that monocytes are the actual targets of MF59[29, 51]. The monocytes targeted by MF59 underwent a phenotypical

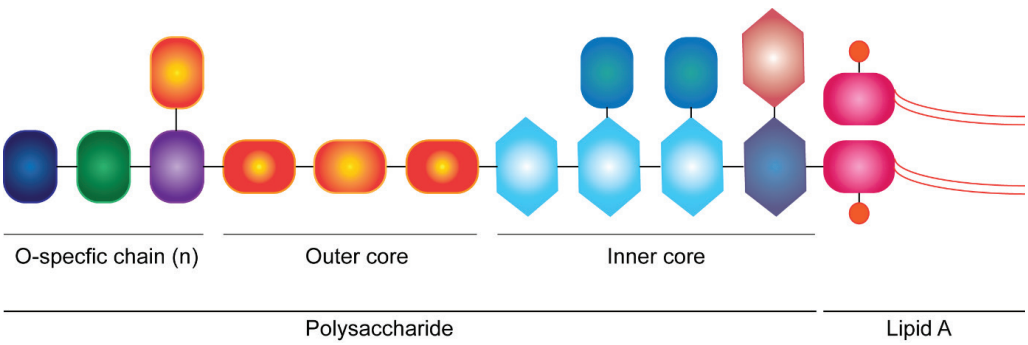

Figure 3. ***LPS structure.***

The O-specific chain is the repeating unit, the outer core consists of oligosaccharides (D galactose and D-glucose), the inner core also consists of oligosaccharides, 3-deoxy-D-manno-oct-2-ulosonic acid and Hep, L-glycero-D-manno-heptose, the lipid A consists of, fatty acids and phosphorylated N-acetylglucosamine (adapted from E. Mahenthiralingam et al.[38] and P. Sperandeo et al.[39].

change to a more DC-like phenotype, resulting in the hypothesis that MF59 induces a *monocyte-to-dendrite* differentiation. In addition to these phenotypical changes, MF59 stimulation increased the cell surface expression of CD86 and HLA class II molecules and the downregulation of CD14, a monocyte cell surface marker. These changes indicate that indeed the cells are differentiating away from a monocytic cell type towards a dendritic cell type *in vitro*[51-52]. *In vivo* studies revealed various mechanisms of action for MF59:

1. the recruitment of white blood cells to the muscle when MF59 was injected intramuscular[53];

2. the induction of chemoattractant molecules like CCL2, CCL4, CCL6, CCL7 and CCL8[30];

3. enhanced antigen processing and presentation;

4. recruitment of MHC II positive cells to the site of injection[30].

MF59 does not bind to TLR receptors[54] nor does it activate the inflammasome, the latter is in contrast to aluminum-based adjuvants[51]. Crucial for the immune response induced by MF59 however, was MyD88, since MyD88 knockout mice did not induce an antibody response upon immunization with MF59[51]. MyD88, is often associated with a TLR induction, however for MF59 the dependence of MyD88 was thought to be independent of TLR activation, since MF59 did not activate any TLRs in vitro[51], thus it was proposed that MF59 is dependent on MyD88 in a TLR independent matter. Perhaps by activating IL-1R, required for the induction of IL-1 and IL-18 or via TAC1, involved in B cell class switch[51, 55] Finally, it may also be that MF59 *in vivo* induces the expression of endogenous TLR ligands thus that the MyD88 dependent immune response could be related to TLR activation[51]. In summary, MF59 has proven to be an adjuvant that recruits both innate and adaptive immune cells to the site of injection and is a safe and efficacious adjuvant in vaccines.

Techniques and comprehensive approach

All mechanistic studies described in the paragraphs above were conducted using acknowledged immunological techniques, most commonly antibody-based assays like ELISAs and flow cytometry. These assays always require a preselection of the targeted effector molecules (cytokines, cell surface receptor and co-stimulatory molecules) and are also biased due to the availability and selection of the antibodies against particular cell markers. The last decades, however, mass spectrometry-based proteomics has emerged as an essential tool in mapping the proteome in biological systems, in an unbiased way. This proteomics approach not only allows identification and quantification of individual proteins, but also can target differentially regulated biological pathways and protein-protein interactions upon defined *stimuli*, although the latter has not been applied in this thesis. With the availability of quantitative mass spectrometry-based proteomics, it is now possible to study the underlying mechanisms of vaccine adjuvants at the level of proteins. This strategy opens new possibilities to further unravel and validate the mechanism of action of the adjuvants.

In this thesis, a comprehensive approach is used for the analysis of mechanisms of action and pathways involved in innate immune activation by adjuvants, consisting of:

1. flow cytometry for the analysis of the maturation/differentiation state of the cells;

2. ELISA-based cytokine analysis, providing inside information about the polarizing messengers secreted by the cell;

3. targeted qPCR for the analysis of 89 immune response genes of the innate and adaptive system;

4. relative quantitative unbiased proteome analysis, in which differentially regulated processes in the cell by the addition of the stimulation condition were analyzed.

Combining the data of these complementary techniques resulted in a comprehensive overview of the mechanisms involved in the activity of a vaccine adjuvant. Targeted transcriptome analysis was performed on stimulated cells with quantitative PCR. With this method the *gene expression* of cytokines, chemokines, cell surface markers and receptors could be determined. For the analysis of the proteome, relative quantitative unbiased proteome analysis was used. This quantitative approach was achieved by using tandem mass tag labeling (TMT) with multiplexing up to ten different conditions (TMT(10)) in one single mass spectrometry analysis.

Thesis outline and objective

The objective of this thesis was to unravel the molecular mechanisms of aluminum-based vaccine adjuvants. In **chapter 2**, the mechanisms of action of $Al(OH)_3$ were investigated *in vitro* in human primary monocytes at the molecular level, combining targeted transcriptomics, proteome analysis and cytokine analysis. Novel pathways elucidated were: type I interferon signaling and HLA class I antigen processing and presentation.

Chapter 3 describes the comparison of the $Al(OH)_3$ mechanism of action in human primary monocytes with the $Al(OH)_3$-adjuvanted DTaP combination vaccine containing Diphtheria, Tetanus and (acellular) Pertussis antigens. Synergistic effects between adjuvants and antigens could be elucidated. It was concluded that the antigens in DTaP influence the innate immune response towards the vaccine adjuvant in a quantitative and qualitative manner.

In **chapter 4**, the response of human monocytes (*in vitro*) and the local response of mice (*in vivo*) induced by either of the two conventional aluminum-based adjuvants, $Al(OH)_3$ and $AlPO_4$, were compared. *In vitro*, $Al(OH)_3$ induced the processes of antigen processing and presentation, while $AlPO_4$ did not. *In vivo*, both adjuvants attract different immune cells to the site of injection.

In **chapter 5**, the immune response to differently shaped and sized aluminum adjuvants were analyzed in human primary monocytes. One conventional adjuvant currently used in vaccines, $Al(OH)_3$, was compared with two different nanoparticles composed of $Al(OH)_3$: gibbsite and boehmite. Clearly, size and shape of the particles affect the strength of the innate immune response induced by these particles.

Chapter 6 describes a new method to map the cellular secretome. This assay utilizes a new generation of chemically modified beads to allow for enrichment of *de novo*-synthesized proteins after administering a stimulus. Isolation of these proteins is based on a single step click chemistry without the addition of agents and/or catalyst that are incompatible with subsequent mass spectrometric analysis. This assay is intended as an unbiased proteomics-based method to target the secreted proteins as an alternative for the biased antibody-based assays (*e.g.* Luminex).

References

1. Rappuoli, R.; Pizza, M.; Del Giudice, G.; De Gregorio, E., Vaccines, new opportunities for a new society. *Proc Natl Acad Sci U S A* 2014, *111* (34), 12288-93.
2. Riedel, S., Edward Jenner and the history of smallpox and vaccination. *Proc (Bayl Univ Med Cent)* 2005, *18* (1), 21-5.
3. Vogel, F. R., Improving vaccine performance with adjuvants. *Clin Infect Dis* 2000, *30 Suppl 3*, S266-70.
4. Glenny, A. T.; Pope, C. G.; Waddington, H.; Wallace, U., Immunological notes. XVII–XXIV. *The Journal of Pathology and Bacteriology* 1926, *29* (1), 31-40.
5. Glenny, A. T.; Buttle, G. A. H.; Stevens, M. F., Rate of disappearance of diphtheria toxoid injected into rabbits and guinea - pigs: Toxoid precipitated with alum. *The Journal of Pathology and Bacteriology* 1931, *34* (2), 267-275.
6. Gupta, R. K.; Siber, G. R., Adjuvants for human vaccines--current status, problems and future prospects. *Vaccine* 1995, *13* (14), 1263-76.
7. Alving, C. R.; Peachman, K. K.; Rao, M.; Reed, S. G., Adjuvants for human vaccines. *Curr Opin Immunol* 2012, *24* (3), 310-5.
8. Awate, S.; Babiuk, L. A.; Mutwiri, G., Mechanisms of action of adjuvants. *Front Immunol* 2013, *4*, 114.
9. Allison, A. C., Adjuvants and immune enhancement. *Int J Technol Assess Health Care* 1994, *10* (1), 107-20.
10. Lambrecht, B. N.; Kool, M.; Willart, M. A.; Hammad, H., Mechanism of action of clinically approved adjuvants. *Curr Opin Immunol* 2009, *21* (1), 23-9.
11. Di Pasquale, A.; Preiss, S.; Tavares Da Silva, F.; Garcon, N., Vaccine Adjuvants: from 1920 to 2015 and Beyond. *Vaccines (Basel)* 2015, *3* (2), 320-43.
12. van de Sandt, C. E.; Kreijtz, J. H.; Rimmelzwaan, G. F., Evasion of influenza A viruses from innate and adaptive immune responses. *Viruses* 2012, *4* (9), 1438-76.
13. Kool, M.; Soullie, T.; van Nimwegen, M.; Willart, M. A.; Muskens, F.; Jung, S.; Hoogsteden, H. C.; Hammad, H.; Lambrecht, B. N., Alum adjuvant boosts adaptive immunity by inducing uric acid and activating inflammatory dendritic cells. *J Exp Med* 2008, *205* (4), 869-82.
14. Kool, M.; Fierens, K.; Lambrecht, B. N., Alum adjuvant: some of the tricks of the oldest adjuvant. *J Med Microbiol* 2012, *61* (Pt 7), 927-34.
15. Marichal, T.; Ohata, K.; Bedoret, D.; Mesnil, C.; Sabatel, C.; Kobiyama, K.; Lekeux, P.; Coban, C.; Akira, S.; Ishii, K. J.; Bureau, F.; Desmet, C. J., DNA released from dying host cells mediates aluminum adjuvant activity. *Nat Med* 2011, *17* (8), 996-1002.
16. Janeway, C. A., Jr., Approaching the asymptote? Evolution and revolution in immunology. *Cold Spring Harb Symp Quant Biol* 1989, *54 Pt 1*, 1-13.
17. Janeway, C. A., Jr.; Medzhitov, R., Innate immune recognition. *Annu Rev Immunol* 2002, *20*, 197-216.
18. Joffre, O.; Nolte, M. A.; Sporri, R.; Reis e Sousa, C., Inflammatory signals in dendritic cell activation and the induction of adaptive immunity. *Immunol Rev* 2009, *227* (1), 234-47.
19. Trombetta, E. S.; Mellman, I., Cell biology of antigen processing in vitro and in vivo. *Annu Rev Immunol* 2005, *23*, 975-1028.
20. Grasis, J. A.; Tsoukas, C. D., Itk: the rheostat of the T cell response. *J Signal Transduct* 2011, *2011*, 297868.
21. Zhu, J.; Yamane, H.; Paul, W. E., Differentiation of effector CD4 T cell populations (*). *Annu Rev Immunol* 2010, *28*, 445-89.
22. Amorij, J. P.; Kersten, G. F.; Saluja, V.; Tonnis, W. F.; Hinrichs, W. L.; Slutter, B.; Bal, S. M.; Bouwstra, J. A.; Huckriede, A.; Jiskoot, W., Towards tailored vaccine delivery: needs, challenges and perspectives. *J Control Release* 2012, *161* (2), 363-76.
23. Holt, L. B., *Developments in Diptheria Prophylaxis*. Heinemann: 1950.

24. Romero Mendez, I. Z.; Shi, Y.; HogenEsch, H.; Hem, S. L., Potentiation of the immune response to non-adsorbed antigens by aluminum-containing adjuvants. *Vaccine* 2007**,** *25* (5), 825-33.
25. Hutchison, S.; Benson, R. A.; Gibson, V. B.; Pollock, A. H.; Garside, P.; Brewer, J. M., Antigen depot is not required for alum adjuvanticity. *FASEB J* 2012**,** *26* (3), 1272-9.
26. Caulfield, M. J.; Shi, L.; Wang, S.; Wang, B.; Tobery, T. W.; Mach, H.; Ahl, P. L.; Cannon, J. L.; Cook, J. C.; Heinrichs, J. H.; Sitrin, R. D., Effect of alternative aluminum adjuvants on the absorption and immunogenicity of HPV16 L1 VLPs in mice. *Hum Vaccin* 2007**,** *3* (4), 139-45.
27. Rimaniol, A. C.; Gras, G.; Clayette, P., In vitro interactions between macrophages and aluminum-containing adjuvants. *Vaccine* 2007**,** *25* (37-38), 6784-92.
28. Ulanova, M.; Tarkowski, A.; Hahn-Zoric, M.; Hanson, L. A., The Common vaccine adjuvant aluminum hydroxide up-regulates accessory properties of human monocytes via an interleukin-4-dependent mechanism. *Infect Immun* 2001**,** *69* (2), 1151-9.
29. Seubert, A.; Monaci, E.; Pizza, M.; O'Hagan, D. T.; Wack, A., The adjuvants aluminum hydroxide and MF59 induce monocyte and granulocyte chemoattractants and enhance monocyte differentiation toward dendritic cells. *J Immunol* 2008**,** *180* (8), 5402-12.
30. Mosca, F.; Tritto, E.; Muzzi, A.; Monaci, E.; Bagnoli, F.; Iavarone, C.; O'Hagan, D.; Rappuoli, R.; De Gregorio, E., Molecular and cellular signatures of human vaccine adjuvants. *Proc Natl Acad Sci U S A* 2008**,** *105* (30), 10501-6.
31. Horohov, D. W.; Dunham, J.; Liu, C.; Betancourt, A.; Stewart, J. C.; Page, A. E.; Chambers, T. M., Characterization of the in situ immunological responses to vaccine adjuvants. *Vet Immunol Immunopathol* 2015**,** *164* (1-2), 24-9.
32. Li, H.; Willingham, S. B.; Ting, J. P.; Re, F., Cutting edge: inflammasome activation by alum and alum's adjuvant effect are mediated by NLRP3. *J Immunol* 2008**,** *181* (1), 17-21.
33. Kool, M.; Petrilli, V.; De Smedt, T.; Rolaz, A.; Hammad, H.; van Nimwegen, M.; Bergen, I. M.; Castillo, R.; Lambrecht, B. N.; Tschopp, J., Cutting edge: alum adjuvant stimulates inflammatory dendritic cells through activation of the NALP3 inflammasome. *J Immunol* 2008**,** *181* (6), 3755-9.
34. Eisenbarth, S. C.; Colegio, O. R.; O'Connor, W.; Sutterwala, F. S.; Flavell, R. A., Crucial role for the Nalp3 inflammasome in the immunostimulatory properties of aluminum adjuvants. *Nature* 2008**,** *453* (7198), 1122-6.
35. Guven, E.; Duus, K.; Laursen, I.; Hojrup, P.; Houen, G., Aluminum hydroxide adjuvant differentially activates the three complement pathways with major involvement of the alternative pathway. *PLoS One* 2013**,** *8* (9), e74445.
36. McKee, A. S.; Burchill, M. A.; Munks, M. W.; Jin, L.; Kappler, J. W.; Friedman, R. S.; Jacobelli, J.; Marrack, P., Host DNA released in response to aluminum adjuvant enhances MHC class II-mediated antigen presentation and prolongs CD4 T-cell interactions with dendritic cells. *Proc Natl Acad Sci U S A* 2013**,** *110* (12), E1122-31.
37. Franchi, L.; Nunez, G., The Nlrp3 inflammasome is critical for aluminum hydroxide-mediated IL-1beta secretion but dispensable for adjuvant activity. *Eur J Immunol* 2008**,** *38* (8), 2085-9.
38. Mahenthiralingam, E.; Urban, T. A.; Goldberg, J. B., The multifarious, multireplicon Burkholderia cepacia complex. *Nat Rev Microbiol* 2005**,** *3* (2), 144-56.
39. Sperandeo, P.; Martorana, A. M.; Polissi, A., Lipopolysaccharide biogenesis and transport at the outer membrane of Gram-negative bacteria. *Biochim Biophys Acta* 2017**,** *1862* (11), 1451-1460.
40. Li, Y.; Wang, Z.; Chen, J.; Ernst, R. K.; Wang, X., Influence of lipid A acylation pattern on membrane permeability and innate immune stimulation. *Mar Drugs* 2013**,** *11* (9), 3197-208.
41. Kong, Q.; Six, D. A.; Roland, K. L.; Liu, Q.; Gu, L.; Reynolds, C. M.; Wang, X.; Raetz, C. R.; Curtiss, R., 3rd, Salmonella synthesizing 1-dephosphorylated [corrected] lipopolysaccharide exhibits low endotoxic activity while retaining its immunogenicity. *J Immunol* 2011**,** *187* (1), 412-23.
42. McAleer, J. P.; Vella, A. T., Understanding how lipopolysaccharide impacts CD4 T-cell immunity. *Crit Rev Immunol* 2008**,** *28* (4), 281-99.

43. Geurtsen, J.; Fransen, F.; Vandebriel, R. J.; Gremmer, E. R.; de la Fonteyne-Blankestijn, L. J.; Kuipers, B.; Tommassen, J.; van der Ley, P., Supplementation of whole-cell pertussis vaccines with lipopolysaccharide analogs: modification of vaccine-induced immune responses. *Vaccine* 2008**,** *26* (7), 899-906.

44. Embry, C. A.; Franchi, L.; Nunez, G.; Mitchell, T. C., Mechanism of impaired NLRP3 inflammasome priming by monophosphoryl lipid A. *Sci Signal* 2011**,** *4* (171), ra28.

45. Casella, C. R.; Mitchell, T. C., Putting endotoxin to work for us: monophosphoryl lipid A as a safe and effective vaccine adjuvant. *Cell Mol Life Sci* 2008**,** *65* (20), 3231-40.

46. Guha, M.; Mackman, N., LPS induction of gene expression in human monocytes. *Cell Signal* 2001**,** *13* (2), 85-94.

47. Kraaij, M. D.; Vereyken, E. J.; Leenen, P. J.; van den Bosch, T. P.; Rezaee, F.; Betjes, M. G.; Baan, C. C.; Rowshani, A. T., Human monocytes produce interferon-gamma upon stimulation with LPS. *Cytokine* 2014**,** *67* (1), 7-12.

48. Rossol, M.; Heine, H.; Meusch, U.; Quandt, D.; Klein, C.; Sweet, M. J.; Hauschildt, S., LPS-induced cytokine production in human monocytes and macrophages. *Crit Rev Immunol* 2011**,** *31* (5), 379-446.

49. Deenick, E. K.; Hasbold, J.; Hodgkin, P. D., Decision criteria for resolving isotype switching conflicts by B cells. *Eur J Immunol* 2005**,** *35* (10), 2949-55.

50. O'Hagan, D. T.; Ott, G. S.; De Gregorio, E.; Seubert, A., The mechanism of action of MF59 - an innately attractive adjuvant formulation. *Vaccine* 2012**,** *30* (29), 4341-8.

51. Seubert, A.; Calabro, S.; Santini, L.; Galli, B.; Genovese, A.; Valentini, S.; Aprea, S.; Colaprico, A.; D'Oro, U.; Giuliani, M. M.; Pallaoro, M.; Pizza, M.; O'Hagan, D. T.; Wack, A.; Rappuoli, R.; De Gregorio, E., Adjuvanticity of the oil-in-water emulsion MF59 is independent of Nlrp3 inflammasome but requires the adaptor protein MyD88. *Proc Natl Acad Sci U S A* 2011**,** *108* (27), 11169-74.

52. Wright, S. D.; Ramos, R. A.; Tobias, P. S.; Ulevitch, R. J.; Mathison, J. C., CD14, a receptor for complexes of lipopolysaccharide (LPS) and LPS binding protein. *Science* 1990**,** *249* (4975), 1431-3.

53. Dupuis, M.; Denis-Mize, K.; LaBarbara, A.; Peters, W.; Charo, I. F.; McDonald, D. M.; Ott, G., Immunization with the adjuvant MF59 induces macrophage trafficking and apoptosis. *Eur J Immunol* 2001**,** *31* (10), 2910-8.

54. Mosaheb, M. M.; Reiser, M. L.; Wetzler, L. M., Toll-Like Receptor Ligand-Based Vaccine Adjuvants Require Intact MyD88 Signaling in Antigen-Presenting Cells for Germinal Center Formation and Antibody Production. *Front Immunol* 2017**,** *8*, 225.

55. Deguine, J.; Barton, G. M., MyD88: a central player in innate immune signaling. *F1000Prime Rep* 2014**,** *6*, 97.

Chapter 2

Novel identified aluminum hydroxide-induced pathways prove monocyte activation and pro-inflammatory preparedness

Sietske Kooijman[1,2], Jolanda Brummelman[3,#a], Cécile A.C.M. van Els[3], Fabio Marino[2,4,#c], Albert J.R. Heck[2,4], Geert P.M. Mommen[1,#b], Bernard Metz[1], Gideon F.A. Kersten[1,6], Jeroen L.A. Pennings[5], Hugo D. Meiring[1*]

1 Intravacc, Bilthoven, The Netherlands
2 Biomolecular Mass Spectrometry and Proteomics, Bijvoet Center for Biomolecular Research and Utrecht Institute for Pharmaceutical Sciences, Science Faculty, Utrecht University, The Netherlands
3 Centre for Infectious Disease Control, National Institute for Public Health and the Environment, Bilthoven, The Netherlands
4 Netherlands Proteomics Centre, Utrecht, The Netherlands
5 Centre for Health Protection, National Institute for Public Health and the Environment, Bilthoven, The Netherlands
6 Leiden Academic Centre for Drug Research, Leiden University, Leiden, The Netherlands
#a Current address: Istituto Clinico Humanitas IRCCS, Milan, Italy
#b Current address: Immunocore, Ltd. Abingdon, United Kingdom
#c Current address: Centre hospitalier Universitaire, Vaudois, Switzerland

Data availability: the authors confirm that all data is available without any restrictions.
Proteome Data is available via ProteomeXchange with identifier PXD008452

Published as: Sietske Kooijman, Jolanda Brummelman, Cécile A.C.M. van Els, Fabio Marino, Albert J.R. Heck, Geert P.M. Mommen, Bernard Metz, Gideon F.A. Kersten, Jeroen L.A. Pennings, Hugo D. Meiring. Novel identified aluminum hydroxide-induced pathways prove monocyte activation and pro-inflammatory preparedness. Journal of Proteomics 175(2018) 144-155. https://doi.org/10.1016/j.jprot.2017.12.021

Abstract

Aluminum-based adjuvants are the most widely used adjuvants in human vaccines. A comprehensive understanding of the mechanism of action of aluminum adjuvants at the molecular level, however, is still elusive. Here, we unravel the effects of aluminum hydroxide $Al(OH)_3$ by a systems-wide analysis of the $Al(OH)_3$-induced monocyte response. Cell response analysis by cytokine release were combined with (targeted) transcriptome and full proteome analysis. Results from this comprehensive study revealed two novel pathways to become activated upon monocyte stimulation with $Al(OH)_3$: the first pathway was IFNβ signaling possibly induced by DAMP sensing pathways like TLR or NOD1 activation, and second the HLA class I antigen processing and presentation pathway. Furthermore, known mechanisms of the adjuvant activity of $Al(OH)_3$ were elucidated in more detail such as inflammasome and complement activation, homeostasis and HLA-class II upregulation, possibly related to increased IFNγ gene expression. Altogether, our study revealed which immunological pathways are activated upon stimulation of monocytes with $Al(OH)_3$, refining our knowledge on the adjuvant effect of $Al(OH)_3$ in primary monocytes.

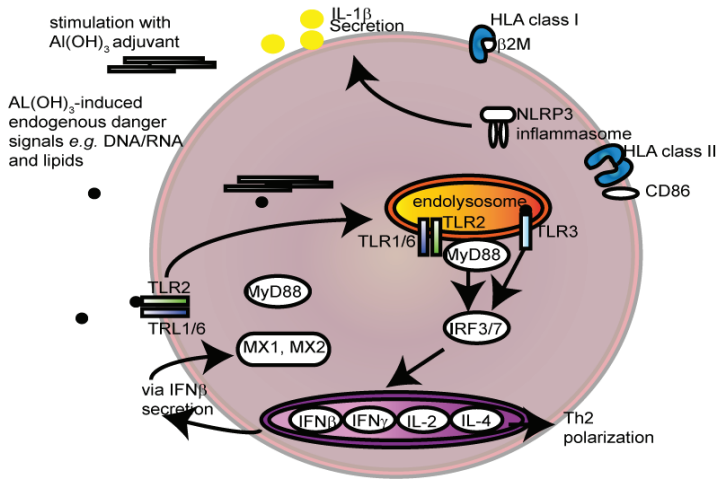

Significance

Aluminum salts are the most used adjuvants in human vaccines but a comprehensive understanding of the working mechanism of alum adjuvants *at the molecular level* is still elusive. Our Systems Vaccinology approach, combining complementary molecular biological, immunological and mass spectrometry-based techniques gave a detailed insight in the molecular mechanisms and pathways induced by $Al(OH)_3$ in primary monocytes. Several novel immunological relevant cellular pathways were identified: type I interferon secretion potentially induced by TLR and/or NOD like signaling, the activation of the inflammasome and the HLA Class-I and Class-II antigen presenting pathways induced by IFNγ. This study highlights the mechanisms of the most commonly used adjuvant in human vaccines by combing proteomics, transcriptomics and cytokine analysis revealing new potential mechanisms of action for $Al(OH)_3$.

Introduction

Since 1926, colloidal aluminum salts are known for their adjuvant features, when Glenny *et al.* discovered that diphtheria toxoid adsorbed to aluminum salts showed a significantly higher antibody titer against the toxoid compared to antigen alone[1]. Since then, aluminum salts have been widely used as vaccine adjuvants, even though the mechanism of action has remained largely unknown. Shortly after Glenny *et al.* discovered its potential, it was observed that the clearance of aluminum salt-adsorbed toxoids was delayed compared to non-adsorbed toxoids[2]. This observation was the basis for the theory that antigen-aluminum salt aggregates form a depot at the site of injection, leading to a slow release of the bound antigen. However, when the aluminum salt deposit was removed at various time points, the immune response was not compromised, suggesting that this is not the only mechanism by which aluminum salts increase the immune response to antigens[3]. It was shown that antigens desorb rapidly from $AlPO_4$ as well as $Al(OH)_3$ after administration, explaining that even when the aluminum salt-deposit is removed, an antibody response is still created[4]. It was demonstrated by flow cytometric analysis that $Al(OH)_3$ causes the differentiation of monocytes to antigen-presenting dendritic cells, which then can elicit a specific immune response in the presence of an antigen[5-7]. $Al(OH)_3$ has been shown to steer the $CD4^+$ T cell response towards a T helper type 2 (Th2) response and induces the recruitment of immune cells (*e.g.* dendritic cells, inflammatory monocytes, eosinophils, neutrophils natural killer cells and $CD11^+$ cells) to the site of injection[7-12].

Additional mechanisms for the adjuvant effect of $Al(OH)_3$ have been described: for example, the activation of the NLRP3 inflammasome, as identified by both *in vivo* and *in vitro* studies[12-15]. Inflammasome activation results in the secretion of IL-1β, a pro-inflammatory cytokine and potent inducer of the adaptive immune response and Th2 polarization[13, 15-16]. The inflammasome, *in vitro*, appeared to be critical for $Al(OH)_3$ dependent IL-1β secretion and antibody responses. *In vivo* however, there is conflicting data about the necessity of the inflammasome to induce a humoral response[13, 15, 17]. Complement activation is another mechanism involved in the adjuvant activity of $Al(OH)_3$[12, 18]. The release of Danger Associated Molecular Patterns (DAMPs) like uric acid and host DNA, is induced by $Al(OH)_3$[13, 19-20]. Uric acid is involved in T cell priming and humoral responses[13, 15]. Besides this, uric acid can also activate the inflammasome *in vitro*[15, 21]. However, *in vivo* IL-1β production did not depend on the presence of uric acid[14-15]. Uric acid is involved in the influx of inflammatory monocytes to the site of injection as is MyD88, since MyD88-deficient mice showed a significant reduction of the influx of inflammatory monocytes[13]. Even though MyD88 appears to be dispensable for antibody production there is a role in the adjuvant activity of $Al(OH)_3$[13]. DNA is also involved in the adjuvant activity of $Al(OH)_3$[19] DNA can result in the secretion of IL-1β or in the secretion of IFNβ and enhances MHC class II antigen presentation[19-20]. In conclusion, there are many potential mechanism described for the adjuvant activity of $Al(OH)_3$. A comprehensive study compiling transcriptome data with proteome data would make it possible to follow pathways in more detail and create an overview of which pathways are actually activated by the $Al(OH)_3$ adjuvant.

In this study, we investigated the $Al(OH)_3$-induced innate cell response at the transcriptome and proteome level, aiming to further complete the overview of molecular

pathways and cellular processes involved in the adjuvant effect of $Al(OH)_3$. Primary monocytes were chosen as a model, since these prominent mononuclear phagocytes play an important role in tissues when activated, bridging the innate and adaptive immune responses[22-23]. Besides there known differentiation into monocyte derived dendritic cells (MDDCs), monocytes can also enforce their antigen presenting role to T cells in response to various stimuli as recently reviewed[24]. In the current study the effect of $Al(OH)_3$ on monocytes will be investigated. The combination of transcriptome/proteome analyses and cytokine measurements enabled the comprehensive identification of molecular pathways in $Al(OH)_3$-stimulated monocytes, further clarifying the mechanism by which $Al(OH)_3$ works.

Materials and methods

Ethics statement

This study was conducted using blood donations, provided by the National Institute for Public Health and the Environment (Bilthoven, The Netherlands), for primary cell isolation. The blood donations for this research goal were specifically approved by the accredited Medical Research Ethics Committee (MREC), METC, Noord-Holland in The Netherlands. The study was conducted according to the principles expressed in the Declaration of Helsinki and written informed consent was obtained from all blood donors before collection and use of their samples. Blood samples were processed anonymously. All human primary cells described in this study were obtained by the rules of this ethical statement.

Reagents used in cell stimulation

Aluminum hydroxide (Alhydrogel 2%; Brenntag; Frederikssund; Denmark) is referred to as $Al(OH)_3$. Lipopolysaccharide (LPS) from *E.coli* K12 (Invivogen; San Diego; California; USA) was used as positive control and is referred to as LPS.

Isolation and stimulation of monocytes

Peripheral blood derived from 7 healthy adult donors and obtained as described in the ethical statement, was used for monocyte isolation. First, peripheral blood mononuclear cells (PBMCs) were obtained by gradient centrifugation at 1,000*x*g for 30 minutes on Lymphoprep (Nycomed; Zurich; Switzerland). Second, monocytes were isolated from the PBMC fraction using MACS in combination with anti-CD14 MACS beads (Miltenyi Biotech; Bergisch Gladbach; Germany). Purity check by flow cytometric analysis of CD14 cell surface expression was performed and only if the purity of the monocyte population was ≥95% the cells were used for proteome and transcriptome analysis.

Monocytes were cultured in a 24-well culture plate (0.6×10^6 cells/ml, 1 ml/well) in RPMI (Gibco/Thermo Fisher; Waltham; Massachusetts; USA) containing 10% Fetal Calf Serum (FCS) (Hyclone), 100 units/ml of penicillin (Gibco) 100 units/ml streptomycin (Gibco), and 2.92 mg/ml L-glutamin (Gibco), hereafter referred to as monocyte culture medium. Isolated monocytes were either left unstimulated in monocyte culture medium, or were stimulated with 500 µl of LPS or $Al(OH)_3$ in monocyte culture medium with a final concentration of 0.1 µg/ml or 10 µg/ml, for 24 or 48 hours respectively, based on the study of Ulanova *et al.*[5].

After incubation, culture supernatants were collected and stored at -80°C for cytokine analysis. Small aliquots were taken from cell suspensions from each donor per time point for flow cytometry analysis.

For proteome analysis, the cells of at least one well per condition per time point per donor (three individuals) were washed with PBS, before adding 500 µl lysis buffer (4 M Guanidine·HCl in phosphate buffer pH 7.5) (Sigma Aldrich; St Louis; Missouri; United States).

For transcriptome analysis, the cells of at least one well per condition per time point per donor (5 individuals) were placed in 350 µl of RLT buffer (Qiagen; Venlo; The Netherlands). The samples for proteome and transcriptome analysis were stored at -80˚C.

Generation and stimulation of primary Monocyte-Derived Dendritic Cells (MDDCs)

Monocytes from the peripheral blood of 6 donors, obtained as described in the ethics statement, were cultured in a 24-well culture plate (0.4 x·10^6 cells/ml, 1 ml/well) in DC culture medium, *i.e.* IMDM (Gibco) containing 1% FCS, 100 units/ml penicillin, 100 units/ml streptomycin, 2.92 mg/ml L-glutamine (Gibco), 500 units/ml GM-CSF (Prepotech; Rocky Hill; New Jersey; USA) and 800 units/ml IL-4 (Sanquin; Amsterdam; The Netherlands) for 6 days. On day 6, the immature MDDCs (iMDDCs) were either left unstimulated, or were stimulated for 48 hours with 250 µl of LPS or $Al(OH)_3$ in DC culture medium containing 250 units/ml GM-CSF, with a final concentration of the stimulus of 0.1 µg/ml or 10 µg/ml. After 48 hours, supernatant were stored at -80° for cytokine analysis. The stimulated MDDCs were harvested and suspended in FACS buffer. Aliquots were taken from cell suspensions for flow cytometric analysis which was used as a quality control for the cell culture procedure. Flow cytometric analysis of monocytes was used as a quality control for the cell culture procedure. LPS served as a positive control and performed as expected, by inducing CD80 expression (Supplementary S1). Samples were only used for further analysis if the monocytes were at least 95% pure.

Culture and stimulation of THP-1 cells

The human monocytic cell line THP-1 (ATCC; Teddington; Middlesex; U.K.) was used for verification experiments of leads identified in primary monocytes. THP-1 cells were cultured according to the supplier's protocol with the addition of 100 units/ml penicillin, 100 µg/ml streptomycin and 300 µg/ml L-glutamine to the medium, hereafter referred to as THP-1 culture medium, in culture flasks.

Cells were primed with 300 ng/ml phorbol 12-myristate 13-acetate (PMA) (Sigma Aldrich) for 24 hours, after which the medium was discarded and new medium without PMA was added. After 24 hours in the refreshed medium, the following stimulations were performed: mock, 50 or 100 µg/ml $Al(OH)_3$ (based on literature[5, 14] and preliminary experiments). Each of these conditions was performed in the presence and absence of 25 µg/ml glybenclamide (Invivogen). An additional cell batch was left completely unstimulated and unprimed. Twenty-four and 48 hours after stimulation, supernatants of cultures were harvested and used for an IL-1β ELISA.

Flow cytometric analysis

For purity analysis, isolated monocytes were stained with PE-conjugated anti CD14 clone (H5E2). Cultured monocyte and MDDC cell suspensions were stained with PE-conjugated anti-CD40 (BD Biosciences; clone 5C3), APC-conjugated anti-CD80 (BioLegend; clone 2D10), FITC-conjugated anti-CD83 (BD Biosciences; clone HB15e), Pacific Blue-conjugated anti-CD86 (BioLegend; clone IT2.2), HLA-DR FITC (Sanquin; clone L243) and finally with LIVE/DEAD Fixable Aqua Dead Cell Stain Kit (Invitrogen) for 30 minutes at 4°C. The cells were washed in FACS buffer and fixed in FACS buffer containing 1% paraformaldehyde (PFA). Data were acquired on a FACS Canto II (BD Biosciences) and analyzed using FlowJo software (Tree Star) by comparing the MFI of the stained control with the MFI of the stained stimulus. The data were corrected for the percentage autofluorescence determined in verification experiments by comparing the unstained stimulated with the stained stimulated cells for each stimulus.

mRNA expression analysis

mRNA was isolated from monocyte samples using the RNeasy mini kit (Qiagen) according to the animal cell spin protocol provided. Isolated RNA concentrations and purities were determined by the spectrophotometric analysis of the 260-nm and 280-nm absorbance on the Nanodrop 2000 (Thermo Fischer). Subsequently, cDNA synthesis was performed with the RT cDNA synthesis kit (Qiagen) and the RT preAMP pathway primer mix, innate and adaptive immunity comprising primers for 89 functional RNA species and controls, on 12 ng of RNA per condition (Qiagen). cDNA was subsequently frozen at -20°C.

qPCR was performed by using the Innate and Adaptive Immune Responses RT^2 Profiler PCR Arrays (PAHS 052ZC) (Qiagen) (Supplementary S2) on a qPCR apparatus (ABI step one plus; Applied Biosystems; Foster City; California; USA) with a melt curve determination as a quality control, included in the measurement.

qPCR data were analyzed with the qPCR statistical web software from Qiagen. Gene expression was normalized to HPRT1 as housekeeping gene, after which the fold change was calculated according to the manufacturer's protocol. Fold change-values greater than one indicate an upregulation, in which the fold regulation is equal to the fold change. Fold change-values less than one indicate a downregulation in which the fold regulation is the negative inverse of the fold change. For donor F (with three technical replicates), *p*-values were calculated based on a Student's *t*-test of the replicate values for each gene in the control group and treatment group. Genes were considered regulated if *p*-value <0.05 and a two-fold change in expression occurred. We validated technical replicate reproducibility with the first donor. The Coefficient of Variation (CV) between technical replicates was 3.5% for all transcriptome data and all the genes that met the two fold difference criterion also had a *p*-value <0.05. Therefore, for the other four donors we used one technical replicate and considered genes regulated if they met the two-fold difference criterion. Overall, genes were considered regulated by $Al(OH)_3$ if they showed a two-fold up- or down-regulation in at least three out of five donors, or were regulated in two donors with a clear trend in at least one other.

LPS served as a control for the time point and for potential artifacts[25] of the cell isolation with CD14 beads, by determining if LPS-related genes were indeed increased. It was confirmed that LPS-related genes were indeed increased after 24 hours (Supplementary S3), indicating that the time point can indeed be used and that artifacts (no induction of LPS-related genes) might not play a role here.

Protein isolation

Monocytes were lysed by adding 500 µl 4 M Guanidine·HCl in 100 mM phosphate buffer (pH=7.5) to the culture plate and incubated for 2 hours at 4°C. During these 2 hours, the cells were subjected to a freeze-thaw step. The protein concentrations were determined with a BCA protein assay (Pierce biotechnology; Waltham Massachusetts; USA) according to the manufacturer's protocol. Lysed cells were stored at -80°C in a culture plate.

Protein digestion

Protein samples from monocytes were diluted 4 times with 100 mM phosphate buffer pH 7.5 to reduce the Guanidine·HCl content to 1 M and adjust the pH to 7.5. Proteins were digested at 37°C with Lys-C (Roche; Basel; Switzerland) in an enzyme-to-sub-

strate ratio of 1:10 (w/w). After 4 hours, fresh Lys-C was added in a 1:10 (w/w) ratio for an overnight incubation.

Protein labeling in monocyte samples

Following the protein digestion, aliquots from the six monocytes samples per donor (three donors) were taken containing equal protein amounts and per condition labeled using tandem mass tag labeling 6-plex (TMT(6), Thermo Fisher). For donor A 25 µg per condition per time point was labeled, for donor B 50 µg protein per condition per time point was labeled and for donor C 25 µg protein and 10 µg per condition was labeled at 24 and 48 hours, respectively. Labeling was performed on Solid Phase Extraction (SPE) columns (Waters; Milford; MA; USA). The SPE columns were equilibrated as described by the manufacturer and washed with 100 mM phosphate buffer pH 7.5. The digested protein samples were loaded onto 6 separate SPE columns using a vacuum manifold (Waters) and washed with 100 mM phosphate buffer pH 7.5. The TMT-label (0.8 mg per TMT-label) was reconstituted in 41 µl acetonitrile (AcN) according to the supplier's protocol. The AcN concentration was reduced to a maximum of 2.5% (v/v) with 100 mM phosphate buffer pH 7.5. The individual TMT labels were loaded onto the 6 SPE columns, leaving 0.5 ml reagent on top of the column for a 30 minute incubation, fresh label was added for another 30 minutes of incubation, after which the columns were washed with water containing 0.5% formic acid (FA). The six samples were eluted with 90% AcN containing 0.5% FA, pooled, dried by centrifugal evaporation and reconstituted in water containing 0.1% trifluoroacetic acid (TFA).

SCX fractionation

Pooled and labeled monocyte-derived protein samples were purified by Strong Cation exchange (SCX) as described previously[26]. The system comprised a HyperCarb trapping column (200 µm I.D. x 5 mm length, 7 µm particle size) and an SCX column (200 µm I.D. x 11 cm length PolySULFOETHYL Aspartamide, 5 µm, PolyLC), both made in-house. The gradient was 12 min at 100% solvent A (water + 0.5% HOAc), after which a linear gradient started to 100% solvent B (250 mM KCl + 35% AcN + 0.5% HOAc in water) in 16.5 min, followed by a second linear gradient to 100% solvent C (500 mM KCl + 35% AcN + 0.5% HOAc in water) in 16.5 min at a column flow rate of 2 µl/min. Twenty-six 4-µL fractions were collected. Fractions were analyzed for peptide content during fractionation using UV. The peptide-containing fractions were subjected to nanoscale LC-MS analysis.

LC-MS/MS analysis

Peptide separation was performed on a Proxeon Easy-nLC 1000 system (Thermo Scientific). Peptides were trapped on a double-fritted trapping column Reprosil C18 (Dr. Maisch; Ammerbuch; Germany; df=3 µm, 2 cm length × 100 µm I.D.) and separated at a column temperature of 40°C on an analytical column Poroshell 120 EC-C18 (Agilent; df=2.7 µm, 50 cm length × 50 µm I.D.) both packed in house. Both columns contained a 1-mm length KASIL frit prepared as described by Meiring *et al.*[27], to retain the packing bed. The second KASIL frit, upstream in the trapping column, was made the same way after flushing the packing bed with helium. Solvent A was 0.1% FA in MilliQ water and solvent B was 0.1% FA in AcN (Biosolve). The peptides were separated in 143 minutes (10 minutes at 2% B for peptide loading onto the trapping column, followed

by a 118-minutes gradient from 2% to 30% B and 5 minutes at 70% B) in a non-linear optimized gradient[28]. After 128 minutes, the system was kept at 5% B for 15 minutes to equilibrate the column. The column effluent was electro-sprayed directly into the MS using a gold-coated fused silica tip with a 5-µm TipID and a spray voltage of 1.8 kV.

Mass spectrometric data were acquired on a Tribrid-Orbitrap Fusion (Thermo Fisher Scientific), where the full scan (MS^1) spectra were acquired with a scan range of *m/z* 350-1500 Da at 120K resolution (FWHM) with an Orbitrap readout. The Automatic Gain Control (AGC) for the MS^1 was set to 200,000 and the maximum injection time to 50 ms in top speed mode with a duration of 3 seconds, where precursor ions with an intensity of >5,000 were selected for fragmentation (MS^2). Charge states between 1 and 7 were selected. MS^2 was performed using Collision-Induced Dissociation (CID) in the linear ion trap with a normalized collision energy of 35%. The AGC for the MS^2 was set to 10,000 and the maximum injection time to 35 ms. Synchronous-Precursor-Selection was enabled to include up to 10 MS^2 fragment ions. These ions were further fragmented by Higher energy Collision Dissociation (HCD) with a normalized collision energy of 50%. TMT reporter ions were analyzed in the Orbitrap analyzer, with the AGC set to 100,000 and a maximum injection time of 120 ms.

Proteomics data were analyzed with Proteome Discoverer 2.1 (PD 2.1) (Thermo Fisher Scientific) using default settings unless stated otherwise. Precursor mass tolerance was set to 5 ppm, MS/MS scans were searched against the human Uniprot database (Nov 2014), containing 23,048 entries, using the Sequest HT search engine with full enzyme specificity for Lys-C, with *b* and *y* type ions enabled for CID and HCD data with a fragment mass tolerance of 0.5 Da. The data was searched with Aspargine deamidation and Methionine oxidation as dynamic modifications. TMT(6) was set as a static modification on the Lysine residues and the peptide N-termini. For relative quantitation, the quantification node was used with TMT(6) as defined quantification method and an integration tolerance of 0.2 Da. A decoy database defined in the Percolator node was used to validate and filter the peptide-to-spectrum matches with a False Discovery Rate (FDR) of <5%. Only medium (FDR <5%) and High (FDR <1%) confident identified proteins were used in the further data analysis.

The protein data from the SCX fractions of an individual donor were combined by PD 2.1 in a consensus report, resulting in one output table per donor/technical replicate. If multiple entries occurred for the same protein, based on Uniprot and NCBI data, the ratios given by Proteome Discoverer were Log2-transformed and averaged for further analysis. Next, a median correction normalization was performed. For donor C, three technical replicates of the medium control and $Al(OH)_3$-stimulated culture conditions were measured (their median CV was 10.5% for the full proteomics data set) and these were combined into a single average value for this donor to make sure each donor is weighed equally in further analysis. For donors A and B, one sample per condition was analyzed. Data of three biological replicates (donors) were compared and proteins that were upregulated or downregulated by 1.5 fold or more in at least two out of three biological replicates were considered substantially regulated. These regulated proteins were imported in STRING (string.embl.de)[29], to identify enriched pathways in these regulated protein sets (FDR<0.05), within Gene Ontology (GO) biological processes.

The mass spectrometry proteomics data have been deposited to the ProteomeXchange Consortium via the PRIDE[30] partner repository with the dataset identifier PXD008452.

IL-1β ELISA

IL-1β levels in culture supernatants were determined using the Human IL-1 beta/IL-1F2 DuoSet ELISA (R&D systems; McKinley; Minneapolis; USA.). The analysis was performed according to the manufacturer's protocol and recorded on a Synergy MX (Biotek; Winooski Vermont; USA).

ELISA data were analyzed with GraphPad Prism®. Significance of difference was determined using a 2-way ANOVA and a Tukey's multiple comparison test with an Alpha of 0.05.

Results

$Al(OH)_3$ induces changes in cell surface markers on monocytes but not on Immature monocyte derived dendritic cells

When immature monocyte-derived dendritic cells (iMDDCs) were stimulated with $Al(OH)_3$, no significant changes in cell surface marker expression were observed, as determined by flow cytometry, whereas LPS stimulation resulted in the upregulation of CD40, CD80 and CD83 (Supplementary S4). Based on the limited effect of $Al(OH)_3$ on iMDDCs, further detailed analyses were only performed using monocytes.

The effect of incubation of monocytes with $Al(OH)_3$ on their cell surface marker expression was investigated at the level of gene expression (with targeted transcriptomics) and protein identification and quantification. $Al(OH)_3$ stimulation upregulated gene expression of, *CD80*, and *CD8A* in monocytes compared to control cells after 24 hours of stimulation. Gene expression of *CD14*, a typical monocyte marker that is lost upon differentiation into iMDDCs and linked to LPS stimulations[31], was downregulated in $Al(OH)_3$-stimulated monocytes after 24 hours (Fig. 1), while gene expression was upregulated in LPS-stimulated monocytes (Supplementary S3, S5). Moreover, at the protein level (analyzed with quantitative mass spectrometry) CD14 was downregulated after 48 hours of $Al(OH)_3$ stimulation (Supplementary S6, S7). $Al(OH)_3$ stimulation of monocytes resulted in an increased protein expression of activation markers CD9 and CD71 (TRFC) after 48 hours (Table 2 and Supplementary S6, S7) (please note: these markers were not analyzed using targeted transcriptomics). These transcriptome and proteome results confirmed that in an $Al(OH)_3$-stimulated monocyte population cells became activated and start changing their cell surface marker phenotype including the loss of CD14 expression.

$Al(OH)_3$ induces changes in immunogenic genes upon monocyte stimulation

Targeted transcriptome analysis of monocytes was performed on an array of 96 genes, comprising innate and adaptive immune system genes, housekeeping genes and control genes (Supplementary S2). In total, 89 functional gene-transcripts could be measured, of which 40 genes were found to be upregulated and 5 genes were downregulated (Table 1 and Fig 1). Some donor variation was observed since genes were not always differentially regulated in all donors. Fig 1 is most representative for all donors used.

Quantitative proteomics reveals up and downregulation of homeostatic and immunogenic processes after $Al(OH)_3$ stimulation of monocytes

Quantitative proteome analysis of $Al(OH)_3$-stimulated monocytes resulted in the identification of over 4,000 unique proteins, of which 3,000 proteins could be relatively quantified. About 200 proteins were upregulated and about 190 proteins were downregulated in $Al(OH)_3$-stimulated monocytes compared to unstimulated monocytes (Supplementary S6-S10). Some of these proteins could be matched to the transcriptome data, *e.g.* HLA-A, HLA-E and CD14 (Table 2). Cytokines were not identified in

the lysates. However, several cytokine inducible proteins were detected in the lysates (*e.g.* Mx1, Mx2 and IFIT3). These proteins are induced by IFNβ[32-34].
Over-representation analysis of GO terms, revealed the involvement of various biological processes (Fig 2 and 3). A comprehensive overview of all differentially regulated proteins and enriched GO terms is represented in Supplementary S7 and S8-10. Immune processes, like *antigen processing and presentation* and *innate immune response* were over-represented as well as processes involved in homeostasis like *metabolic processes*, *localization* and *transport*(Fig 2). Specific pathways that were induced after 24 hours were related to *localization* and *copper homeostasis*: specified proteins related to this process were, *e.g.* copper-transporting ATPase 2 (ATP7B) and Amyloid-beta A4 (APP). After 48 hours of stimulation, additional GO terms were enriched in the upregulated protein sets as compared to 24 hours of stimulation including: *intracellular transport processes* (*e.g. protein transport, protein localization)* and *response to stress* (Fig 3B). Processes related to cell death were also increased after $Al(OH)_3$ stimulation (*programmed cell death*). A complete overview can be found in Supplementary S8-S9.

Within the set of downregulated proteins after 24 hours of $Al(OH)_3$ stimulation, no GO terms were over-represented. However, in the data set representing downregulated proteins after 48 hours, over-representation of various GO terms was identified *i.e. blood coagulation, inflammatory response, regulation of immune system process* and *response to stress* (Supplementary S10). These data show that $Al(OH)_3$ regulated both processes involved in homeostasis as well as in the immune response.

IL-1β production as a consequence of $Al(OH)_3$ stimulation is partially inflammasome dependent

Inflammasome-related gene expression was increased in transcriptome analysis after 24 hours of $Al(OH)_3$ stimulation, *i.e. NOD1 and IL-1R1*, while *CASP1* and *MyD88* were upregulated in two donors (Fig 1). IL-1β ELISA analysis in the culture supernatant of two donors showed a trend towards increased IL-1β secretion (Supplementary S11). Cytokine analysis with an IL-β ELISA in THP-1 cells confirmed the upregulation of IL-1β after 48 hours (Fig 4 and Supplementary S12).

To investigate the involvement of the inflammasome in IL-1β production upon $Al(OH)_3$ stimulation in more detail, THP-1 cells (a human monocytic cell line) were differentiated into macrophages by addition of PMA and stimulated with 50 μg/ml of $Al(OH)_3$ in the presence and absence of the inflammasome blocker glybenclamide. Measurement of IL-1β in cell culture supernatants of THP-1 cells revealed that IL-1β secretion upon $Al(OH)_3$ stimulation decreased in the presence of glybenclamide (Fig 4 and Supplementary S12). A similar trend was observed when tested in primary monocytes: one donor with blocking (donor A) and one donor without blocking experiment (donor B) (Supplementary S11). However, this response was less pronounced if compared to the response in PMA-primed THP-1 cells. The loss of IL-1β production upon glybenclamide addition provided evidence that the IL-1β production of $Al(OH)_3$-stimulated monocytic cells is indeed partially dependent on the activation of the inflammasome.

$Al(OH)_3$ activates the complement system

Our proteomics data of $Al(OH)_3$-stimulated primary monocytes identified the altered expression of proteins from all complement pathways: C4 (lectin pathway), C8 (alter-

native pathway), and C5aR (classical pathway) were significantly upregulated after 24 hours of stimulation (Table 2 and Supplementary S7). In addition, gene expression of *C3* was upregulated and *CASP1* was upregulated in two donors (Table 1).

$Al(OH)_3$ promotes the production of Th2 and Th1 related cytokines

Notably, in $Al(OH)_3$-stimulated monocytes, the Th1-associated gene *IFNγ* [35-36] was upregulated after 24 hours (Fig 1 and Supplementary S5). Proteins involved in the response to IFNγ, IFNγR1 and IFI30, were also upregulated (Supplementary S7). Other cytokine genes increased after $Al(OH)_3$ stimulation, were *IL-2*, *IL-5*, *IL-17A*, *IL-23A* and *IFNβ* (Fig 1, Table 1 and Supplementary S5). Interferon-induced protein with tetratricopeptide repeats 3 (IFIT3) and the interferon-induced GTP-binding proteins Mx1 and Mx2 were also upregulated (Table 2). In addition, increased expression of the Th2 polarizing gene *IL-4* was observed, after 24 hours of stimulation (Table 1 and Fig 1).

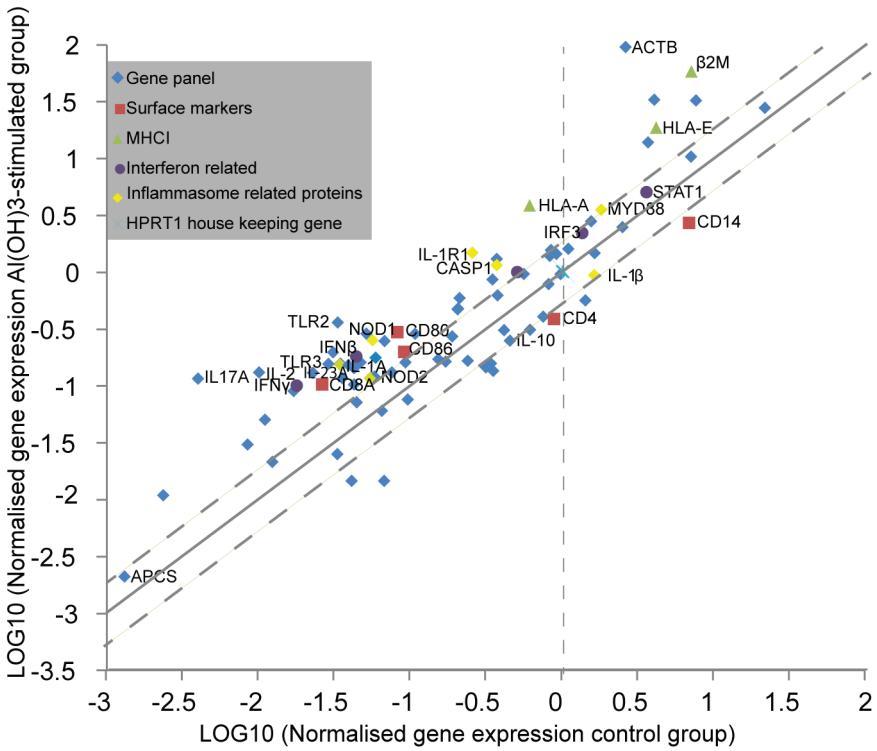

Figure 1. ***Gene expression profile of $Al(OH)_3$-stimulated monocytes after 24 hours.***
Gene expression was normalized to a housekeeping gene. This figure depicts the LOG10(normalized) gene expression profile after 24 hours of $Al(OH)_3$ stimulation (10μg/ml) compared to the control, of two representative biological replicas (for an overview of all the altered genes in three out of five donors see Table 1). The genes above the upper dotted line are significantly upregulated by at least a factor of 2 as a result of the $Al(OH)_3$ stimulation, while the genes below the lower dotted lines are downregulated by at least a factor of 2 due to the $Al(OH)_3$ stimulation

Table 1. ***Genes differentially expressed upon Al(OH)$_3$ (10 µg/ml) stimulation of monocytes.***

Pattern recognition receptors (PPRs) and signaling	*Cytokines and chemokines*	*Cytokine and chemokine receptors*	*Surface markers*	*Transcription factors*	*Complement system*	*Antigen presentation*	*Others*
NOD1[2]	CCL2[2]	CCR6[2]	CD8A[2]	FoxP3[2]	C3[2]	β2M[2]	ACTβ[2]
TLR2[2]	CSF2[2]	CCR8[2]	CD80[2]	GATA3[2]	*CASP1*[2]	HLA-A[2]	CD40LG[2]
TLR3[2]	IL-2[2]	CXCR3[2]	*CD4*[1]	*IRF3*[2]		*HLA-E*[2]	CRP[2]
MYD88[2]	IL-4[2]	IL-1R1[2]	CD14[1]	IRF7[2]			MPO[2]
IRAK1[2]	IL-5			*TBX21*[1]			MX1[2]
TICAM1[2]	IL-17A[2]						RAG1[2]
DDX58[2]	IL-23A						STAT1[2]
	IFNαR1[2]						STAT3[2]
	IFNβ1[2]						STAT6[2]
	IFNg[2]						TYK2[2]
	TNF[2]						*TRAF6*[2]
	IL-1β[1]						MAPK1[2]
	IL-18[1]						MAPK8[2]
							RORC[2]
							LY96[2]
							LYZ[1]
							NLRP3[1]

[1] *annotated genes that are downregulated by at least a factor of 2 in at least 3 donors.*
[2] *annotated genes that are upregulated by at least factor of 2 in at least 3 donors.*
Italic genes: genes that are upregulated/downregulated in 2 donors and a trend towards upregulation in at least one additional donor.

Table 2. ***Selection of proteins and their fold changes after 24 and 48 hours of $Al(OH)_3$ (10 µg/ml) stimulation compared to control in primary monocytes.***

Accession number	*Protein*	*Fold changes after 24 hours*	*Fold changes after 48 hours*
P05534	HLA-A	1.05	15.53
P13747	HLA-E	2.65	15.01
Q8TCT9	HM13	2.11	4.01
Q99538	LGMN	2.20	3.08
P07339	CTSD	2.43	3.35
P07711	CTSL	7.04	6.85
P25774	CTSS	1.22	1.71
O60911	CSTV	2.53	2.39
P21926	CD9	1.57	2.82
P08571	CD14	0.67	0.20
P02786	TFRC	1.47	3.32
P20591	MX1	1.36	1.62
P20592	MX2	1.26	1.72
P13284	IFI30	2.31	1.49
O14879	IFIT3	1.62	2.53
P26951	IL3RA	3.37	90.58
P15260	IFNγR1	2.02	3.37
Q9UHD2	TBK1	0.92	0.99
P0C0L4	C4	1.86	1.74
P21730	C5aR1	1.50	1.97
P07357	C8a	2.64	1.77
P07358	C8b	6.86	0.93

However, in the presence of the Th1-associated gene *IFNγ* , which was also increased after 24 hours of stimulation.

Stimulation with $Al(OH)_3$ increases the chemotactic capacity of the monocytes

Transcriptome data showed that $Al(OH)_3$-stimulated monocytes regulated mechanisms to attract other immune cells. The gene expression of *CCL2* was upregulated in $Al(OH)_3$-stimulated monocytes (Table 1); this gene encodes for a molecule involved in monocyte trafficking. $Al(OH)_3$ stimulation also induced the expression of chemokine receptors *CCR6* and *CCR8* (Table 1).

Figure 2. ***Heatmap of all $Al(OH)_3$-regulated proteins in monocytes.***

The heatmap represents the median of all upregulated (red) and downregulated (green) proteins from 3 biological replicates on a LOG(2) scale after 24 and 48 hours of $Al(OH)_3$ stimulation (10µg/ml). Regulated proteins were at least altered by a factor 1.5 compared to the control in at least two out of three biological replicates. Enrichment analysis of GO biological processes was performed on the regulated proteins; depicted processes have FDRs <0.05. The proteins were clustered by GO term as described in Supplementary S7.

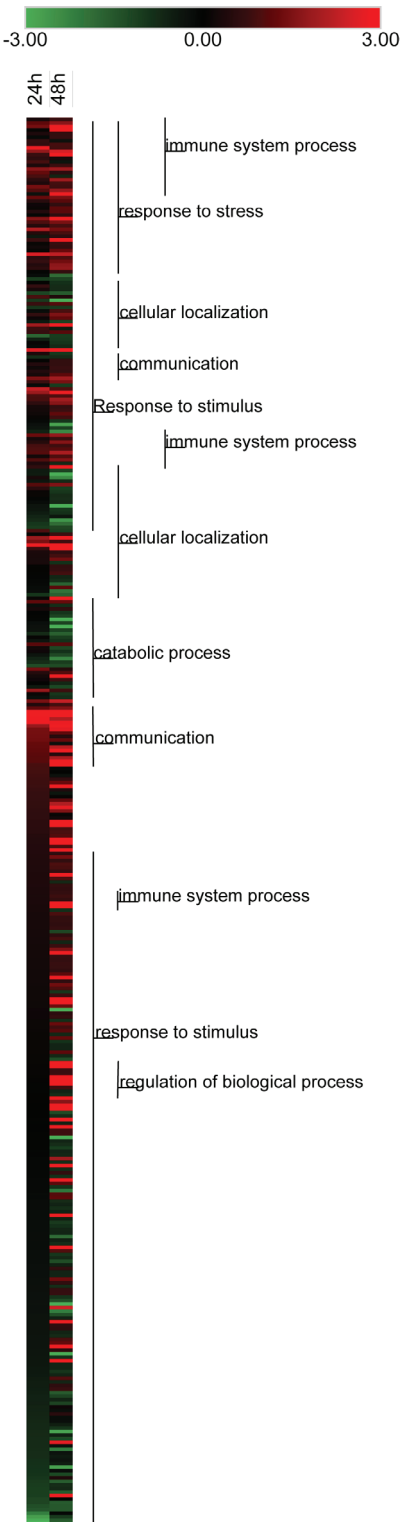

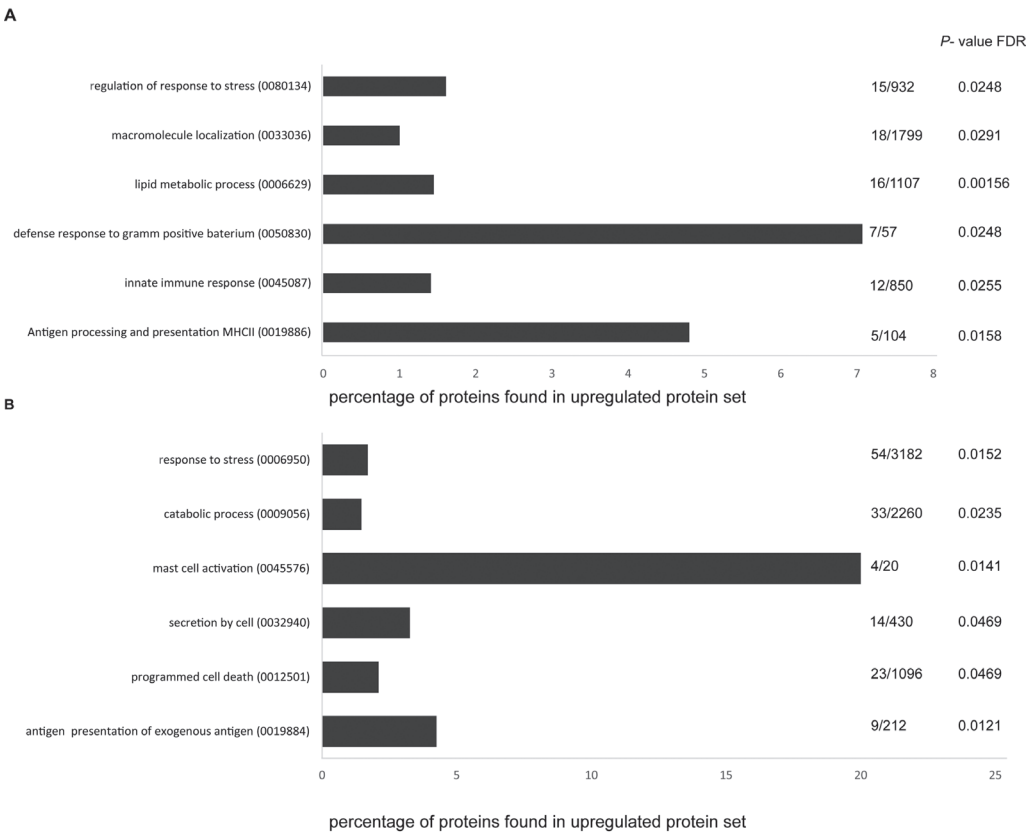

Figure 3. ***Enriched GO biological process terms in the upregulated protein set after 24 and 48 hours of Al(OH)$_3$stimulation of monocytes.***

The GO terms are biological processes that are significantly overexpressed (p-values <0.1) in the upregulated protein data set after 24 hours of Al(OH)$_3$ stimulation (10μg/ml) (3A) and 48 hours (3B) from three biological replicates. The bars depict the percentage of upregulated proteins out of the total proteins in this GO term. the numbers display the ratios between upregulated proteins and total proteins in this GO term and the numbers between brackets are referring to the specified GO term.

Al(OH)$_3$ induces upregulation of components of the HLA processing and presentation pathways in monocytes

The upregulation of HLA class II pathways in monocytes induced by Al(OH)$_3$ was observed at the level of the proteome. The pathway antigen processing and presentation by HLA class II was enriched in the upregulated protein data set of Al(OH)$_3$-stimulated monocytes. HLA class II-related upregulated proteins included Legumain[37-39] and Cathepsin D, S and L (Table 2 and Supplementary S7)[40]. mRNA expression of *IFNγ* was upregulated as was the protein expression of IL-3R, both synergizing in increasing HLA class II expression[41-42].

In addition to HLA class II pathway upregulation, induction of HLA class I-related genes and proteins was observed. Al(OH)$_3$ stimulation of monocytes increased gene and protein expression of HLA-A and HLA-E, as well as the gene expression of β2*M*

compared to controls (Table 1 and Fig 1). HLA class I-related proteins were also upregulated upon $Al(OH)_3$ stimulation *i.e.* heat shock protein 90 (HSP90) and Minor Histocompatibility Complex HM13 (Table 2).

$Al(OH)_3$ stimulation of monocytes induces IFNβ secretion potentially by upregulating TLR or NOD like signaling

$Al(OH)_3$ stimulation of monocytes resulted in a significantly increased *IFN*β gene expression (p <0.01*)*. Protein expression of proteins downstream of IFNβ: *i.e.* Mx1, Mx2, and IFIT3 was increased in $Al(OH)_3$-stimulated monocytes (Supplementary S7), as was the gene expression of *Mx1.* This provides evidence that IFNβ indeed has been secreted, since these proteins would otherwise not have been increased. These proteins could be induced by IFNβ via STAT1. Indeed, gene expression of *STAT1* was upregulated in $Al(OH)_3$-stimulated monocytes (Fig 1 and Supplementary S5). These data confirm the secretion and consumption of IFNβ.

Indications of IFNβ transcription were also found since the gene expression of *IRF7* a key transcriptional regulator was found to be increased (Fig 1). *IRF3* gene expression was increased in two donors. Genes involved in the pathways via which IRF7 can mediate the induction of type I interferons were increased, *i.e. TICAM1* and *IRAK1* while *MyD88*, and *TRAF6* clearly trended towards upregulation (Table 1 and Supplementary S5)[43]. The protein TBK1 in the IRF7 signaling pathway was identified at the level of the proteome but was not increased (Supplementary S6). Upstream of both *MyD88/IRAK1* and *TICAM/TRAF6*, TLR and NOD signaling could be involved, although $Al(OH)_3$ is not a ligand for both TLRs and NOD1. However, $Al(OH)_3$ induced cell stress and cell death (Supplementary S8 and S9)[13, 16, 19], resulting in the release of DAMPs/endogenous ligands. These endogenous ligands can bind various receptors leading to the secretion

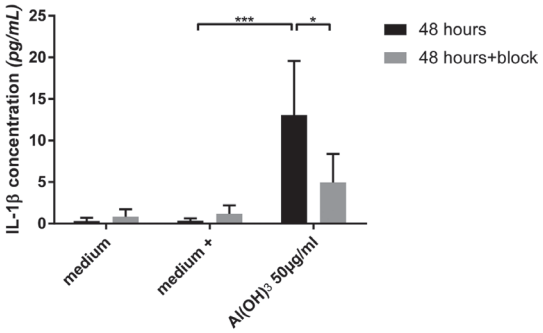

Figure 4. ***IL-β levels in supernatants of THP-1 cell cultures upon $Al(OH)_3$ stimulation of THP-1 cells.***

*PMA-treated THP-1 cells were stimulated with 50 µg/ml $Al(OH)_3$ with or without the inflammasome blocker glybenclamide. IL-1β levels, measured after 48 hours of stimulation, were compared to non-blocked $Al(OH)_3$- stimulated cells. Data are represented as the mean and the standard deviation of three independent experiments (biological replicates), each, with at least two technical replicates p-values <0.05 are depicted as * and p-values < 0.005 are depicted as ***. Medium represents control cells, medium+ represents medium with the PMA prime and 50 µg $Al(OH)_3$ represents the PMA-primed, $Al(OH)_3$-stimulated group.*

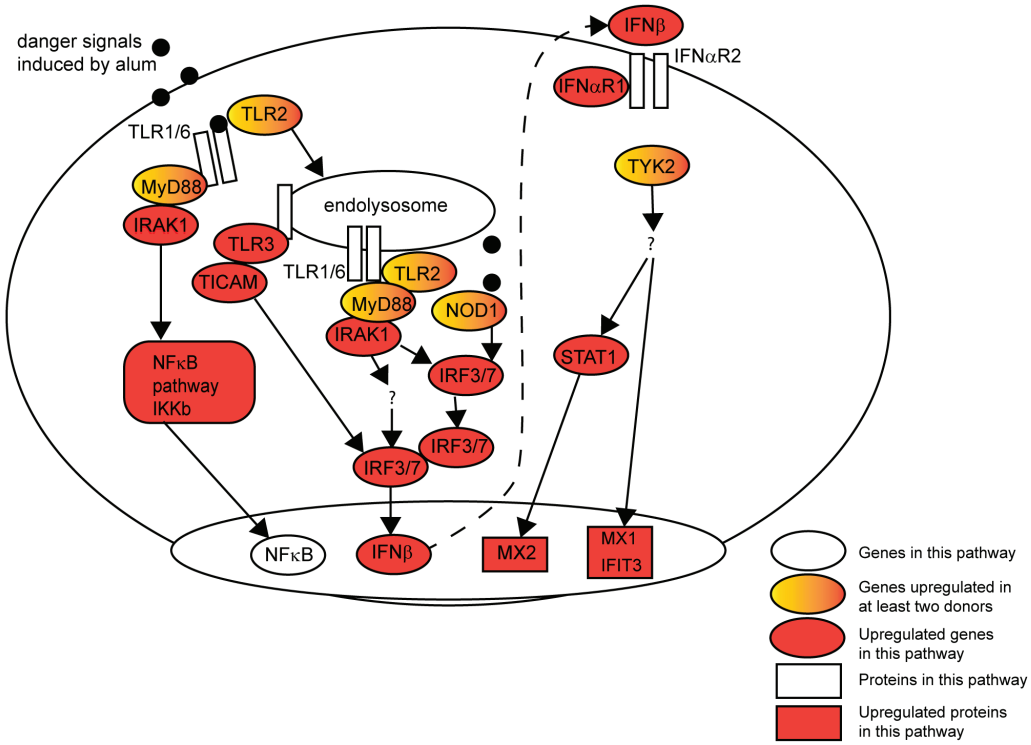

Fig 5. ***Hypothetical pathways resulting in IFNβ secretion, potentially via TLR2/TLR3 and NOD1 pathways that become activated upon Al(OH)$_3$ stimulation of monocytes.*** *TLR2 and TLR3 can be activated by DAMPS, after which two pathways can be activated: one leading to the formation of NFκB and the second pathway leading to the formation of IFNβ and downstream proteins. NOD1 activation leads to the secretion of IFNβ. Genes are annotated in circles, proteins are annotated in boxes.*

of type I interferons. Gene expression of a subset of these DAMP sensors was identified in this data set, specifically DDX58, (no further pathway evidence identified) TLR2 (upregulated in two donors but downregulated in one), TLR3 (upregulated in four donors) and NOD1 (in two donors tending towards upregulation in at least one more) (Fig 1). TLR3 can be activated by endogenous mRNA[44-46] resulting in the secretion of type I interferons, via the induction of TICAM1, TRAF6, TBK1 and IRF7[44-45, 47]. TLR2 (upregulated in two donors and downregulated in one donor) can be induced by endogenous ligands and induce the secretion of type I interferons via the pathway described by Dietrich *et al.*[48]. NOD1 can also be induced by endogenous ligands and results in the formation of type I interferons[49-50]. These data indicate the TLR signaling and NOD1 signaling could be involved in the induction of type I interferons by DAMP sensing.

Although involvement of other DNA sensors cannot be excluded, hypothetical Al(OH)$_3$-induced pathways resulting in the release of type I interferons, based on the data described and the literature are depicted in Fig 5.

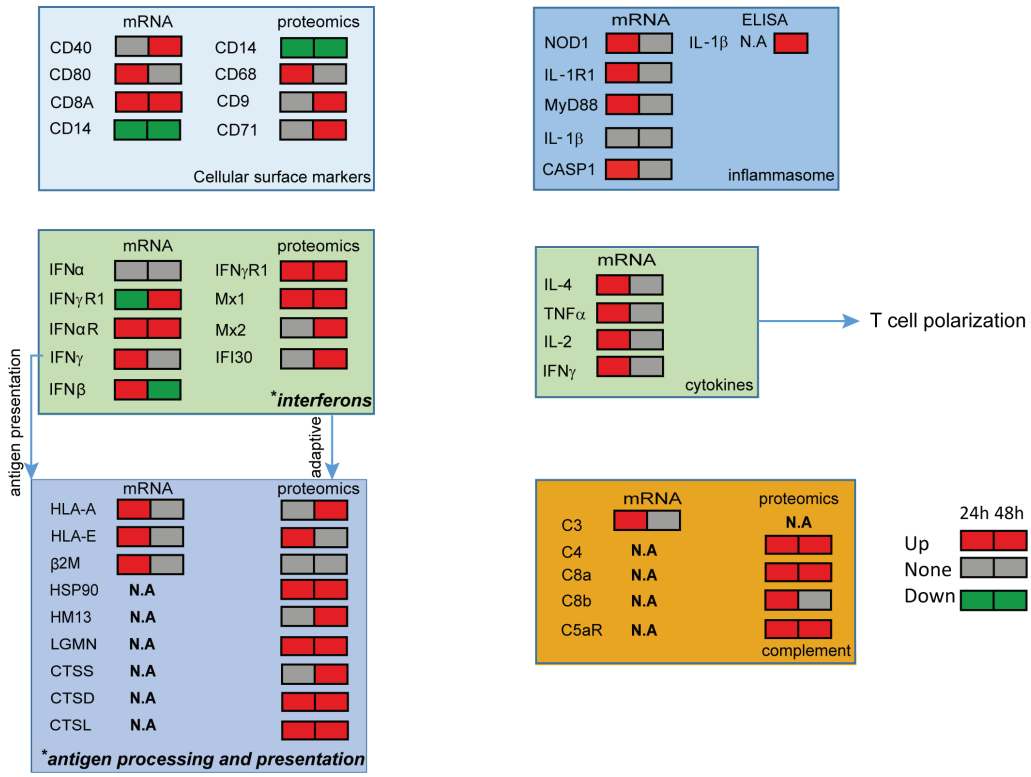

Fig 6. ***Overview of the kinetics from the monocyte response towards $Al(OH)_3$ in combination with the analytical tool used.***

The green blocks represent cytokines and related proteins. The light blue blocks represent the surface markers. The purple blocks represent the HLA-class I and class II antigen presentation pathways. The dark blue blocks represent the inflammasome activation. The orange blocks represent complement activation

Discussion

A comprehensive analysis of the effects of $Al(OH)_3$ on monocytes revealed two novel cellular processes to be involved in the adjuvant action of $Al(OH)_3$: first, IFNβ secretion via NOD1 or TLR signaling and second, the upregulation of antigen processing and presentation via HLA class I-related proteins, potentially leading to more antigen processing and presentation when an antigen is present. Together with a deeper elucidation of known $Al(OH)_3$-affected mechanisms, these novel processes emphasize that $Al(OH)_3$-stimulated monocytes prepare for a pro-inflammatory function and antigen presentation in the immune response[22-24].

Known mechanisms of $Al(OH)_3$ (as reviewed by He *et al.*[12]) were elucidated in more detail: inflammasome activation, complement activation, cytokine induction, monocyte activation and differentiation and induced HLA-class II activation possibly due to increased *IFNγ* gene expression. It is noteworthy that *IFNγ* gene expression is induced as a result of $Al(OH)_3$ stimulation. As the gene targets were measured at mRNA level and the proteins induced by these measured genes were determined to be increased by proteomics-enabled mass spectrometry, it can be stated that the genes actually have been translated into proteins and subsequently induced downstream pathways; *e.g.* IFNβ induction was measured at the gene expression level and Mx1, Mx2 and IFIT3 were measured at protein level (Table 2 and Supplementary S7), these proteins are specifically induced by type I interferons[32-33]. By combining the transcriptome and proteome analysis, pathways can be identified in more detail, despite the sometimes relative low coherence between protein and gene expression with respect to the same Uniprot entry. This might be related to the limited set of genes investigated, due to differences in kinetics or due to the fact that secreted proteins probably have not been identified in the cell lysates. By combining these techniques it is possible to analyze activated pathways, based on the identification of selected cytokines and downstream proteins.

One of the novel processes identified is the induction of IFNβ secretion resulting from $Al(OH)_3$ stimulation, most likely due to TLR2, TLR3, NOD like or other DAMP signaling. *IFNβ* gene expression was increased in $Al(OH)_3$-stimulated monocytes. Downstream of IFNβ, various proteins were induced: *e.g.* Mx1, Mx2 and IFIT3 were increased in $Al(OH)_3$-stimulated monocytes. These proteins can be induced by IFNβ via *STAT1.* Indeed, gene expression of *STAT1* was upregulated in $Al(OH)_3$-stimulated monocytes (Fig 1). Upstream of IFNβ, *IRF7* gene expression was increased as was the expression of *IRF3* in two biological replicates. These inducers of type I interferon secretion can be activated via various pathways. Multiple of these inducers were identified and upregulated at the level of gene expression: *TICAM1*, *TRAF6*, *MyD88* and *IRAK1*. Upstream of these molecules, TLR signaling can be involved. In this data set, *TLR3* was upregulated at the level of gene expression. *TLR2* was upregulated in two donors (Table 1). $Al(OH)_3$ is not a direct ligand for either of these pathways, however $Al(OH)_3$ causes the release of endogenous ligands by inducing cell death[13, 16, 19]. Indeed, markers of cell stress and cell death were identified in the protein dataset in this study (Fig 3A, 3B, Supplementary S6-S9). These endogenous ligands can activate TLR3 and downstream signaling[44-46] and TLR2 directly or indirectly via TLR3[51-54]. The activation of TLR3 results in recruitment of TICAM1 followed by the activation of IRF3/IRF7 leading to type I Interferon transcription. The activation of TLR2 can result in the formation of a complex

with MyD88 and the internalization of this complex towards the endolysosome where this complex binds IRAK1. Subsequently, IRAK1 phosphorylates IRF3/IRF7, resulting in the transcription and secretion of type I interferons[48]. Many of the genes involved in these pathways were found to be upregulated as can be seen in Fig 5. Since TLR2 was upregulated in two donors but downregulated in one donor, the pathway via TLR3 is more likely to be involved in type I Interferon induction than the pathway via TLR2.

Detection of cytosolic DNA or other DAMPs is another possible cause of IFNβ induction[16]. Two of those DAMP sensors are NOD1 and DDX58[19, 49-50]. *NOD1* gene expression was found to be increased. Activation of NOD1 results in a similar pathway as the TLR2/TLR3 signaling pathway (Fig 7). *DDX58* gene expression was upregulated in this data set, however, no further evidence of the activation of this pathway was identified. This is in agreement with the data from Marichal *et al.* describing that the DDX58-STING pathway might not be involved in the adjuvant effect of $Al(OH)_3$[12, 19]. However, based on this data this pathway cannot be excluded. TLR8 and TLR9 are other potential DAMP sensors. Protein expression of TLR8 was downregulated and the gene expression of *TLR8* and *TLR9* was not increased in $Al(OH)_3$-stimulated monocytes, probably excluding TLR8 and TLR9 from a role in the adjuvant effect of $Al(OH)_3$. These results show that $Al(OH)_3$-induced DAMPS could be involved in the formation of IFNβ, most likely by activation TLR2 and/or TLR3 and by NOD1 signaling pathways, since many genes and proteins were upregulated in $Al(OH)_3$-stimulated cells that belong to these pathways. Other potential sensors for DNA in the cytoplasm signaling via the Caspase recruitment and activation domain (CARD) were not identified in the proteomics data, but cannot be excluded from being involved in Interferon secretion. It has been described that TLR signaling is not involved in the Ab response in $Al(OH)_3$-stimulated DCs[12, 15], however, a potential role for TLR signaling in the induction of interferons has been described earlier[16], as is the interaction with the inflammasome[55-57]. This data indicate that TLR signaling can be involved in the adjuvant effect of $Al(OH)_3$.

The induction and secretion of type I interferons can be related to processes described above, amongst others: differentiation away from a monocytic cell type, chemotaxis via the induction of CCL2, the increase of HLA class I and class II, activate complement and induce or inhibit the secretion of various cytokines as described previously[58-60]. This implies that type I interferons are crucial mediators of the innate immune response induced by $Al(OH)_3$. In addition, secretion of type I interferons (IFNβ) after $Al(OH)_3$ stimulation, might have several effects if the effects induce innate memory. Innate memory is the phenomenon of innate immune cells, like NK cells and macrophages, that are permanently changed after stimulation. Interferons play a role in inducing this innate memory[61]. First, type I interferons induced via TLR signaling are essential in the host response to virus. Second, they prime NK cells and macrophages[62-63], of major importance for an early clearance of infections and the maturation of Th1 cells, which can be needed to induce memory[64-65]. Third, type I interferons are essential for the survival of both $CD4^+$ and $CD8^+$ T cells[63], but most relevant for the immune response upon vaccination is the stimulation of local B cells by type I Interferons[66]. Therefore, IFNβ secretion can be important in the adjuvant effect of $Al(OH)_3$.

The other novel mechanism identified in this study is the increased activation of the antigen presentation pathway via HLA class I. It was recently described that activated monocytes have a fundamental role in antigen presentation to T cells in the lymph nodes and that antigen presenting monocytes can in fact cross present to HLA class

I[24]. This study showed an upregulation of HLA class I molecules HLA-A and HLA-E, on both the level of gene expression and protein expression. Moreover, an increased protein expression of HM13 and an increased gene expression of *β2M* and *IFNγ* was observed, all related to antigen presentation via HLA class I[41, 67]. These results show that $Al(OH)_3$ increased the expression of HLA class I molecules on monocytes which leads to enhanced antigen presentation. Although $Al(OH)_3$ is capable of activating $CD8^+$ T cells, these T cells will likely not develop into mature cytotoxic T cells but rather into $CD8^+$ memory T cells[8, 13, 68-70]. Nevertheless, $Al(OH)_3$ is mainly considered an inducer of $CD4^+$ T cells[5, 13, 71]. HLA-E plays a role in the stimulation of NK cells. NK cells specifically recognize the HLA-E-peptide complex, which can inhibit and excite the response, depending if the peptide is self or foreign, such as a viral peptide[72-73]. This is a useful process in inducing the immune response or preventing autoimmunity.

Besides increased expression of HLA class I molecules, an increased expression of components of the HLA class II pathway after $Al(OH)_3$ stimulation was observed, like Legumain, Cathepsins S, L, B and D. There is conflicting literature regarding the effect of $Al(OH)_3$ on HLA class II expression[5-6, 74,]. The increased expression of HLA class II molecules by $Al(OH)_3$ might be due to IFNγ signaling[41]. Indeed, in our study mRNA of *IFNγ* was increased. Moreover, protein expression of IFNγR1, and IFI30, a downstream molecule of the IFNγ signaling pathway, was increased. IFNγ-induced increase of HLA class II can be synergized by IL-3 and the IL-3R receptor, of which protein expression was increased[42]. The detection of several Cathepsins (S, L, D) and IFI30, which is required for antigen presentation via HLA class II, supports the hypothesis that $Al(OH)_3$ increases HLA class II antigen presentation by monocytes and that the increase of HLA class II molecules in monocytes might be due to the induction of IFNγ and subsequent signaling.

As described previously, $Al(OH)_3$ induced the downregulation of CD14[6]. This finding indicates that $Al(OH)_3$-stimulated monocytes are starting to differentiate away from a monocytic cell type and that the cells become activated, which was confirmed by the increase of activation marker CD71 for monocytes. For the response to $Al(OH)_3$ it was expected that the response would be well measureable after 24 hours, since the responses towards LPS could still be detected after 24 hours; this time point was also based on the study of Ulanova *et al.*[75-77].

Induction of cytokines by an adjuvant is important in steering the immune response. $Al(OH)_3$ is described as an adjuvant that primes for a Th2 response by inducing IL-4[5]. Indeed, our results show production of the Th2 polarizing cytokine *IL-4* by monocytes upon $Al(OH)_3$ stimulation. Presumably, the IL-4 response is dominant and may inhibit Th1 polarization in response to $Al(OH)_3$. However, innate IFNγ is associated with a Th1 response[36, 69]. A more Th1-related response to $Al(OH)_3$ was observed in multiple studies related to $Al(OH)_3$[69]. IFNγ was secreted in IL-4 knockout mice[9] resulting in a more Th1-related response. IFNγ has more functions then solely being a Th1-associated cytokine. Thus, the polarization towards a Th2 type response occurs upon $Al(OH)_3$ stimulation despite the IFNγ produced.

One of the known mechanisms in the adjuvant activity of $Al(OH)_3$ besides preparing the innate immune system for antigen presentation and T cell activation, is the activation of the inflammasome leading to the secretion of IL-1β. This was confirmed in primary monocytes, by the increased gene expression of *NOD1*, *IL1R1* and a trend in *CASP1* and *MyD88*. In addition, a trend towards increased IL-1β secretion was observed in

primary monocytes (2 donors) as was the reduction of IL-1β secretion when the inflammasome was blocked (1 donor). In PMA-primed THP-1 cells, an inflammasome inhibition experiment was performed that resulted in a reduced IL-1β secretion. PMA-primed THP-1 cells were used to further elucidate the inflammasome dependent origin of IL-β. THP-1 cells were used because, the levels of IL-1β detected in primary monocytes were low and THP-1 cells are a useful model since PMA priming causes the production of pro IL-1β and subsequent exposure to $Al(OH)_3$ can increase actual IL-1β, mimicking the two step activation required for inflammasome induction[78-80]. THP-1 cells are immortalized cells that differ in sensitivity form primary monocytes in response to stimuli such as LPS, due to differences in the cell surface marker expression of[81-82]. However, the confirmation of the role of the inflammasome pathway in the IL-1β secretion in THP-1 cells suggests a similar involvement of the inflammasome in primary monocytes, since leads were also found in the primary monocyte data.

Complement activation is another mechanism described to be induced by $Al(OH)_3$[18], either by $Al(OH)_3$ directly or by dying cells; genes and proteins related to the classical, alternative and lectin pathways were upregulated in this dataset[18]. In our study, transcriptome data revealed the upregulation of *C3* showing the initiation of the complement cascade, while at the level of the proteome C4, C5A and C8 were upregulated, representing the different complement pathways. These results show that combined use of transcriptomics and proteomics is valuable. At the transcriptome level, the initiation of the complement cascade was observed while with the proteome data the specific pathways were determined. The activation of complement pathways can be useful for bacterial lysis, and clearing apoptotic cells, which could prevent autoimmunity[83].

This study demonstrates that the response to $Al(OH)_3$ is very complex (Fig 6), but also indicates that there might be considerable differences between *in vivo* and *in vitro* models. This might be caused by the use of a single cell type *in vitro* versus the availability of an intact, coherent immune system *in vivo*. Also, the species difference between cells from humans and mice might play a role. In mouse models, it was observed that $Al(OH)_3$ skews to a Th2 response[84]. In this study we indeed observed a polarization of the immune response towards a Th2 response, but in the presence of the Th1-associated gene IFNγ.

Conclusion

The immune response is a complex interplay of many molecules, residing in different tissues and cellular compartments. Hence, our model system, utilizing primary monocytes, does not include the coherent adaptive immune response upon $Al(OH)_3$ stimulus. Moreover, the present study did not include a particular antigen adsorbed to $Al(OH)_3$ which might also contribute to the innate immune response induced by $Al(OH)_3$.

Our systems biology-based approach revealed a detailed overview of the molecular mechanisms of $Al(OH)_3$ as an adjuvant for monocyte responsiveness (Fig 6). Most important, the monocyte response to $Al(OH)_3$ is broad as illustrated by the induction of Th2-polarizing factors, the induction of type I and type II interferons and the upregulation of both HLA class I and HLA class II pathways, even in the absence of antigens. In this study, two new modes of action of $Al(OH)_3$ were elucidated, *i.e.* the upregulation of IFNγ in relation to HLA regulation and antigen presentation and the IFNβ secretion possibly as a result of TLR2, TLR3 or NOD1 activation. Finally, by combining complementary techniques, *e.g.* functional assays, transcriptome data and proteome data, it was possible to create a detailed overview of cellular processes in response to $Al(OH)_3$, which are important in the adjuvant effect of $Al(OH)_3$.

Acknowledgements

Sietske Kooijman is funded by a strategic research grant (SOR) of the Ministry of Health (IS200107). This work was also partly supported by the Proteins@Work, a program of the Netherlands Proteomics Centre financed by the Netherlands Organisation for Scientific Research (NWO) as part of the National Roadmap Large-scale Research Facilities of the Netherlands (project number 184.032.201).

We acknowledge Hilde Vrieling for performing the autofluorescent verification experiments for the flow cytometry data and for the THP-1 set up experiments.

References

1. Glenny, A. T.; Pope, C. G.; Waddington, H.; Wallace, U., Immunological notes. XVII–XXIV. *The Journal of Pathology and Bacteriology* 1926, *29* (1), 31-40.
2. Glenny, A. T.; Buttle, G. A. H.; Stevens, M. F., Rate of disappearance of diphtheria toxoid injected into rabbits and guinea - pigs: Toxoid precipitated with alum. *The Journal of Pathology and Bacteriology* 1931, *34* (2), 267-275.
3. Holt, L. B., *Developments in Diptheria Prophylaxis*. Heinemann: 1950.
4. Hem, S. L., Elimination of aluminum adjuvants. *Vaccine* 2002, *20 Suppl 3*, S40-3.
5. Ulanova, M.; Tarkowski, A.; Hahn-Zoric, M.; Hanson, L. A., The Common vaccine adjuvant aluminum hydroxide up-regulates accessory properties of human monocytes via an interleukin-4-dependent mechanism. *Infect Immun* 2001, *69* (2), 1151-9.
6. Seubert, A.; Monaci, E.; Pizza, M.; O'Hagan, D. T.; Wack, A., The adjuvants aluminum hydroxide and MF59 induce monocyte and granulocyte chemoattractants and enhance monocyte differentiation toward dendritic cells. *J Immunol* 2008, *180* (8), 5402-12.
7. Brewer, J. M.; Conacher, M.; Hunter, C. A.; Mohrs, M.; Brombacher, F.; Alexander, J., Aluminium hydroxide adjuvant initiates strong antigen-specific Th2 responses in the absence of IL-4- or IL-13-mediated signaling. *J Immunol* 1999, *163* (12), 6448-54.
8. McKee, A. S.; Munks, M. W.; MacLeod, M. K.; Fleenor, C. J.; Van Rooijen, N.; Kappler, J. W.; Marrack, P., Alum induces innate immune responses through macrophage and mast cell sensors, but these sensors are not required for alum to act as an adjuvant for specific immunity. *J Immunol* 2009, *183* (7), 4403-14.
9. Brewer, J. M.; Conacher, M.; Satoskar, A.; Bluethmann, H.; Alexander, J., In interleukin-4-deficient mice, alum not only generates T helper 1 responses equivalent to freund's complete adjuvant, but continues to induce T helper 2 cytokine production. *Eur J Immunol* 1996, *26* (9), 2062-6.
10. Sokolovska, A.; Hem, S. L.; HogenEsch, H., Activation of dendritic cells and induction of CD4(+) T cell differentiation by aluminum-containing adjuvants. *Vaccine* 2007, *25* (23), 4575-85.
11. Calabro, S.; Tortoli, M.; Baudner, B. C.; Pacitto, A.; Cortese, M.; O'Hagan, D. T.; De Gregorio, E.; Seubert, A.; Wack, A., Vaccine adjuvants alum and MF59 induce rapid recruitment of neutrophils and monocytes that participate in antigen transport to draining lymph nodes. *Vaccine* 2011, *29* (9), 1812-23.
12. He, P.; Zou, Y.; Hu, Z., Advances in aluminum hydroxide-based adjuvant research and its mechanism. *Hum Vaccin Immunother* 2015, *11* (2), 477-88.
13. Kool, M.; Soullie, T.; van Nimwegen, M.; Willart, M. A.; Muskens, F.; Jung, S.; Hoogsteden, H. C.; Hammad, H.; Lambrecht, B. N., Alum adjuvant boosts adaptive immunity by inducing uric acid and activating inflammatory dendritic cells. *J Exp Med* 2008, *205* (4), 869-82.
14. Li, H.; Willingham, S. B.; Ting, J. P.; Re, F., Cutting edge: inflammasome activation by alum and alum's adjuvant effect are mediated by NLRP3. *J Immunol* 2008, *181* (1), 17-21.
15. Kool, M.; Petrilli, V.; De Smedt, T.; Rolaz, A.; Hammad, H.; van Nimwegen, M.; Bergen, I. M.; Castillo, R.; Lambrecht, B. N.; Tschopp, J., Cutting edge: alum adjuvant stimulates inflammatory dendritic cells through activation of the NALP3 inflammasome. *J Immunol* 2008, *181* (6), 3755-9.
16. Kool, M.; Fierens, K.; Lambrecht, B. N., Alum adjuvant: some of the tricks of the oldest adjuvant. *J Med Microbiol* 2012, *61* (Pt 7), 927-34.
17. Franchi, L.; Nunez, G., The Nlrp3 inflammasome is critical for aluminium hydroxide-mediated IL-1beta secretion but dispensable for adjuvant activity. *Eur J Immunol* 2008, *38* (8), 2085-9.
18. Guven, E.; Duus, K.; Laursen, I.; Hojrup, P.; Houen, G., Aluminum hydroxide adjuvant differentially activates the three complement pathways with major involvement of the alternative pathway. *PLoS One* 2013, *8* (9), e74445.

19. Marichal, T.; Ohata, K.; Bedoret, D.; Mesnil, C.; Sabatel, C.; Kobiyama, K.; Lekeux, P.; Coban, C.; Akira, S.; Ishii, K. J.; Bureau, F.; Desmet, C. J., DNA released from dying host cells mediates aluminum adjuvant activity. *Nat Med* 2011, *17* (8), 996-1002.

20. McKee, A. S.; Burchill, M. A.; Munks, M. W.; Jin, L.; Kappler, J. W.; Friedman, R. S.; Jacobelli, J.; Marrack, P., Host DNA released in response to aluminum adjuvant enhances MHC class II-mediated antigen presentation and prolongs CD4 T-cell interactions with dendritic cells. *Proc Natl Acad Sci U S A* 2013, *110* (12), E1122-31.

21. Eisenbarth, S. C.; Colegio, O. R.; O'Connor, W.; Sutterwala, F. S.; Flavell, R. A., Crucial role for the Nalp3 inflammasome in the immunostimulatory properties of aluminium adjuvants. *Nature* 2008, *453* (7198), 1122-6.

22. Rossi, M.; Young, J. W., Human dendritic cells: potent antigen-presenting cells at the crossroads of innate and adaptive immunity. *J Immunol* 2005, *175* (3), 1373-81.

23. Rivera, A.; Siracusa, M. C.; Yap, G. S.; Gause, W. C., Innate cell communication kick-starts pathogen-specific immunity. *Nat Immunol* 2016, *17* (4), 356-63.

24. Jakubzick, C. V.; Randolph, G. J.; Henson, P. M., Monocyte differentiation and antigen-presenting functions. *Nat Rev Immunol* 2017, *17* (6), 349-362.

25. Elkord, E.; Williams, P. E.; Kynaston, H.; Rowbottom, A. W., Human monocyte isolation methods influence cytokine production from in vitro generated dendritic cells. *Immunology* 2005, *114* (2), 204-12.

26. Meiring, H. D.; Soethout, E. C.; Poelen, M. C.; Mooibroek, D.; Hoogerbrugge, R.; Timmermans, H.; Boog, C. J.; Heck, A. J.; de Jong, A. P.; van Els, C. A., Stable isotope tagging of epitopes: a highly selective strategy for the identification of major histocompatibility complex class I-associated peptides induced upon viral infection. *Mol Cell Proteomics* 2006, *5* (5), 902-13.

27. Meiring, H. D.; van der Heeft, E.; ten Hove, G. J.; de Jong, A. P. J. M., Nanoscale LC-MS(n) : technical design and applications to peptide and protein analysis. *Journal of Separation Science* 2002, *25* (9), 557-568.

28. Moruz, L.; Pichler, P.; Stranzl, T.; Mechtler, K.; Kall, L., Optimized nonlinear gradients for reversed-phase liquid chromatography in shotgun proteomics. *Anal Chem* 2013, *85* (16), 7777-85.

29. Szklarczyk, D.; Franceschini, A.; Wyder, S.; Forslund, K.; Heller, D.; Huerta-Cepas, J.; Simonovic, M.; Roth, A.; Santos, A.; Tsafou, K. P.; Kuhn, M.; Bork, P.; Jensen, L. J.; von Mering, C., STRING v10: protein-protein interaction networks, integrated over the tree of life. *Nucleic Acids Res* 2015, *43* (Database issue), D447-52.

30. Vizcaino, J. A.; Csordas, A.; Del-Toro, N.; Dianes, J. A.; Griss, J.; Lavidas, I.; Mayer, G.; Perez-Riverol, Y.; Reisinger, F.; Ternent, T.; Xu, Q. W.; Wang, R.; Hermjakob, H., 2016 update of the PRIDE database and its related tools. *Nucleic Acids Res* 2016, *44* (22), 11033.

31. Wright, S. D.; Ramos, R. A.; Tobias, P. S.; Ulevitch, R. J.; Mathison, J. C., CD14, a receptor for complexes of lipopolysaccharide (LPS) and LPS binding protein. *Science* 1990, *249* (4975), 1431-3.

32. Holzinger, D.; Jorns, C.; Stertz, S.; Boisson-Dupuis, S.; Thimme, R.; Weidmann, M.; Casanova, J. L.; Haller, O.; Kochs, G., Induction of MxA gene expression by influenza A virus requires type I or type III interferon signaling. *J Virol* 2007, *81* (14), 7776-85.

33. Pletneva, L. M.; Haller, O.; Porter, D. D.; Prince, G. A.; Blanco, J. C., Induction of type I interferons and interferon-inducible Mx genes during respiratory syncytial virus infection and reinfection in cotton rats. *J Gen Virol* 2008, *89* (Pt 1), 261-70.

34. Simon, A.; Fah, J.; Haller, O.; Staeheli, P., Interferon-regulated Mx genes are not responsive to interleukin-1, tumor necrosis factor, and other cytokines. *J Virol* 1991, *65* (2), 968-71.

35. Dubois Cauwelaert, N.; Desbien, A. L.; Hudson, T. E.; Pine, S. O.; Reed, S. G.; Coler, R. N.; Orr, M. T., The TLR4 Agonist Vaccine Adjuvant, GLA-SE, Requires Canonical and Atypical Mechanisms of Action for TH1 Induction. *PLoS One* 2016, *11* (1), e0146372.

36. O'Garra, A., Cytokines induce the development of functionally heterogeneous T helper cell subsets. *Immunity* 1998, *8* (3), 275-83.

37. Antoniou, A. N.; Blackwood, S. L.; Mazzeo, D.; Watts, C., Control of antigen presentation by a single protease cleavage site. *Immunity* 2000, *12* (4), 391-8.

38. Wolk, K.; Grutz, G.; Witte, K.; Volk, H. D.; Sabat, R., The expression of legumain, an asparaginyl endopeptidase that controls antigen processing, is reduced in endotoxin-tolerant monocytes. *Genes Immun* 2005, *6* (5), 452-6.
39. Manoury, B.; Hewitt, E. W.; Morrice, N.; Dando, P. M.; Barrett, A. J.; Watts, C., An asparaginyl endopeptidase processes a microbial antigen for class II MHC presentation. *Nature* 1998, *396* (6712), 695-9.
40. Tulone, C.; Sponaas, A. M.; Raiber, E. A.; Tabor, A. B.; Langhorne, J.; Chain, B. M., Differential requirement for cathepsin D for processing of the full length and C-terminal fragment of the malaria antigen MSP1. *PLoS One* 2011, *6* (10), e24886.
41. Keskinen, P.; Ronni, T.; Matikainen, S.; Lehtonen, A.; Julkunen, I., Regulation of HLA class I and II expression by interferons and influenza A virus in human peripheral blood mononuclear cells. *Immunology* 1997, *91* (3), 421-9.
42. Korpelainen, E. I.; Gamble, J. R.; Smith, W. B.; Dottore, M.; Vadas, M. A.; Lopez, A. F., Interferon-gamma upregulates interleukin-3 (IL-3) receptor expression in human endothelial cells and synergizes with IL-3 in stimulating major histocompatibility complex class II expression and cytokine production. *Blood* 1995, *86* (1), 176-82.
43. Honda, K.; Taniguchi, T., IRFs: master regulators of signalling by Toll-like receptors and cytosolic pattern-recognition receptors. *Nat Rev Immunol* 2006, *6* (9), 644-58.
44. Kariko, K.; Ni, H.; Capodici, J.; Lamphier, M.; Weissman, D., mRNA is an endogenous ligand for Toll-like receptor 3. *J Biol Chem* 2004, *279* (13), 12542-50.
45. Cavassani, K. A.; Ishii, M.; Wen, H.; Schaller, M. A.; Lincoln, P. M.; Lukacs, N. W.; Hogaboam, C. M.; Kunkel, S. L., TLR3 is an endogenous sensor of tissue necrosis during acute inflammatory events. *J Exp Med* 2008, *205* (11), 2609-21.
46. Zhang, X.; Mosser, D. M., Macrophage activation by endogenous danger signals. *J Pathol* 2008, *214* (2), 161-78.
47. Ishii, K. J.; Koyama, S.; Nakagawa, A.; Coban, C.; Akira, S., Host innate immune receptors and beyond: making sense of microbial infections. *Cell Host Microbe* 2008, *3* (6), 352-63.
48. Dietrich, N.; Lienenklaus, S.; Weiss, S.; Gekara, N. O., Murine toll-like receptor 2 activation induces type I interferon responses from endolysosomal compartments. *PLoS One* 2010, *5* (4), e10250.
49. Antosz, H.; Osiak, M., NOD1 and NOD2 receptors: integral members of the innate and adaptive immunity system. *Acta Biochim Pol* 2013, *60* (3), 351-60.
50. Shigeoka, A. A.; Kambo, A.; Mathison, J. C.; King, A. J.; Hall, W. F.; da Silva Correia, J.; Ulevitch, R. J.; McKay, D. B., Nod1 and nod2 are expressed in human and murine renal tubular epithelial cells and participate in renal ischemia reperfusion injury. *J Immunol* 2010, *184* (5), 2297-304.
51. Lichtnekert, J.; Vielhauer, V.; Zecher, D.; Kulkarni, O. P.; Clauss, S.; Segerer, S.; Hornung, V.; Mayadas, T. N.; Beutler, B.; Akira, S.; Anders, H. J., Trif is not required for immune complex glomerulonephritis: dying cells activate mesangial cells via Tlr2/Myd88 rather than Tlr3/Trif. *Am J Physiol Renal Physiol* 2009, *296* (4), F867-74.
52. Mori, K.; Yanagita, M.; Hasegawa, S.; Kubota, M.; Yamashita, M.; Yamada, S.; Kitamura, M.; Murakami, S., Necrosis-induced TLR3 Activation Promotes TLR2 Expression in Gingival Cells. *J Dent Res* 2015, *94* (8), 1149-57.
53. Scheibner, K. A.; Lutz, M. A.; Boodoo, S.; Fenton, M. J.; Powell, J. D.; Horton, M. R., Hyaluronan fragments act as an endogenous danger signal by engaging TLR2. *J Immunol* 2006, *177* (2), 1272-81.
54. Yu, L.; Wang, L.; Chen, S., Endogenous toll-like receptor ligands and their biological significance. *J Cell Mol Med* 2010, *14* (11), 2592-603.
55. Suresh, M. V.; Thomas, B.; Machado-Aranda, D.; Dolgachev, V. A.; Kumar Ramakrishnan, S.; Talarico, N.; Cavassani, K.; Sherman, M. A.; Hemmila, M. R.; Kunkel, S. L.; Walter, N. G.; Hogaboam, C. M.; Raghavendran, K., Double-Stranded RNA Interacts With Toll-Like Receptor 3 in Driving the Acute Inflammatory Response Following Lung Contusion. *Crit Care Med* 2016, *44* (11), e1054-e1066.
56. Becker, C. E.; O'Neill, L. A., Inflammasomes in inflammatory disorders: the role of TLRs and their interactions with NLRs. *Semin Immunopathol* 2007, *29* (3), 239-48.
57. Grishman, E. K.; White, P. C.; Savani, R. C., Toll-like receptors, the NLRP3 inflammasome, and interleukin-1beta in the development and progression of type 1 diabetes. *Pediatr Res* 2012, *71* (6), 626-32.

58. Rauch, I.; Muller, M.; Decker, T., The regulation of inflammation by interferons and their STATs. *JAKSTAT* 2013, *2* (1), e23820.

59. Asokan, R.; Hua, J.; Young, K. A.; Gould, H. J.; Hannan, J. P.; Kraus, D. M.; Szakonyi, G.; Grundy, G. J.; Chen, X. S.; Crow, M. K.; Holers, V. M., Characterization of human complement receptor type 2 (CR2/CD21) as a receptor for IFN-alpha: a potential role in systemic lupus erythematosus. *J Immunol* 2006, *177* (1), 383-94.

60. Hervas-Stubbs, S.; Perez-Gracia, J. L.; Rouzaut, A.; Sanmamed, M. F.; Le Bon, A.; Melero, I., Direct effects of type I interferons on cells of the immune system. *Clin Cancer Res* 2011, *17* (9), 2619-27.

61. Netea, M. G.; Joosten, L. A.; Latz, E.; Mills, K. H.; Natoli, G.; Stunnenberg, H. G.; O'Neill, L. A.; Xavier, R. J., Trained immunity: A program of innate immune memory in health and disease. *Science* 2016, *352* (6284), aaf1098.

62. Szomolanyi-Tsuda, E.; Liang, X.; Welsh, R. M.; Kurt-Jones, E. A.; Finberg, R. W., Role for TLR2 in NK cell-mediated control of murine cytomegalovirus in vivo. *J Virol* 2006, *80* (9), 4286-91.

63. Siegal, F. P.; Kadowaki, N.; Shodell, M.; Fitzgerald-Bocarsly, P. A.; Shah, K.; Ho, S.; Antonenko, S.; Liu, Y. J., The nature of the principal type 1 interferon-producing cells in human blood. *Science* 1999, *284* (5421), 1835-7.

64. Joffre, O.; Nolte, M. A.; Sporri, R.; Reis e Sousa, C., Inflammatory signals in dendritic cell activation and the induction of adaptive immunity. *Immunol Rev* 2009, *227* (1), 234-47.

65. Longhi, M. P.; Trumpfheller, C.; Idoyaga, J.; Caskey, M.; Matos, I.; Kluger, C.; Salazar, A. M.; Colonna, M.; Steinman, R. M., Dendritic cells require a systemic type I interferon response to mature and induce CD4+ Th1 immunity with poly IC as adjuvant. *J Exp Med* 2009, *206* (7), 1589-602.

66. Coro, E. S.; Chang, W. L.; Baumgarth, N., Type I IFN receptor signals directly stimulate local B cells early following influenza virus infection. *J Immunol* 2006, *176* (7), 4343-51.

67. Lemberg, M. K.; Bland, F. A.; Weihofen, A.; Braud, V. M.; Martoglio, B., Intramembrane proteolysis of signal peptides: an essential step in the generation of HLA-E epitopes. *J Immunol* 2001, *167* (11), 6441-6.

68. Dillon, S. B.; Demuth, S. G.; Schneider, M. A.; Weston, C. B.; Jones, C. S.; Young, J. F.; Scott, M.; Bhatnaghar, P. K.; LoCastro, S.; Hanna, N., Induction of protective class I MHC-restricted CTL in mice by a recombinant influenza vaccine in aluminium hydroxide adjuvant. *Vaccine* 1992, *10* (5), 309-18.

69. Hogenesch, H., Mechanism of immunopotentiation and safety of aluminum adjuvants. *Front Immunol* 2012, *3*, 406.

70. MacLeod, M. K.; McKee, A. S.; David, A.; Wang, J.; Mason, R.; Kappler, J. W.; Marrack, P., Vaccine adjuvants aluminum and monophosphoryl lipid A provide distinct signals to generate protective cytotoxic memory CD8 T cells. *Proc Natl Acad Sci U S A* 2011, *108* (19), 7914-9.

71. Lindblad, E. B., Aluminium compounds for use in vaccines. *Immunol Cell Biol* 2004, *82* (5), 497-505.

72. Braud, V. M.; Allan, D. S.; O'Callaghan, C. A.; Soderstrom, K.; D'Andrea, A.; Ogg, G. S.; Lazetic, S.; Young, N. T.; Bell, J. I.; Phillips, J. H.; Lanier, L. L.; McMichael, A. J., HLA-E binds to natural killer cell receptors CD94/NKG2A, B and C. *Nature* 1998, *391* (6669), 795-9.

73. Brooks, A. G.; Borrego, F.; Posch, P. E.; Patamawenu, A.; Scorzelli, C. J.; Ulbrecht, M.; Weiss, E. H.; Coligan, J. E., Specific recognition of HLA-E, but not classical, HLA class I molecules by soluble CD94/NKG2A and NK cells. *J Immunol* 1999, *162* (1), 305-13.

74. Sun, H.; Pollock, K. G.; Brewer, J. M., Analysis of the role of vaccine adjuvants in modulating dendritic cell activation and antigen presentation in vitro. *Vaccine* 2003, *21* (9-10), 849-55.

75. Zheng, Y.; Manzotti, C. N.; Liu, M.; Burke, F.; Mead, K. I.; Sansom, D. M., CD86 and CD80 differentially modulate the suppressive function of human regulatory T cells. *J Immunol* 2004, *172* (5), 2778-84.

76. Lang, T. J.; Nguyen, P.; Peach, R.; Gause, W. C.; Via, C. S., In vivo CD86 blockade inhibits CD4+ T cell activation, whereas CD80 blockade potentiates CD8+ T cell activation and CTL effector function. *J Immunol* 2002, *168* (8), 3786-92.

77. Odobasic, D.; Leech, M. T.; Xue, J. R.; Holdsworth, S. R., Distinct in vivo roles of CD80 and CD86 in the effector T-cell responses inducing antigen-induced arthritis. *Immunology* 2008, *124* (4), 503-13.

78. Guo, H.; Callaway, J. B.; Ting, J. P., Inflammasomes: mechanism of action, role in disease, and therapeutics. *Nat Med* 2015, *21* (7), 677-87.

79. Ghonime, M. G.; Shamaa, O. R.; Das, S.; Eldomany, R. A.; Fernandes-Alnemri, T.; Alnemri, E. S.; Gavrilin, M. A.; Wewers, M. D., Inflammasome priming by lipopolysaccharide is dependent upon ERK signaling and proteasome function. *J Immunol* 2014, *192* (8), 3881-8.

80. Cullen, S. P.; Kearney, C. J.; Clancy, D. M.; Martin, S. J., Diverse Activators of the NLRP3 Inflammasome Promote IL-1beta Secretion by Triggering Necrosis. *Cell Rep* 2015, *11* (10), 1535-48.

81. Chanput, W.; Mes, J. J.; Wichers, H. J., THP-1 cell line: an in vitro cell model for immune modulation approach. *Int Immunopharmacol* 2014, *23* (1), 37-45.

82. Bosshart, H.; Heinzelmann, M., THP-1 cells as a model for human monocytes. *Ann Transl Med* 2016, *4* (21), 438.

83. Fishelson, Z.; Attali, G.; Mevorach, D., Complement and apoptosis. *Mol Immunol* 2001, *38* (2-3), 207-19.

84. Mosca, F.; Tritto, E.; Muzzi, A.; Monaci, E.; Bagnoli, F.; Iavarone, C.; O'Hagan, D.; Rappuoli, R.; De Gregorio, E., Molecular and cellular signatures of human vaccine adjuvants. *Proc Natl Acad Sci U S A* 2008, *105* (30), 10501-6.

Legends to the Supplementary data

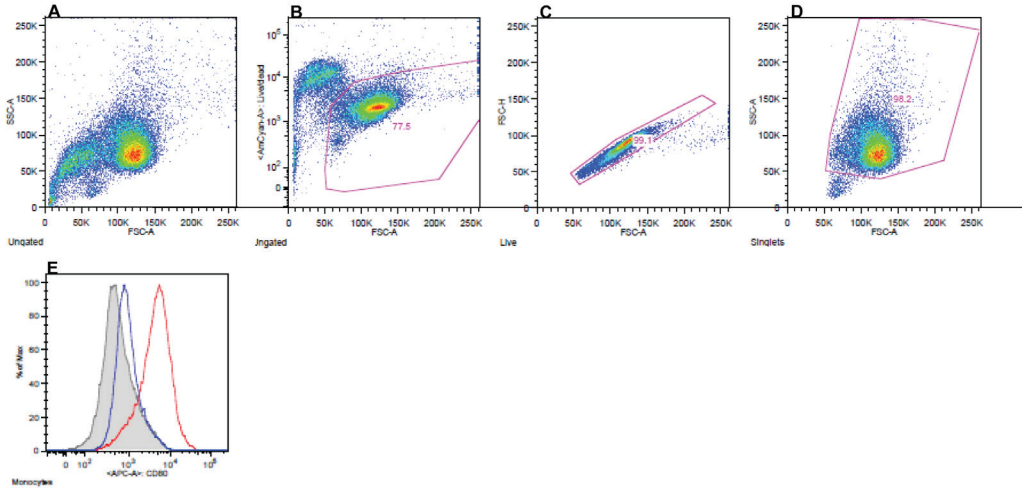

Supplementary S1. *Gating staining strategy used for the monocytes.*
S1A: all cells without any gating. S1B: gating set around the live cells. S1C: the single-stained cells within the gate of the live cells. S1D: CD14⁺ monocytes within the gate of the single stained cells. S1E: the histogram of a single representative donor for CD80 after 24 hours of stimulation. In these histograms the grey-filled line represents the medium-stimulated monocytes, whereas the red line represents the LPS-stimulated monocytes and the blue line the $Al(OH)_3$-stimulated (10 µg/ml) monocytes.

Supplementary S2. *All measured genes on the qPCR array except for controls.*

Pattern Recognition Receptors (PPRs) and signaling	Cytokines: and chemokines	Cytokine and chemokine receptors	Surface markers	Transcription factors	Complement system	Antigen presentation	Others
DDX58	CCL2	CCR4	CD4	FoxP3	C3	HLA-A	ACTβ
NLRP3	CCL5	CCR5	CD8A	GATA3	CASP1	HLA-E	APCS
NOD1	CSF2	CCR6	CD14	IRF3	MBL2	β2M	CD40LG
NOD2	IL-1α	CCR8	CD40	IRF7			CRP
TLR1	IL-1β	CXCR3	CD80	NFκB1			FASLG
TLR2	IL-2	IL1R1	CD86	NFκB1A			GAPDH
TLR3	IL-4	IFNαR1		TBX21			HPRT1
TLR4	IL-5	IFNγR1					ICAM1
TLR5	IL-6						ITGAM
TLR6	IL-8						JAK2
TLR7	IL-10						LYZ
TLR8	IL-13						MAPK1
TLR9	IL-17A						MAPK8
MYD88	IL-18						MPO
IRAK1	IL-23A						MX1
TICAM	IFNα1						RAG1
LY96	IFNβ1						RORC
	IFNγ						RPLP0
	TNF						STAT1
	CXCL8						STAT3
	CXCL10						STAT4
	SLC11A1						STAT6
							TRAF6
							TYK2

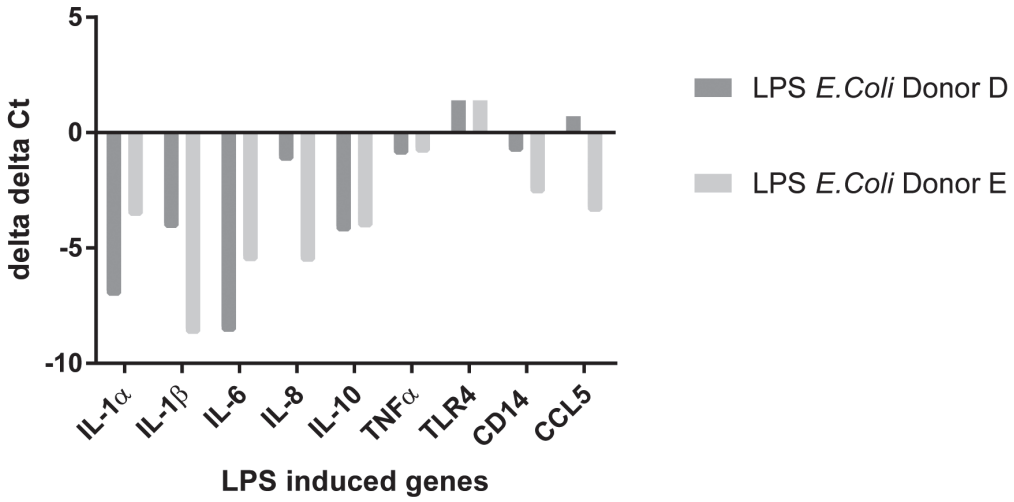

Supplementary S3. *LPS-related genes.*
The gene expression of known LPS-related genes is depicted for two biological replicates with each two technical replicates upon LPS stimulation (100 ng/ml). The graph depicts the delta delta Ct values of those replicates, in which the delta delta Ct value is inversely proportional to the gene regulation.

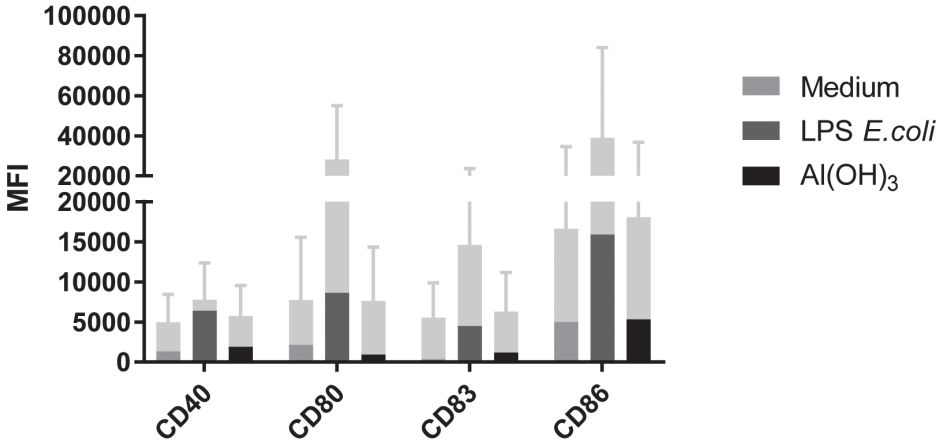

Supplementary S4. *Cell surface marker expression of stimulated iMDDCs.*
Cell surface marker expression values obtained by flow cytometric analysis are depicted by the mean fluorescent intensities (MFI and SD). The intensities and error bars depict the mean relative intensity and the standard deviation of 5 biological replicates. The lower dark-colored part of each bar represents the MFI corrected for the autofluorescence.

Supplementary S5. ***qPCR raw data table.***
Ct Values and delta delta Ct values for a given donor and stimulation condition ($Al(OH)_3$) or LPS, 10 µg/ml and 100 ng/ml, respectively) after 24 hours of stimulation. For $Al(OH)_3$ five biological replicates are depicted, with one of these donors (donor F) analyzed with three technical replicates. For LPS two biological replicates are depicted, each with two technical replicates.

Supplementary S6. ***LC-MS/MS raw data table.***
The worksheet 'Raw' contains all raw data combined for all three donors, empty cells indicate that a protein was not detected for a given condition. All values are LOG transformed. The worksheet 'Normalized' contains all data median normalized, LOG(2) transformed and pooled on Uniprot entry. The worksheets 'Donor C' (three technical replicates) and 'Donor A' and 'Donor B' contain all the raw data per donor and technical replicate extracted from proteome discoverer 2.1.

Supplementary S7. ***Proteins regulated by $Al(OH)_3$.***
Regulation factors for all proteins affected by $Al(OH)_3$ stimulation (10 µg/ml) after both 24 and 48 hours. These values are the median-normalized expression values of the three biological replicates and the GO clustering after 24 and 48 hours is depicted. The gene code represents the Uniprot geneID and the values represent the normalized expression values of the proteins. Proteins of the three biological replicates were median-normalized; the proteins depicted in this table are at least regulated by a factor of 1.5 in two out of three donors. This table includes the grouping used to create the heatmap in Figure 2.

Supplementary S8. ***Enriched GO terms in the upregulated protein set after 24 hours of $Al(OH)_3$ stimulation.***
The GO terms represented by the upregulated proteins after 24 hours of $Al(OH)_3$ (10 µg/ml) are depicted. The table represents the GO_ID of the enriched processes in the set of upregulated proteins after 24 hours of $Al(OH)_3$ stimulation. The table represents the term, the number of proteins identified and the FDR of the process enrichment.

Supplementary S9. ***Enriched GO terms in the upregulated set after 48 hours of $Al(OH)_3$ stimulation.***
The GO terms represented by the upregulated proteins after 48 hours of $Al(OH)_3$ (10 µg/ml) are depicted. The table represents the GO_ID of the enriched processes in the set of upregulated proteins after 48 hours of $Al(OH)_3$ stimulation. The table represents the term, the number of proteins identified and the FDR of the process enrichment.

Supplementary S10. ***Enriched GO terms in the downregulated set after 48 hours of $Al(OH)_3$ stimulation.***

The GO terms represented by the downregulated proteins after 48 hours of $Al(OH)_3$ (10 µg/ml) are depicted. The table represents the GO_ID of the enriched processes in the set of downregulated proteins after 48 hours of $Al(OH)_3$ stimulation. The table represents the term, the number of proteins identified in the dataset and the FDR of the process enrichment.

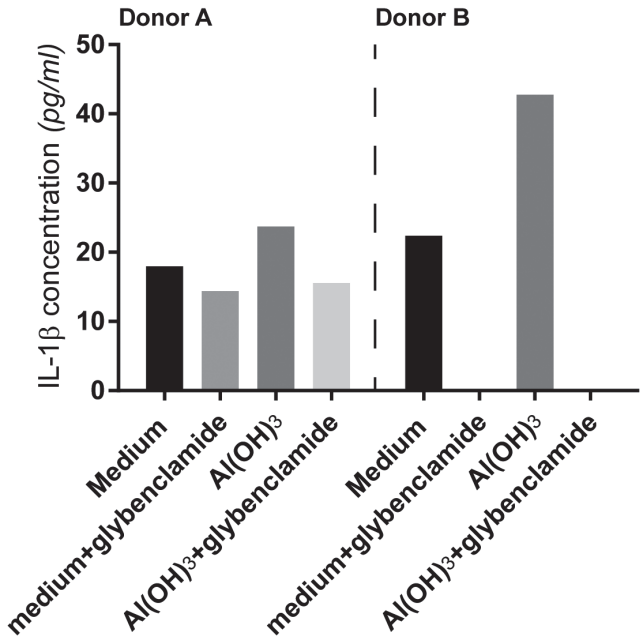

Supplementary S11. ***IL-1β secretion in primary human monocytes.***

The IL-1β secretion of two biological replicas is depicted in 1 donor on which a blocking experiment was performed (donor A) and in the other donor without blocking experiment (donor B) in which 'medium' represents the control stimulation, 'medium + glybenclamide' represents the control cells with the inflammasome blocker glybenclamide (25 µg/ml), 'Al(OH)$_3$' represents cells stimulated with 10 µg/ml Al(OH)$_3$ and 'Al(OH)$_3$ + glybenclamide' represent the Al(OH)$_3$-stimulated cells in the presence of 25 µg/ml glybenclamide.

Supplementary S12. ***Raw IL-1β ELISA data.***

Measured IL-1β concentrations in pg/ml for the three individual stimulation experiments (biological replicates) with at least two technical replicates after stimulation with 50 µg/ml $Al(OH)_3$ in THP-1 cells.

	medium	*medium +PMA*	*medium +PMA +block*	*$Al(OH)_3$*	*$Al(OH)_3$+ PMA+block*
IL-1β (pg/ml)	0,00	0,00	0,00	9,31	2,79
IL-1β (pg/ml)	0,00	0,63	0,04	9,36	2,75
IL-1β (pg/ml)	0,00	0,04	0,39	8,47	3,01
IL-1β (pg/ml)	0,83	0,62	0,62	9,91	2,27
IL-1β (pg/ml)	0,70	0,43	1,53	9,65	3,91
IL-1β (pg/ml)	0,40	0,39	2,35	19,86	9,84
IL-1β (pg/ml)	0,00	0,39	2,29	24,81	10,01

Chapter 3

Vaccine antigens modulate the innate response of monocytes to $Al(OH)_3$

Sietske Kooijman[1,2], Jolanda Brummelman[3,#a], Cécile A.C.M. van Els[3], Fabio Marino[2,4,#b], Albert J.R. Heck[2,4], Elly van Riet[1], Bernard Metz[1], Gideon F.A. Kersten[1,6], Jeroen L.A. Pennings[5], Hugo D. Meiring[1*]

1 Intravacc, Bilthoven, The Netherlands
2 Biomolecular Mass Spectrometry and Proteomics, Bijvoet Center for Biomolecular Research and Utrecht Institute for Pharmaceutical Sciences, Science Faculty, Utrecht University, The Netherlands
3 Centre for Infectious Disease Control, National Institute for Public Health and the Environment, Bilthoven, The Netherlands
4 Netherlands Proteomics Centre, Utrecht, The Netherlands
5 Centre for Health Protection, National Institute for Public Health and the Environment, Bilthoven, The Netherlands
6 Leiden Academic Centre for Drug Research, Leiden University, Leiden, The Netherlands
#a Current address: Humanitas Clinical and Research Center, Rozzano, Italy
#b Current address: Centre Hospitalier Universitaire Vaudois, Switzerland

Published as: Sietske Kooijman, Jolanda Brummelman, Cécile A.C.M. van Els, Fabio Marino, Albert J.R. Heck, Elly van Riet, Bernard Metz, Gideon F.A. Kersten, Jeroen L.A. Pennings, Hugo D. Meiring. Vaccine antigens modulate the innate response of monocytes to $Al(OH)_3$.
PLoS ONE 13 (5): e0197885. https://doi.org/10.1371/journal.pone.0197885

Abstract

Aluminum-based adjuvants have widely been used in human vaccines since 1926. In the absence of antigens, aluminum-based adjuvants can initiate the inflammatory preparedness of innate cells, yet the impact of antigens on this response has not been investigated so far. In this study, we address the modulating effect of vaccine antigens on the monocyte-derived innate response by comparing processes initiated by $Al(OH)_3$ and by Infanrix, an $Al(OH)_3$-adjuvanted trivalent combination vaccine (DTaP), containing diphtheria toxoid (D), tetanus toxoid (T) and acellular pertussis (aP) vaccine antigens. A systems-wide analysis of stimulated monocytes was performed in which full proteome analysis was combined with targeted transcriptome analysis and cytokine analysis. This comprehensive study revealed four major differences in the monocyte response, between plain $Al(OH)_3$ and DTaP stimulation conditions: (I) DTaP increased the anti-inflammatory cytokine IL-10, whereas $Al(OH)_3$ did not; (II) $Al(OH)_3$ increased the gene expression of *IFNγ*, *IL-2* and *IL-17a* in contrast to the limited induction or even downregulation by DTaP; (III) increased expression of type I interferons-induced proteins was not observed upon DTaP stimulation, but was observed upon $Al(OH)_3$ stimulation; (IV) opposing regulation of protein localization pathways was observed for $Al(OH)_3$ and DTaP stimulation, related to the induction of exocytosis by $Al(OH)_3$ alone. This study highlights that vaccine antigens can antagonize $Al(OH)_3$-induced programming of the innate immune responses at the monocyte level.

Introduction

In 1926, the adjuvant features of colloidal aluminum salts were discovered by observing that diphtheria toxoid adsorbed to aluminum induced a significantly higher antibody titer against the toxoid than the antigen alone[1]. Since the discovery of their adjuvant activity, aluminum salts have been widely used as vaccine adjuvants in human vaccines. For a long time the mechanism of action of aluminum adjuvants was largely unknown. Based on the observation that aluminum salt-adsorbed toxoids were cleared more slowly from the injection site than non-adsorbed toxoids[1], it was hypothesized that antigen-aluminum salts act as a depot at the site of injection, causing a slow antigen release. However, in guinea pig experiments, the immune response was not compromised when the salt deposit was removed from the injection site[2-3], indicating that this is at least not the only mechanism by which Al(OH)$_3$ affects the immune response towards antigens. Other modes of action suggested for the adjuvant effect of Al(OH)$_3$ include early innate mechanisms such as differentiation of monocytes to antigen-presenting dendritic cells[4], triggering and recognition of Danger Associated Molecular Patterns (DAMPs)[5-7] promoting T-helper (Th) 2 differentiation[4, 8], recruitment of immune cells to the site of injection[9-10], inflammasome activation[7, 11-12], complement activation[13], increasing antigen presentation via HLA class I and II[14], enhanced phagocytosis[15].

Most of the previous studies analyzed the effect of Al(OH)$_3$ with either Al(OH)$_3$[4, 14, 16] alone or in combination with a model antigen like ovalbumin or alpha casein[7-8, 11, 15]. Since antigens may have a distinct effect on innate immune cells, the question arises to what extent particular antigens skew the innate effects of the adjuvant.

DTaP vaccine was implemented for active immunization against diphtheria, tetanus and pertussis in infants and children. Besides diphtheria toxoid and tetanus toxoid, DTaP comprises *Bordetella pertussis*-derived filamentous hemagglutinin, pertussis toxoid and pertactin P.69 antigens. DTaP vaccination typically induces a Th2-biased and regulatory T cell response[15, 17-18] not optimally conferring long-term protective immunity to pertussis. For vaccine development it is important to understand whether antigens affect the innate phase of the immune response or the instructions of the adaptive response of the adjuvant, or both.

In this study, we compared the innate immune responses induced by Al(OH)$_3$ alone *versus* that of a licensed combination DTaP vaccine containing Al(OH)$_3$, using cytokine analysis, transcriptomics and proteomics, to determine unique, shared and potential synergistic or antagonistic effects of adjuvant and antigen components. Primary human monocytes were used as the main innate cell platform since these are prominent mononuclear phagocytes in the blood and play, when activated, an important role in bridging the innate and adaptive immune response in tissue[19-20]. Besides this, their known differentiation into monocyte-derived dendritic cells (MoDCs) monocyte can also enforce their antigen presenting role to T cells in response to various stimuli[21]. This systems-based approach results in a comprehensive insight in the molecular pathways involved in innate immune activation of monocytes upon stimulation with Al(OH)$_3$-based vaccines.

Materials and methods

Ethics statement

This study was conducted according to the principles expressed in the Declaration of Helsinki. Written informed consent was obtained from all blood donors before collection and use of their samples. All blood samples were processed anonymously. All blood donations, provided by the Dutch National Institute for Public Health and the Environment (RIVM, Bilthoven; The Netherlands), were specifically given for primary cell isolation, a research goal explicitly approved by the accredited Medical Research Ethics Committee (MREC), METC, Noord-Holland in The Netherlands.

Materials used for cell stimulation

Aluminum hydroxide ($Al(OH)_3$) Alhydrogel 2%, Brenntag (Frederikssund; Denmark) was used as the adjuvant. The registered DTaP vaccine Infanrix was obtained from GlaxoSmithKline (Brentford; Middlesex; UK). The vaccine contains combined antigens, *i.e.* a minimum of 30 international units (I.U.) diphtheria toxoid, a minimum of 40 I.U. tetanus toxoid, 25 μg filamentous hemagglutinin (FHA), 25 μg pertussis toxoid, and 8 μg pertactin P.69 (PRN), all absorbed to 0.5 mg of $Al(OH)_3$ per dose. LPS from *E.coli* K12 (Invivogen; San Diego; California; USA) was used as positive control. Non-adsorbed *Bordetella pertussis* antigens PRN and Pertussis toxin (PTx) were obtained from Biotrend (Cologne; Germany) and FHA was purchased from Sigma Aldrich (Darmstadt; Germany).

Monocyte isolation and stimulation

Blood from 5 healthy adult donors was used for Peripheral blood mononuclear cell (PBMC) isolation and subsequent monocyte isolation. PBMCs were obtained by density gradient centrifugation on Lymphoprep (Nycomed; Zurich; Switzerland) at 1,000*x*g for 30 minutes. Subsequently, monocytes were isolated from the obtained PBMC fraction using anti-CD14 MACS beads in combination with MACS (Miltenyi Biotech; Bergisch Gladbach; Germany). A purity check of the monocytes was performed by flow cytometric analysis of CD14 cell surface expression and only if the purity of the monocyte population was ≥95% the cells were used for proteome and transcriptome analysis.

The isolated monocytes, 600,000 cells/well were cultured in a 24-wells plate (Corning; Corning; New York; USA) in 1.5 ml of RPMI (Gibco/Thermo Fisher; Waltham; Massachusetts; USA) containing 10% Fetal Calf Serum (FSC) (Hyclone), 100 units/ml of penicillin (Gibco) 100 units/ml streptomycin (Gibco) and 2.92 mg/ml L-glutamin (Gibco) (culture medium). Monocytes were either left unstimulated or were stimulated with a final concentration of 0.1 μg/ml LPS, 10 μg/ml $Al(OH)_3$ or DTaP containing a final concentration of 10 μg/ml $Al(OH)_3$ per stimulation condition per donor. After 24 and 48 hours of stimulation, culture supernatants were collected for cytokine assays and monocytes were harvested for targeted transcriptome and whole proteome analysis. For both proteomics and gene expression analysis, the material of three individual donors was available. LPS was used as a positive control for the cell culture and only when LPS performed as expected, by inducing CD80, as described previously[16] (S1 Fig), the samples were used.

Culture and stimulation of THP-1 cells

A human monocytic cell line THP-1 (ATCC; Teddington; Middlesex; U.K.), was used to verify pathways or leads identified in primary monocytes, *i.e.* Inflammasome activation and IL-10 secretion.

THP-1 cells were cultured according to the supplier's protocol. To investigate the IL-1β secretion induced by Al(OH)$_3$ or DTaP, the cells were primed with 300 ng/ml phorbol 12-myristate (PMA) (Sigma-Aldrich; Darmstadt, Germany) for 24 hours. After 24 hours of priming, the cells were placed in culture medium without PMA for 24 hours[16]. The medium was refreshed again and cells were either left unstimulated or stimulated with 50 µg/ml DTaP or the same concentration of Al(OH)$_3$ (based on a dose response curve in THP-1 cells), in the presence or absence of 25 µg/ml of an inflammasome blocker (Glybenclamide) (Invivogen; San Diego; California; USA) for 48 hours.

For determination of the IL-10-inducing component, THP-1 cells were stimulated with 50 or 100 µg/ml Al(OH)$_3$ alone or the same concentrations of Al(OH)$_3$ in DTaP or with PTx (0.165 µg/ml to 5.28 µg/ml), FHA (0.165 µg/ml to 5.28 µg/ml), PRN (0.05 µg/ml to 1.6 µg/ml) alone all in a twofold dilution series. The concentration range used was based on the concentrations of the individual antigens in the complete vaccine. Synergy in a complete vaccine cannot be excluded; therefore the concentration range started just below the lowest vaccine dose used in THP-1 cell stimulations. The DTaP stimulations contained 0.33 or 0.66 µg/ml of PTx or 0.33 or 0.66 µg/ml of FHA or 0.2 or 0.4 µg/ml of PRN, respectively. Cells were stimulated for 48 hours. Supernatants were analyzed for the presence of IL-10 by ELISA.

mRNA Expression analysis

mRNA Isolation from monocytes (from three different donors) was performed using the RNeasy mini kit (Qiagen; Venlo; The Netherlands), according to the manufacturer's animal cell spin protocol. RNA purity and concentration was determined using spectrophotometric analysis of the 260-nm and 280-nm absorbance, on the NanoDrop 2000 (Thermo Fisher; Waltham MA; USA). cDNA synthesis of 12 ng of RNA was performed using the RT cDNA synthesis kit and the RT preAMP pathway primer mix innate and adaptive immunity (both from Qiagen; Venlo; The Netherlands); cDNA was frozen at -20°C. qPCR measurements were performed using the Roche Light Cycler 96 (Roche; Basel; Switzerland) and the innate and adaptive immune response RT^2 profiler arrays (Qiagen; Venlo; The Netherlands), comprising 89 functional genes and 7 controls. A melt curve determination was included in the measurement for quality control[16].

Gene expression of each donor was normalized to the three most stable house-keeping genes ACTB, HPRT1 and RPLP0. After normalization, the fold-change was determined, meaning normalized gene expression ($2^{-}\Delta^{Ct}$) in the test sample divided by the normalized gene expression ($2^{-}\Delta^{Ct}$) in the control sample. Fold change values greater than one indicates an up-regulation of 2^1 or more. Fold-change values less than one indicate down-regulation. Genes were considered regulated when they differed a factor 2 or more from the control in two out of three donors, based on the SD between technical replicates of 0.13*x*Ct values, corresponding to a coefficient of variation (CV) of 9.4% (S1 Table). This means that a two-fold change in gene expression more than three times exceeds the CV and is a meaningful difference.

Protein isolation, digestion and labeling

To isolate the proteins from the monocytes (from 3 three different donors) the cells were incubated with 500 µl of 4 M guanidine·HCl in phosphate buffer, pH 7.5, at 4°C for two hours. During incubation, the cells were subjected to a freeze-thaw step. After the cell lysis, 50 µl of the lysate of each sample was used to determine the protein concentration using the BCA protein assay (Pierce Biotechnology; Waltham; Massachusetts; USA), according to the manufacturer's protocol. The remaining lysed cells were stored at -80°C.

To reduce the guanidine·HCl concentration, protein samples were diluted four times with 100 mM phosphate buffer pH 7.5. Subsequently, the proteins were digested with Lys-C (Roche) in an enzyme-to-substrate ratio of 1:10 (w/w) at 37°C. After 4 hours, fresh Lys-C was added in a 1:10 (w/w) enzyme-to-substrate ratio for an overnight incubation.

Normalization on protein content was performed on aliquots of the digested protein samples from the 6 conditions (medium, $Al(OH)_3$ and DTaP all at 24 and 48 hours) per individual donor. The samples were labeled per condition on solid phase extraction (SPE) columns (Waters; Milford; MA; USA) using tandem mass tag labeling-6plex (TMT(6), Thermo Fisher). The SPE columns were equilibrated as described by the manufacturer. Columns were washed with 100 mM phosphate buffer pH 7.5.

The digested samples were loaded onto individual SPE columns per condition, using a vacuum manifold (Waters), after which samples were washed with 100 mM phosphate buffer pH 7.5. The labeling reagent (TMT(6)) was reconstituted in acetonitrile (AcN) according to the supplier's protocol (0.8 mg per individual label in 41 µl AcN), after which the AcN concentration was reduced to a maximum of 2.5% (v/v) with 100 mM phosphate buffer pH 7.5. The individual TMT(6) labels were loaded onto the 6 individual SPE columns leaving 0.5 ml reagent on top of the column for a 30 minute incubation. After 30 minutes, fresh label was added for another 30 minutes of incubation subsequently, the columns were washed with water containing 0.5% formic acid (FA). The individual stimulation conditions per donor were eluted from the column with 90% Acetonitrile (AcN) containing 0.5% formic acid (FA), were pooled and then dried by centrifugation under reduced pressure and reconstituted in Trifluoroacetic acid (0.1%TFA).

Peptide fractionation by SCX

To purify and fractionate the labeled monocyte-derived digested protein samples, Strong Cation eXchange (SCX) was used as described previously[22]. The system comprised an in-house made Hypercarb trapping column (200 µm I.D. x 5 mm length, 7 µm particle size) and an in-house made SCX column (200 µm I.D. x 11 cm length PolySULFOETHYL Aspartamide, 5 µm, PolyLC). Elution was 12 min at 100% solvent A (water + 0.5% HOAc) followed by a 16.5 minute linear gradient to 100% solvent B (250 mM KCl + 35% AcN+ 0.5% HOAc in water) and a second linear gradient of 16.5 min to 100% solvent C (500 mM KCl + 35% AcN+ 0.5% HOAc in water). Twenty-six SCX fractions were obtained and of each 4 µL was subjected to nanoscale LC-MS analysis.

LC-MS/MS analysis

Peptide separation of the individual SCX fractions was performed on a Proxeon Easy-nLC 1000 system (Thermo Scientific; San Jose; CA; USA). Peptides were trapped on

a double-fritted trapping column Reprosil (Dr. Maisch; Ammerbuch; Germany) C18; df=3 µm, 2 cm length × 100 µm I.D., made in-house and separated on an in-house-packed analytical column Poroshell (Agilent; Waldbron; Germany) 120 EC-C18; df=2.7 µm, 50 cm length × 50 µm I.D.), at a column temperature of 40°C. Solvent A was MilliQ water containing 0.1% FA and solvent B was 0.1% FA in AcN (Biosolve). The peptides were separated in 133 minutes (10 minutes at 2% B, from 2% to 30% B in 118 minutes and 5 minutes at 70% B) in a non-linear gradient optimized as described by Morus *et al*.[23]. After 133 minutes, the system was kept at 5% B for 15 minutes to equilibrate the column for the next injection. The column effluent was electro-sprayed directly into the MS using a gold-coated fused silica tapered tip of 5 µm, at a spray voltage of 1.8 kV.

Mass spectrometric data were acquired on a Tribrid-Orbitrap Fusion (Thermo Fisher Scientific; San Jose; CA; USA). The full scan (MS^1) spectra were acquired with a scan mass range of *m/z* 350-1500 at 120,000 resolution (FWHM) with an Orbitrap readout. For the MS^1 the maximum injection time was 50 ms and the automatic gain control (AGC) was set to 200,000. Top speed mode was chosen with a duration of 3 s where precursor ions with an intensity >5,000 were selected for fragmentation (MS^2). For MS^2 charge states between 1 and 7 were selected. MS^2 was performed using Collision-Induced Dissociation (CID) in the linear ion trap (LTQ) with a normalized collision energy of 35%. In MS^2 the AGC was set to 10,000 and the maximum injection time was 35 ms. Synchronous-Precursor-Selection (SPS) was used to include up to 10 MS^2 fragment ions in MS^3. These fragment ions were further fragmented by Higher energy Collision Dissociation (HCD) with a normalized collision energy of 50%. The TMT reporter ions were analyzed in the Orbitrap with a maximum injection time of 120 ms, and an AGC of 100,000.

Proteomics data were analyzed with Proteome Discoverer 1.4, (Thermo Fisher Scientific; San Jose; CA; USA). Default settings were used, unless stated otherwise. Precursor mass tolerance was set to 5 ppm. MS^2 scans were searched, with the Sequest HT search engine and a full enzyme specificity for Lys-C, against the human Uniprot database from November 2014, containing 23,048 entries. *b*-Type ions and *y*-type ions were enabled for CID and HCD data using a fragment mass tolerance of 0.5 Da. The quantification node was used to obtain relative expression values, where TMT(6) was defined as the quantification method, with an integration tolerance of 0.2 Da. Percolator was used to filter the peptide to spectrum mass with a false discovery rate (FDR) of <5%. The data was searched with Aspargine deamidation and Methionine oxidation as dynamic modifications and TMT(6) was set as a static modification on the N-termini and Lysine residues.

The results of the separate SCX fractions were integrated in the data analysis for each individual donor. When multiple entries occurred, based on Uniprot and NCBI data for the same protein, the ratios as provided by Proteome Discoverer were Log2-transformed and these entries were averaged for further analysis. Next, data were normalized by performing a median correction. Data of three individual donors were compared: proteins that were upregulated or downregulated by 1.5-fold or more compared to control in at least two out of three biological replicates were considered regulated. The fold change of 1.5 was based upon being 3 times the median coefficient of variation (CV) of the technical variation, which corresponds to a p-value of < 0.01. The regulated proteins were imported in STRING (string.embl.de)[24] and Protein Center to iden-

tify enriched pathways (FDR<0.1), within functional annotations provided by Gene Ontology (GO) biological processes and Kyoto Encyclopedia of Genes and Genomes (KEGG) using the following String settings: medium confidence and the interactions sources: experiments, co- expression, co-occurrence and database.

Venn diagrams were created using http://bioinfogp.cnb.csic.es/tools/venny/ with the regulated proteins for each condition and time point incorporated.

Protein network was created using Cytoscape based on the enriched pathways in each up or downregulated protein set. String network analysis of the gene expression data was performed.

Cytokine ELISA

In the supernatants of THP-1 cultures, IL-1β was determined by using the Human IL-1 beta/IL-1F2 DuoSet ELISA (R&D systems; McKinley; Minneapolis; USA) and IL-10 by human IL-10 ELISA Ready set go (Affymetrix; eBiosciences; San Diego; CA; USA), both according to the manufacturer's protocol. Samples were measured on a Synergy MX (Biotek; Winooski; Vermont; USA). ELISA data were analyzed with Graphpad Prism®. Significance of difference between stimulation conditions was determined using multiple T-tests one per row with the FDR approach with the two-stage linear setup procedure of Benjamini, Q=5%.

Results

DTaP, like Al(OH)$_3$, induces differentiation of monocytes

To first assess whether primary monocytes show characteristics of activation and differentiation when stimulated with the Al(OH)$_3$-adjunvanted vaccine DTaP or with Al(OH)$_3$ alone, the expression of known cell surface markers was surveyed selectively with targeted transcriptome analysis and unbiased by mass spectrometry-based proteomics. Al(OH)$_3$ increased the expression of activation markers, at the protein level[16]. The activation marker TFRC (*i.e.* CD71, after 48 hours) was increased at least two-fold in both Al(OH)$_3$ and DTaP-stimulated monocytes (Fig 1, Table 1). Another protein indicating an active function of the monocytes, CD44 (involved in the adhesion of leukocytes), was significantly upregulated in DTaP-stimulated cells, after 48 hours. In addition, the gene expression of the costimulatory marker *CD80* was induced by DTaP also when compared to plain Al(OH)$_3$, after 24 hours of stimulation[16] (Fig 2).

The expression of the monocyte differentiation antigen CD14[25-26], was downregulated after 48 hours of Al(OH)$_3$ stimulation[16]. This was also the case in response to the Al(OH)$_3$-containing vaccine DTaP after 48 hours of stimulation (Fig 1, Table 1). The loss of CD14 indicates that both DTaP-stimulated monocytes and Al(OH)$_3$-stimulated monocytes differentiate away from a monocytic cell type.

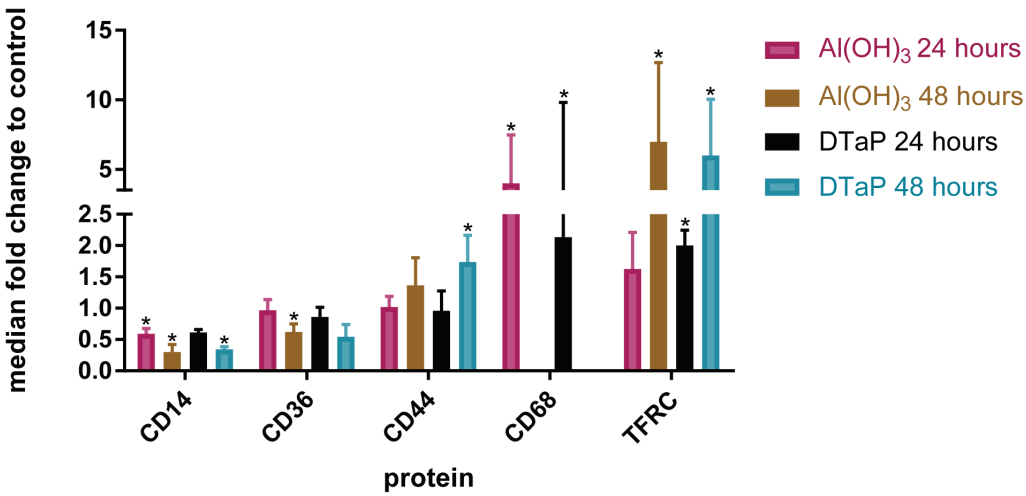

Figure 1: Expression profiles of cell surface proteins of stimulated monocytes as determined by mass spectrometry.

*Fold changes (average and range) of the expression at the protein level of indicated cell surface markers by monocytes under the indicated stimulation conditions. Both contain 10 µg of Al(OH)$_3$. The absence of a bar means that this marker was quantified not more than once for this stimulation condition. Significance of difference compared to control were determined with a student t-test with Bonferroni set up p-values <0.05 are depicted with an *.*

Table 1. ***Proteins involved in the processes described and their median fold changes after 24 and 48 hours of stimulation of three donors.***

Protein	*Fold changes*			
	DTAP stimulation		*$Al(OH)_3$ stimulation*	
	24 hours	*48 hours*	*24 hours*	*48 hours*
HLA-A	*0.85*	1.95	*1.04*	2.47
HLA-E	1.84	N.D.	1.75	N.D.
HSP90AA1	*1.16*	*1.29*	1.60	*1.31*
Minor histocompatibility antigen H13	*1.06*	1.68	N.D.	2.01
Full-length cDNA clone CS0DI002YH20 of Placenta of Homo sapiens (human) Legumain	*1.43*	1.75	2.09	1.83
Cathepsin B	*1.27*	1.95	*1.39*	*0.99*
Cathepsin D	2.11	2.50	2.73	2.16
Cathepsin L1	2.95	2.48	4.66	2.29
Cathepsin S	*1.11*	1.73	*1.14*	1.78
CD9 antigen	N.D.	1.4	1.28	1.61
Monocyte differentiation antigen CD14, urinary form CD14*	*0.69*	*0.44*	*0.68*	*0.44*
Macrosialin	2.12	N.D.	3.13	N.D.
CD71 (TFRC)	2.00	4.96	1.70	5.75
MX1	*1.07*	1.99	1.50	1.64
MX2	*1.00*	*1.32*	*1.23*	1.90
IFI30	1.61	*1.39*	2.33	*1.4*
IFIT2	*1.03*	*1.44*	N.D.	*1.44*
IFIT3	*1.05*	2.13	1.64	2.62
IL3RA	1.73	1.55	2.22	1.61
IFNγR1	*1.03*	*1.29*	1.90	3.08
IRF5	*1.06*	1.73	*1.15*	*1.21*
C4	*0.78*	2.31	1.82	1.65
C5aR	1.57	2.19	*1.48*	2.10
C8a	1.75	*0.95*	1.87	*1.48*

* CD14 was only identified in one donor twice.

N.D. there were no quantitative data at this time point.

Median fold change of three biological replicates of monocytes: a fold change ≥1.5 compared to medium-stimulated monocytes was considered significant. Non-significant genes are depicted in *italic*.

Quantitative proteomics reveals distinct protein expression and pathway enrichments in monocytes induced by DTaP compared to Al(OH)$_3$

Quantitative proteomics of Al(OH)$_3$ and DTaP-stimulated monocytes resulted in the identification of 4,000 unique proteins of which 3,000 proteins were relatively quantified. 650 Proteins were regulated as a result of one of the stimulation conditions compared to unstimulated control (Figs 3A and 3B, S2 Table). Proteins were clustered in GO terms and KEGG pathways and the differences in these terms and pathways between the stimulations and control were identified with a pathway overrepresentation analysis (S3 Table). It was previously observed that after 24 hours of stimulation with Al(OH)$_3$, several immunological relevant GO terms were overrepresented[16]. In addition, localization processes were also enriched[16]. Also processes requiring localization such as, *vesicle mediated transport* and *exocytosis* were enriched (Fig 3C, S3 Table). After 48 hours of Al(OH)$_3$ stimulation, the immune system-related pathways were still enriched, as were the localization processes and the processes requiring localization, *e.g. secretion by cell* and *exocytosis*. The inflammatory response was downregulated after 48 hours of Al(OH)$_3$ stimulation[16] (Table 2, Fig 3C, S3 Table).

In contrast, upon 24 hours of DTaP stimulation (adjuvanted with Al(OH)$_3$) no immune response-related GO terms were overrepresented (Table 2, S3 Table). Amongst the 4 KEGG pathways identified, one immune system-related KEGG pathway was found: *activation of complement* and *coagulation pathway*s (S3 Table). *Endocytosis* was overrepresented in both the up and downregulated protein set (Table 2, Figs 3C and 3D, S3 Table). The downregulated protein set overrepresented *localization pathways* (Table 2, Fig 3C, S3 Table). After 48 hours of DTaP stimulation, the upregulated processes also included multiple immune system-related processes, *e.g. antigen processing and presentation* and *interferon induced signaling* and *exocytosis* (Table 2, Figs 3C and 3E, S3 Table). Interestingly, the GO-annotated term *positive regulation/activation of immune system processes* was downregulated after 48 hours of DTaP stimulation (Tabel 2 and S3 Table).

These data reveal several differences in the processes induced by plain Al(OH)$_3$ or the Al(OH)$_3$ containing vaccine DTaP: early activation of the antigen processing and presentation pathways after Al(OH)$_3$ stimulation, with a delayed response upon DTaP stimulation. Furthermore, DTaP did not induce processes requiring localization, *e.g.* exocytosis after 24 hours of stimulation and less strong, compared to Al(OH)$_3$ after 48 hours of stimulation. Finally, re-localization processes were also found to be differentially activated upon stimulation with Al(OH)$_3$ (upregulated) or DTaP (downregulated) (S3 Table). Thus, the antigens in a vaccine alter the processes activated, in a cell, by the adjuvant.

DTaP is a stronger activator of the inflammasome than Al(OH)$_3$ alone

Part of the adjuvant effect of Al(OH)$_3$ is often assigned to activation of the inflammasome[11-12, 16]. To determine if the presence of antigens influences this inflammasome activation, transcriptome analysis and an IL-1β ELISA were performed. As was observed previously for stimulation with Al(OH)$_3$ alone[16], DTaP stimulation also induced gene expression of the inflammasome-related genes, in particular *IL1R1*. Moreover, DTaP induced the expression of *CASP1* and a trend towards upregulation in *MyD88* expression (Fig 2, S1 Table).

Table 2. *Overview of enriched processes identified by quantitative proteomics extracted from S3 Table.*

DTaP up 24 hrs	*DTaP up 48 hrs*	*DTaP down 24 hrs*	*DTaP down 48 hrs*	*Al(OH)$_3$ up 24 hrs*	*Al(OH)$_3$ up 48 hrs*	*Al(OH)$_3$ down 24 hrs*	*Al(OH)$_3$ down 48 hrs*
Endocytosis	Endocytosis	Endocytosis	Coagulation	Lysosome	Lysosme	None	Inflammatory response
Complement and coagulation cascades	Defense response	Cell activation	Localization	Immune system process	Immune system process		Defense response
	Antigen processing and presentation	Regulation of T cell activation	Response to stress	Antigen processing and presentation	Antigen processing and presentation		Response to stress
	Exocytosis	Platelet activation	Exocytosis	Exocytosis	Exocytosis		
	Immune response	Transport	Positive regulation/ activation of immune system process	Transport	Transport		
	Cell proliferation	Localization		Localization	Localization		
	Cytokine-mediated signaling pathway			Metabolic processes	Metabolic pathways		
	Autophagy			Catabolic processes	Regulation of cell death		
	Translation			Complement and coagulation cascades	Vesicle-mediated transport		
	Interferon-gamma-mediated signaling pathway			Valine, leucine and isoleucine biosynthesis			

To verify if the enhanced activation after DTaP stimulation resulted in an increased secretion of IL-1β, the presence of IL-1β was measured in culture supernatants of stimulated and PMA-primed THP-1 cells. Medium and medium with PMA do not differ significantly in the induction of IL-1β both with and without blockage, indicating that the prime with PMA does not induce IL-1β secretion[16]. DTaP, however, significantly enhanced the secretion of IL-1β compared to plain Al(OH)$_3$ (Fig 4, S4 Table)[16], supporting the transcriptomics data. Subsequently, the role of the inflammasome activation in IL-1β secretion was investigated by adding the inflammasome blocker Glybenclamide during stimulation of the cells. DTaP-induced secretion of IL-1β was dependent on the inflammasome, since 60% of the secretion was inhibited when the inflammasome was blocked (Fig 4), which is less than the inhibition of 80% found in Al(OH)$_3$-stimulated cells (Fig 4).

The loss of IL-1β secretion upon inflammasome blockage implies that DTaP, like Al(OH)$_3$ depends on the inflammasome for the induction of IL-1β. The substantially higher levels of IL-1β induced by DTaP indicate that the antigens in the vaccine significantly contribute to IL-1β secretion.

Al(OH)$_3$ and DTaP induce different chemokine-related genes

Al(OH)$_3$ induces a Th2 polarization[16, 27]. Additionally, the presence of Th1-related and inflammatory cytokines (*IL-2*, *IL-17A* and *IFNγ*) was observed[16] (S1 Table, schematically depicted in Fig 2). DTaP stimulation also induced the Th2 polarization. Increased gene expression of *IL-4* (in one donor with a trend towards upregulation in another donor) and of *IL-5* was found. These expression levels of IL-4 and IL-5 were lower (factor 10 and 2, respectively) than the levels induced by plain Al(OH)$_3$ (Fig 2). In addition, DTaP also induced the gene expression of *IL-8* and the anti-inflammatory cytokine *IL-10*. IL-10 represses the formation of IL-2, IL-17A and IFNγ. Transcripts for *IL-2* were a 12-fold less regulated in DTaP-stimulated cells compared to Al(OH)$_3$ stimulated cells, while *IL-17A* was even downregulated in DTaP-stimulated monocytes (Fig 2, S1 Table). Expression of *IFNγ* was increased by DTaP stimulation. The gene expression of *CCL2* and *CCL5 w*as induced by DTaP stimulation as was the gene expression of *CCR6* and *CXCR3*.

The data show that Al(OH)$_3$ and DTaP differentially regulated the expression of genes involved in the innate immune response. Thus, antigens qualitatively alter the innate immune response induced by Al(OH)$_3$ at the level of gene expression towards a less pro-inflammatory profile represented by a decrease in IL-2 and IL-17A gene expression (compared to Al(OH)$_3$) and an increase in IL-10 gene expression.

IL-10 is mainly induced by FHA

Next, we investigated whether the difference in *IL-10* gene transcription also resulted in increased levels of the IL-10 protein. For this we stimulated PMA-primed THP-1 cells as a monocyte model and IL-10 was measured in the culture supernatant. To identify the antigen responsible for the induction of IL-10, THP-1 cells were stimulated with DTaP, with single antigens of *Bordetella pertussis* that are present in the vaccine, FHA, PTx or PRN, a combination of these antigens without Al(OH)$_3$ or with plain Al(OH)$_3$ for 48 hours. In accordance with the transcriptome data, DTaP induced the secretion of IL-10, whereas plain Al(OH)$_3$ did not. In addition, the combination of antigens without Al(OH)$_3$ also enhanced the secretion of the anti-inflammatory cytokine IL-10. FHA

Function	gene name	DTaP	$Al(OH)_3$
HLA I	HLA-A	5.84	3.17
	HLA-E	2.52	1.18
IFN signaling	DDX58	5.95	3.30
	IRAK1	4.31	6.65
	MX1	3.85	3.59
	STAT1	3.66	3.19
	IFNG	3.45	2.43
	TICAM1	2.82	2.72
	IFNAR1	2.72	1.28
	IRF7	2.47	1.75
	ICAM1	2.47	1.10
	IFNGR1	2.24	1.02
	IL10	2.09	1.23
	IFNA1	0.97	0.35
Inflammatory	CCL2	10.15	2.98
	STAT3	4.15	2.74
	IL2	3.45	42.32
	IL23A	3.12	1.91
	MPO	2.96	3.19
	IL8	2.58	1.32
	CCL5	2.78	1.20
	STAT6	2.20	2.35
	IL5	2.00	4.07
	IL4	1.30	11.42
	CSF2	0.78	0.35
	RORC	0.73	8.71
	IL17A	0.09	7.03
	IL13	0.04	0.35
	MBL2	0.04	0.72
Inflammasome	C3	8.36	2.57
	IL1R1	3.17	2.16
	CASP1	3.98	1.62
	IL1A	1.24	0.36
	IL1B	0.93	0.36
	NLRP3	0.58	0.28
TLR signaling	TLR5	4.12	2.27
	TLR8	2.23	1.63
	TLR3	2.21	2.52
	TRAF6	1.83	2.37
	TLR7	1.63	2.26
chemokine receptors	CCR6	5.29	3.82
	CXCR3	2.61	0.34
	CCR4	1.10	0.16
	CCR8	0.41	18.94
transcription factors	GATA3	3.28	2.93
	NFKB1	3.31	2.48
	TBX21	2.27	1.61
cell surface marker-related	CD80	3.69	1.59
	CD14	0.61	0.21
	CD40LG	0.19	0.25
MAP kinases	MAPK8	2.26	2.09
	MAPK1	2.07	1.31
remaining	RAG1	2.05	2.59
	LYZ	0.49	0.45
	LY96	0.36	0.20
	CRP	0.15	0.37
	APCS	0.12	0.02

←

Figure 2. ***Gene expression after 24 h of stimulation of monocytes.***
Regulated genes in monocytes (at least a factor 2 up or down) are depicted after 24 hours of $Al(OH)_3$ or DTaP stimulation. The median fold change from the 3 donors is depicted. The genes are clustered in a heatmap based on their molecular function.

→

Figure 3. ***Venn diagram and protein network analysis of regulated proteins.***
Venn diagrams indicate numbers of sharing and upregulated (A) and downregulated (B) proteins in DTaP versus $Al(OH)_3$ adjuvant-stimulated monocytes after 24 hours and 48 hours. Purple represents $Al(OH)_3$ 24 hours, yellow represents DTaP 24 hours, green represents $Al(OH)_3$ 48 hours and red represents DTaP 48 hours. All proteins depicted in these Venn diagrams were regulated by a factor of at least 1.5 in at least two out of three donors. Up and downregulated proteins, identified per stimulation condition and per time point by mass spectrometric analysis, were assessed based on Gene Ontology biological process enrichment (GO terms). An overview of the main enriched pathways is depicted in a protein network (C). The yellow circles represent the stimulation conditions, the purple squares represent the processes. Green lines from a condition towards a process represent downregulated pathways. Red lines from a condition towards a process represent an enrichment of these processes in the upregulated protein sets. The width of the line represents the significance of the enrichment factor: the thicker the line the more significantly enriched the process; the thinnest lines represent a p-value <0.05, the medium lines represent a p-value <0.01 and the thickest lines represent a p-value <0.001. The black arrows connect daughter terms with the mother term.

*All terms are at least enriched with a False Discovery Rate p value of <0.05. Bar graphs of the number of proteins found to be regulated upon the stimulation conditions after 24 hours (D) and 48 hours (E), in which red represents that process was enriched in the upregulated proteins set and green represents that the process is enriched in the downregulated protein set. The * depicts the significantly regulated pathways.*

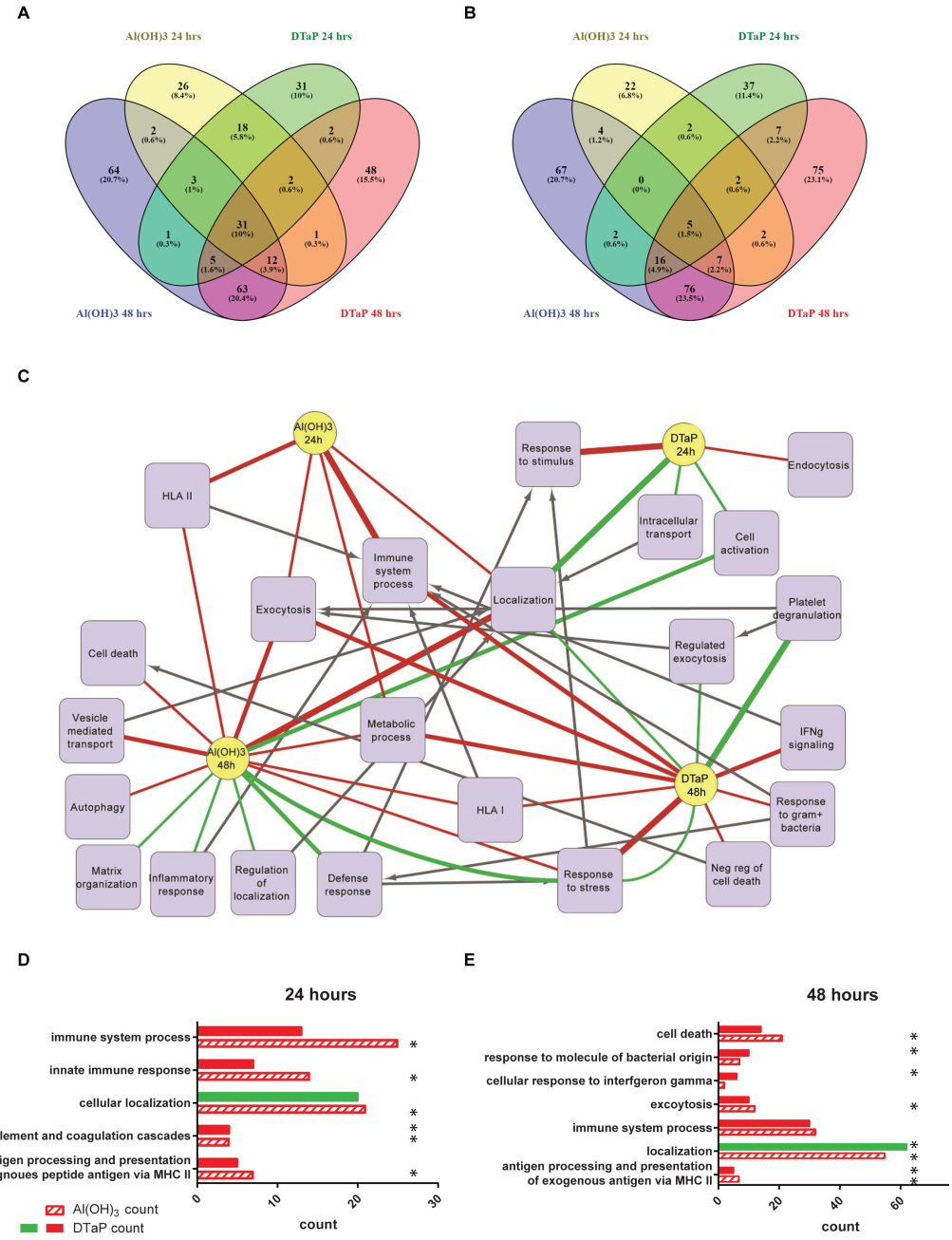

was the only individual antigen that induced significant amounts of IL-10 (Fig 5, S5 Table); PRN and PTx contributed marginally.

DTaP induces type I interferons and IFNγ, but downstream signaling is stronger in monocytes stimulated with plain $Al(OH)_3$

After 24 hours of stimulation, both $Al(OH)_3$ and DTaP-stimulated monocytes showed a trend towards increased gene expression of the type I interferon *IFNβ*. We showed before that $Al(OH)_3$ significantly induced proteins downstream of IFNβ[16]. The expressions of two antiviral proteins MX1 and IFIT3, that are specifically induced by type I interferons[28-33], were significantly lower in DTaP-stimulated monocytes compared to the expression in $Al(OH)_3$-stimulated monocytes (p-value≤ 0.05) (Fig 6). After 24 hours, DTaP specifically induced gene expression of the receptor for IFNβ, *IFNαR1*.

After 48 hours, gene expression levels of all IFN-related genes were reduced to levels lower than naïve cells in both DTaP and $Al(OH)_3$-stimulated cells (Table 3). However, proteins downstream of IFNβ were still upregulated: MX1 and IFIT3 in both stimulation conditions and MX2 specifically in $Al(OH)_3$-stimulated monocytes (a factor 1.44 stronger compared to DTaP). DTaP specifically induced IRF5, a transcription factor of type I interferons, a 1.43-fold stronger compared to $Al(OH)_3$ (Fig 6, Table 1). Although both proteins were not significantly regulated compared to the other stimulation condition a clear trend was observed.

With respect to type 2 interferons, *IFNγ* gene expression was induced by $Al(OH)_3$, as was the expression of the downstream proteins IFI30 and IFNγR1[16]. DTaP stimulation also induced the gene expression of IFNγ, however, unlike $Al(OH)_3$, DTaP did not induce the expression of IFNγ-induced proteins (Table 1). The protein expression of *IFNγR1* was more than a 1.5-fold lower and the expression IFI30 was a 1.48-fold lower in DTaP-stimulated monocytes compared to the effect of $Al(OH)_3$ (Table 1, extracted from S2 Table). In addition, after 24 hours, DTaP specifically induced the gene expression of *IFNγR1* in monocytes (Fig 2).

These data provide evidence that $Al(OH)_3$ alone as well as formulated in DTaP induce *IFNβ* and *IFNγ* gene expression. However, downstream signaling is impacted by the antigens in DTaP, since this downstream signaling was not evident for IFNβ after 24 hours of DTaP stimulation, while this was the case in $Al(OH)_3$-stimulated monocytes.

Table 3. ***Fold changes of interferon-related genes relative to control after 48 hours of stimulation.***

Gene	DTaP fold change 48 hours	$Al(OH)_3$ fold change 48 hours
IFNα	0.47	0.60
IFNαR1	0.76	0.62
IFNβ	0.13	0.11
IFNγ	1.34 (2 times up one time down)	1.42
IFNγR1	0.16	0.15

Data are depicted as an average from three biological replicates.

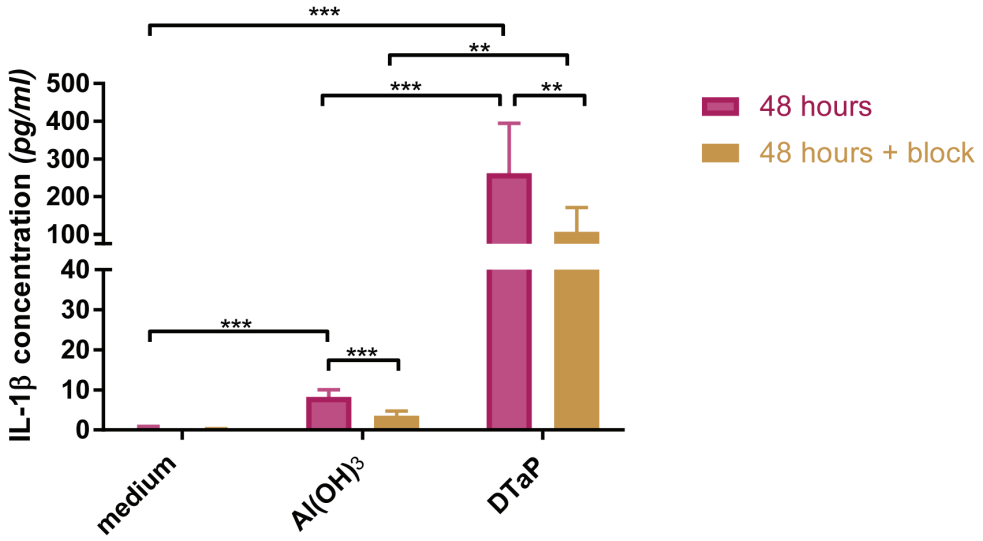

Figure 4: IL-1β secretion profile.
*Concentrations of IL-1β (average and range) present in supernatants of Al(OH)$_3$ or DTaP-stimulated THP-1 cells in the absence or presence of Glybenclamide. Data are from three individual experiments, with two technical replicates. 'Medium +' is the PMA-primed medium. Significant values were identified with a t-test with a two stage setup method of Benjamini. p-Values <0.05 are indicated as * p-values <0.01 are indicated as **, whereas p-values <0.001 are indicated as ***.*

In addition, signaling downstream of IFNγ was induced much stronger in monocytes stimulated by plain Al(OH)$_3$.

Antigens in DTaP do not enhance antigen processing and presentation pathways compared to induction by Al(OH)$_3$

Antigen processing and presentation by HLA class II and HLA class I is crucial for the activation of CD4 helper T-cells and cytotoxic CD8 T-cells, respectively. The process of antigen processing and presentation was enriched after 24 hours of Al(OH)$_3$ stimulation[16]. Notably, this was not the case after 24 hours of DTaP stimulation, determined upon pathway analysis of the upregulated proteins (Fig 3). DTaP induced the protein expression of HLA-E after 24 hours, but not the expression of HSP90, while Al(OH)$_3$ did. The expression of HLA-A and HM13 was enhanced after 48 hours of DTaP stimulation similar to the response induced by Al(OH)$_3$ alone (Table 1, S2 Table). Additionally, as for Al(OH)$_3$ the gene expression of *HLA-A* was increased by DTaP (S2 Table, summarized in Table 1)[16]. Moreover, DTaP induced the gene expression of *HLA-E* after 24 hours of stimulation (Fig 2, S2 Table).

Various proteins related to antigen processing and presentation were increased upon Al(OH)$_3$ stimulation, *i.e.* Cathepsin D, Cathepsin L and Legumain[16]. DTaP also induced the protein expression of Cathepsin D and Cathepsin L, with the latter showing a modest increase in expression as compared to Al(OH)$_3$ (S2 Table summarized in Table 1). Contrary to the Al(OH)$_3$ stimulus, the expression of Legumain, a protease involved in antigen presentation by HLA class II[34-36], was not increased upon DTaP stimulation.

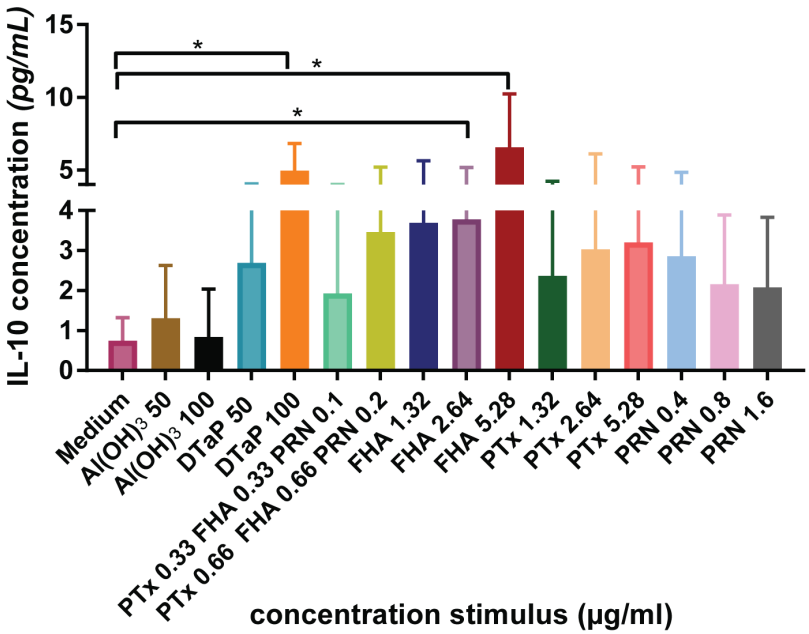

Figure 5. ***IL-10 secretion profile.***
*The concentration (average and range) of IL-10 induced by the indicated stimulation conditions in pg/ml in THP-1 cells. Data are from three individual experiments. Significant values were identified with a t-test with a two stage setup method of Benjamini. p-Values <0.05 are indicated as *.*

After 48 hours, both stimulation conditions increased the protein expression of Cathepsin S (involved in HLA class II antigen presentation) and Legumain, while Cathepsin B was only induced by DTaP, also compared to $Al(OH)_3$. The similar strength in the induction of antigen processing and presentation pathways and associated proteins, indicates that $Al(OH)_3$ adjuvant alone is sufficient to activate antigen processing and presentation pathways and that the antigens in DTaP do not enhance these processes further.

Discussion

Aluminum salts have been used as adjuvants in a wide variety of vaccines and these formulations are known to induce a Th2-biased response. In this study, we investigated the immune skewing of one such vaccine, DTaP, in detail and compared the *in vitro* innate immune response with those initiated by a plain Al(OH)$_3$ stimulus as described in our previous study[16]. Combined proteomics and transcriptomics analysis revealed several similarities between the monocyte responses towards the vaccine and the plain Al(OH)$_3$ adjuvant, like activation of the inflammasome. Flow cytometry analysis could not be used in the presence of an Al(OH)$_3$ suspension because the particles cause a substantial background masking the specific signals. Nevertheless, predominant differences were found with respect to interferon and IL-10 signaling: (*i*) the induction of the anti-inflammatory cytokine IL-10 by DTaP, (*ii*) gene expression of the pro-inflammatory cytokines *IFNγ*, *IL-2* and IL-17A by Al(OH)$_3$, (*iii*) differences in the production of IFN-induced proteins between stimulation conditions and (*iv*) processes involved in re-localization of proteins and macromolecules being induced by Al(OH)$_3$, but down-regulated by DTaP, which could be related to the induction of exocytosis and endocytosis, respectively. However, the implications of this difference for the functional immune response need further investigation.

The unique induction of *IL-2* and *IL-17A* by plain Al(OH)$_3$ and the unique induction of IL-10 by DTaP (annotated as differences (*i*) and (*ii*) in the previous paragraph, respectively) are likely related, since IL-10 inhibits the formation of IL-2, IL-17A and IFNγ[37-43] (Fig 7). Note: IFNγ was equally induced by both stimulation conditions. The induction of IL-10 by DTaP could be attributed to the *B. pertussis* antigens present in

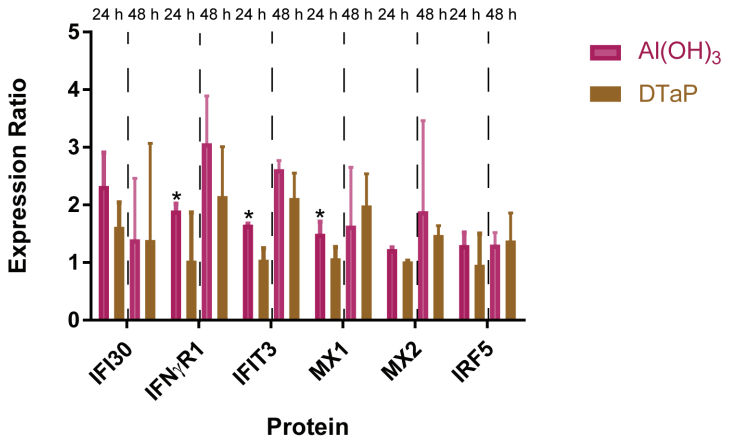

Figure 6. ***Interferon-related protein expression ratios of stimulated monocytes.***
*The protein expression ratios (median and range of three biological replicates) of indicated interferon-related proteins normalized to medium control (1.0) after 24 and 48 hours of Al(OH)$_3$ or DTaP stimulation are depicted. Significance of difference is determined with a t-test with a two stage setup method of Benjamini, p-Values <0.05 are denoted as: * when upregulated compared to the other stimulation condition.*

the vaccine and more specifically to FHA with a minor contribution for PRN; this is in agreement with previously described data[18, 44-46].

IL-2 and IL-17A are important pro-inflammatory cytokines in the protective response towards bacteria and viruses. IL-2 is involved in activating and steering NK cells and is required for T-cell survival[47-49]. IL-17A is a pro-inflammatory cytokine involved in cell trafficking and inflammation and induces in innate immune cells IL-12 secretion, resulting in Th1 polarization[50-51]. IFNγ plays a role in the induction of HLA class II expression on the cell surface and is related to the polarization of a Th1 response partly by the inhibition of a Th2 response[52-55]. By inducing IL-10, the monocyte response to DTaP might have become less inflammatory and less Th1-related. For bacteria, the secretion of anti-inflammatory components, such as the *B. pertussis* antigen FHA, can be very effective in evading the human immune response. To improve current DTaP vaccines it may be relevant to select the antigenic composition not only based on immunogenicity but also on innate immune modulating effects of the antigens.

The third difference, the specific upregulation of IFNβ-induced proteins upon $Al(OH)_3$ stimulation could be related to the induction of IL-10 by DTaP, since IFNβ

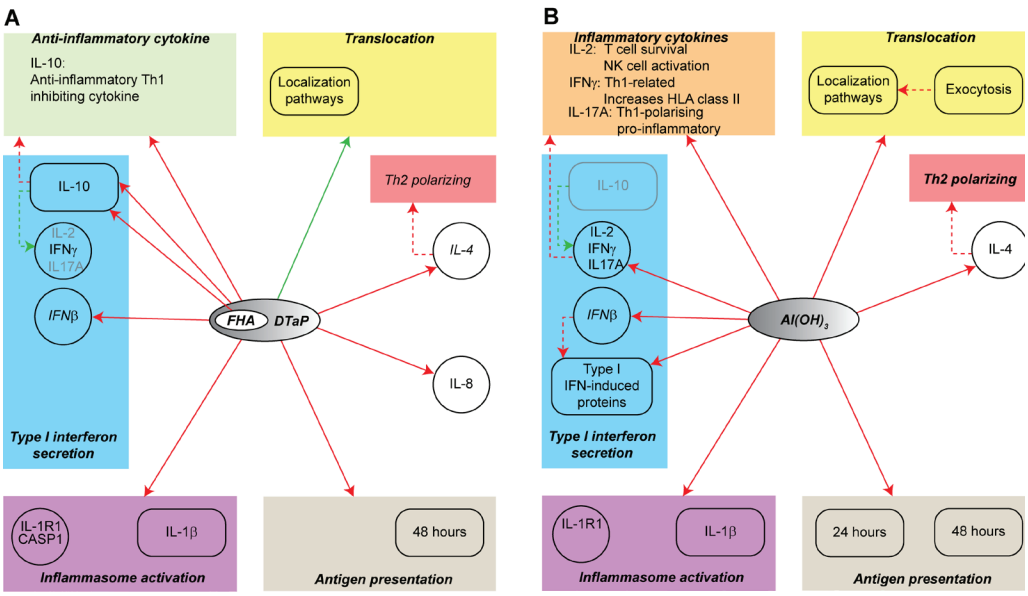

Figure 7. ***Overview of all data.***

The different effects of $Al(OH)_3$ and DTaP stimulation on monocyte functions are summarized. The red arrows from a stimulation DTaP and FHA (A) or $Al(OH)_3$ (B) represent an upregulation, the green arrows represent a down regulation. Red arrows towards a box indicate that the genes/proteins in the box are upregulated. The title in the box represents the process regulated. For interferon secretion, individual arrows indicate if genes or processes are upregulated. The dashed arrows represent connections based on the literature. The circles represent measurements at the gene expression level while the rounded boxes represent measurements at the protein level. The green and orange rectangles represent consequences of an inhibition or activation by one of the stimulations.

can be consumed by monocytes to produce IL-10[56]. This results in an apparently limited upregulation of IFNβ-induced proteins as observed after DTaP stimulation, as well as the increased IL-10 secretion. The proteins downstream of IFNβ are all proteins involved in the defense response against viruses, thus perhaps not functional in the response against the bacterial antigens in the DTaP vaccine. This explains why these are not formed upon DTaP stimulation and provide evidence that the specific response against the antigens of DTaP can antagonize the underlying broad spectrum innate response against the adjuvant.

As described previously, Al(OH)$_3$ stimulation of monocytes induced re-localization processes[16]. In DTaP-stimulated monocytes, these processes were downregulated after 24 hours of stimulation. Processes requiring protein localization include *secretion*, *exocytosis*, *vesicle mediated transport*, *communication* and *signal transduction*[57]. Al(OH)$_3$ did induce processes requiring localization after 24 and 48 hours of stimulation, whereas in DTaP-stimulated monocytes the processes requiring localization were not evident after 24 hours of stimulation. Upon prolonged stimulation, these particular processes were enriched in DTaP stimulated monocytes. However, the enrichment was less strong compared to Al(OH)$_3$-stimulated monocytes, implicating that this could partly explain the differences in localization processes. In contrast to the secretory pathways, DTaP specifically induced the process of endocytosis after 24 hours. Endocytosis plays a role in antigen processing and presentation and cross-presentation[58-59], which is unlikely occur in the cells where no exogenous antigen is present; this is confirmed by the stimulation with plain Al(OH)$_3$ after which we did not observe enhanced endocytosis[16].

Processes induced by both Al(OH)$_3$ and DTaP are activation of the inflammasome and the secretion of IL-1β[16], however, much stronger by DTaP than by Al(OH)$_3$. This implies that the antigens in the vaccine boost the secretion of IL-1β (Fig 7). IL-1β is a cytokine involved in many innate immune system-related processes, *e.g.* the induction of adhesion molecules on the cell surface, being co-stimulatory for T cells and induce Th17 polarization[60-61]. The stronger induction of IL-1β by DTaP most likely results in a stronger co-stimulation for T cells and induction of the adaptive immune response.

Other processes being regulated both by Al(OH)$_3$ and DTaP are the activation of complement and antigen processing and presentation. Al(OH)$_3$ stimulation alone is enough to induce proteins related to antigen processing and presentation by both HLA class I and class II[16]. This induction is not affected further when the complete vaccine is used as a stimulus (Fig 6). This indicates that Al(OH)$_3$ plays a role in antigen processing and presentation previously thought to be related to antigens.

These *in vitro* data show that we indeed find the described Th2 profile often assigned to Al(OH)$_3$ and Al(OH)$_3$-adjuvanted vaccines, like DTaP[8, 62-63]. However, our findings clearly show that the effect of the adjuvant can be influenced significantly by the antigens in the vaccine, since Al(OH)$_3$ induced a mixed Th1/Th2 profile and that the antigens in the vaccine formulation influence this to a great extent. This difference, the mixed response we observe for Al(OH)$_3$ compared to the Th2 response described in literature[27], could be related to responses in mice *versus* human: in mice, Al(OH)$_3$ is specifically a Th2 polarizing adjuvant while in human it induces a more mixed innate response[8, 46-49, 62-63]. These differences between *in vivo* mice data and *in vitro* human data indicate that our model of human monocytes can be important in the translation of *in vivo* mice to human data. However, in this analysis only one cell type was used to determine the induced immune responses, thus we would miss interactions

between different cell types, involved in the immune response. An additional consideration could be that for some proteins their functions are not annotated, thus the link to the pathways they would have been involved in. The comprehensive systems approach allows for the identification of multiple differences in innate pathway activation in monocytes between an adjuvant alone and a complete adjuvanted vaccine. Our results show that antigens can have a profound impact on the adjuvant activity of a vaccine. A possible explanation could be that DTaP contains $Al(OH)_3$ particles with different physicochemical interactions due to inhomogeneous antigen distribution. For example, bare $Al(OH)_3$ particles may exist next to particles with adsorbed antigen, or the different antigens are adsorbed on different particles in case the formulation of the final bulk is done by mixing pre-adsorbed individual antigens. This is unlikely since studies have shown that any inhomogeneous distribution is equilibrated due to rearrangements of the $Al(OH)_3$ primary particles and/or antigen[64]. Most likely, the distinct innate effects between plain $Al(OH)_3$ and an $Al(OH)_3$-adjuvanted vaccine are caused by intrinsic adjuvant actions of some antigens present, *e.g.* the ability of FHA to induce IL-10 as shown here and by others[65]. Our study clearly reveals that the combination of antigen and the adjuvant determine the innate effects caused by a vaccine.

Author contributions

Conceptualization: BM EvR GFAK HDM SK.
Formal analysis: JB JLAP SK.
Funding acquisition: HDM.
Investigation: JB FM SK.
Methodology: BM EvR GFAK HDM JB SK.
Project administration: HDM.
Software: HDM JLAP.
Supervision: AJRH BM CACMvE EvR GFAK HDM.
Validation: JLAP.
Visualisation: JB SK.
Writing-original draft: SK.
Writing-review & editing: AJRH BM CACMvE EvR GFAK HDM JB SK.

Additional information

Competing Interest: The authors have the following competing interest to declare: BM, GFAK, HDM and SK are affiliated with the commercial company, Intravacc. There are no patents, products in development or marketed products to declare. This affiliation does not alter authors' adherence to data sharing policies of PLoSOne. The authors declare no competing financial interest.

Funding statement: SK is funded by a strategic research grant (SOR) of the Ministry of Health and Welfare, The Netherlands (AS200107). The Ministry of Health and Welfare funded the project and the salary of SK but the Ministry did not have any role in the study design, data collection and analysis, decision to publish or preparation of the manuscript. The specific roles of this author is articulated in the 'author contributions' section.

This work was also partly supported by the *Proteins@Work*, a program of the Netherlands Proteomics Centre financed by the Netherlands Organisation for Scientific Research (NWO) as part of the National Roadmap Large-scale Research Facilities of the Netherlands (project number 184.032.201). *Proteins@Work* funded the salary of FM but did not have a role in the study design, data collection and analysis, decision to publish or preparation of the manuscript. The specific roles of this authors are articulated in the 'author contributions' section.

References

1. Glenny, A. T.; Pope, C. G.; Waddington, H.; Wallace, U., Immunological notes. XVII–XXIV. *The Journal of Pathology and Bacteriology* 1926, *29* (1), 31-40.
2. Holt, L. B., *Developments in Diptheria Prophylaxis*. Heinemann: 1950.
3. Hem, S. L., Elimination of aluminum adjuvants. *Vaccine* 2002, *20 Suppl 3*, S40-3.
4. Ulanova, M.; Tarkowski, A.; Hahn-Zoric, M.; Hanson, L. A., The Common vaccine adjuvant aluminum hydroxide up-regulates accessory properties of human monocytes via an interleukin-4-dependent mechanism. *Infect Immun* 2001, *69* (2), 1151-9.
5. McKee, A. S.; Burchill, M. A.; Munks, M. W.; Jin, L.; Kappler, J. W.; Friedman, R. S.; Jacobelli, J.; Marrack, P., Host DNA released in response to aluminum adjuvant enhances MHC class II-mediated antigen presentation and prolongs CD4 T-cell interactions with dendritic cells. *Proc Natl Acad Sci U S A* 2013, *110* (12), E1122-31.
6. Marichal, T.; Ohata, K.; Bedoret, D.; Mesnil, C.; Sabatel, C.; Kobiyama, K.; Lekeux, P.; Coban, C.; Akira, S.; Ishii, K. J.; Bureau, F.; Desmet, C. J., DNA released from dying host cells mediates aluminum adjuvant activity. *Nat Med* 2011, *17* (8), 996-1002.
7. Kool, M.; Soullie, T.; van Nimwegen, M.; Willart, M. A.; Muskens, F.; Jung, S.; Hoogsteden, H. C.; Hammad, H.; Lambrecht, B. N., Alum adjuvant boosts adaptive immunity by inducing uric acid and activating inflammatory dendritic cells. *J Exp Med* 2008, *205* (4), 869-82.
8. Sokolovska, A.; Hem, S. L.; HogenEsch, H., Activation of dendritic cells and induction of CD4(+) T cell differentiation by aluminum-containing adjuvants. *Vaccine* 2007, *25* (23), 4575-85.
9. McKee, A. S.; Munks, M. W.; MacLeod, M. K.; Fleenor, C. J.; Van Rooijen, N.; Kappler, J. W.; Marrack, P., Alum induces innate immune responses through macrophage and mast cell sensors, but these sensors are not required for alum to act as an adjuvant for specific immunity. *J Immunol* 2009, *183* (7), 4403-14.
10. Seubert, A.; Monaci, E.; Pizza, M.; O'Hagan, D. T.; Wack, A., The adjuvants aluminum hydroxide and MF59 induce monocyte and granulocyte chemoattractants and enhance monocyte differentiation toward dendritic cells. *J Immunol* 2008, *180* (8), 5402-12.
11. Kool, M.; Petrilli, V.; De Smedt, T.; Rolaz, A.; Hammad, H.; van Nimwegen, M.; Bergen, I. M.; Castillo, R.; Lambrecht, B. N.; Tschopp, J., Cutting edge: alum adjuvant stimulates inflammatory dendritic cells through activation of the NALP3 inflammasome. *J Immunol* 2008, *181* (6), 3755-9.
12. Li, H.; Willingham, S. B.; Ting, J. P.; Re, F., Cutting edge: inflammasome activation by alum and alum's adjuvant effect are mediated by NLRP3. *J Immunol* 2008, *181* (1), 17-21.
13. Guven, E.; Duus, K.; Laursen, I.; Hojrup, P.; Houen, G., Aluminum hydroxide adjuvant differentially activates the three complement pathways with major involvement of the alternative pathway. *PLoS One* 2013, *8* (9), e74445.
14. Mosca, F.; Tritto, E.; Muzzi, A.; Monaci, E.; Bagnoli, F.; Iavarone, C.; O'Hagan, D.; Rappuoli, R.; De Gregorio, E., Molecular and cellular signatures of human vaccine adjuvants. *Proc Natl Acad Sci U S A* 2008, *105* (30), 10501-6.
15. Morefield, G. L.; Sokolovska, A.; Jiang, D.; HogenEsch, H.; Robinson, J. P.; Hem, S. L., Role of aluminum-containing adjuvants in antigen internalization by dendritic cells in vitro. *Vaccine* 2005, *23* (13), 1588-95.
16. Kooijman, S.; Brummelman, J.; van Els, C.; Marino, F.; Heck, A. J. R.; Mommen, G. P. M.; Metz, B.; Kersten, G. F. A.; Pennings, J. L. A.; Meiring, H. D., Novel identified aluminum hydroxide-induced pathways prove monocyte activation and pro-inflammatory preparedness. *J Proteomics* 2018.
17. Brummelman, J.; Wilk, M. M.; Han, W. G.; van Els, C. A.; Mills, K. H., Roads to the development of improved pertussis vaccines paved by immunology. *Pathog Dis* 2015, *73* (8), ftv067.

18. Brummelman, J.; Helm, K.; Hamstra, H. J.; van der Ley, P.; Boog, C. J.; Han, W. G.; van Els, C. A., Modulation of the CD4(+) T cell response after acellular pertussis vaccination in the presence of TLR4 ligation. *Vaccine* 2015, *33* (12), 1483-91.

19. Rivera, A.; Siracusa, M. C.; Yap, G. S.; Gause, W. C., Innate cell communication kick-starts pathogen-specific immunity. *Nat Immunol* 2016, *17* (4), 356-63.

20. Rossi, M.; Young, J. W., Human dendritic cells: potent antigen-presenting cells at the crossroads of innate and adaptive immunity. *J Immunol* 2005, *175* (3), 1373-81.

21. Jakubzick, C. V.; Randolph, G. J.; Henson, P. M., Monocyte differentiation and antigen-presenting functions. *Nat Rev Immunol* 2017, *17* (6), 349-362.

22. Meiring, H. D.; Soethout, E. C.; Poelen, M. C.; Mooibroek, D.; Hoogerbrugge, R.; Timmermans, H.; Boog, C. J.; Heck, A. J.; de Jong, A. P.; van Els, C. A., Stable isotope tagging of epitopes: a highly selective strategy for the identification of major histocompatibility complex class I-associated peptides induced upon viral infection. *Mol Cell Proteomics* 2006, *5* (5), 902-13.

23. Moruz, L.; Pichler, P.; Stranzl, T.; Mechtler, K.; Kall, L., Optimized nonlinear gradients for reversed-phase liquid chromatography in shotgun proteomics. *Anal Chem* 2013, *85* (16), 7777-85.

24. Szklarczyk, D.; Franceschini, A.; Wyder, S.; Forslund, K.; Heller, D.; Huerta-Cepas, J.; Simonovic, M.; Roth, A.; Santos, A.; Tsafou, K. P.; Kuhn, M.; Bork, P.; Jensen, L. J.; von Mering, C., STRING v10: protein-protein interaction networks, integrated over the tree of life. *Nucleic Acids Res* 2015, *43* (Database issue), D447-52.

25. Wright, S. D.; Ramos, R. A.; Tobias, P. S.; Ulevitch, R. J.; Mathison, J. C., CD14, a receptor for complexes of lipopolysaccharide (LPS) and LPS binding protein. *Science* 1990, *249* (4975), 1431-3.

26. Zhou, L. J.; Tedder, T. F., CD14+ blood monocytes can differentiate into functionally mature CD83+ dendritic cells. *Proc Natl Acad Sci U S A* 1996, *93* (6), 2588-92.

27. Brewer, J. M.; Conacher, M.; Hunter, C. A.; Mohrs, M.; Brombacher, F.; Alexander, J., Aluminium hydroxide adjuvant initiates strong antigen-specific Th2 responses in the absence of IL-4- or IL-13-mediated signaling. *J Immunol* 1999, *163* (12), 6448-54.

28. Haller, O.; Arnheiter, H.; Horisberger, M. A.; Gresser, I.; Lindenmann, J., Interaction between interferon and host genes in antiviral defense. *Ann N Y Acad Sci* 1980, *350*, 558-65.

29. Holzinger, D.; Jorns, C.; Stertz, S.; Boisson-Dupuis, S.; Thimme, R.; Weidmann, M.; Casanova, J. L.; Haller, O.; Kochs, G., Induction of MxA gene expression by influenza A virus requires type I or type III interferon signaling. *J Virol* 2007, *81* (14), 7776-85.

30. Simon, A.; Fah, J.; Haller, O.; Staeheli, P., Interferon-regulated Mx genes are not responsive to interleukin-1, tumor necrosis factor, and other cytokines. *J Virol* 1991, *65* (2), 968-71.

31. Roers, A.; Hochkeppel, H. K.; Horisberger, M. A.; Hovanessian, A.; Haller, O., MxA gene expression after live virus vaccination: a sensitive marker for endogenous type I interferon. *J Infect Dis* 1994, *169* (4), 807-13.

32. Pletneva, L. M.; Haller, O.; Porter, D. D.; Prince, G. A.; Blanco, J. C., Induction of type I interferons and interferon-inducible Mx genes during respiratory syncytial virus infection and reinfection in cotton rats. *J Gen Virol* 2008, *89* (Pt 1), 261-70.

33. Zhou, X.; Michal, J. J.; Zhang, L.; Ding, B.; Lunney, J. K.; Liu, B.; Jiang, Z., Interferon induced IFIT family genes in host antiviral defense. *Int J Biol Sci* 2013, *9* (2), 200-8.

34. Antoniou, A. N.; Blackwood, S. L.; Mazzeo, D.; Watts, C., Control of antigen presentation by a single protease cleavage site. *Immunity* 2000, *12* (4), 391-8.

35. Manoury, B.; Hewitt, E. W.; Morrice, N.; Dando, P. M.; Barrett, A. J.; Watts, C., An asparaginyl endopeptidase processes a microbial antigen for class II MHC presentation. *Nature* 1998, *396* (6712), 695-9.

36. Wolk, K.; Grutz, G.; Witte, K.; Volk, H. D.; Sabat, R., The expression of legumain, an asparaginyl endopeptidase that controls antigen processing, is reduced in endotoxin-tolerant monocytes. *Genes Immun* 2005, *6* (5), 452-6.

37. Chomarat, P.; Rissoan, M. C.; Banchereau, J.; Miossec, P., Interferon gamma inhibits interleukin 10 production by monocytes. *J Exp Med* 1993, *177* (2), 523-7.

38. Saraiva, M.; O'Garra, A., The regulation of IL-10 production by immune cells. *Nat Rev Immunol* 2010, *10* (3), 170-81.

39. Fiorentino, D. F.; Zlotnik, A.; Mosmann, T. R.; Howard, M.; O'Garra, A., IL-10 inhibits cytokine production by activated macrophages. *J Immunol* 1991, *147* (11), 3815-22.

40. Fiorentino, D. F.; Zlotnik, A.; Vieira, P.; Mosmann, T. R.; Howard, M.; Moore, K. W.; O'Garra, A., IL-10 acts on the antigen-presenting cell to inhibit cytokine production by Th1 cells. *J Immunol* 1991, *146* (10), 3444-51.

41. Taga, K.; Tosato, G., IL-10 inhibits human T cell proliferation and IL-2 production. *J Immunol* 1992, *148* (4), 1143-8.

42. Gu, Y.; Yang, J.; Ouyang, X.; Liu, W.; Li, H.; Yang, J.; Bromberg, J.; Chen, S. H.; Mayer, L.; Unkeless, J. C.; Xiong, H., Interleukin 10 suppresses Th17 cytokines secreted by macrophages and T cells. *Eur J Immunol* 2008, *38* (7), 1807-13.

43. Redford, P. S.; Murray, P. J.; O'Garra, A., The role of IL-10 in immune regulation during M. tuberculosis infection. *Mucosal Immunol* 2011, *4* (3), 261-70.

44. McGuirk, P.; Mills, K. H., Direct anti-inflammatory effect of a bacterial virulence factor: IL-10-dependent suppression of IL-12 production by filamentous hemagglutinin from Bordetella pertussis. *Eur J Immunol* 2000, *30* (2), 415-22.

45. Raeven, R. H.; Brummelman, J.; Pennings, J. L.; Nijst, O. E.; Kuipers, B.; Blok, L. E.; Helm, K.; van Riet, E.; Jiskoot, W.; van Els, C. A.; Han, W. G.; Kersten, G. F.; Metz, B., Molecular signatures of the evolving immune response in mice following a Bordetella pertussis infection. *PLoS One* 2014, *9* (8), e104548.

46. Brummelman, J.; Raeven, R. H.; Helm, K.; Pennings, J. L.; Metz, B.; van Eden, W.; van Els, C. A.; Han, W. G., Transcriptome signature for dampened Th2 dominance in acellular pertussis vaccine-induced CD4(+) T cell responses through TLR4 ligation. *Sci Rep* 2016, *6*, 25064.

47. Boyman, O.; Sprent, J., The role of interleukin-2 during homeostasis and activation of the immune system. *Nat Rev Immunol* 2012, *12* (3), 180-90.

48. Gruenbacher, G.; Gander, H.; Nussbaumer, O.; Nussbaumer, W.; Rahm, A.; Thurnher, M., IL-2 costimulation enables statin-mediated activation of human NK cells, preferentially through a mechanism involving CD56+ dendritic cells. *Cancer Res* 2010, *70* (23), 9611-20.

49. de Rham, C.; Ferrari-Lacraz, S.; Jendly, S.; Schneiter, G.; Dayer, J. M.; Villard, J., The proinflammatory cytokines IL-2, IL-15 and IL-21 modulate the repertoire of mature human natural killer cell receptors. *Arthritis Res Ther* 2007, *9* (6), R125.

50. Onishi, R. M.; Gaffen, S. L., Interleukin-17 and its target genes: mechanisms of interleukin-17 function in disease. *Immunology* 2010, *129* (3), 311-21.

51. Lin, Y.; Ritchea, S.; Logar, A.; Slight, S.; Messmer, M.; Rangel-Moreno, J.; Guglani, L.; Alcorn, J. F.; Strawbridge, H.; Park, S. M.; Onishi, R.; Nyugen, N.; Walter, M. J.; Pociask, D.; Randall, T. D.; Gaffen, S. L.; Iwakura, Y.; Kolls, J. K.; Khader, S. A., Interleukin-17 is required for T helper 1 cell immunity and host resistance to the intracellular pathogen Francisella tularensis. *Immunity* 2009, *31* (5), 799-810.

52. Korpelainen, E. I.; Gamble, J. R.; Smith, W. B.; Dottore, M.; Vadas, M. A.; Lopez, A. F., Interferon-gamma upregulates interleukin-3 (IL-3) receptor expression in human endothelial cells and synergizes with IL-3 in stimulating major histocompatibility complex class II expression and cytokine production. *Blood* 1995, *86* (1), 176-82.

53. Korpelainen, E. I.; Gamble, J. R.; Vadas, M. A.; Lopez, A. F., IL-3 receptor expression, regulation and function in cells of the vasculature. *Immunol Cell Biol* 1996, *74* (1), 1-7.

54. O'Garra, A., Cytokines induce the development of functionally heterogeneous T helper cell subsets. *Immunity* 1998, *8* (3), 275-83.

55. O'Garra, A.; Arai, N., The molecular basis of T helper 1 and T helper 2 cell differentiation. *Trends Cell Biol* 2000, *10* (12), 542-50.

56. Chang, E. Y.; Guo, B.; Doyle, S. E.; Cheng, G., Cutting edge: involvement of the type I IFN production and signaling pathway in lipopolysaccharide-induced IL-10 production. *J Immunol* 2007, *178* (11), 6705-9.

57. Kintaka, R.; Makanae, K.; Moriya, H., Cellular growth defects triggered by an overload of protein localization processes. *Sci Rep* 2016, *6*, 31774.

58. Burgdorf, S.; Kautz, A.; Bohnert, V.; Knolle, P. A.; Kurts, C., Distinct pathways of antigen uptake and intracellular routing in CD4 and CD8 T cell activation. *Science* 2007, *316* (5824), 612-6.

59. Burgdorf, S.; Scholz, C.; Kautz, A.; Tampe, R.; Kurts, C., Spatial and mechanistic separation of cross-presentation and endogenous antigen presentation. *Nat Immunol* 2008, *9* (5), 558-66.

60. Dinarello, C. A., Immunological and inflammatory functions of the interleukin-1 family. *Annu Rev Immunol* 2009, *27*, 519-50.

61. Garlanda, C.; Dinarello, C. A.; Mantovani, A., The interleukin-1 family: back to the future. *Immunity* 2013, *39* (6), 1003-18.

62. Ghimire, T. R., The mechanisms of action of vaccines containing aluminum adjuvants: an in vitro vs in vivo paradigm. *Springerplus* 2015, *4*, 181.

63. Brewer, J. M.; Conacher, M.; Satoskar, A.; Bluethmann, H.; Alexander, J., In interleukin-4-deficient mice, alum not only generates T helper 1 responses equivalent to freund's complete adjuvant, but continues to induce T helper 2 cytokine production. *Eur J Immunol* 1996, *26* (9), 2062-6.

64. Morefield, G. L.; HogenEsch, H.; Robinson, J. P.; Hem, S. L., Distribution of adsorbed antigen in mono-valent and combination vaccines. *Vaccine* 2004, *22* (15-16), 1973-84.

65. de Gouw, D.; Diavatopoulos, D. A.; Bootsma, H. J.; Hermans, P. W.; Mooi, F. R., Pertussis: a matter of immune modulation. *FEMS Microbiol Rev* 2011, *35* (3), 441-74.

Legends to the Supplementary data

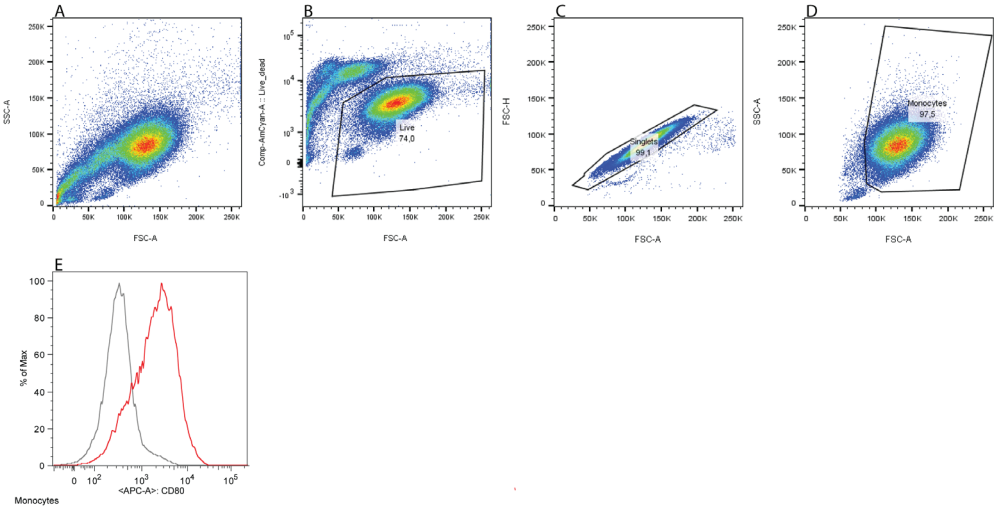

Supplementary S1 Fig. Flow cytometry data gating staining
Data of one representative donor to illustrate the gating strategy used: (A) represents ungated monocytes, in (B) the live cells are gated, (C) represents the single stained cells inside the live cells, (D) represents the monocytes inside the single stained cells and (E) is a histogram of CD80-stained cell in which the grey line represents medium control and the red line represents LPS as a positive control.

Supplementary S1 Table. qPCR raw data table
Values are Ct values, Delta Ct values, DeltaDelta Ct values and ratios to control for a given donor and stimulation condition ($Al(OH)_3$ or DTaP) after 24 hours of stimulation. The technical replicates used for the determination of the significance threshold are also depicted in the tab 'Technical replicates'. A heap map of all the individual donors is depicted in the tab 'heatmap individual donors'.

Supplementary S2 Table. LC-MS/MS raw data table
LOG(2) ratios as obtained by Proteome Discoverer for the individual proteins are depicted. To combine multiple entries for the same protein, columns B and C contain the information used to remove redundancy in protein accession numbers (column A). Blank values indicate that no quantification data were available. The tab 'Regulated Proteins' contains the proteins that were regulated with at least a factor 1.5 in one of the stimulation conditions, after pooling and normalization. The fold changes are depicted as LOG(2) factors.

Supplementary S3 Table. Enriched pathways and GO terms
The pathways that are enriched after a specific stimulation condition and time point. The pathways are GO terms or KEGG pathways, which are enriched after one of the stimulation conditions with an FDR of <0.1. The proteins were at least a factor 1.5 regulated compared to control in 2 out of 3 donors.

Supplementary S4 Table. Raw IL-1β ELISA

Measured IL-1β concentrations in pg/ml for the individual experiments.

	Medium+PMA	*Medium+PMA+block*	*Al(OH)$_3$ + PMA*	*Al(OH)$_3$+PMA+block*	*DTaP (PMA)*	*DTaP+PMA+block*
IL-1β pg/ml	0	0,62	9,308	2,265	392,127	140,09
IL-1β pg/ml	0	0	9,932	5,32	342,686	138,24
IL-1β pg/ml	0	0	9,914	2,746	374,274	193,34
IL-1β pg/ml	0,63	0	8,36	3,94	262,31	38,68
IL-1β pg/ml	0,39	0,038	6,06	3,04	102,838	26,6
IL-1β pg/ml	1,355	0	5,979	4,28	98,728	103,65

Supplementary S5 Table. Raw IL-10 ELISA

Measured IL-10 concentrations in pg/ml for the individual experiments.

Medium	1,40
	0,32
	0,51
Al(OH)$_3$ 50 µg/ml	2,59
	2,31
	0,15
	0,20
Al(OH)$_3$ 100 µg/ml	2,54
	0,00
	0,83
	0,00
DTaP 50 µg/ml	4,33
	2,87
	1,00
	1,38
DTaP 100 µg/ml	4,99
	7,03
	5,33
	2,50
PTx 0.33 µg/ml + FHA 0.33 µg/ml + PRN 0.1 µg/ml	2,15
	4,75
	0,80
PTx 0.66 µg/ml + FHA 0.66 µg/ml + PRN 0.2 µg/ml	2,37
	5,12
	4,76
	1,61
FHA 1.32 µg/ml	5,21
	4,60
	0,87
	4,08
FHA 2.64 µg/ml	4,78
	4,56
	1,72
	4,06
FHA 5.28 µg/ml	4,45
	11,84
	3,72
	6,22
PRN 0.4 µg/ml	2,23
	4,68
	0,32
	4,40
PRN 0.8 µg/ml	2,16
	4,23
	0,00
	2,24
PRN 1.6 µg/ml	2,18
	4,28
	0,00
	1,85
PTx 1.32 µg/ml	
	0,66
	2,10
	4,35
PTx 2.64 µg/ml	2,15
	6,46
	0,48
PTx 5.28 µg/ml	4,29
	4,45
	0,87

All amounts are pg/ml

Chapter 4

The aluminum hydroxide and aluminum phosphate adjuvants elicit a different innate immune response

Sietske Kooijman[1,2], Hilde Vrieling[1,3], Lisa Verhagen[1], Justin de Ridder[1], Alex de Haan[1], Peter C. Soema[1], Elly van Riet[1], Albert J.R. Heck[2,4], Gideon F.A. Kersten[1,3], Jeroen L.A. Pennings[5], Bernard Metz[1], Hugo D. Meiring[1*]

1 Intravacc, Bilthoven, the Netherlands
2 Biomolecular Mass Spectrometry and Proteomics, Bijvoet Center for Biomolecular Research and Utrecht Institute for Pharmaceutical Sciences, Science Faculty, Utrecht University, Utrecht the Netherlands
3 Leiden Academic Centre for Drug Research, Leiden University, Leiden, the Netherlands
4 Netherlands Proteomics Centre, Utrecht, the Netherlands
5 Centre for Health Protection, National Institute for Public Health and the Environment, Bilthoven, the Netherlands

Manuscript in preparation

Abstract

Aluminum hydroxide ($Al(OH)_3$) and aluminum phosphate ($AlPO_4$) are widely used adjuvants in human vaccines. However, a rationale to choose one or the other is lacking since the differences between molecular mechanisms of action of these adjuvants are unknown. In the current study, we compared the innate immune response induced by both adjuvants *in vitro* and *in vivo*. Proteome analysis of human primary monocytes was used to determine the immunological pathways activated by these adjuvants. Subsequently, analysis of immune cells present at the site of injection and proteome analysis of the muscle tissue revealed the differentially regulated processes related to the innate immune response *in vivo*. $Al(OH)_3$ specifically enhanced the activation of antigen processing and presentation pathways *in vitro*. *In vivo* experiments showed that only $Al(OH)_3$ attracted neutrophils, while $AlPO_4$ attracted monocytes to the site of injection. In addition, $Al(OH)_3$ enhanced the process of hemostasis after 96 hours, related to neutrophilic extracellular trap formation, while $AlPO_4$ did not. Both adjuvants differentially regulated various immune system-related processes. The results show that $Al(OH)_3$ and $AlPO_4$ act differently on the innate immune system. We speculate that this is related to the different physicochemical properties of both adjuvants, affecting the interaction with cells.

Introduction

Most of the inactivated vaccines currently available require the use of an adjuvant to boost the immune response. Since the early 20th century, aluminum salts are known for their adjuvant activity[1]. Many vaccines contain aluminum hydroxide ($Al(OH)_3$) or aluminum phosphate ($AlPO_4$)[2]. The immunological mechanisms of action attributed to aluminum salts are several: 1) *Depot effect*. Glenny *et al*. observed that the clearance of toxoids adsorbed to aluminum potassium sulfate was delayed compared to non-adsorbed toxoids *in vivo*[3]; 2) *Activation and maturation* of antigen presenting cells by both aluminum-based adjuvants occur both *in vivo* and *in vitro* with and without antigen present[4-5]; 3) *Enhancement of the expression of chemotactic proteins in vitro*. $Al(OH)_3$ and $AlPO_4$ attract immune cells to the site of injection, *e.g*. inflammatory monocytes, dendritic cells, neutrophils, natural killer cells, eosinophils and $CD11^+$ cells, in the presence and absence of an antigen, *in vivo*[4-9]; 4) Activation of the *inflammasome*, inducing the secretion of inflammatory cytokine IL-1β both *in vitro* and *in vivo*, upon $Al(OH)_3$ stimulation in the presence of an antigen[10-11]; 5) *Complement activation* in human sera (*in vitro*) upon $Al(OH)_3$ stimulation, in the presence of an antigen[12]; 6) *Release of Danger Associated Molecular Patterns* (DAMPs) upon cell death, induced by $Al(OH)_3$. DAMPs like Uric Acid and DNA can induce cell priming, inflammasome activation, IL-1β secretion, and MHC class II antigen presentation *in vitro* and *in vivo*, in the presence of an antigen[13-15]. 7) The induction of a T helper (Th) type 2 response, by inducing IL-4 secretion, *in vivo* and *in vitro*[6, 9].

Most of the molecular mechanisms described above were obtained in studies focused on $Al(OH)_3$ but not on $AlPO_4$. These studies are mostly conducted with classical immunological techniques, such as flow cytometry, ELISA and multiplex immune assays (MIA). More recently, comprehensive, non-biased approaches have emerged, *e.g*. genomics and proteomics[16-17]. However, the use of these techniques in adjuvant research is limited as of now.

In many vaccine formulations either of the two adjuvants are used, apparently without a clear rationale of choosing between the two adjuvants. Sometimes the degree of antigen adsorption is used as a criterion. Because of its high isoelectric point (IEP), $Al(OH)_3$ often adsorbs antigen more efficiently as compared to $AlPO_4$ with a neutral or slightly acidic IEP.

However, the link between antigen adsorption in the formulation and immunogenicity does not always hold true[18]. Antigens may rapidly desorb from the adjuvant *in vivo*[19]. Sometimes, however, a link between adsorption and adjuvant activity is described, both positive and negative[20-21], although it is not clear whether a link between degree of adsorption and adjuvant effect is causal. There may be other effects than adsorption of antigen causing the adjuvant effect, *e.g*. interaction with antigen presenting cells. Thus, knowledge on the immune-modulating effect of both adjuvants is important to substantiate the use of $Al(OH)_3$ *versus* $AlPO_4$ as an adjuvant.

In the current study, we compared the effects of $Al(OH)_3$ and $AlPO_4$ *in vitro* and *in vivo* by flow cytometric assays and quantitative mass spectrometry-based proteomics. *In vitro*, the adjuvant effects were studied in human primary monocytes, since these prominent mononuclear phagocytes play an important role in bridging the innate and adaptive immune response[22]. In addition, we focused on the site of injection *in vivo* to

study the initiation of the immune response in mice. The recruitment of immune cells to the site of injection was studied, as well as changes in the proteome of the site of injection. The results of this study show that both adjuvants attract different cell types to the site of injection and are different in inducing immune system-related processes.

Materials and methods

Ethics statement

The human monocyte study was conducted according to the principles expressed in the Declaration of Helsinki. All blood donors gave written-informed consent before collection and use of their samples. All blood donations, provided by the Dutch National Institute for Public Health and the Environment (RIVM, Bilthoven; the Netherlands) were specifically donated for primary cell isolation. This research goal was explicitly approved by the accredited Medical Research Ethics Committee (MREC), METC, Noord-Holland in the Netherlands. All blood samples were processed anonymously.

Animal studies complied with the ARRIVE guideline and were approved by the central committee animal studies (CCD The Hague; the Netherlands) following the procedures of European legislation guideline (2010/63/EU and law for animal testing (WOD) the Netherlands). The specific experiment was approved by the authority for animal welfare (IvD) and the Scientific committee (WTC) of Intravacc (Bilthoven; the Netherlands).

Reagents used for cell stimulation

$Al(OH)_3$ is Alhydrogel 2% (Brenntag; Frederikssund; Denmark). Aluminum phosphate, referred to as $AlPO_4$, is AdjuPhos (Brenntag; Frederikssund; Denmark). Lipopolysaccharide (LPS) from *E.coli* K12 was used as a positive control and is referred to as LPS and was obtained from Invivogen (San Diego; USA).

Primary monocyte culture and adjuvant stimulation

Fresh peripheral blood was obtained from four healthy volunteers and collected in heparin-coated tubes. Peripheral Blood Mononuclear Cells (PBMCs) were isolated from the blood using Ficoll density centrifugation at 1,000x*g* for 30 minutes. Monocytes were isolated from the PBMC fraction using positive selection by CD14 micro beads and magnetic LS MACS columns (Miltenyi Biotech; Bergisch Gladbach; Germany). A purity check was performed by flow cytometric analysis of CD14 cell surface expression[23]. Monocytes were ≥95% pure. The monocytes were cultured in a 24-well culture plate at a density of 0.6×10^6 cells/ml, 1 ml/well, in RPMI (Gibco/Themo Fisher; Waltham; Massachusetts; USA) supplemented with 10% Fetal Calf Serum (FCS) (Serana Germany) and 100 units/ml penicillin, 100 µg/ml streptomycin and 0.3 µg/ml L-glutamine (P/S/G) (Invitrogen/Thermo Fisher Scientific; Waltham; Massachusetts; USA). Isolated monocytes were either left unstimulated, or were stimulated with $Al(OH)_3$ or $AlPO_4$ with a final concentration of 10 µg/ml aluminum for 24 or 48 hours. LPS (100 ng/ml) was used as a culture control.

Protein isolation, digestion and labeling

To disrupt the cells and isolate the proteins from the cells, 500 µl of 4 M guanidine·HCl in 100 mM phosphate buffer pH 7.5 was added to the cell culture plates. The cell suspensions were incubated at 4°C for 30 minutes. During this incubation step, the cell suspensions were subjected to a freeze-thaw step. Lysed cells were stored at -80°C. After the cell lysis, a 50-µl aliquot of each sample was used to determine the protein

concentration with the BCA protein assay (Pierce Biotechnology; Waltham; Massachusetts; USA). To adjust the pH of the lysates and to reduce the concentration of Guanidine·HCl to 1 M, the samples were diluted four times in 100 mM phosphate buffer pH 7.5. Next, the isolated proteins were digested with Lys-C (Roche; enzyme-to-substrate ratio 1/10) for 4 hours at 37°C, after which fresh Lys-C was added (enzyme-to-substrate ratio 1/10) for an overnight incubation at 37°C. Samples were normalized on protein content, desalted using solid phase extraction (SPE) on C18 columns (Waters) according to the manufacturer's protocol and dried with centrifugation under reduced pressure, after which the samples were labeled per condition using Tandem Mass Tag labeling-10plex (TMT(10) (Thermo Fisher; Waltham; Massachusetts; USA) according to the manufacturer's protocol. Samples were pooled and dried by centrifugation under reduced pressure. Next, the pooled samples were dissolved in MilliQ water containing 5% dimethyl sulfoxide (DMSO) and 0.1% formic acid (FA) for mass spectrometry based-proteome analysis.

In vivo studies

Female (20 individuals) and male (30 individuals) BALB/c mice (age 6-8 weeks, specified pathogen free) were obtained from Charles River Laboratories. Mice were randomly divided in ten groups of five mice (three male and two female mice per group). The males and females were housed separately and per group in Macrolon II cages with top filter. Three groups were injected Intramuscularly (I.M.) in both quadriceps with $Al(OH)_3$ (100 µg aluminum), in 50 µl Phosphate-buffered saline (PBS) pH 7.2 (Gibco; 10.6 mM KH_2PO_4, 150 mM NaCl, 29.7 mM Na_2HPO_4). Three groups were injected I.M in both quadriceps with $AlPO_4$ (100 µg aluminum) in 50 µl PBS. One control group was not treated at all and euthanized after 96 hours and three other control groups were injected with PBS only. Injections were given under anesthesia (isoflurane/oxygen). Groups were euthanized and muscles were taken from individual mice after 24, 48 and 96 hours of immunization and placed in All Protect (Qiagen; Venlo; the Netherlands).

Muscle cell isolation

During sample collection, the same part of each muscle was separated, sliced in small cubes placed in DMEM culture medium (Gibco) and kept on ice. Samples were supplemented with Hanks-Balanced Salt Solution (HBSS) and 0.2% Collagenase B (Roche; Basel; Switzerland). Samples were rotated at 37°C for 30 minutes, after which the same amount of collagenase B was added and samples were again rotated for 30 minutes at 37°C. The remaining cell suspensions were filtered over a cell strainer (0.7 µm) and washed with DMEM containing 10% FCS and P/S/G. Samples were frozen at -135°C in DMEM medium, containing 40% FCS and 10% DMSO for subsequent analysis.

Muscle protein extraction and labeling

Whole muscles were homogenized in the All Prep Lysis buffer (1 ml, Qiagen; Venlo; the Netherlands) with the Fast Prep-24 Classic instrument: the samples were shaken 6 times 30 seconds at speed 6 meters/second (m/s), with cooling between each 30 seconds of shaking. Next, 500 µl was used for protein extraction with the All Prep kit (Qiagen; Venlo; the Netherlands) according to the manufacturer's protocol. Protein pellets were reconstituted in 8 M urea (which was degassed with helium to prevent carbamylation of proteins) in 100 mM phosphate buffer pH 7.5. After reconstitution, urea concentra-

tions were reduced to 1 M. A protein content analysis was performed using the BCA kit (Pierce Bioscience) according to the manufacturer's protocol. Samples were normalized on protein content and digested with proteinase Lys-C in a 1:10 enzyme-to-substrate ratio at 37°C. After 4 hours, fresh Lys-C was added in a 1:10 enzyme-to-substrate-ratio for an overnight incubation at 37°C. The individual protein samples were labeled with TMT(10) (Thermo Fisher) according to the manufacturer's protocol. Each 10-plex contained the isolated proteins from the muscle of one mouse per group. Individual samples were pooled and dried with centrifugation under reduced pressure and a subsequent C18 solid phase extraction clean-up was performed, after which the samples were eluted with 90% acetonitrile and 0.5% acetic acid in MilliQ water. Samples were centrifuged under reduced pressure and reconstituted in MilliQ water containing 5% DMSO and 0.1 %FA for further analysis.

Flow cytometry

The muscle samples frozen in medium were rapidly thawed at 37°C in a water bath. Subsequently, they were placed in a 15-ml tube with the addition of 4 ml medium (RPMI supplemented with P/S/G and 10% FCS). Samples were washed with medium and subsequently with FACS buffer (PBS + 0.5% Bovine Serum Albumin (BSA) + 0.5 mM Ethylenediaminetetraacetic acid (EDTA)). Samples were divided into two fractions. One of the fractions was left unstained and was used as a control. The other fraction was stained with AF488-conjugated Ly-6G (BioLegend clone 1A8), PE-conjugated CD115 (BD Biosciences clone T38-320), BV510-conjugated CD11b (BD Biosciences clone m1/70) and BV711 conjugated-F4/80 (BD Biosciences clone T45-2342), all in a 1/50 dilution and Live Dead fixable viability stain 780 (BD Biosciences) in a 1/2000 dilution in FACS buffer for 30 minutes at 4°C. The muscle cells were washed and re-suspended in FACS buffer containing 1% paraformaldehyde (PFA). Data were acquired on a flow cytometer (Attune Next, Thermo Fisher Scientific). Samples were compared to their unstained control and to the PBS control group at the corresponding time point. Data was analyzed using FlowJo software version 10 (Three Star).

LC MS/MS analysis of human monocytes and mouse muscle cells

Peptide separation was performed on an Agilent 1290 system (Santa Clara; California; USA). Peptides were trapped on a trapping column (Reprosil-Pur C18-AQ, df=5 µm, 2 cm length × 100 µm I.D.; Dr. Maisch; Ammerbuch; Germany) and separation was performed on an analytical column (Reprosil-Pur C18-AQ, df=3 µm, 30 cm length x 50 µm I.D.; Dr. Maisch; Ammerbuch; Germany), both packed in-house. Solvent A was 0.1% FA in MilliQ water and solvent B was 0.1% FA in AcN (Biosolve). The peptides were separated in 195 minutes in a non-linear gradient (15 minutes at 0% B for peptide loading on the trapping column, subsequently followed by a gradient of 160 minutes from 0% to 30% B, a 15-minutes gradient to 45% B and 5 minutes at 65% B) optimized as described by Morus *et al.*[24]. The column effluent was electro-sprayed directly into the MS using a gold-coated fused silica tip of 3.5 µm tipID, with a spray voltage of 1.8 KV.

Mass spectrometric data were acquired on a Tribrid-Orbitrap Fusion Lumos (Thermo Fisher Scientific). The full scan (MS^1) spectra were acquired with a scan mass range of 350-1500 at 120,000 resolution (FWHM) with an Orbitrap readout. For the MS^1, the automatic gain control (AGC) was set to 400,000 and the maximum injection time was 50 ms. Top speed mode was used with a duration of 3 sec for the *in vitro* samples and 5

sec for *in vivo* mouse muscle cells, where precursor ions were selected with an intensity >5,000 for fragmentation (MS^2). Charge states between 2 and 7 were selected for MS^2 and fragmentation was performed using Collision-Induced Dissociation (CID) in the linear ion trap (LTQ) with a normalized collision energy of 35%. In MS^2, the AGC was set to 10,000 and the maximum injection time was 100 ms. Synchronous-Precursor-Selection (SPS) was enabled to include up to 5 MS^2 fragment ions in MS^3. The fragment ions were further fragmented by higher energy collision dissociation (HCD) with a normalized collision energy of 60%. The TMT reporter ions were analyzed in the Orbitrap analyzer, the AGC was set to 100,000 and the maximum injection time was set to 240 ms for the *in vitro* samples and 160 ms for the *in vivo* mouse muscles. Each individual sample was analyzed three times to optimize protein identification and quantification.

Data analysis of proteomics data

Proteomics data were analyzed with Proteome Discoverer 2.1 (Thermo Fisher Scientific) with default settings unless stated otherwise. Precursor mass tolerance was set to 5 ppm. MS^2 scans were searched against the Human Uniprot protein database from November 2014, containing 23,048 entries or the *Mus musculus* database, using the SequestHT search engine with a full enzyme specificity for Lys-C as described previously[23]. The quantification node was used to obtain relative expression values, where TMT(10) was defined as the quantification method, with an integration tolerance of 0.2 Da. Cite Percolator was used to filter the peptide to spectrum mass with a False Discovery Rate (FDR) of <5%.

Data were normalized by performing a median correction as described previously[23]. Data of three biological replicates for human samples and five biological replicates for mice samples were compared. Proteins that were upregulated or downregulated by 1.5 fold or more compared to control (based on being >2.5x the median coefficient of variation (CV) as described previously[23] in at least two out of three replicates (human monocyte samples) or a factor 2 in three out of five mice per group) were considered significantly regulated. This factor 2 was based on approximately 3x the median CV of 28%, analogously to our previous studies[23]. The regulated proteins were imported in Panther[25] to identify regulated pathways (FDR<0.05), within functional annotations provided by Gene Ontology (GO) biological processes.

Statistics

Flow cytometry data was analyzed with Graphpad Prism®. Significance of difference was determined with a two way ANOVA and a Tukey test for multiple comparison correction.

Results

$AlPO_4$ and $Al(OH)_3$ induce different pathways related to immune activation in human primary monocytes

Monocytes were stimulated with $AlPO_4$ and $Al(OH)_3$ for 24 and 48 hours. Quantitative proteome analysis resulted in about 1200 quantified proteins in all samples. After 24 hours, in both $AlPO_4$ and $Al(OH)_3$-stimulated cells about 100 proteins were up- or downregulated compared to the expression in unstimulated cells. These changes are reflected in the enrichment of various immune system-related pathways induced by both $AlPO_4$ and $Al(OH)_3$ (GO terms) (Figure 1), including known $Al(OH)_3$-induced pathways *regulation of complement activation*[12] and *regulation of the humoral response*. In addition, $Al(OH)_3$ specifically induced *regulation of the acute inflammatory response* and *immune response* after 24 hours of stimulation. The pathways specifically enriched by $AlPO_4$ were related to *viral transcription* and *viral gene expression*. After 24 hours of $AlPO_4$ stimulation, the pathway *antigen processing and presentation* was downregulated, while this was not the case in $Al(OH)_3$-stimulated monocytes.

After 48 hours of stimulation, both adjuvants induced many immunologically relevant pathways, *e.g. (positive regulation of) defense response*, *immune response*, *viral process* and *blood coagulation*, *Antigen processing and presentation* pathways were also upregulated by both stimuli, although much stronger for $Al(OH)_3$ compared to $AlPO_4$ (Figure 1). Upon $Al(OH)_3$ stimulation, typical proteins related to antigen processing and presentation via both HLA class I and class II were upregulated. Proteins related to antigen presentation via HLA class I specifically regulated by $Al(OH)_3$ included: various proteasomal subunits related to antigen processing and presentation, *e.g.* proteasome subunits alpha type-3 (PSMA2) and beta type-3 (PSMB3) and 26S proteasome non-ATPase regulatory subunits 3 and 13 (PSMD3 and PSMD13, respectively). Proteins specifically upregulated by $Al(OH)_3$ that are related to antigen presentation via HLA class II consisted of: cathepsin (CTS) L1, dynactin subunit 2 (DCTN2), cytoplasmic dynin II chain (DYNC1i2) and legumain (LGMN) (Supplementary S1). Pathways uniquely induced upon 48 hours of $Al(OH)_3$ stimulation included: *positive regulation of type IIa hypersensitivity* and *positive regulation of adaptive immune response*. After 48 hours of stimulation, $AlPO_4$ uniquely induced *positive regulation of complement activation* (Figure 1, Supplementary S2).

These data show that both adjuvants activate the immune system and immune system-related pathways in monocytes. Distinct differences in the quality and kinetics of the immunogenicity of both adjuvants were observed. Figure 1 clearly shows that the *in vitro* immune response towards $Al(OH)_3$ is more pronounced compared to $AlPO_4$, in particular after prolonged stimulation (48 hours). Another important difference was found with respect to *antigen presentation and processing*, which was downregulated after 24 hours of stimulation with $AlPO_4$ (with no regulation upon $Al(OH)_3$ stimulation at this time point), whereas this pathway was strongly upregulated after 48 hours of stimulation with $Al(OH)_3$, with a minimal induction for $AlPO_4$.

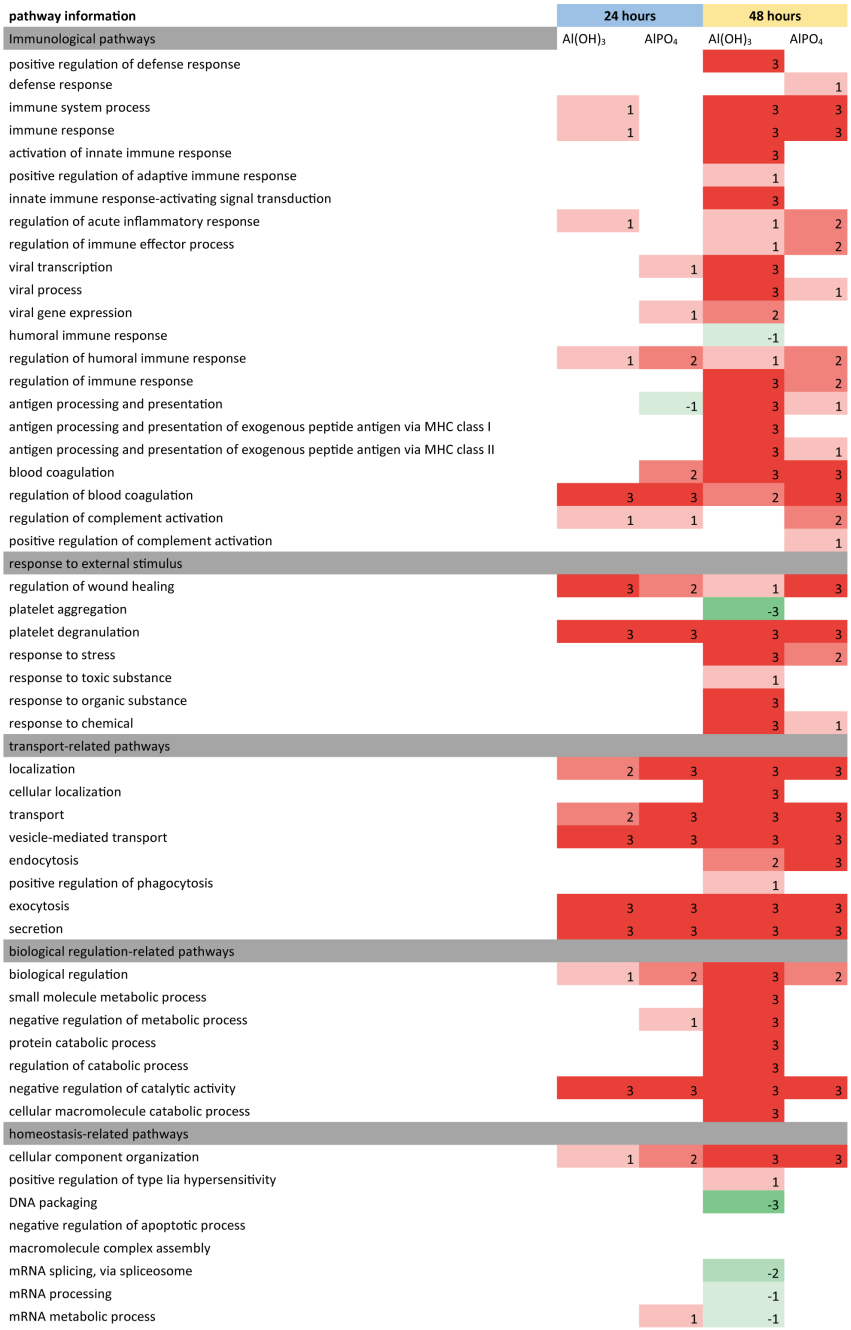

pathway information	24 hours		48 hours	
Immunological pathways	$Al(OH)_3$	$AlPO_4$	$Al(OH)_3$	$AlPO_4$
positive regulation of defense response			3	
defense response				1
immune system process	1		3	3
immune response	1		3	3
activation of innate immune response			3	
positive regulation of adaptive immune response			1	
innate immune response-activating signal transduction			3	
regulation of acute inflammatory response	1		1	2
regulation of immune effector process			1	2
viral transcription		1	3	
viral process			3	1
viral gene expression		1	2	
humoral immune response			-1	
regulation of humoral immune response	1	2	1	2
regulation of immune response			3	2
antigen processing and presentation		-1	3	1
antigen processing and presentation of exogenous peptide antigen via MHC class I			3	
antigen processing and presentation of exogenous peptide antigen via MHC class II			3	1
blood coagulation		2	3	3
regulation of blood coagulation	3	3	2	3
regulation of complement activation	1	1		2
positive regulation of complement activation				1
response to external stimulus				
regulation of wound healing	3	2	1	3
platelet aggregation			-3	
platelet degranulation	3	3	3	3
response to stress			3	2
response to toxic substance			1	
response to organic substance			3	
response to chemical			3	1
transport-related pathways				
localization	2	3	3	3
cellular localization			3	
transport	2	3	3	3
vesicle-mediated transport	3	3	3	3
endocytosis			2	3
positive regulation of phagocytosis			1	
exocytosis	3	3	3	3
secretion	3	3	3	3
biological regulation-related pathways				
biological regulation	1	2	3	2
small molecule metabolic process			3	
negative regulation of metabolic process		1	3	
protein catabolic process			3	
regulation of catabolic process			3	
negative regulation of catalytic activity	3	3	3	3
cellular macromolecule catabolic process			3	
homeostasis-related pathways				
cellular component organization	1	2	3	3
positive regulation of type Iia hypersensitivity			1	
DNA packaging			-3	
negative regulation of apoptotic process				
macromolecule complex assembly				
mRNA splicing, via spliceosome			-2	
mRNA processing			-1	
mRNA metabolic process		1	-1	

Figure 1. ***Heatmap of regulated processes in human monocytes.***
For each stimulation condition a summary of the enriched pathways is depicted. The pathways are grouped based on immunological and homeostatic features. The intensity of the color and the numbers correspond to the significance of the pathway: 1, 2 and 3 correspond to a p-value of <0.05, <0.01 and <0.001 respectively.

$Al(OH)_3$ but not $AlPO_4$ attracts neutrophils to the site of injection

To determine whether the differences identified *in vitro* could also be observed in *in vivo* experiments, mice were intramuscularly injected with the adjuvants. The cell types present at the site of injection after 24, 48 and 96 hours of administration were analyzed with flow cytometry (gating strategy specified in Supplementary S3). Twenty-four hours after administration of $Al(OH)_3$ or $AlPO_4$, no significant increase in any cell population was observed compared to the control group (PBS injected mice) (Figure 2A-C). However, after both 48 and 96 hours, $Al(OH)_3$ significantly increased neutrophil ($CD11b^+$ $F4/80^-$ $Ly6G^+$) influx at the site of injection compared to the control group, while for $AlPO_4$ this neutrophil population was not significantly different from the control group. After 96 hours, the influx of neutrophils induced by $Al(OH)_3$ was significantly higher compared to control and $AlPO_4$-administered mice (Figure 2A). In addition, $Al(OH)_3$ significantly increased the monocyte population at the site of injection after 48 hours. After 96 hours, both adjuvants induced a significant increase in macrophages ($CD11b^+$ $F4/80^+$ $Ly6G^-$ SSC^{int}) (Figure 2B). In addition, monocytes ($CD11b^+$ $F4/80^{\pm}$ $Ly6G^-$ SSC^{low}) appeared 96 hours after $AlPO_4$ administration (Figure 2C). Thus, both $AlPO_4$ and $Al(OH)_3$ attracted immune cells to the site of injection, but there is a difference in the numbers of monocytes. Also, $Al(OH)_3$ attracted significant numbers of neutrophils, while $AlPO_4$ did not induce significant amounts of monocytes.

Distinct protein expression at the site of injection after administration of $Al(OH)_3$ and $AlPO_4$

Twenty-four hours after administration of the $Al(OH)_3$ and $AlPO_4$ stimulus, protein analysis of mouse muscles showed a large overlap (67%) in upregulated proteins between the two adjuvants. Proteins that were highly upregulated in both stimulation conditions were S100-A8 and S100-A9 (Supplementary S4); these proteins are related to the presence of neutrophils. The pathway (GO term) *neutrophil aggregation* (attraction of neutrophils) was enriched in both stimulation conditions. Moreover, (*antibacterial*) *humoral immune response*, *hemostasis* and the related Gene Ontology process *negative regulation (i.e.* inhibition*) of hemostasis* were also enriched. In addition, the processes *monocyte chemotaxis* and *acute phase response* were specifically enhanced by $Al(OH)_3$ (Figure 3 extracted from supplementary S5). $AlPO_4$ uniquely induced the pathway *localization*, a pathway related to the movement of, *e.g.* proteins, macromolecules and organelles in the cell, after 24 hours of stimulation (Figure 3).

After 48 hours of stimulation, the overlap between the upregulated proteins by $Al(OH)_3$ and $AlPO_4$ at the site of injection was 62%. Both adjuvants still enhanced *neutrophil aggregation*, *hemostasis* and the Gene Ontology-related term *negative regulation* (*i.e.* inhibition) *of hemostasis.* In addition, various immune system-related processes, *e.g. adaptive immune response* and *innate immune response* were enriched (Figure 3). Moreover, $Al(OH)_3$ specifically induced various pathways, such as *regulation of cell death* and *regulation of interleukin-8 production.* IL-8 is one of the main neutrophil chemoattractant molecules, thus its upregulation is in accordance with the detection of neutrophils at the injection site in response to $Al(OH)_3$ only. $AlPO_4$ did not regulate any immunological pathways not being regulated by $Al(OH)_3$.

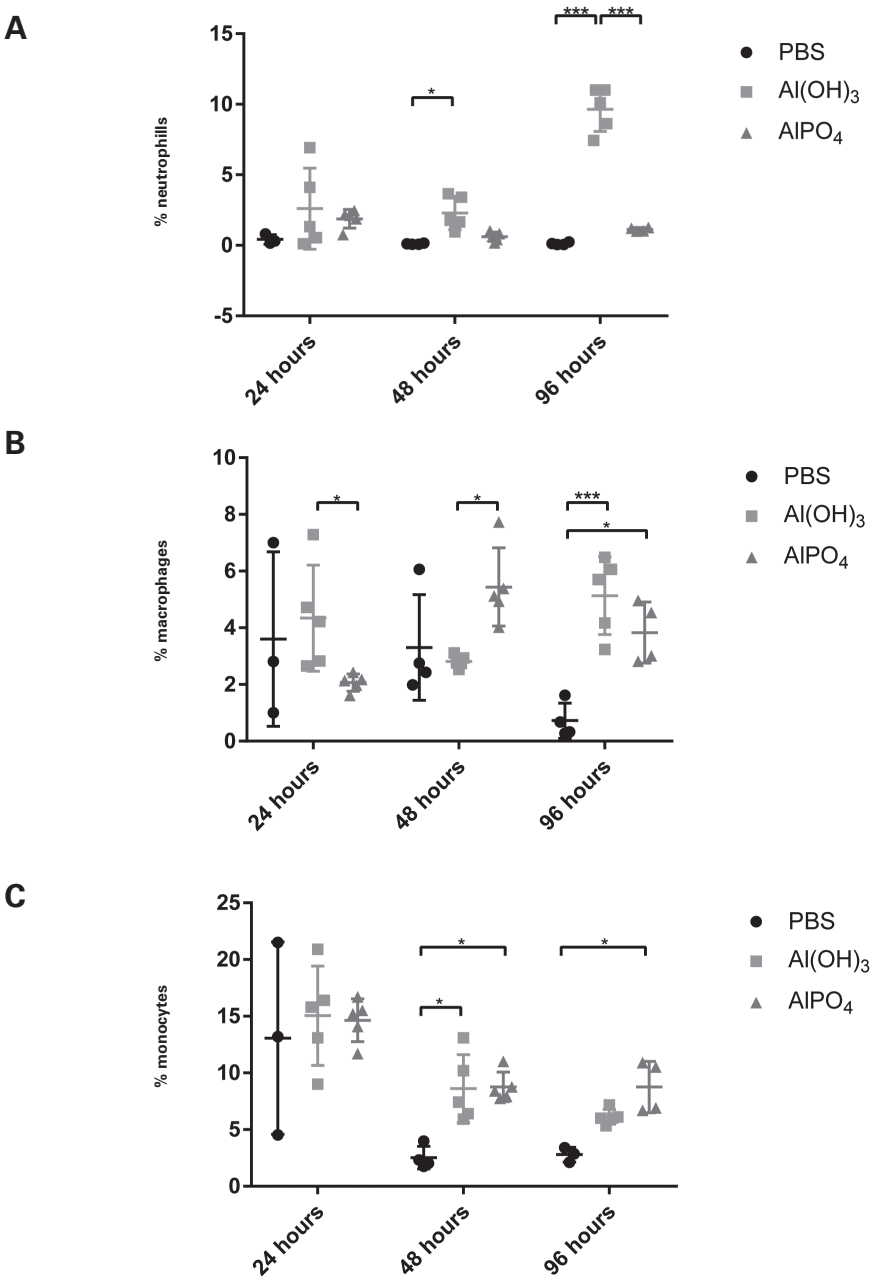

Figure 2. ***Cell populations at the site of injection in mice muscles.***
*Percentage of neutrophils (A), percentage of F4/80⁺ cells (macrophages) from single cells (B) and percentage of F4/80⁺CD11β⁺ (monocytes) cell of single cells isolated from muscle (C). Significance of difference was determined with a 2-way ANOVA with Tukey testing for multiple comparison, p-values <0.05 are indicated with an *, p-value <0.01 are indicated as ** and p-values <0.001 are indicated as***.*

Pathway	$Al(OH)_3$ 24 hrs up	$AlPO_4$ 24 hrs up	$Al(OH)_3$ 48 hrs up	$AlPO_4$ 48 hrs up	$Al(OH)_3$ 96 hrs up	$AlPO_4$ 96 hrs up
chemotaxis-related pathways						
neutrophil aggregation (GO:0070488)	2	2	3	2	2	2
neutrophil migration (GO:1990266)	2	1			1	
neutrophil chemotaxis (GO:0030593)	2	1			2	
mononuclear cell migration (GO:0071674)	1					
monocyte chemotaxis (GO:0002548)	1					
leukocyte cell-cell adhesion (GO:0007159)	2	2	2	1	2	2
leukocyte aggregation (GO:0070486)	2	1	2	2	1	1
leukocyte migration involved in inflammatory response (GO:0002523)	1	1	2	1	1	1
leukocyte chemotaxis (GO:0030595)	2	2	2	1	2	
granulocyte chemotaxis (GO:0071621)	3	3	2	2	2	1
positive regulation of cell-cell adhesion (GO:0022409)	2	1	2	2		1
chemotaxis (GO:0006935)	2	1	1	1	1	
immune system-related pathways						
regulation of cytokine secretion involved in immune response (GO:0002739)	1	1	2	2	1	1
negative regulation of cytokine production involved in immune response (GO:0002719)	1	1	1	1	1	1
regulation of cytokine secretion (GO:0050707)	1		1	1		
regulation of interleukin-8 production (GO:0032677)			1			
immune response (GO:0006955)	2	3	3	2	2	2
innate immune response (GO:0045087)	3	3	3	3	3	3
inflammatory response (GO:0006954)	2	2	2	2		2
acute-phase response (GO:0006953)	1					
adaptive immune response (GO:0002250)	1	1	2	2		1
negative regulation of immune system process (GO:0002683)	1				1	
negative regulation of immune effector process (GO:0002698)	2	2	2	1	2	
antimicrobial humoral response (GO:0019730)	2	2	2	2	2	2
induction of bacterial agglutination (GO:0043152)	2	2	2	2	2	2
antibacterial humoral response (GO:0019731)	1		1	1	1	
humoral immune response (GO:0006959)		2	2	2		1
defense response (GO:0006952)	3	3	3	3	2	3
wouding and chromatin proccsing pathwyas						
hemostasis (GO:0007599)	2	3	3	3	2	3
negative regulation of hemostasis (GO:1900047)	2	2	2	2		2
blood coagulation (GO:0007596)	2	3	3	3	2	3
wound healing (GO:0042060)	2	3	3	3	2	2
response to wounding (GO:0009611)	2	3	3	3	2	2
blood coagulation, fibrin clot formation (GO:0072378)	3	3	3	3	2	3
regulation of blood coagulation (GO:0030193)	3	3	3	3	2	3
chromatin assembly (GO:0031497)					1	
chromatin assembly or disassembly (GO:0006333)					1	
cell death-related pathways						
regulation of cell death (GO:0010941)	1	1	1			
regulation of programmed cell death (GO:0043067)	2	1	1	1		
negative regulation of extrinsic apoptotic signaling pathway (GO:2001237)	3	2	2	2	1	1
regulation of extrinsic apoptotic signaling pathway (GO:2001236)	2	2	1	1		1
negative regulation of apoptotic signaling pathway (GO:2001234)	2	1	1	1		
homeostasis-related pathways						
localization (GO:0051179)		1	1			
neutral lipid metabolic process (GO:0006638)	2	2	3		1	1
cholesterol metabolic process (GO:0008203)	1	2	3		1	1
lipoprotein metabolic process (GO:0042157)	1	2	3		1	1
positive regulation of metabolic process (GO:0009893)			2	1		1
neutral lipid catabolic process (GO:0046461)	3	2	3	1	2	2
positive regulation of lipid catabolic process (GO:0050996)	3	2	3	1	2	2

Figure 3. *Pathway analysis in mouse muscle cells.*
A subset of pathways extracted from Supplementary S5 that were upregulated by either $Al(OH)_3$ or $AlPO_4$ relative to PBS injected controls at 24, 48 and 96 hours post injection. The numbers 1-3 indicate the significance of the regulations with false discovery rates of <0.05, <0.01 and <0.001, respectively. The empty cells indicate that there was no regulation of the specific pathway for that stimulation condition.

After 96 hours of stimulation, the overlap in the upregulated proteins in mice muscles between $Al(OH)_3$ and $AlPO_4$ was 57%. Both adjuvants induced immune system-related processes, *e.g. innate immune response*, *(antimicrobial) humoral response*, *hemostasis* and *defense response*. In contrast to *immune cell/leukocyte aggregation*, which was upregulated by both adjuvants at all time points, $Al(OH)_3$ uniquely induced *neutrophil chemotaxis* and *neutrophil migration*, showing that pathways related to neutrophil influx are specifically upregulated by $Al(OH)_3$ (Figure 3), which is in agreement with the flow cytometry data, showing the presence of a large population of neutrophils upon $Al(OH)_3$ stimulation.

Other immunological processes that were upregulated by $Al(OH)_3$ were negative regulation or inhibition processes, *e.g. negative regulation of immune system process*, which could either represent tolerance to the adjuvant or the contraction phase after initiation. $AlPO_4$ specifically enhanced *positive regulation of cell-cell adhesion*, the *inflammatory response*, *adaptive immune response* and *negative regulation* (inhibition) *of hemostasis* (Figure 3).

These data prove that the innate immune response induced by both aluminum-based adjuvants is quite similar at 24 hours after injection, but after 96 hours differences were observed between $Al(OH)_3$ and $AlPO_4$ responses. This included strong induction of neutrophil-related pathways in $Al(OH)_3$-stimulated muscles, that was much less prominent after $AlPO_4$ injection. Also, there was a difference in the processes related to hemostasis after 96 hours: the adjuvants both induced and inhibited the processes of hemostasis, except after 96 hours when $Al(OH)_3$ only induced hemostasis.

Discussion

Aluminum-containing adjuvants are often used in human vaccines. Although the mechanisms of action have been extensively studied in recent years, comparison of the molecular responses to $Al(OH)_3$ *versus* $AlPO_4$ has not been performed. This study reveals that both $Al(OH)_3$ and $AlPO_4$ activate innate immune responses. However, two main differences were observed: *1*) antigen processing and presentation pathways in monocyte cultures were mainly upregulated by $Al(OH)_3$ and *2*) $Al(OH)_3$ attracted more neutrophils to the site of injection *in vivo*, possibly related to NET formation and hemostasis.

Activated monocytes play a fundamental role in antigen processing and presentation[22]. A clear difference was observed in the activation of antigen processing and presentation pathways between $Al(OH)_3$ and $AlPO_4$: $Al(OH)_3$ strongly activated the pathway of *antigen processing and presentation* in monocytes, both via HLA class I and HLA class II, as described previously[14, 17, 23], while $AlPO_4$ only induced a limited response. This may be related to the fact that $Al(OH)_3$ is taken up better by cells than $AlPO_4$[26]. This enhanced uptake is most likely related to the physicochemical properties of the adjuvants, in particular charge and size. With respect to charge, $Al(OH)_3$ is positively charged at physiological pH, even though this charge may be partly shielded by proteins and salts in the culture medium[26]. This positive charge of $Al(OH)_3$ allows for stronger interactions with the negatively charged cell membrane, compared to the slightly negatively charged $AlPO_4$[27]. With respect to size, $Al(OH)_3$ particles are expected to have a more suitable size (smaller) for phagocytosis by monocytes as compared to $AlPO_4$ as described by Mold *et al.*[26]. This is also observed in the current study, since only $Al(OH)_3$ activated phagocytosis. Thus, both size and charge probably lead to increased uptake of $Al(OH)_3$ and enhanced antigen processing and presentation as well as related pathways, *e.g. activation of immune response* and *innate immune response-activating signal transduction*.

The attraction of neutrophils to the site of injection was affected by $Al(OH)_3$ administration after 48 and 96 hours, but not after $AlPO_4$ administration. In agreement with this, $Al(OH)_3$ uniquely induced *neutrophil chemotaxis* and *neutrophil migration* after 96 hours. Neutrophils are capable of eliciting an inflammatory response by binding and ingesting bacteria when activated[28]. In addition, neutrophil presence can result in the formation of Neutrophil Extracellular Traps (NETs). Extracellular Traps (ETs) are networks of chromatin and histones, which are extruded from immune cells. NETs are specifically extruded from neutrophils and can trap and kill bacteria[29] and further amplify neutrophil recruitment upon $Al(OH)_3$ stimulation[30]. Moreover, neutrophils, both alive and dead due to netosis, contribute to the adjuvant effect of $Al(OH)_3$ by inducing antigen specific T cell expansion, B cell differentiation and B cell class switch in the presence of an antigen. Mice deficient in netosis had significantly less antigen specific T cells and germinal B cell centers[30]. This shows that trap formation indeed contributes to the adjuvant effect of $Al(OH)_3$ upon vaccination. Upon $AlPO_4$ administration, there was no increase observed in neutrophils at the site of injection, so $AlPO_4$ will probably not induce NET formation. However, the formation of nodules that resemble ETs was described previously for $AlPO_4$[31]. These ETs did not depend on the presence of neutrophils but on the presence of fibrinogen (FETs) and were induced by both $Al(OH)_3$ and

$AlPO_4$[31]. However, these FETs were observed after intraperitoneal administration of the adjuvants. Via this route, the adjuvants are exposed to many types of immune cells which are also able to form ETs[30, 32-33] implying that the route of administration may have an effect on ET formation.

The formation of NETs and FETs is also related to the processes of *hemostasis*[30-31, 34-36]. After 96 hours of $Al(OH)_3$ stimulation, hemostasis was upregulated by $Al(OH)_3$ and $AlPO_4$. However, only for $Al(OH)_3$ this coincided with the presence of a significant population of neutrophils and the enrichment of histone 1.3 and 2A, proteins that are often found in NETs[31]. Finally, also the pathways *neutrophil degranulation* and *neutrophil migration* were upregulated. Together, these data, for the 96 hours $Al(OH)_3$-administered group, are in agreement with NET formation that was found previously[30]. Other proteins found in (F)ETs were upregulated by both adjuvants, *e.g.* fibrinogen alpha chain and histone 4 (Supplementary S4). This upregulation of proteins associated with (F)ETs, upon both $Al(OH)_3$ and $AlPO_4$ stimulation implies that (F)ET formation might also occur upon I.M. injection of $Al(OH)_3$ and $AlPO_4$.

Attracting neutrophils to the site of injection and the activation of more immunological pathways by $Al(OH)_3$ implies that this is perhaps a more pro-inflammatory adjuvant compared to $AlPO_4$. This might result in more side effects since neutrophils also contain high levels of cytotoxic compounds, often associated with tissue inflammation and potential side effects[28]. Whether this results in a stronger adjuvant effect is not clear. Studies comparing the adjuvant effect of $Al(OH)_3$ or $AlPO_4$, *i.e.* in the presence of antigen, have been contradicting. Either no differences between the antibody titers were reported[27, 37-38] or a trend towards a stronger response towards antigen adsorbed to $AlPO_4$[27] or a better response when $Al(OH)_3$ was used as an adjuvant[20]. The stronger response towards $Al(OH)_3$ was associated with higher adsorption of the antigen to $Al(OH)_3$[20]. Other potential explanations might be, intrinsic immunogenicity of the adjuvant, as suggested by Berthold *et al.*, antigen-adjuvant ratio and the dose of both the adjuvant and the antigen[38]. Finally, the ability of the antigen to desorb from the adjuvant when bound can also be involved. If the interaction is too strong, the adjuvant effect can be negatively influenced as reviewed by Clapp *et al.*[18].

One major difference between the mechanisms identified *in vitro* and *in vivo* is that, unlike the *in vitro* data, indications for antigen processing and presentation were not identified in the *in vivo* data. The reason for this difference is not known. $Al(OH)_3$ may be coated by serum proteins present in the culture medium which might result in the cell entrance of adjuvant-serum protein complexes during *in vitro* experiments. This might not happen *in vivo*, upon $Al(OH)_3$ I.M. injection since interstitial fluid is lower in protein content compared to serum[39-40]. In addition, proteins in culture medium might be identified as non-self (enhanced antigen presentation) while proteins in interstitial fluid are self. However, enhanced antigen processing and presentation upon $Al(OH)_3$ I.M. injection was described previously[17]. The reason that this is not identified in the current study could be that different outcome parameters are used: mRNA versus protein, *in vivo* the expression of antigen processing-related proteins might occur predominantly at different locations, *e.g.* draining lymph nodes, or the presence of other APCs than only monocytes.

Some mechanisms of action of alum-based adjuvants were confirmed in this study, *e.g. in vitro* upregulation of *complement activation* and *cell death* by $Al(OH)_3$[12-14] and *recruitment of immune cells to the site of injection* by both $Al(OH)_3$ and $AlPO_4$[8, 9, 41-42]. In

addition, differences between in the innate immune response after $Al(OH)_3$ or $AlPO_4$ stimulation were observed *in vitro*. However, it needs to be taken into account that we have analyzed the cellular proteins and not the secreted proteins. In addition, some processes related to $Al(OH)_3$ adjuvant activity require the presence of an antigen or other additional components, such as activation of the inflammasome[43]. *In vitro* culture of monocytes was studied, in which effects of interaction between different cell types cannot be taken into account.

The current study demonstrates that two commercially available aluminum-based adjuvants, $Al(OH)_3$ and $AlPO_4$, have a very distinct impact on the innate immune response both *in vitro* on human primary monocytes as well as *in vivo* in mice. Based on current data, $Al(OH)_3$ induces a more immunogenic response compared to $AlPO_4$ since $Al(OH)_3$ upregulated antigen processing and presentation pathways more strongly than $AlPO_4$. Additionally much more immune system-related pathways were induced by $Al(OH)_3$ and *in vivo* more neutrophils were attracted to the site of injection as compared to $AlPO_4$.

References

1. Glenny, A. T.; Pope, C. G.; Waddington, H.; Wallace, U., Immunological notes. XVII–XXIV. *The Journal of Pathology and Bacteriology* 1926, *29* (1), 31-40.
2. Gupta, R. K., Aluminum compounds as vaccine adjuvants. *Adv Drug Deliv Rev* 1998, *32* (3), 155-172.
3. Glenny, A. T.; Buttle, G. A. H.; Stevens, M. F., Rate of disappearance of diphtheria toxoid injected into rabbits and guinea - pigs: Toxoid precipitated with alum. *The Journal of Pathology and Bacteriology* 1931, *34* (2), 267-275.
4. Seubert, A.; Monaci, E.; Pizza, M.; O'Hagan, D. T.; Wack, A., The adjuvants aluminum hydroxide and MF59 induce monocyte and granulocyte chemoattractants and enhance monocyte differentiation toward dendritic cells. *J Immunol* 2008, *180* (8), 5402-12.
5. Verdier, F.; Burnett, R.; Michelet-Habchi, C.; Moretto, P.; Fievet-Groyne, F.; Sauzeat, E., Aluminium assay and evaluation of the local reaction at several time points after intramuscular administration of aluminium containing vaccines in the Cynomolgus monkey. *Vaccine* 2005, *23* (11), 1359-1367.
6. Brewer, J. M.; Conacher, M.; Hunter, C. A.; Mohrs, M.; Brombacher, F.; Alexander, J., Aluminium hydroxide adjuvant initiates strong antigen-specific Th2 responses in the absence of IL-4- or IL-13-mediated signaling. *J Immunol* 1999, *163* (12), 6448-54.
7. Calabro, S.; Tortoli, M.; Baudner, B. C.; Pacitto, A.; Cortese, M.; O'Hagan, D. T.; De Gregorio, E.; Seubert, A.; Wack, A., Vaccine adjuvants alum and MF59 induce rapid recruitment of neutrophils and monocytes that participate in antigen transport to draining lymph nodes. *Vaccine* 2011, *29* (9), 1812-23.
8. McKee, A. S.; Munks, M. W.; MacLeod, M. K.; Fleenor, C. J.; Van Rooijen, N.; Kappler, J. W.; Marrack, P., Alum induces innate immune responses through macrophage and mast cell sensors, but these sensors are not required for alum to act as an adjuvant for specific immunity. *J Immunol* 2009, *183* (7), 4403-14.
9. Sokolovska, A.; Hem, S. L.; HogenEsch, H., Activation of dendritic cells and induction of CD4(+) T cell differentiation by aluminum-containing adjuvants. *Vaccine* 2007, *25* (23), 4575-85.
10. Kool, M.; Petrilli, V.; De Smedt, T.; Rolaz, A.; Hammad, H.; van Nimwegen, M.; Bergen, I. M.; Castillo, R.; Lambrecht, B. N.; Tschopp, J., Cutting edge: alum adjuvant stimulates inflammatory dendritic cells through activation of the NALP3 inflammasome. *J Immunol* 2008, *181* (6), 3755-9.
11. Li, H.; Willingham, S. B.; Ting, J. P.; Re, F., Cutting edge: inflammasome activation by alum and alum's adjuvant effect are mediated by NLRP3. *J Immunol* 2008, *181* (1), 17-21.
12. Guven, E.; Duus, K.; Laursen, I.; Hojrup, P.; Houen, G., Aluminum hydroxide adjuvant differentially activates the three complement pathways with major involvement of the alternative pathway. *PLoS One* 2013, *8* (9), e74445.
13. Marichal, T.; Ohata, K.; Bedoret, D.; Mesnil, C.; Sabatel, C.; Kobiyama, K.; Lekeux, P.; Coban, C.; Akira, S.; Ishii, K. J.; Bureau, F.; Desmet, C. J., DNA released from dying host cells mediates aluminum adjuvant activity. *Nat Med* 2011, *17* (8), 996-1002.
14. McKee, A. S.; Burchill, M. A.; Munks, M. W.; Jin, L.; Kappler, J. W.; Friedman, R. S.; Jacobelli, J.; Marrack, P., Host DNA released in response to aluminum adjuvant enhances MHC class II-mediated antigen presentation and prolongs CD4 T-cell interactions with dendritic cells. *Proc Natl Acad Sci U S A* 2013, *110* (12), E1122-31.
15. Kool, M.; Soullie, T.; van Nimwegen, M.; Willart, M. A.; Muskens, F.; Jung, S.; Hoogsteden, H. C.; Hammad, H.; Lambrecht, B. N., Alum adjuvant boosts adaptive immunity by inducing uric acid and activating inflammatory dendritic cells. *J Exp Med* 2008, *205* (4), 869-82.
16. Oh, D.Y.; Dowling, D. J.; Ahmed, S.; Choi, H.; Brightman, S.; Bergelson, I.; Berger, S. T.; Sauld, J. F.; Pettengill, M.; Kho, A. T.; Pollack, H. J.; Steen, H.; Levy, O., Adjuvant-induced Human Monocyte Secretome Profiles Reveal Adjuvant- and Age-specific Protein Signatures. *Mol Cell Proteomics* 2016, *15* (6), 1877-94.

17. Mosca, F.; Tritto, E.; Muzzi, A.; Monaci, E.; Bagnoli, F.; Iavarone, C.; O'Hagan, D.; Rappuoli, R.; De Gregorio, E., Molecular and cellular signatures of human vaccine adjuvants. *Proc Natl Acad Sci U S A* 2008, *105* (30), 10501-6.

18. Clapp, T.; Siebert, P.; Chen, D.; Jones Braun, L., Vaccines with aluminum-containing adjuvants: optimizing vaccine efficacy and thermal stability. *J Pharm Sci* 2011, *100* (2), 388-401.

19. Exley, C.; Siesjo, P.; Eriksson, H., The immunobiology of aluminium adjuvants: how do they really work? *Trends Immunol* 2010, *31* (3), 103-9.

20. Westdijk, J.; Koedam, P.; Barro, M.; Steil, B. P.; Collin, N.; Vedvick, T. S.; Bakker, W. A.; van der Ley, P.; Kersten, G., Antigen sparing with adjuvanted inactivated polio vaccine based on Sabin strains. *Vaccine* 2013, *31* (9), 1298-304.

21. Hansen, B.; Sokolovska, A.; HogenEsch, H.; Hem, S. L., Relationship between the strength of antigen adsorption to an aluminum-containing adjuvant and the immune response. *Vaccine* 2007, *25* (36), 6618-24.

22. Jakubzick, C. V.; Randolph, G. J.; Henson, P. M., Monocyte differentiation and antigen-presenting functions. *Nat Rev Immunol* 2017, *17* (6), 349-362.

23. Kooijman, S.; Brummelman, J.; van Els, C.; Marino, F.; Heck, A. J. R.; Mommen, G. P. M.; Metz, B.; Kersten, G. F. A.; Pennings, J. L. A.; Meiring, H. D., Novel identified aluminum hydroxide-induced pathways prove monocyte activation and pro-inflammatory preparedness. *J Proteomics* 2018.

24. Moruz, L.; Pichler, P.; Stranzl, T.; Mechtler, K.; Kall, L., Optimized nonlinear gradients for reversed-phase liquid chromatography in shotgun proteomics. *Anal Chem* 2013, *85* (16), 7777-85.

25. Mi, H.; Huang, X.; Muruganujan, A.; Tang, H.; Mills, C.; Kang, D.; Thomas, P. D., PANTHER version 11: expanded annotation data from Gene Ontology and Reactome pathways, and data analysis tool enhancements. *Nucleic Acids Res* 2017, *45* (D1), D183-D189.

26. Mold, M.; Shardlow, E.; Exley, C., Insight into the cellular fate and toxicity of aluminium adjuvants used in clinically approved human vaccinations. *Sci Rep* 2016, *6*, 31578.

27. Caulfield, M. J.; Shi, L.; Wang, S.; Wang, B.; Tobery, T. W.; Mach, H.; Ahl, P. L.; Cannon, J. L.; Cook, J. C.; Heinrichs, J. H.; Sitrin, R. D., Effect of alternative aluminum adjuvants on the absorption and immunogenicity of HPV16 L1 VLPs in mice. *Hum Vaccin* 2007, *3* (4), 139-45.

28. Kobayashi, S. D.; DeLeo, F. R., Role of neutrophils in innate immunity: a systems biology-level approach. *Wiley Interdiscip Rev Syst Biol Med* 2009, *1* (3), 309-33.

29. Brinkmann, V.; Reichard, U.; Goosmann, C.; Fauler, B.; Uhlemann, Y.; Weiss, D. S.; Weinrauch, Y.; Zychlinsky, A., Neutrophil extracellular traps kill bacteria. *Science* 2004, *303* (5663), 1532-5.

30. Stephen, J.; Scales, H. E.; Benson, R. A.; Erben, D.; Garside, P.; Brewer, J. M., Neutrophil swarming and extracellular trap formation play a significant role in Alum adjuvant activity. *NPJ Vaccines* 2017, *2*, 1.

31. Munks, M. W.; McKee, A. S.; Macleod, M. K.; Powell, R. L.; Degen, J. L.; Reisdorph, N. A.; Kappler, J. W.; Marrack, P., Aluminum adjuvants elicit fibrin-dependent extracellular traps in vivo. *Blood* 2010, *116* (24), 5191-9.

32. Goldmann, O.; Medina, E., The expanding world of extracellular traps: not only neutrophils but much more. *Front Immunol* 2012, *3*, 420.

33. Doster, R. S.; Rogers, L. M.; Gaddy, J. A.; Aronoff, D. M., Macrophage Extracellular Traps: A Scoping Review. *J Innate Immun* 2018, *10* (1), 3-13.

34. Savchenko, A. S.; Martinod, K.; Seidman, M. A.; Wong, S. L.; Borissoff, J. I.; Piazza, G.; Libby, P.; Goldhaber, S. Z.; Mitchell, R. N.; Wagner, D. D., Neutrophil extracellular traps form predominantly during the organizing stage of human venous thromboembolism development. *J Thromb Haemost* 2014, *12* (6), 860-70.

35. Jenne, C. N.; Urrutia, R.; Kubes, P., Platelets: bridging hemostasis, inflammation, and immunity. *Int J Lab Hematol* 2013, *35* (3), 254-61.

36. Martinod, K.; Wagner, D. D., Thrombosis: tangled up in NETs. *Blood* 2014, *123* (18), 2768-76.

37. Fenje, P.; Pinteric, L., Potentiation of tissue culture rabies vaccine by adjuvants. *Am J Public Health Nations Health* 1966, *56* (12), 2106-13.

38. Berthold, I.; Pombo, M. L.; Wagner, L.; Arciniega, J. L., Immunogenicity in mice of anthrax recombinant protective antigen in the presence of aluminum adjuvants. *Vaccine* 2005, *23* (16), 1993-9.

39. Sloop, C. H.; Dory, L.; Roheim, P. S., Interstitial fluid lipoproteins. *J Lipid Res* 1987, *28* (3), 225-37.

40. Ellmerer, M.; Schaupp, L.; Brunner, G. A.; Sendlhofer, G.; Wutte, A.; Wach, P.; Pieber, T. R., Measurement of interstitial albumin in human skeletal muscle and adipose tissue by open-flow microperfusion. *Am J Physiol Endocrinol Metab* 2000, *278* (2), E352-6.

41. Lambrecht, B. N.; Kool, M.; Willart, M. A.; Hammad, H., Mechanism of action of clinically approved adjuvants. *Curr Opin Immunol* 2009, *21* (1), 23-9.

42. HogenEsch, H., Mechanisms of stimulation of the immune response by aluminum adjuvants. *Vaccine* 2002, *20 Suppl 3*, S34-9.

43. Cullen, S. P.; Kearney, C. J.; Clancy, D. M.; Martin, S. J., Diverse Activators of the NLRP3 Inflammasome Promote IL-1beta Secretion by Triggering Necrosis. *Cell Rep* 2015, *11* (10), 1535-48.

Supplementary figures

Supplementary S1. ***Raw and normalized proteomics data from human monocytes.***
Results table generated by Proteome Discoverer 2.1. Each multiplex refers to a TMT(10)-plex containing quantitative ratios compared to control for both $Al(OH)_3$ and $AlPO_4$. The raw data were combined in one output table 'raw data combined'. The data was median-normalized (presented in the worksheet 'normalized data') and the upregulated proteins (fold change >1.5) per condition are given in the worksheet 'upregulated protein table'. Downregulated proteins (fold change <0.667) are depicted in the worksheet 'downregulated protein table'.

Supplementary S2. ***GO term analysis of up and downregulated proteins.***
GO terms represented by the upregulated proteins in human primary monocytes after stimulation with $Al(OH)_3$ or $AlPO_4$ for 24 or 48 hours. The table shows the GO_ID of the enriched processes in the set of upregulated proteins after 24 and 48 hours of $Al(OH)_3$ or $AlPO_4$ stimulation. The table depicts the GO term, the number of proteins identified in the dataset and the FDR of the process enrichment.

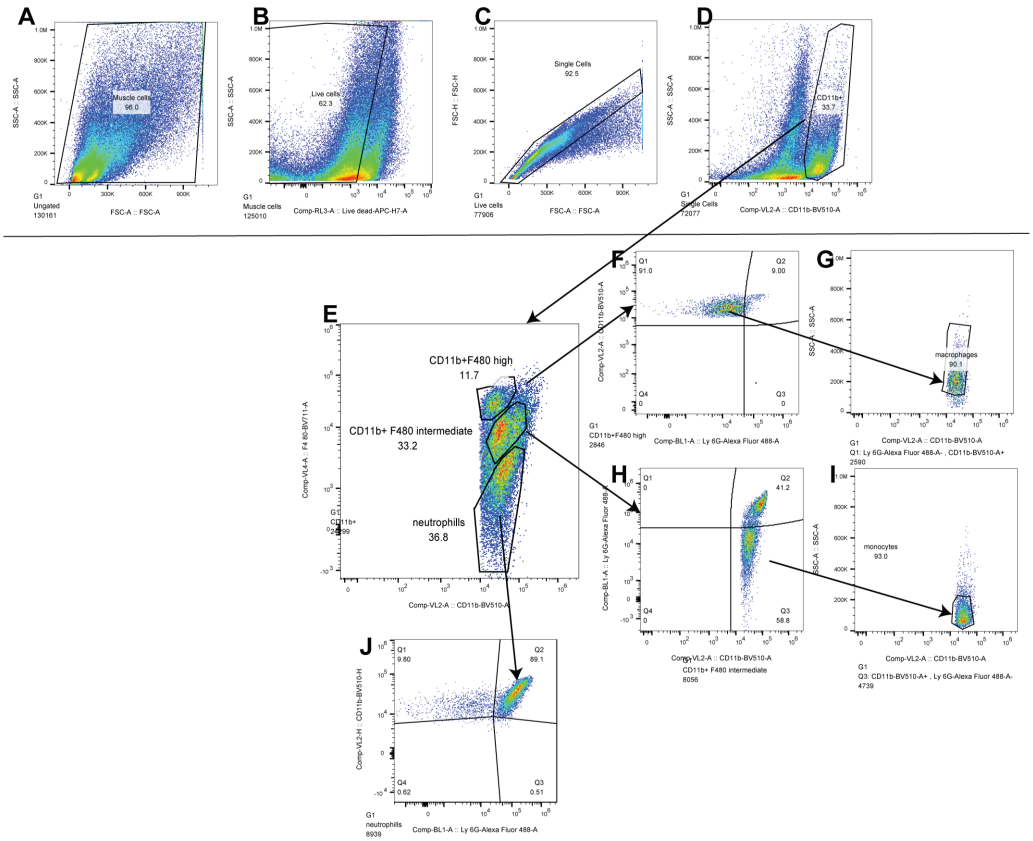

Supplementary S3. ***Gating staining strategy applied to flow cytometric analysis of mice muscle cells.***

Gating strategy is presented for (A) the cell gate, (B) the live cell gate, (C) the single cell gate and (D) the CD11b$^+$ gate. Further gating of markers is given for (E) gating on F4/80: F4/80$^-$, F4/80$^\pm$ and F4/80$^+$, (F) the Ly6g$^-$CD11b$^+$ F4/80$^+$ gate, (G) the macrophage gate (Ly6g$^-$CD11b$^+$ F4/80$^\pm$ SSC low SSC intermediate), (H) the Ly6g$^-$CD11b$^+$ F4/80$^\pm$ gate, (I) the monocyte gate (Ly6g$^-$CD11b$^+$ F4/80$^\pm$ SSC low) and (J) the neutrophil gate (CD11b$^+$Ly6G$^+$ F4/80$^-$).

Supplementary S4. ***Raw and normalized proteomics data from mouse muscle tissue.***

The labels of the individual samples can be found in 'labels'. Raw data per condition per run is depicted in 'raw data' and normalized data is depicted in the tab 'normalized'. The median for up and down-regulated protein determination is given in 'Stat.Median'.

Supplementary S5. ***Proteomics pathway analysis of mouse muscle tissue.***

All pathways that are overrepresented in the upregulated protein set after 24, 48 and 96 hours of $Al(OH)_3$ or $AlPO_4$ stimulation. The table depicts the GO term, the number of proteins in the pathway, the number of upregulated proteins in the pathway the FDR.

Acknowledgement

Sietske Kooijman is funded by a strategic research grant (SOR) of the Ministry of Health (IS200107). This work was also partly supported by the Proteins@Work, a program of the Netherlands Proteomics Centre financed by the Netherlands Organisation for Scientific Research (NWO) as part of the National Roadmap Large-scale Research Facilities of the Netherlands (project number 184.032.201).We acknowledge the colleagues from the Animal Research Center for their contribution to this study.

Chapter 5

The size and shape of aluminum hydroxide particles determine the innate immune response in human monocytes

*Sietske Kooijman[1,2], *Hilde Vrieling[1,3], Justin de Ridder[1], Wim Jiskoot[3], Elly van Riet[1], Albert Heck[2,4], Gideon Kersten[1,3], Hugo Meiring[1], Bernard Metz[1]

Manuscript in preparation

* Authors contributed equally

1 Intravacc (Institute for Translational Vaccinology), Bilthoven, the Netherlands
2 Biomolecular Mass Spectrometry and Proteomics, Bijvoet Center for Biomolecular Research and Utrecht Institute for Pharmaceutical Sciences, Science Faculty, Utrecht University, the Netherlands
3 Division of Drug Delivery Technology, Leiden Academic Centre for Drug Research (LACDR), Leiden University, Leiden, the Netherlands
4 Netherlands Proteomics Centre, Utrecht, the Netherlands

Keywords: Aluminum salts; vaccine adjuvant; nanoparticles; molecular mechanism; proteomics

Abstract

Background Aluminum salts are widely used vaccine adjuvants. These salts consist of micrometre-sized aggregates. In the past decades, nanoparticles have emerged as promising adjuvant candidates. In this study, the responses of human monocytes to aluminum hydroxide nanoparticles (hexagonal-shaped gibbsite) and aluminum oxyhydroxide nanoparticles (needle-shaped boehmite) were investigated and compared with classical aluminum oxyhydroxide (Alhydrogel®).

Methods Human primary monocytes were cultured in the presence of Alhydrogel®, gibbsite or boehmite. The transcriptome and proteome were investigated using quantitative polymerase chain reaction and mass spectrometry. In addition, human monocytic THP-1 cells were used to investigate the cellular maturation, differentiation and cytokine secretion, which was demonstrated by enzyme-linked immuno sorbent assay and flow cytometry.

Results Alhydrogel®, gibbsite and boehmite caused changes in gene expression related to the pro-inflammatory interferons and the Th2 polarizing cytokine IL-4. In addition, each compound resulted in a specific gene expression profile. After 24 hours, Alhydrogel® specifically induced the pro-inflammatory cytokine IL-2, which was down-regulated by the nanoparticles. Both nanoparticles increased the expression of the immune system-related transcription factor NFκb1. Proteome analysis revealed that Alhydrogel® activated both homeostatic and immunological pathways after 24 hours of stimulation. Gibbsite and boehmite induced limited activation of both immunogenic and homeostatic pathways. After 48 hours, the effect of Alhydrogel® was even stronger than the response after 24 hours, while boehmite induced a more specific immune system-related (non-homeostatic) response. Of the seven surface markers investigated, only CD80 was significantly upregulated by Alhydrogel® and neither by gibbsite or boehmite. IL-1β secretion was significantly upregulated by Alhydrogel®.

Conclusion The *in vitro* innate immune response induced by adjuvants depends on the composition, size and shape of the adjuvant. Boehmite induced a stronger immune response and a less stress response-related response and is therefore a promising nanoparticle adjuvant candidate.

Introduction

Many prophylactic vaccines contain adjuvants, which enhance the immune response after vaccination. Aluminum-based adjuvants activate and maturate antigen-presenting cells (APCs), which have a key role in the activation of the specific immune system[1]. Traditional aluminum-based adjuvants consist of aluminum salts that form aggregates of 0.5-10 µm upon dispersion in water[2]. However, aluminum-based nanoparticles have drawn the attention to improve the immune response compared to the traditional adjuvants[3,4]. In the past decades, studies investigating the effect of size and shape of aluminum-based nanoparticles on the immune response have been performed. For example, ovalbumin and *Bacillus anthracis* antigens induced a stronger antigen-specific antibody response in mice when adsorbed to nanoparticles of aluminum hydroxide than microparticles[5]. In addition, Sun *et al.* found that the size of aluminum oxyhydroxide nanorods was positively related to the adaptive humoral immune response using ovalbumin as model antigen, and that rod-shaped nanoparticles were more potent adjuvants compared to plates and polyhedra[6]. Moreover, aluminum (oxy)hydroxide nanoparticles induced higher levels of uric acid compared to microparticles both *in vitro* and *in vivo*[7]. Thus, aluminum hydroxide nanoparticles may have a stronger adjuvant effect than microparticles. These studies mostly address the adaptive immune response and so have been done in the presence of antigen. Not much is known about the intrinsic capacity of these particles to activate the innate immune system.

To investigate the role of adjuvants, classical immunological assays such as enzyme-linked immuno sorbent assay (ELISA), multiplex immune assays and flow cytometry, have been utilised, analysing secreted proteins and cell surface markers, respectively, to profile the immune response. However, modern, systems-based omics-approaches, analysing protein expression and mRNA expression, may attribute to further unravelling the molecular signatures that are induced by adjuvants[8]. Few studies have been done on the analysis of protein and gene expression. For example, the secretome of human monocytes stimulated *in vitro* with Adju-Phos®, MPLA and R848 in absence of an antigen or complete vaccines have been investigated with mass spectrometry[9]. In addition, Alhydrogel®, MF59 and CPG induced distinct gene expression profiles at the site of injection in mouse muscle cells without the presence of an antigen[10]. Transcriptome and proteome analysis may thus help to unravel the mechanism by which adjuvants work.

In this study, two experimental aluminum (oxy)hydroxides, gibbsite and boehmite, and a commercially available aluminum oxyhydroxide adjuvant (Alhydrogel®, often referred to as aluminum hydroxide) were used to identify differences of the size and shape on the innate immune response. The effects of these particles on the transcriptome and proteome in human monocytes were investigated and related to cellular pathways. The results demonstrate that the size and shape of aluminum salts influence the induction of the innate immune response.

Materials and methods

Materials

Alhydrogel® 2% (batch 9394) was purchased from Brenntag Biosector. Ultrapure lipopolysaccharide (LPS) from E. coli K was obtained from Invivogen. Bovine serum albumin (BSA), ethylenediaminetetraacetic acid (EDTA), aluminum-iso-propoxide, aluminum-*sec*-butoxide, $AlCl_3$, dodecyltrimethylammonium bromide, Eriochrome cyanide R and Ficoll® were purchased from Sigma-Aldrich.

Hank's balanced salt solution (HBSS) was purchased from Gibco. Phosphate-buffered saline (PBS, 10.6 mM KH_2PO_4, 1.5 M NaCl, 29.7 mM Na_2HPO_4) pH 7.2, Roswell Park Memorial Institute Media 1640 (RPMI) and Penicillin/Streptomycin/L-Glutamin (P/S/G) were obtained from Invitrogen (ThermoFisher Scientific). Fetal calf serum (FCS) was purchased from Serana.

Human CD14 microbeads were from Miltenyi Biotec. Fluorescently labelled antibodies CD83-APC (HB15E), CD40-BV711 (5C3), CD86-BV510 (FUN-1), CD14-PE (H5E2), CD11c-BV421 (B-ly6/3.9) and CD80-BB515 (L307.4), and Fixable Viability Stain 780 were obtained from BD Biosciences (New Yersey, USA). HLA-DR-PerCP (L243) was purchased from BioLegend.

Human IL-1β ELISA Ready-Set-Go! was from eBioscience (ThermoFisher Scientific). IL-6 human uncoated ELISA kits were from Invitrogen (ThermoFisher Scientific). Human IL-18 matched antibody pair was from Invitrogen (ThermoFisher Scientific).

Synthesis of boehmite and gibbsite

Boehmite and gibbsite were synthesised as previously described by Buining *et al*[11]. Briefly, 80 mM aluminum-iso-propoxide was mixed with 80 mM aluminum-*sec*-butoxide in 90 mM HCl. The solution was stirred for at least 10 days. After hydrothermal treatment at 150°C (boehmite) or 85°C (gibbsite) for 36h, the suspension was dialysed against water (MilliQ, resistivity = 18.2 MΩ.cm, total organic carbon < 5 ppb) using dialysis cassettes with a cut-off of 10,000 Da for at least 14 days. During this procedure, the dialysate was replaced at least 8 times. Suspensions were autoclaved and stored at room temperature.

Aluminum determination

The quantification of Al^{3+} ions was performed using a colorimetric assay. Standards were prepared by diluting 150 µM $AlCl_3$ in 6 M KOH so that the final range of the calibration line was 0-15 µM Al^{3+} ions. Samples were diluted in 6 M KOH so that the maximum concentration Al^{3+} ions was not higher than 0.85 mM. Samples were heated at 100°C for 60 min to dissolve aluminum salts. After cooling to RT, standards and samples were diluted in 1 M sodium acetate buffer pH 5.5 so that the expected final concentration was between 0.1 and 8.5 nM Al^{3+}. 50 µL of each sample or standard was added to a transparent polystyrene flat-bottom 96-wells plate (Greiner bio one) in triplicate. To each well, 50 µL of 12 mM dodecyltrimethylammonium bromide, 50 µL of 600 µM Eriochrome cyanide R and 50 µL of 1 M sodium acetate buffer pH 5.5 was added. The plate was incubated on a plate shaker at 600 rpm at RT for 15 min. The absorbance was determined at 584 nm using a SynergyMx reader (BioTek). Aluminum

concentrations in samples were calculated based on the standard curve using Gentech 5 software (BioTek).

Transmission Electron Microscopy (TEM)

Transmission electron microscopy (TEM) was performed using a Philips Tecnai 10 electron microscope, typically operating at 100kV. The samples were prepared by drying a drop of diluted, aqueous particle dispersion on top of polymer-coated copper grids.

Dynamic Light Scattering (DLS)

The hydrodynamic size was measured by DLS using a zetasizer (Zetasizer Nano ZS, Malvern Instruments Ltd.). 60 µL of each sample diluted 80x (Alhydrogel®) or 8x (gibbsite and boehmite) in 1 mM NaCl or cell culture medium was measured in single-use polystyrene UV micro cuvettes (BRAND®). The Dispersion Technology Software (version 7.11) was used for collection and analysis of the data. Each sample was measured at 25°C in triplicate with an automatic attenuator. The number of runs and the measurement duration were automatically optimised by the software.

Laser-Doppler electrophoresis

The zeta potential was measured using a zetasizer (Zetasizer Nano ZS, Malvern Instruments Ltd.). Folded capillary cells (DTS1070, Malvern Instruments Ltd.) were filled with 800 µL sample containing 1.2 mg/mL Al^{3+} ions diluted in 1 mM NaCl or in cell culture medium. The Dispersion Technology Software (version 7.11) was used for collection and analysis of the data. Each sample was measured at 25°C in triplicate with an automatic attenuator. The number of runs and the measurement duration were automatically optimised by the software.

Cell culture

The human monocyte study was conducted according to the principles expressed in the Declaration of Helsinki. All blood donors gave written-informed consent before collection and use of their samples. All blood donations, provided by the Dutch National Institute for Public Health and the Environment (RIVM, Bilthoven, the Netherlands) were specifically donated for primary cell isolation. This research goal was explicitly approved by the accredited Medical Research Ethics Committee (MREC), METC, Noord-Holland in the Netherlands. All blood samples were processed anonymously.

Fresh peripheral blood was collected from healthy volunteers and collected in heparin-coated tubes. Peripheral blood mononuclear cells (PBMCs) were isolated from whole blood using Ficoll® density centrifugation at 1000x*g* for 30 min. Monocytes were isolated by positive selection using CD14 microbeads and a magnetic LS MACS column (Miltenyi Biotech). Monocytes were cultured at 400,000 cells/well in 24-wells plates in cell culture medium (RPMI containing 10% FCS, 100 units/mL penicillin, 100 µg/mL streptomycin and 0.3 µg/mL L-glutamine) in the presence of Alhydrogel®, gibbsite or boehmite (each at a concentration of 10 µg/mL Al^{3+} ions), in the presence of 100 ng/mL LPS or were left unstimulated for 6, 24 or 48 hours.

Human THP-1 cells were grown in cell culture medium at 37°C with 5% CO_2. Cells were primed overnight with 300 ng/mL PMA in a 96-wells plate containing 100,000 cells/well in 200 µL. After priming, cells were washed three times with culture medium by centrifugation at 300x*g* for 5 min. The supernatant was discarded and Alhydrogel®,

gibbsite and boehmite were added at a final concentration of 0.1 mg/mL Al^{3+} ions in the presence of 2.5 ng/mL LPS in culture medium in a total volume of 200 µL/well. Cells were incubated at 37°C with 5% CO_2 for 24h and centrifuged at 300x*g* for 5 min. Supernatants (170 µL/well) were stored at -20 °C until further use. Cells were immediately processed for surface marker analysis as described under"flow cytometry".

Flow cytometry

After 24h of stimulation, THP-1 cells were washed twice with FACS buffer (0.5% BSA and 0.5 mM EDTA in PBS, pH 7.2) by centrifugation at 300x*g* for 3 min. After centrifugation (300x*g*, 3 min) pellets were resuspended in 100 µL FACS buffer containing CD83-APC (HB15E), CD40-BV711 (5C3), CD86-BV510 (FUN-1), CD14-PE (H5E2), CD11c-BV421 (B-ly6/3.9), CD80-BB515 (L307.4) or HLA-DR-PerCP (L243) in a 1:20 dilution. Cells were incubated at 4°C for 30 min. After staining, cells were washed with FACS buffer and resuspended in 150 µL FACS buffer. Cell populations were analysed by flow cytometry using Attune NxT (Thermo Fisher Scientific). Attune™ NxT Software V2.6 was used for data collection. Samples were analysed using FlowJo software, version 10.2 (Treestar). Surface marker expression is reported as the percentage of cells in the positive gate using unstained controls per stimulation. The gating strategy can be observed in Supplementary S1.

Cytokine secretion

Cytokine concentrations (IL-1β, IL-4, IL-6, IL-10, IL-17A and IL-18) were measured in the culture supernatants of primary monocytes and THP-1 cells using ELISA kits according to the manufacturer's instructions. The light absorbance was determined at 450 nm using a SynergyMx reader (BioTek). Cytokine concentrations in samples were calculated based on the standard curves using Gentech 5 software (BioTek).

mRNA expression

The mRNA produced by 89 genes which are involved in innate and adaptive immunity and 7 controls were determined. Monocytes were lysed with RLT buffer (Qiagen). Subsequently, mRNA was extracted using the RNeasy mini kit (Qiagen), according to the manufacturer's animal cell spin protocol. RNA purity and concentration were determined using spectrophotometric analysis at 260 nm and 280 nm, samples were measured on a Synergy MX (Biotek). Depending on the amount of mRNA available, 10 or 12 ng of cDNA was synthesised. Each sample was compared to a control sample with the same amount of cDNA. Analysis was performed using the RT cDNA synthesis kit and the RT preAMP Pathway primer mix"Innate and Adaptive immunity" (Qiagen) according to the manufacturer's protocol. cDNA was stored at -20°C.

Subsequently, qPCR analysis was executed with the 'Innate and Adaptive Immune response RT2 profiler arrays' (Qiagen), comprising 89 functional genes and 7 controls for determining the reliability of the experiments. The PCR was performed using the Roche light cycler 96 (Roche). Melting curves were measured of each cDNA and were included for quality control.

The PCR array contained 5 housekeeping genes (ACTβ, β2M, GAPDH, HPRT1 and RPLP0). For each time point, the four most stable housekeeping genes were used in the calculations (β2M, GAPDH, HPRT1 and RPLP0 after 6 hour of stimulation; ACTβ, β2M, HPRT1 and RPLP0 after 24 hours of stimulation). The Ct values of these four

genes were averaged to a general housekeeping gene value. The target gene expression values of each gene were normalised based on the general value (Supplementary S2). Changes in target gene expression *versus* medium control were calculated as the ΔΔCt. Expression changes for three donors were compared and genes that showed a twofold increase or decrease in at least two out of three biological replicates were considered differentially expressed. For these genes the median values across the three biological replicates were visualised as a heatmap combined with hierarchical clustering (Euclidean distance, Ward.D linkage) using R statistical software (version 3.4.0).

Isolation, digestion and labelling of proteins

Cells were centrifuged at 300x*g* for 5 min and washed twice with 500 µL of ice-cold PBS. Subsequently, 500 µL of guanidine-HCl solution (4 M guanidine-HCl in 100 mM phosphate buffer, pH 7.5) was added to the culture plates to disrupt the cells and to denature the proteins. Samples were freeze-thawed and subsequently incubated with the lysis buffer at 4°C for 30 minutes. After the cell lysis, 50 µL of the lysate of each sample was used to determine the protein concentration with the BCA protein assay (Pierce Biotechnology), according to the manufacturer's protocol. The remaining lysates were stored at -80°C in the lysis buffer.

The lysates were diluted four times with a 100 mM phosphate buffer pH 7.5 to lower the concentration of guanidine-HCl and to adjust the pH. Subsequently, the proteins were digested with Lys-C (Roche) in an enzyme to substrate ratio of 1:10 (w/w) at 37°C. After 4 hours, fresh Lys-C was added in a 1:10 (w/w) enzyme to substrate ratio for an overnight incubation.

The protein content of the digested protein samples, from the eight incubations conditions (medium, Alhydrogel®, gibbsite and boehmite, each at 24 and 48 hours incubation times) per biological replicate, was normalised on protein content and diluted in 100 mM phosphate buffer pH 7.5. Samples were desalted using C18 Solid Phase Extraction (Waters) according to the manufacturer's protocol and dried by centrifugation under reduced pressure. The samples were labelled per condition using tandem mass tag labelling-10plex (TMT(10)), (ThermoFisher Scientific), pooled and dried by centrifugation under reduced pressure. Subsequently, samples were dissolved in MilliQ water with 5% DMSO and 0.1% Formic Acid (FA) for proteome analysis.

LC-MS/MS analysis

Peptide separation was performed on an Agilent 1290 system (Santa Clara). Peptides were trapped on a fritted trapping column Reprosil-Pur C18-AQ, df=5 µm, 2 cm x 100 µm I.D. (Dr. Maisch), made in-house and separated on an in-house packed analytical column (Reprosil-Pur C18-AQ, df=3 µm, 30 cm x 50 µm I.D., Dr Maisch). Solvent A was 0.1% FA in MilliQ water and solvent B was 0.1% FA in acetonitrile (AcN) (Biosolve). The peptides were separated in 195 minutes at a column flow rate of 125 nL/min in a non-linear gradient (15 minutes at 0% B, a gradient of 160 minutes from 0% to 30% B, a 15 minutes gradient to 45% B and 5 minutes at 65% B) optimised as described by Morus *et al.*(20). The column effluent was electro-sprayed directly into the MS using a gold-coated fused silica tip of 3.5 µm, with a spray voltage of 2.1 kV.

Mass spectrometric data were acquired on a Tribrid-Orbitrap Fusion Lumos (ThermoFisher Scientific). The full scan (MS^1) spectra were acquired with a scan mass range of 350-1500 m/z at 120,000 resolution (FWHM) with an Orbitrap readout. For the MS^1,

the automatic gain control (AGC) was set to 400,000 and the maximum injection time was 50 ms. Top speed mode was chosen with a duration of 3 s where precursor ions with an intensity > 5,000 were selected for fragmentation (MS^2). Charge states between 1 and 7 were selected for MS^2 which was performed using collision-induced dissociation (CID) in the linear ion trap (LTQ) with a normalised collision energy of 35%. In MS^2, the AGC was set to 10,000 and the maximum injection time was 100 ms. Synchronous-precursor-selection (SPS) was enabled to include up to 5 MS^2 fragment ions for MS^3. These fragment ions were further fragmented by higher energy collision dissociation (HCD) with a normalised collision energy of 60%. The TMT reporter ions were analysed in the Orbitrap analyser, the AGC was set to 100,000 and the maximum injection time was set to 240 ms.

Proteomics data were analysed with Proteome Discoverer 2.1 (ThermoFisher Scientific); unless stated otherwise default settings were used. Precursor mass tolerance was set to 5 ppm. MS^2 scans were searched against the human Uniprot database from November 2014, containing 23,048 entries, using the Sequest HT search engine with a full enzyme specificity for Lys-C as described previously. The quantification node was used to obtain relative expression values, where TMT(10) was defined as the quantification method, with an integration tolerance of 0.2 Da. Cite Percolator was used to filter the peptide to spectrum mass with a false discovery rate (FDR) of <5%.

Next, data were normalised by performing a median correction. Data of three biological replicates were compared, proteins that were upregulated or downregulated by 1.5 fold or more compared to control, in at least two out of three replicates were considered significantly regulated as described previously[1]. The regulated proteins were imported in STRING (string.embl.de)to identify enriched pathways (FDR<0.1), within functional annotations provided by Gene Ontology (GO) biological processes and Kyoto Encyclopedia of Genes and Genomes (KEGG) pathways.

Results

Characterisation

To investigate the effects of aluminum salts on monocytes, a commercially available aluminum-based adjuvant, Alhydrogel®, and 2 experimental aluminum salts, gibbsite and boehmite, were used. Alhydrogel® and boehmite consisted of needle-shaped particles, while gibbsite consisted of hexagonal particles (Figure 1). The Alhydrogel® primary particles were aggregated to particles with a hydrodynamic diameter of 744 ± 5 d.nm, while gibbsite and boehmite consisted of individual particles of 155 ± 2 and 502 ± 13 d.nm (Table 1). The hydrodynamic diameter and polydisphersity index (PdI) increased after dispersion in culture medium for all particles except for Alhydrogel® (Table 1). The zeta potential of the aluminum hydroxides in MilliQ was positively charged, varying from 12 to 53 mV (Table 1). However, the zeta potential of all particles was reduced to less than -10 mV upon dispersion in culture medium. This can be attributed to the presence of salts and proteins in the culture medium.

Gene expression

Human primary monocytes were stimulated with each of the aluminum-based adjuvants for 6 hours, after which the adjuvant's effects on monocyte gene expression were assessed related to the innate and adaptive immune response. Alhydrogel® altered the gene expression of 34 immune system-related genes (of which 32 were upregulated and 2 were downregulated) (Supplementary S2). Also gibbsite and boehmite altered the gene expression of immune system-related genes significantly, although in smaller numbers: gibbsite 14 (13 up and one down) and boehmite 9 (8 up and one down) (Figure 2A and Supplementary S2). Stimulations with the three aluminum salts increased the expression of *IFNα* and *IFNβ* (both pro-inflammatory cytokines), *APCS* (an acute phase-related gene) and *IL-4* (a Th2 polarizing cytokine) (Figure 2A). Alhydrogel® specifically increased the gene expression of *HLA-A*, *IL-2*, *IL-6* and *IL-17A* (all pro-inflammatory cytokines) and the cell surface marker *CD8A* (related to an inflammatory response and co-activation of FcγR)[12]. Gibbsite specifically increased mRNA levels of

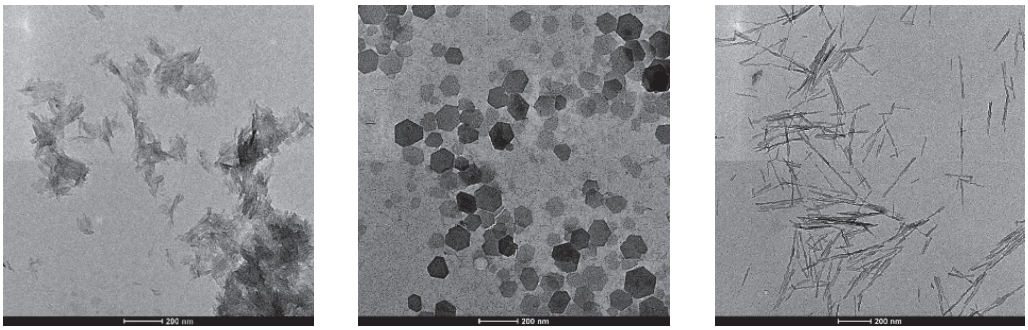

Figure 1. ***Representative TEM images of Alhydrogel® (A), gibbsite (B) and boehmite (C).***

Table 1. ***Physicochemical properties of aluminum salts. Data is presented as mean ± SD (n = 3).***

	Composition	*MilliQ*			*culture medium*		
		Z-average (d.nm)	*PdI*	*zeta potential (mV)*	*Z-average (d.nm)*	*PdI*	*zeta potential (mV)*
Alhydrogel®	Aluminum oxyhydroxide	744± 5	0.162 ± 0.074	12 ± 0.3	583 ± 5	0.72 ± 0.037	-9 ± 1
gibbsite	Aluminum oxyhydroxide	155 ± 2	0.085 ± 0.023	53 ± 1	1467 ± 188	0.564 ± 0.046	-9 ± 0
boehmite	Aluminum oxyhydroxide	502 ± 13	0.234 ± 0.017	33 ± 1	1110 ± 120	0.427 ± 0.083	-9 ± 1

CD4, (associated with the differentiation to functional macrophages)[13], and *TICAM1* (involved in TLR-mediated interferon regulatory factor signalling). In addition, gibbsite shared gene expression upregulation with Alhydrogel®, *e.g. IL-5* (a Th2-related cytokine) and *IFNγ* (a Th1-related cytokine) (Figure 2A). Boehmite specifically induced *CSF2,* which is related to the proliferation of monocyte-derived pro-inflammatory macrophages[14], and *CCR6* (a chemoattractant for DCs and effector/memory B and T cells). Thus, based on this data the gene expression profiles of Alhydrogel®, boemite and gibbsite appear to generate a mixed Th1/Th2 response as described previously for Alhydrogel®[1]. In addition, the response induced by Alhydrogel® is more pro-inflammatory compared to the response induced by gibbsite and boehmite after 6 hours of stimulation.

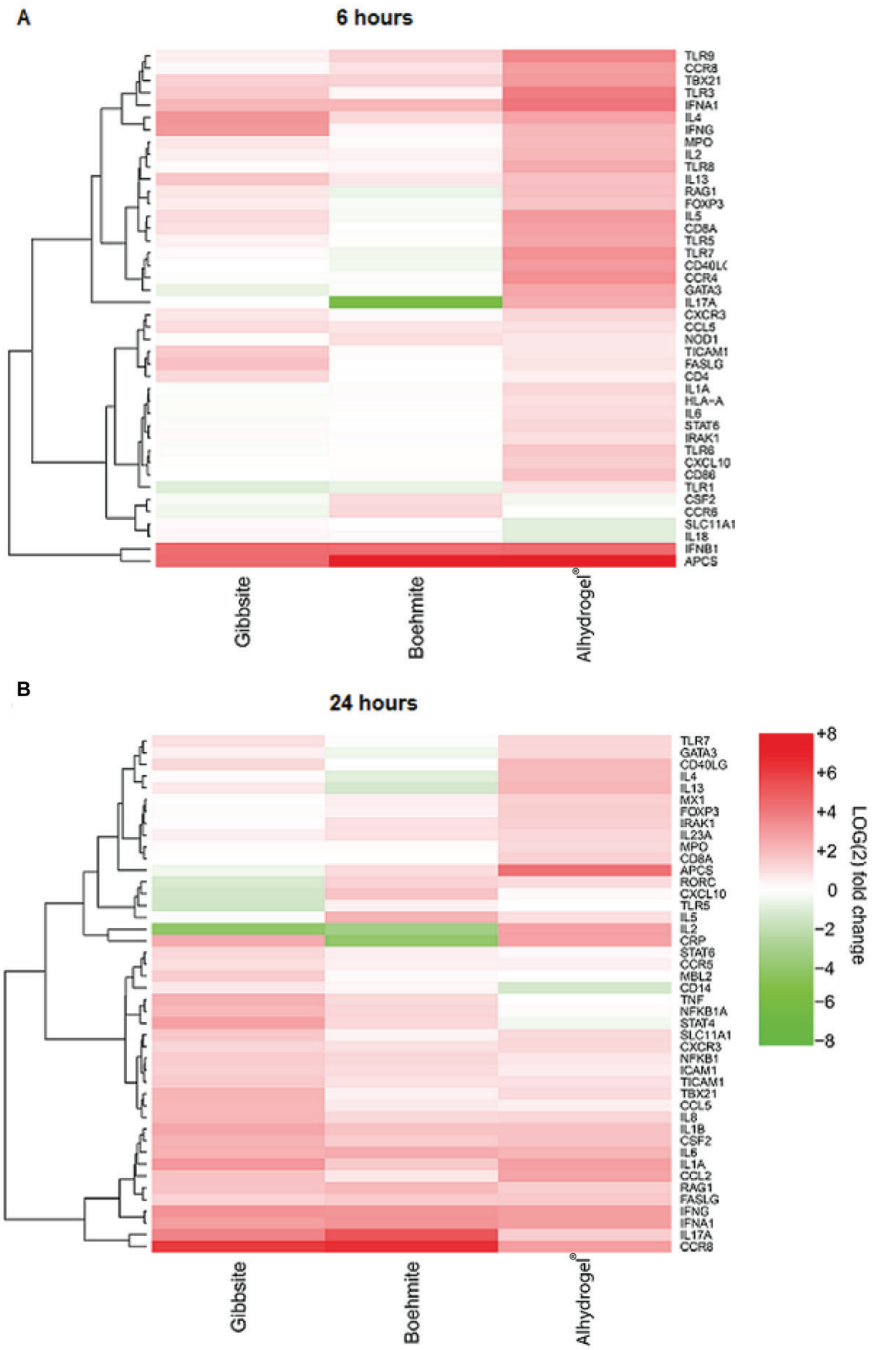

Figure 2. ***Heatmap of differentially expressed genes.***
The genes that induced a fold changes of 2 or greater in one of the stimulation conditions after 6 hours (A) and 24 hours (B) were clustered using Euclidean distance. In this heatmap green and red represent a down and upregulation, respectively, of the gene expression.

After 24 hours of stimulation with the adjuvants, the gene expression profiles of the monocytes were determined a second time. All adjuvants increased the gene expression of *CCR8* (a chemokine receptor involved in monocyte chemotaxis). Moreover, *IFNα* (a pro-inflammatory cytokine) expression remained upregulated by all adjuvants. In addition, Alhydrogel® continued to induce *IL-17A* (a pro-inflammatory cytokine) expression. Moreover, gibbsite and boehmite also induced the expression of *IL-17A* after 24 hours of stimulation. *IFNγ* was induced by all adjuvants (Figure 2B, Supplementary S2). Besides this overlap in gene expression, differences between Alhydrogel® on one hand and gibbsite and boehmite on the other hand were also identified: (*i*) *IL-2* (a cytokine involved in Natural Killer cell steering and required for T cell survival) was still specifically induced by Alhydrogel® and downregulated by both gibbsite and boehmite (Figure 2B), (*ii*) *CD14* (a monocyte differentiation marker) was specifically downregulated by Alhydrogel® after 24 hours of stimulation, while (*iii*) *CD8A* was still uniquely upregulated upon Alhydrogel® stimulation, (*iv) IL-4* (a cytokine involved in Th2 polarization) was specifically induced by Alhydrogel®. In contrast, the nanoparticles specifically induced various genes, *e.g. NFκB1*, *NFκB1a* (transcription factors) and *STAT4* (involved in regulating the differentiation of T cells). Additionally, *TNFα* (a pro-inflammatory cytokine mainly secreted by macrophages) and *ICAM1* (involved in leukocyte adhesion) were increased (Figure 2B).

Besides these particle size-related differences, there were also genes that were affected by one of the nanoparticles only. Gibbsite increased the expression of *CCR5* and its ligand *CCL5* (responsible for attracting monocytes and memory T cells) and the toll like receptor adaptor molecule *TICAM1*. Boehmite specifically induced the expression for *CXCL10*, an IFNγ-induced transcript and a chemoattractant for monocytes, DCs and T cells.

These data indicate that gibbsite induced similar genes compared to Alhydrogel®, but less strong. In addition, there is a particle size effect observed, since both gibbsite and boehmite are less strong in inducing the expression of immune system-related genes compared to Alhydrogel®. Moreover, the nanoparticles induced the expression of genes related to the differentiation towards macrophages at 6 and 24 hours, while this is not the case for Alhydrogel®. Finally, Alhydrogel® appears to be the stronger Th2 inducer, since *IL-4* gene expression is induced after both 6 and 24 hours of stimulation while gibbsite and boehmite only induce *IL-4* after 24 hours of stimulation. All adjuvants induced mRNA coding for pro-inflammatory cytokines. Based on these gene expression profiles it might be so that Alhydrogel® is a more potent adjuvant compared to gibbsite and boehmite thus that the particle size indeed influences the innate immune response at the level of gene expression.

Effects on protein expression

Monocytes were stimulated with the different aluminum-based adjuvants for 24 and 48 hours, after which a quantitative proteome analysis was performed. The proteome analysis revealed about 1200 quantified proteins between all the conditions (Supplementary S3). Alhydrogel® induced the regulation of the most proteins (72), while gibbsite and boehmite resulted in 40 differentially expressed proteins (Supplementary S3). All 40 regulation induced by gibbsite were also regulated in the same direction by Alhydrogel®. After 24 and 48 hours, the protein expression profile of boehmite differed from both Alhydrogel® and gibbsite.

pathway information	24 hours			48 hours		
immunological pathways	Alhydrogel®	Gibbsite	Boehmite	Alhydrogel®	Gibbsite	Boehmite
defense response				2		
immune system process				3		1
innate immune response				3		1
activation of immune response				2		1
innate immune response-activating signal transduction				1		1
regulation of inflammatory response	1			1		2
regulation of immune effector process				1		
viral transcription				3		
viral process				3		2
viral gene expression				3		
regulation of humoral immune response		1		3		
regulation of immune response				3		1
Kegg antigen processing and presentation				2		
antigen processing and presentation				3		
antigen processing and presentation of exogenous peptide antigen via MHC class I				3		1
antigen processing and presentation of exogenous peptide antigen via MHC class II				1		
Kegg complement and coagulation cascades	3	1		2		
blood coagulation	3			3		2
regulation of complement activation	3			2		
positive regulation of complement activation						
complement activation, lectin pathway						-1
response to external stimulus						
wound healing	3			3		2
platelet aggregation				-3		
platelet activation	3			3		
platelet degranulation	3			3	-1	
cell activation	2			1	-1	
response to stress				3		
response to metal ion	1					
response to organic substance				2		1
response to chemical				3		1
transport-related pathways						
localization				3		
cellular localization				3	-1	
transport				3		1
vesicle mediated transport	2			3	-1	
endocytosis				3		
phagocytosis				1		
exocytosis						
secretion	1			1		
biological regulation-related pathways						
biological regulation				3		
small molcule metabolic process				1		
negative regulation of metabolic process				3		1
protein catabolic process				2		1
regulation of catabolic process					-1	
negative regulation of catalytic activity	3			3		3
cellular macromolecule catabolic process				3		1
homeostasis-related pathways						
cellular component organization				3		
positive regulation of type Iia hypersensitivity				2		
DNA packaging						-2
negative regulation of apoptotic process				2		1
macromolecule complex assembly						-2
spliceosome				-3		-2
mRNA processing				-1		-1
mRNA metabolic process				-2		-2

Figure 3. ***Heatmap view of regulated processes.***
For each stimulation condition, a summary of the enriched pathways is depicted. The pathways are grouped based on immunogenic and homeostatic features. The intensity of the colour and the numbers in the cells correspond to the significance of the pathway: 1 corresponds to a p-value <0.05, 2 corresponds to a p-value < 0.01 and 3 corresponds to a p-value <0.005.

After 24 hours of Alhydrogel® stimulation, two immune system-related pathways, *i.e. regulation of the inflammatory response* and *regulation of complement activation* were induced (Supplementary S4). Gibbsite stimulation also resulted in the upregulation of two immune system-related pathways (*regulation of humoral immune response* and *complement and coagulation cascade*), while boehmite stimulation did not result in the induction of immunological pathways (Figure 3 and Supplementary S4).

After 48 hours of stimulation with Alhydrogel®, homeostatic and immunological pathways were enriched in the upregulated protein set, *e.g. defense response*, *antigen processing and presentatio*n, *negative regulation of metabolic process*, *response to stress* and *secretion*. Noteworthy, Alhydrogel® stimulation resulted in *positive regulation of type II a hypersensitivity pathway*, which is related to an allergic reaction, while none of the other stimulations conditions did (Figure 3 and Supplementary S4). After 48 hours of gibbsite stimulation, no immunological pathway were induced. However, even though immunological pathways were not induced by gibbsite, individual proteins that are related to an immune response were upregulated, *e.g.* C4 (involved in complement pathways), CD71 (a monocyte activation marker), Cathepsin D (involved in antigen processing and presentation) and LGALS3 which binds IgE and is involved in the innate immune response. After 48 hours of boehmite stimulation, relevant immunogenic pathways were induced, *e.g. immune system process*, *innate immune response* and a*ntigen presentation of exogenous peptide via HLA class I* (Figure 3). The significance of this pathway enrichment was lower compared to Alhydrogel®. However, unlike Alhydrogel®, boehmite stimulation only resulted in the induction of a limited number of stress-related pathways with a much lower inducing power compared to Alhydrogel® (Figure 3).

After 24-hours of stimulation, none of the adjuvants induced a downregulation of pathways. (Figure 3). After 48 hours of stimulation, Alhydrogel® induced the downregulation of the process of, *e.g*. *mRNA processing*, while gibbsite stimulation resulted in the downregulation of amongst others *cell activation* and boehmite stimulation induced the downregulation of several pathways, *e.g. complement activation*, *lectin pathway.*

In summary, our data strongly suggest that large alum particles are more potent immune activators as compared to nanoparticles after 24 hours of stimulation of monocytes. Alhydrogel® stimulation resulted in the induction of an immune response after 24 hours of stimulation and this immune response is stronger after 48 hours of stimulation, since additional immunological pathways were enriched (Figure 3). In contrast, the response of monocytes to the needle-shaped nanoparticles (*i.e.* boehmite), only resulted in the induction of immune system-relate pathways after 48 hours of stimulation (Figure 3). Gibbsite stimulation only resulted in the induction of immunological pathways after 24 hours of stimulation.

Effects on cytokine secretion

The effects of Alhydrogel®, gibbsite and boehmite on cytokine secretion of human primary monocytes seemed minimal. No cytokines could be detected in the culture supernatants. This does not mean that no cytokines were produced. Low extracellular levels may be due to consumption of the cytokines by the cells, or to the absence of co-stimulatory agents. Therefore, a human monocytic cell line (THP-1 cells) was used instead of human of primary monocytes. This cell line is a suitable model to study monocyte responsiveness[15]. For this cell line it is known that for cytokine expression an additional stimulus besides the adjuvants is required[16]. THP1 cells were stimulated

with the different aluminum-based adjuvants for 24 hours, after which the IL-1β and IL-6 concentrations in the supernatants were determined. Only Alhydrogel® induced significant highest IL-1β secretion than unstimulated cells (Figure 4A). IL-6 was not significantly induced by any of the stimuli (Figure 4B).

Effects on differentiation

In addition to cytokine secretion, cell differentiation was analysed using THP-1 cells by assessing the expression of CD11c, CD14, CD40, CD80, CD83, CD86 and HLA-DR. Cells stimulated with Alhydrogel® showed a significantly higher percentage of CD80-positive cells compared to unstimulated cells and cells stimulated with gibbsite or boehmite (Figure 5). The percentage of positive cells for the other markers was not affected by the stimuli.

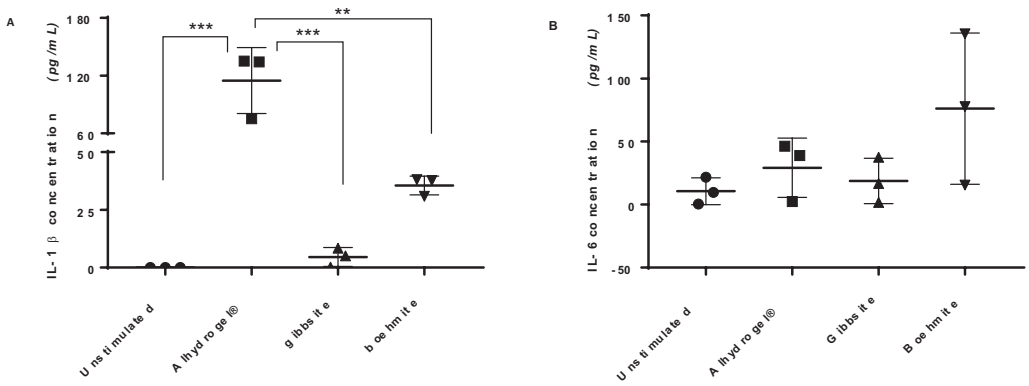

Figure 4. ***Secretion of IL-1β (A) and IL-6 (B) after stimulation of PMA-primed THP-1 cells that were stimulated with Alhydrogel®, gibbsite or boehmite.***

Data is presented as mean ± SD (n = 3). p-values were determined by one-way ANOVA with multiple comparison (= p<0.05, ** = p<0.01, *** = p<0.001 and **** = p<0.0001).*

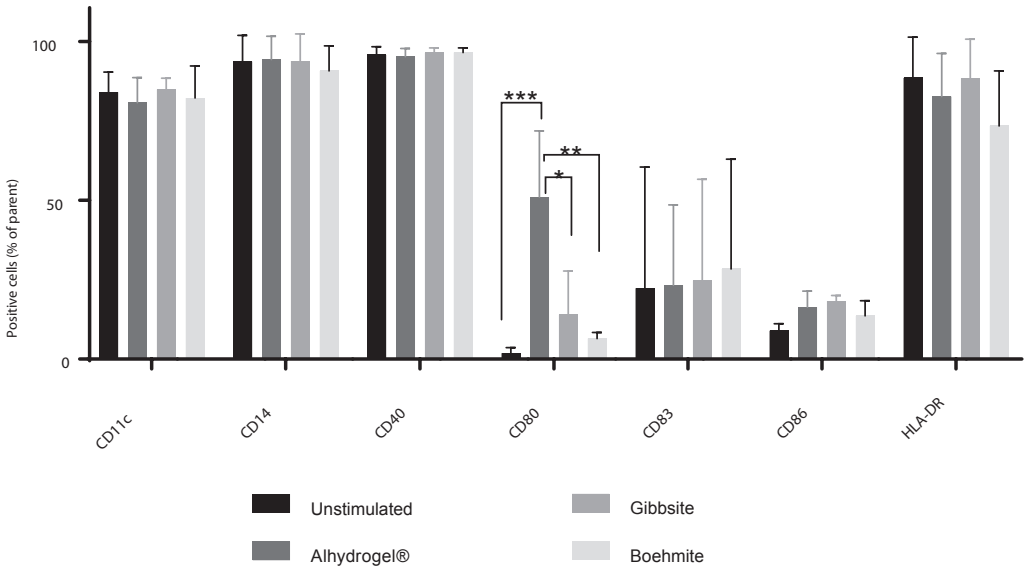

Figure 5. ***Surface marker expression on PMA-primed THP-1 cells after stimulation with Alhydrogel®, gibbsite or boehmite.***

Data is presented as mean ± SD (n=3). p-values were determined by one-way ANOVA with multiple comparison (= p<0.05, ** = p<0.01, *** = p<0.001.*

Discussion

In this study, the effects of the particle size and shape on the immunological effects of aluminum-containing particles have been investigated *in vitro*. For this purpose, three different particles were used: Alhydrogel® (aluminum oxyhydroxide microparticles), gibbsite (hexagonal-shaped aluminum hydroxide nanoparticles) and boehmite (needle-shaped aluminum oxyhydroxide nanoparticles). Mapping the transcriptome and proteome of PBMCs after stimulation with Alhydrogel®, gibbsite and boehmite clearly showed distinct differences and skewing of the immune response. The innate immune response towards gibbsite and boehmite was substantially less strong when compared to the innate response towards Alhydrogel®. Gibbsite hardly induced immunological pathways, while boehmite did induce an immune response but less pronounced compared to Alhydrogel®.

Although only small effects of Alhydrogel®, gibbsite and boehmite were detected on cytokine secretion and marker expression, effects on gene and protein level were more pronounced. For example, IL-2, which is an essential cytokine for T cell survival and NK polarization, was upregulated by Alhydrogel®, while gibbsite and boehmite downregulated this pro-inflammatory cytokine. Thus, gibbsite and boehmite might induce a less inflammatory response compared to Alhydrogel® as described previously[5]. This was also observed in the cytokine secretion analysis were Alhydrogel® strongly induced the expression of IL-1β in THP-1 cells, also significantly more compared to gibbsite and boehmite. ELISA data and transcriptome analysis together imply that Alhydrogel® induces a more inflammatory response than gibbsite and boehmite. However, it needs to be taken into account that the dosage that was administered to the cells was based on aluminum concentration and not on total salt content or concentrations of the particles, which might have impacted the outcomes.

Gibbsite induced gene expression of CD4, which is related to monocyte differentiation towards *functional* mature macrophages[13]. Boehmite induced CSF2, which is related to the differentiation of monocytes towards *pro-inflammatory* macrophages. Both gibbsite and boehmite induced gene expression of TNFα, which is a cytokine mainly secreted by macrophages, while Alhydrogel® induced the differentiation towards DCs[17]. This is supported by the increased HLA-A gene expression observed in this study. Thus, boehmite and Alhydrogel® induce monocyte differentiation towards pro-inflammatory macrophages and DCs, which are mainly involved in initiating the *tissue immune response*, while gibbsite induces monocyte differentiation towards functional macrophages, which are mainly involved in *tissue integrity* and suppress inflammation[18]. For the use in vaccines, a pro-inflammatory response is desired. Gibbsite thus seems a less suitable vaccine adjuvant than boehmite and Alhydrogel®. This may also be related to the shape: needle-shaped particles trigger monocyte differentiation towards inflammatory APCs.

Furthermore, Alhydrogel® induced pathways related to allergy, which was not the case for gibbsite and boehmite. The local side effects that are induced by the nanoparticles may be milder, which has also been described by Li et al[5].

Although gibbsite stimulation of the cells resulted in the upregulation of individual immune system-related proteins, no pathways could be assigned as being significantly regulated. Boehmite had no effect on protein level after 24 hours, but after 48

hours several pro-inflammatory pathways were induced. Compared to Alhydrogel®, less stress response-related pathways were induced, which may be related to milder side effects as described above.

Because the Z-potentials of gibbsite and boehmite were comparable, the differences in response between gibbsite and boehmite are likely due to the shape of the particles. The cellular uptake of nanoparticles is influenced by amongst others its shape, with rod-shaped particles being internalised at a higher rate and quantity than spheres and cubes[19-21]. Particle uptake is required for activation of the inflammasome, which in turn induces IL-1β secretion. Thus, it is possible that the increased biological activity of boehmite compared to gibbsite is due to an increased uptake of boehmite. In addition, needle-shaped particles induce more cell damage by puncturing the cell membrane than particles that are less sharp[22,23], which also influences the immune response through the release of uric acid and DNA[24]. In this regard, the needle-shaped boehmite may induce more cell damage and thus activate more pro-inflammatory immune pathways than the hexagonal-shaped gibbsite.

Sun *et al.* investigated the effects of shape and size of aluminum hydroxide nanoparticles *in vitro* and *in vivo*. They found that the size of aluminum oxyhydroxide nanorods was directly correlated to the activation of the NLRP3 inflammasome in THP-1 cells and in bone marrow-derived dendritic cells (BMDCs), resulting in increased IL-1β secretion and to the expression of the surface markers MHCII, CD80, CD86 and CD40 by BMDCs[6]. In contrast to Sun *et al.*[6], no effect of the particle size was found on cytokine secretion nor surface marker expression in this study. This may be due to the different cell types and culture conditions used, such as different pre-treatment of the cells with PMA (300 ng/mL in our study vs 1 µg/mL by Sun *et al.*) and the addition of LPS for increased cytokine secretion (2.5 ng/mL in our study vs 10 ng/mL by Sun *et al.*) . In addition, Sun *et al.* used Imject alum as a control. This is a mixture of aluminum hydroxide and magnesium hydroxide[25]. It is thus likely that Imject alum differently induces cytokine secretion than Alhydrogel®. Also, the doses of aluminum (oxy)hydroxide differed: Sun *et al.* used 500 µg/mL particles, while in this study 10 and 100 µg Al^{3+}/mL were used for primary monocytes and THP-1 cells, respectively. Because the maximum dose of adjuvant that is allowed in vaccines is based on the aluminum content, the aluminum-based dose may be more comparable. However, it is possible that a higher dose induces a more pronounced effect.

Seubert *et al.* found that the expression of MHC II and CD86 on monocytes was increased after stimulation with aluminum hydroxide[17], which was not observed in this study. However, not only monocytes were isolated as in our study, but all PBMCs were used in the cell culture. Since PBMCs include lymphocytes (T cells, B cells, and NK cells), monocytes and dendritic cells, it is possible that the interaction between these different cell types influences the expression of surface markers. For example, T cells are needed to increase MHC II on monocytes, and no increase in MHC II was detected with purified monocytes[26].

In the current study, the innate immune response of aluminum-based vaccine adjuvants was studied, without the presence of an antigen. It needs to be taken into account that comparing this response with the innate immune response of complete vaccine formulations with the same adjuvants, differences can occur. Since, antigens can alter the innate immune response towards an adjuvant and the complete formulation will determine the final response, as described by Kooijman *et al.*[27].

We have shown that the particle size and shape clearly affects the innate immune response towards a vaccine adjuvant. The nanosized hexagonal-shaped gibbsite did not induce a functional response, while the nanosized needle-shaped boehmite induced several immunological pathways. Hence, needle-shaped nanoparticles are more favourable than hexagonal-shaped nanoparticles. The immune response towards Alhydrogel® was stronger compared to the immune response towards the nanosized needle-shaped particles. However, the stress response-related pathways were also much stronger induced by Alhydrogel®, possibly resulting in more side effects compared to the side effects induced by the needle-shaped nanoparticles. Alhydrogel®, which consisted of aggregated needle-shaped nanoparticles, induced many pathways, both pro-inflammatory and homeostatic. The latter may be related to local side effects that appear after immunisation with an aluminum-containing adjuvant. Because boehmite induced a much milder stress response-related response, but still activated the immune system, these needle-shaped nanoparticles may be a suitable alternative for the currently licenced aluminum hydroxide adjuvant.

References

1 Kooijman, S. et al. Novel identified aluminum hydroxide-induced pathways prove monocyte activation and pro-inflammatory preparedness. J Proteomics 175, 144-155, doi:10.1016/j.jprot.2017.12.021 (2018).

2 Hem, J. D. & Roberson, C. E. Form and stability of aluminum hydroxide complexes in dilute solution. Geological Survey Water-supply Paper 1827-A, 60 (1967).

3 Boraschi, D. et al. Nanoparticles and innate immunity: new perspectives on host defence. Semin Immunol 34, 33-51, doi:10.1016/j.smim.2017.08.013 (2017).

4 O'Hagan, D. T. & Fox, C. B. New generation adjuvants--from empiricism to rational design. Vaccine 33 Suppl 2, B14-20, doi:10.1016/j.vaccine.2015.01.088 (2015).

5 Li, X., Aldayel, A. M. & Cui, Z. Aluminum hydroxide nanoparticles show a stronger vaccine adjuvant activity than traditional aluminum hydroxide microparticles. J Control Release 173, 148-157, doi:10.1016/j.jconrel.2013.10.032 (2014).

6 Sun, B. et al. Engineering an effective immune adjuvant by designed control of shape and crystallinity of aluminum oxyhydroxide nanoparticles. ACS Nano 7, 15 (2013).

7 Thakkar, S. G., Xu, H., Li, X. & Cui, Z. Uric acid and the vaccine adjuvant activity of aluminum (oxy)hydroxide nanoparticles. J Drug Target, 1-23, doi:10.1080/1061186X.2018.1428808 (2018).

8 Olafsdottir, T., Lindqvist, M. & Harandi, A. M. Molecular signatures of vaccine adjuvants. Vaccine 33, 5302-5307, doi:10.1016/j.vaccine.2015.04.099 (2015).

9 Oh, D. Y. et al. Adjuvant-induced Human Monocyte Secretome Profiles Reveal Adjuvant- and Age-specific Protein Signatures. Mol Cell Proteomics 15, 1877-1894, doi:10.1074/mcp.M115.055541 (2016).

10 Mosca, F. et al. Molecular and cellular signatures of human vaccine adjuvants. PNAS 105, 6 (2008).

11 Buining, P. A., Pathmamanoharan, C., Jansen, J. B. H. & Lekkerkerker, H. N. W. Preparation of Colloidal Boehmite Needles by Hydrothermal Treatment of Aluminum Alkoxide Precursors. J. Am. Ceram. Soc. 74, 5 (1992).

12 Gibbings, D. J., Marcet-Palacios, M., Sekar, Y., Ng, M. C. & Befus, A. D. CD8 alpha is expressed by human monocytes and enhances Fc gamma R-dependent responses. BMC Immunol 8, 12, doi:10.1186/1471-2172-8-12 (2007).

13 Zhen, A. et al. CD4 ligation on human blood monocytes triggers macrophage differentiation and enhances HIV infection. J Virol 88, 9934-9946, doi:10.1128/JVI.00616-14 (2014).

14 Italiani, P. & Boraschi, D. From Monocytes to M1/M2 Macrophages: Phenotypical vs. Functional Differentiation. Front Immunol 5, 514, doi:10.3389/fimmu.2014.00514 (2014).

15 Chanput, W., Mes, J. J. & Wichers, H. J. THP-1 cell line: an in vitro cell model for immune modulation approach. Int Immunopharmacol 23, 37-45, doi:10.1016/j.intimp.2014.08.002 (2014).

16 Cullen, S. P., Kearney, C. J., Clancy, D. M. & Martin, S. J. Diverse Activators of the NLRP3 Inflammasome Promote IL-1beta Secretion by Triggering Necrosis. Cell Rep 11, 1535-1548, doi:10.1016/j.celrep.2015.05.003 (2015).

17 Seubert, A., Monaci, E., Pizza, M., O'Hagan, D. T. & Wack, A. The Adjuvants Aluminum Hydroxide and MF59 Induce Monocyte and Granulocyte Chemoattractants and Enhance Monocyte Differentiation toward Dendritic Cells. The Journal of Immunology 180, 5402-5412, doi:10.4049/jimmunol.180.8.5402 (2008).

18 Gordon, S. & Taylor, P. R. Monocyte and macrophage heterogeneity. Nat Rev Immunol 5, 953-964, doi:10.1038/nri1733 (2005).

19 Niikura, K. et al. Gold nanoparticles as vaccine platform - influence of size and shape on immunological responses in vitro and in vivo. ACS Nano 7, 13 (2013).

20 Zheng, M. & Yu, J. The effect of particle shape and size on cellular uptake. Drug Deliv Transl Res 6, 67-72, doi:10.1007/s13346-015-0270-y (2016).

21 Gratton, S. E. A. et al. The effect of particle design on cellular internatization pathways. PNAS 105, 6 (2008).

22 Doshi, N. & Mitragotri, S. Needle-shaped polymeric particles induce transient disruption of cell membranes. J R Soc Interface 7 Suppl 4, S403-410, doi:10.1098/rsif.2010.0134.focus (2010).
23 Laquerriere, P. et al. MMP-2, MMP-9 and their inhibitors TIMP-2 and TIMP-1 production by human monocytes in vitro in the presence of different forms of hydroxyapatite particles. Biomaterials 25, 2515-2524, doi:10.1016/j.biomaterials.2003.09.034 (2004).
24 Kool, M., Fierens, K. & Lambrecht, B. N. Alum adjuvant: some of the tricks of the oldest adjuvant. J Med Microbiol 61, 927-934, doi:10.1099/jmm.0.038943-0 (2012).
25 Hem, S. L., Johnston, C. T. & HogenEsch, H. Imject Alum is not aluminum hydroxide adjuvant or aluminum phosphate adjuvant. Vaccine 25, 4985-4986, doi:10.1016/j.vaccine.2007.04.078 (2007).
26 Ulanova, M., Tarkowski, A., Hahn-Zoric, M. & Hanson, L. A. The Common vaccine adjuvant aluminum hydroxide up-regulates accessory properties of human monocytes via an interleukin-4-dependent mechanism. Infect Immun 69, 1151-1159, doi:10.1128/IAI.69.2.1151-1159.2001 (2001).
27 Kooijman, S et al. Vaccine antigens modulate the innate response of monocytes to Alhydrogel®. PloS One. 2018 mannuscript in press

Supplementary figures

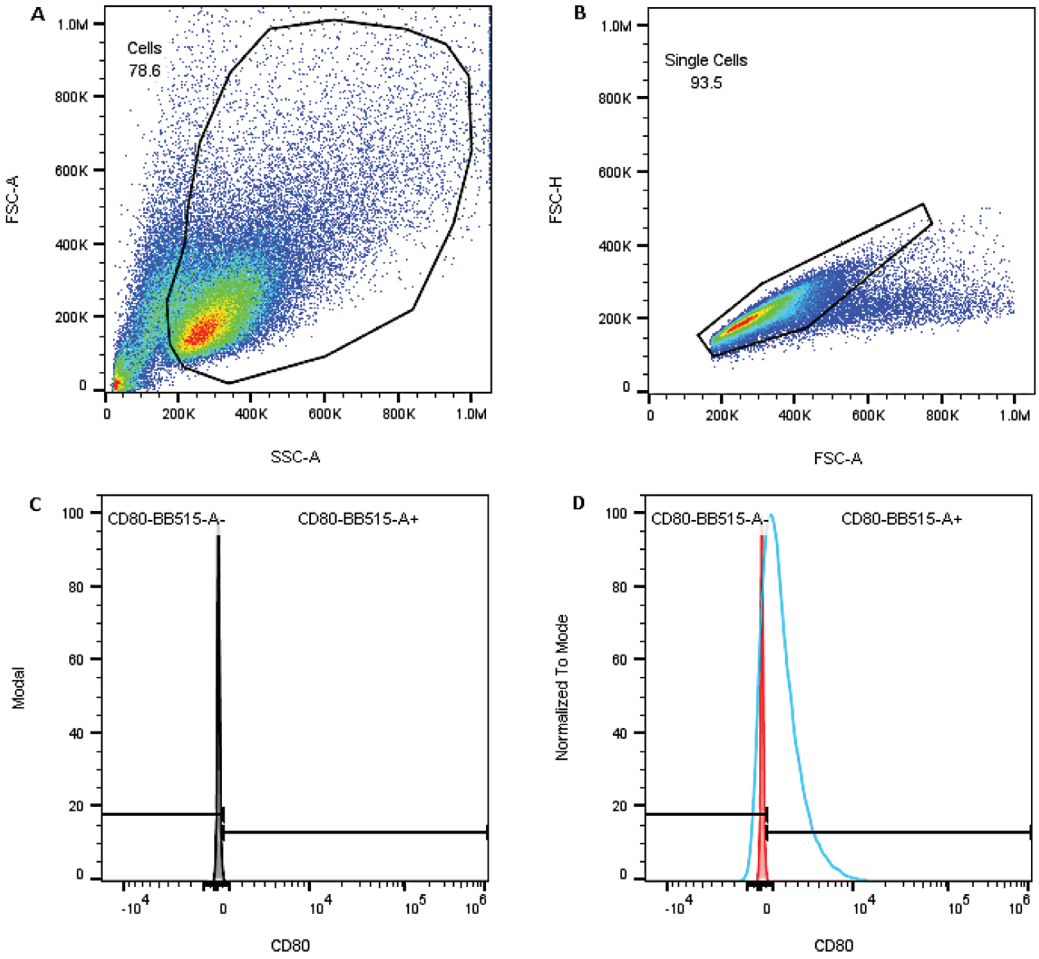

Supplementary S1. ***Representative gating strategy used for the THP-1 cells.***
S1A: gating set around the cell population to exclude debris. S1B: gating set around single cells within the cell population to exclude doublet cells. S1C: The histogram for CD80 after 24 hours of stimulation with Alhydrogel®. The gate was set using an unstained cell population. S1D: The histogram for CD80 after 24 hours of stimulation. An unstained control (red) and stained sample (blue) are shown.

Supplementary S2. ***qPCR data***

'raw data' contains the Ct values, of the individual donors, upon stimulation with the adjuvants, after 6 hours 'raw data 6hrs and 24 hours 'raw data 24 hrs'. these data are normalised towards a housekeeping gene and towards control. These ΔΔCt values are depicted in tab 'after normalization 6 hrs' for the 6 hour time point and 'after normalization 24 hrs' for the 24 hours time point. The median ΔΔCt per condition is depicted in 'median 6 hours'for the 6 hours time point and 'median 24 hours for the 24 hours time point, respectively.

Supplementary S3. ***proteomics data set***

All mass spectrometry data is depicted, the output from proteome discoverer 2.1 is depicted in the 'plex 1' to 'plex 4'tabs. All raw data combined is depicted in the tab ' raw data combined'and the median normalised data can be found in the tab 'normalized data'.

Supplementary S4. ***Regulated pathways***

The pathways over represented in the upregulated protein set upon stimulation with one of the adjuvants for 24 hours are depicted in the '.. 24 hrs up' the pathways overrepresented in the downregulated protein set after24 hours of stimulation are in the tabs ' 24 hrs down'. The pathways over represented after 48 hours can be found in '..48 hours up' and '48 hours down' respectively. The GO ID, pathway description and, the number of proteins regulated and the false discovery rate are depicted.

Chapter 6

Design of a Catalyst-free Enrichment Method for the Capture and Analysis of Cell-Secreted Proteins

Sietske Kooijman,[1,2] Joost P. Uittenbogaard,[1] Marieke Hoonakker,[2]
Hugo D. Meiring,[1,*] Gideon F. A. Kersten,[1,3] Bernard Metz[1]
and Maarten Danial[1,*]

Manuscript submitted to analytical chemistry

1 Intravacc (Institute for Translational Vaccinology), Bilthoven, The Netherlands.
2 Biomolecular Mass Spectrometry and proteomics, Bijvoet center for Biomolecular Research and Utrecht Institute for Pharmaceutical sciences, Science faculty, Utrecht University, The Netherlands.
3 Division of Drug Delivery Technology, Leiden Academic Centre for Drug Research, Leiden, The Netherlands.

Abstract

In this paper a catalyst-free resin-based enrichment process coupled to mass spectrometry was developed. To facilitate the enrichment technique, agarose resin was functionalized with cyclooctyne that permits rapid and bioorthogonal capture of azido-modified moieties via strain-promoted azide-alkyne cycloaddition (SPAAC) chemistry. The loading and efficiency of the cyclooctyne-functionalized agarose resin was assessed through capturing of l-azidohomoalanine and an l-azidohomoalanine-functionalized model peptide. The versatility the capturing process was demonstrated through the capturing of azido–modified lysozyme and lactoperoxidase, which represents a small and large protein, respectively. Application of the cyclooctyne functionalized resin to analyzing the secretome of THP-1 monocytes in response to stimulation with Escherichia coli-derived lipopolysaccharide (LPS), demonstrating that high-throughput identification and quantification of secreted cytokines and chemokines offering numerous advantages over techniques that typically require expensive reagents or monoclonal antibodies. The catalyst-free enrichment method is envisioned to be a highly valuable tool that facilitates examination of cellular responses to vaccines or cellular responses in disease progression.

Introduction

Secreted proteins, such as cytokines, chemokines, hormones, growth factors and enzymes make up the majority of actors in the communication processes between cells. The analysis of the cell secretome has provided valuable insights in the fundamental understanding of cell communications in particular in the onset of diseases such as cancer, virus infections[1] and bacterial infections.[2,3] The effects of immunogens, toxoids and adjuvants on cell-secreted proteins have also yielded a better understanding of cell immunology and have led to important developments in vaccine design.[4-7] Furthermore, the adoption of sensitive techniques to analyze cell secretomes could be of great benefit in diagnostic applications,[8,9] especially at early development stages of disease progression.

There are a number of analytical methodologies that could be utilized to study secretomes including those of bacterial cells,[10-12] mammalian cells,[13] stem cells[14] and cancer cells.[15] Of these methods, antibody-based assays (e.g. Luminex multiplex assays) are popular since they enable high-throughput detection and quantitation of multiple secreted proteins.[16] Alternatively, liquid chromatography tandem mass spectrometric (LC-MS/MS) methods are increasingly applied due to the potential to provide a higher degree of analytical capability in secretome studies. Most importantly, mass spectrometry-based approaches are unbiased compared to antibody-based assays in terms of comprehensively mapping the secretome; *i.e.* no preselection of antibodies targeting a specific subset of the secreted proteins is required. For instance, in-gel LC-MS/MS methods like two-dimensional gel electrophoresis or difference gel electrophoresis have led to the isolation and identification of unknown secretory proteins. However, this technique remains a low-throughput method as spots have to be individually excised from the gel.[10,11] Alternatively, gel-independent LC-MS/MS methods like tandem mass tag (TMT)[17] or isobaric tag for relative and absolute quantitation (iTRAQ)[18] analysis have permitted elucidation of the relative protein abundance from different sources in a single experiment. Stable isotope labeling by amino acids in cell culture (SILAC)[19] has also allowed for a comprehensive analysis of cell proteomes. However, in part due to the low abundance of secreted proteins (in the low ng/mL range) relative to the total concentration of serum proteins in culture media (~6 mg/mL) as well as the use of media conditioned with dual-labelled ^{15}N and ^{13}C amino acid isotopes of L-lysine and L-arginine, SILAC alone is a costly technique for secretome analysis. Although the low signal-to-noise ratio of secreted proteins can be overcome through the use of serum free media, the non-natural environment for cells could lead to the unnatural secretion of proteins that are typically expressed in response to stress.

To this end, enrichment processes have enabled more reliable identification of the cell proteome without the use of serum-free conditioned media. Such an enrichment process was achieved by a "pulsed" introduction of the non-canonical amino acid L-azidohomoalanine (Aha) in cell culture medium.[20,21] Aha serves as a surrogate for methionine and is incorporated in newly synthesized proteins by cells in methionine-deficient media. Using an alkyne-functionalized resin, these newly synthesized proteins are captured via copper-catalyzed azide-alkyne cycloaddition (CuAAC) reaction,[22,23] which permits these proteins to be distinguished from pre-existing and serum proteins. Applying this CuAAc-based enrichment technique to secretome studies has allowed the

detection and quantitation of secreted proteins in nanogram-per-milliliter amounts.[24] One major drawback, however, is the copper catalyst employed for attachment of the newly formed azido-containing proteins to the alkyne functionalized resin. Copper(I) is known to induce unwanted oxidative side-reactions on proteins,[25] which complicates the quantitation and identification of secreted proteins. In addition, the copper(II) precursor often used in CuAAC reactions can chelate to amine groups of amino acids[26] as well as amide bonds of peptides and proteins[27,28] hampering the capturing efficiency of the alkyne-based affinity resin.

In contrast to CuAAC, strain-promoted azide-alkyne cycloaddition (SPAAC)[29] allows for a catalyst-free, azide-alkyne conjugation route which has proven to be an efficient and versatile bioorthogonal chemistry tool in biological and non-biological "click" conjugations that can be carried out in various solvents and temperatures.[30-32] As such, SPAAC would eliminate the occurrence of side-reactions and maintain the integrity of the protein primary structure of cell-secreted proteins. In addition, any risks associated with inefficient protein capturing by CuAAC and incomplete enzymatic processing would be alleviated using SPAAC, leading to improved reliability of protein analysis as well as possible identification of novel secreted proteins.

In this paper, we describe the development of a cyclooctyne-functionalized agarose resin that permits a catalyst-free capture of azide-functionalized proteins via SPAAC. The efficiency of SPAAC applied to the affinity-based capture is demonstrated with an Aha-functionalized peptide (1.4 kDa) as well as model proteins lysozyme (14.3 kDa) and lactoperoxidase (78 kDa) functionalized with an azide. Furthermore, the enrichment, the capture, enrichment and analysis of secreted proteins from lipopolysaccharide (LPS)-stimulated human monocytic THP-1 cells is also demonstrated, thereby paving the way to a catalyst-free, straightforward approach to stimulated cell secretome analytics.

Experimental section

Materials

Ammonium bicarbonate (NH_4HCO_3, >99%), *N*-[(1*R*,8*S*,9*s*)-bicyclo[6.1.0]non-4-yn-9-ylmethyloxycarbonyl]-1,8-diamino-3,6-dioxaoctane (BCN-amine), chloroform-*d* ($CDCl_3$, 99.8 atom % D), complete EDTA-free protease inhibitors, dimethylformamide (DMF, 99%), deuterium oxide (D_2O, 99.9 atom % D), ethanolamine (>99%), lactoperoxidase from bovine milk (essentially salt free), l-leucine-13C_6 (98 atom % 13C, 95 % (CP)), lysozyme from chicken egg white (90%), phorbol 12-myristate 13-acetate (PMA), phosphate-buffered saline (foil pouches, BioPerformance Certified, pH 7.4), 3-(trimethylsilyl)propionic-2,2,3,3-d_4 acid sodium salt (TMSP-d_4, 98 atom % D), triethylamine (Et_3N, BioUltra > 99.5 %), triethylammonium bicarbonate buffer (TEAB, 1.0 M pH 8.5), urea (for analysis) were purchased from Sigma-Aldrich (Schnelldorf, Germany). l-Azidohomoalanine (Aha, also known as H-γ-azido-Abu-OH, >99 %) was purchased from Bachem (Budendorf, Switzerland). Bond breaker tris(2-carboxyethyl) phosphine (TCEP) solution (0.5 M solution), dry NHS-activated agarose, RPMI medium, methionine and leucine-free RPMI medium, and TMTduplex™ isobaric label reagent set (5 x 0.8 mg) were purchased from Thermo-Fisher (Venlo, The Netherlands). Lipopolysaccharide (LPS) from E.coli K12 was obtained from Invivogen (San Diego, California USA). The endoprotease LysC was purchased from Promega (The Netherlands). Micro Bio-spin™ filter columns were purchased from Bio-Rad (United States). The azido-PEG_3-maleimide preparation kit (CLK-AZ107-100), which contains maleimido NHS-ester (in vial 1) and azido-PEG_3-amine (in vial 2) was purchased from Jena Bioscience (Germany). Peptide 4, Ac-[Aha]SAKEATRVAYVK-OH (free C-terminus) utilized in this study was custom synthesized and purchased from Pepscan b.v. (Lelystad, The Netherlands).

Deuterated PBS (10 mM phosphates, 138 mM NaCl, 2.7 mM KCl, pD 7.8) was prepared by dissolving 973.5 mg of PBS powder in D_2O (9.1 mL) followed by the addition of 900 μL of TMSP-d_4 stock (0.75 % in D_2O). For other purposes, PBS (10 mM phosphates, pH 7.2) from Gibco was utilized.

Synthesis of cyclooctyne (BCN)-functionalized agarose resin

Dry NHS-activated agarose (154 mg) was added to DMF (1 mL). After a pre-incubation of 30 min, 0.5 mL of DMF supernatant is removed. In a separate vessel, BCN-amine (**1,** 15 mg, 46.2 μmol) is dissolved in $CDCl_3$ (1 mL) containing TMS 0.03%. Et_3N (19.3 μL, 139 μmol, 3 equiv) is then added to the solution after which it is added to the vessel containing the agarose beads. The reaction is allowed to proceed at room temperature under rotation for 16 hours after which the agarose is centrifuged (16200 × g) for 5 minutes using a Biofuge benchtop centrifuge (Heraeus) and the supernatant is analyzed for residual BCN-amine by ^{1}H-NMR. Any NHS groups remaining on the agarose resin was quenched by the addition of ethanolamine (50 μL, 832 μmol, 18 equiv). Removal of residual NHS moieties was performed at room temperature for 3 hours. The resin was centrifuged (16200 × g) for 5 minutes. The resin was resuspended in H_2O and transferred to a biospin filter. The agarose resin was washed 5-fold with water by successive

centrifuge runs at 400 × g. The washed beads (**2**) were recovered from the Bio-spin™ columns and stored at 4 °C until further usage.

Capture and analysis of L-azidohomoalanine and azido-modified peptide by BCN-functionalized agarose resin

Solutions (1 mL) containing 1, 2 and 4 μmol Aha and 1, 2 and 3.6 μmol azido-functionalized peptide **4** were prepared in deuterated PBS (10 mM phosphates, pD 7.8) or in 4 M urea (in D_2O). These solutions were analyzed by ^{1}H-NMR, subsequently added to 1.5-mL Eppendorf tubes containing 20 mg BCN-functionalized resin **2** and shaken for 16 hours at room temperature. After incubation the samples were centrifuged (16200 × g) and the supernatant was transferred to an NMR tube and analyzed by ^{1}H-NMR.

The efficiency of Aha and peptide (**4**) captured by 20 mg BCN-functionalized resin **2** was calculated by determining the difference in ^{1}H-NMR integrals of the Aha or peptide **4** in the solution before and after incubation. More specifically, an ^{1}H-NMR spectrum of the solution containing Aha or peptide **4** before incubation with resin **2** was acquired and the integrals of the species were determined relative to the internal standard TMSP-d_4 (-0.10 ppm). Following the incubation with resin **2**, the sample was centrifuged (16200 × g) and the supernatant was transferred to an NMR tube and subsequently analyzed by ^{1}H-NMR. The amount of Aha coupled to the resin **2** was determined using the integral of the multiplet at 2.00 ppm relative to the internal standard TMSP-d_4. The amount of peptide **4** coupled to resin **2** was determined using the tyrosine integrals of the doublets at 6.70 and 7.05 ppm relative to the internal standard TMSP-d_4.

Capture of azido-PEG$_3$-thiosuccinimide-modified lysozyme and lactoperoxidase by BCN-functionalized agarose resin

Azido-PEG$_3$-thiosuccinimide-modified lysozyme (**5**, 1 mg) and azido-PEG$_3$-thiosuccinimide-modified lactoperoxidase (**6**, 1 mg) were each dissolved in 500 μL PBS (10 mM phosphates, pH 7.2). From these stock solutions, the following solutions were prepared in 1.5-mL Eppendorf tubes: (*i*) 0.5 μL of **5** or **6** dissolved in 599 μL PBS (10 mM, pH 7.2), (*ii*) 0.5 μL of **5** or **6** dissolved in 249 μL PBS and 250 μL 8 M urea and (*iii*) 0.5 μL of **5** or **6** dissolved in 249 μL serum containing medium and 250 μL 8 M urea. These solutions were each added to the BCN-functionalized agarose resin (10 mg) and shaken for 16 hours at room temperature.

Mass spectrometry analysis of captured azido-modified peptide and proteins

Following successful capturing of the azido-modified peptide, the resin was transferred into a Bio-Spin™ filter and washed using aliquots of water (4 × 0.7 mL), 10 mM CHAPS (1 × 0.7 mL) and water (5 × 0.7 mL). The Bio-Spin™ filters were centrifuged at 400 × g for 1 to 2 minutes between each wash. Then, based on the amount of peptide **4** that was coupled to the resin **2** (determined by ^{1}H-NMR), LysC was added in an enzyme-to-substrate mass ratio of 1:10. This reaction was left to stir overnight at 37 °C. In addition, two control samples were analyzed. One sample contained peptide **4** in the same concentration without the presence of the agarose resin. Another control sample consisted of the same amount of peptide in the presence of 20 mg agarose resin that was inactivated by treatment with ethanolamine (agarose resin **3**). These samples were

analyzed with a mass spectrometry method: peptides were trapped for 10 minutes in solvent A (0.1% formic acid (FA) in MilliQ) on an in-house manufactured trapping column (Reprosil-Pur C18-AQ, df=5 µm, pore size=120Å) (Dr. Maisch, Ammerbuch, Germany) 2 cm in length x 100 µm I.D., after which they were separated on an analytical column Reprosil-Pur C18-AQ, df=3 µm, pore size=120Å (Dr. Maisch, Ammerbuch, Germany) 30 cm length x 50 µm I.D. (manufactured in-house), using a non-linear gradient: first, a step to 7.5% solvent B (0.1% FA in acetonitrile (Biosolve)) followed by a gradient of 25 minutes with 2%/min to 57.5% solvent B.

Mass spectrometry data were acquired using a Tribrid-Orbitrap Fusion Lumos (Thermo Fisher Scientific, San Jose, CA, USA). The full scan MS spectra were acquired with an Orbitrap read out and a resolution of 120K Full Width Half Maximum (FHMW) using a scan range of *m/z* 350-1500, a maximum injection time of 100 ms and the automatic gain control (AGC) set at 200000. MS^2 fragmentation was performed by selecting the precursor ions with charge states 2-7 and a corresponding intensity threshold of 50,000. For the reporter peptide derived from peptide **4**, a targeted *m/z* value of 518.79 was set for the proteolyzed peptide. When this mass was not identified, MS/MS was performed on the highest abundant peak in the chromatogram. For the MS/MS experiments, an injection time of 150 ms was used with the AGC was set at 30,000. Peptides were fragmented with Collision-Induced Dissociation (CID) using a normalized collision energy of 35% and with Higher energy Collision Dissociation (HCD) using a normalized collision energy of 35%. Proteomics data were analyzed with Proteome Discoverer 2.1 (Thermo Fisher Scientific) using default settings unless stated otherwise. Precursor mass tolerance was set to 5 ppm and MS/MS scans were searched against the lysozyme sequence (P00698) or the lactoperoxidase sequence (P80025) with a full enzyme specificity for LysC and *b* and *y* ions enabled for CID and HCD data, with a fragment mass tolerance of 0.5 Da. Asparagine deamidation and methionine oxidation were set as dynamic modification as was the addition of the hydrolyzed azide-PEG_3-thiosuccinimide linker (387.1754 Da). The percolator node was used to filter the Peptide-to-Spectrum Matches (PSMs) with an False Discovery Rate (FDR) of < 5%.

Cell culture and stimulation

For cell stimulation experiments, the human monocytic cell line THP-1 (ATCC; Teddington; Middlesex, U.K.) was cultured according to the supplier's protocol. Cells were cultured in RPMI medium with the addition of 10% FCS, 100 units/mL penicillin, 100 µg/mL streptomycin and 300 µg/mL L-glutamine (THP-1 culture medium) to a density of 0.8×10^6 cells per mL. Four T25 flasks were each prepared with 10 mL of the above-mentioned THP-1 stock. To adhere the cells to the culture flasks, cells were primed for 24 hours with 100 ng/mL PMA in THP-1 culture medium. After 24 hours, the PMA-containing culture medium was removed. The THP-1 cells were washed with PBS and then placed in THP-1 culture medium that was devoid of PMA for 24 hours. The THP-1 culture medium was then replaced with THP-1 medium containing dialyzed 10% (v/v) FCS but devoid of L-methionine and L-leucine for one hour. After one hour, RPMI medium containing dialyzed 10% FCS (v/v) was prepared containing L-azidohomoalanine (0.10 mM) and L-leucine-$^{13}C_6$ (0.38 mM) in lieu of L-methionine and L-leucine, respectively. This modified RPMI medium was filtered using a vacuum drive sterile filter, 0.22 µm pore size (Stericup, Merck Millipore) and added to the THP-1 cells each T25 flask. LPS *E. coli* (100 ng/mL) was added to two T25 flasks. No further

additions were made to the two remaining control T25 flasks. After a 24-hour incubation, the supernatants were removed and centrifuged at 400 × *g* to remove cell debris. Complete EDTA protease inhibitors were added and supernatants were frozen at -80 °C until further use.

Cell-secreted protein enrichment

The supernatant from each culture flask was centrifuged through an Amicon centrifuge filter (15 mL, 3.5 kDa MWCO) to yield a 500-μL concentrate from which the residual leucine-$^{13}C_6$ and Aha was removed. The obtained supernatant concentrate was then diluted to 10 mL with an aqueous solution consisting of 4 M urea and ammonium bicarbonate (50 mM). This solution was then transferred to a 15 mL Falcon tube that contained 35 mg BCN-functionalized agarose resin **2**. The supernatants were placed on a rotating stand and incubated for 16 hours. Subsequently, the resin suspensions were transferred into Bio-Spin™ filters and washed with aliquots of water (4 × 0.8 mL), 10 mM CHAPS (2 × 0.8 mL) and water (8 × 0.8 mL). The Bio-Spin™ filters containing the resin were centrifuged at 400 × g for 1 to 2 minutes between each wash. The resins were then transferred to a 1.5-mL Eppendorf tube, suspended in 500 μL TEAB buffer (diluted to 50 mM with MilliQ) in which proteolysis was performed with LysC (1:10 enzyme:substrate mass ratio). Formic acid (15 μL of 10 % v/v solution) was added to each of the proteolyzed samples to pH 7.4. Subsequently, the proteolyzed samples were labeled with a tandem mass tag using the TMTduplex™ isobaric reagent label set (0.4 mg of the reagent per proteolyzed sample) for relative quantitation of the proteins.

Secreted protein data analysis

The TMTduplex™ labeled samples were analyzed with mass spectrometry using the LC gradient and MS settings as described by Kooijman et al[33], with the addition of an exclusion list, containing the highest abundant bovine peptide masses (Table S1). Data analysis was performed with Proteome Discoverer 2.1 as described previously[33], with the incorporation of dynamic modifications of Aha for L-methionine and L-leucine-$^{13}C_6$ for L-leucine . In addition, the data was also searched against a database containing bovine contaminants previously identified in agarose resin experiments. Proteins were considered to be novel and secreted when L-leucine-$^{13}C_6$ and/or Aha was incorporated in one of the peptides, and the Gene Ontology Description contained the keywords "secreted" or "extracellular", or the Uniprot key term included "secreted". A protein was considered regulated when, after median normalization, the fold change was ≥ 1.5 in either direction, as described previously[33].

Results and discussion

Design and Synthesis of Protein Capturing Platform

The platform was envisioned to capture newly synthesized peptides and proteins that could be distinguished from pre-existing proteins, including serum proteins present in the medium. The newly synthesized proteins therefore require an orthogonal moiety that can be specifically introduced and allowed to react with the platform without significantly disrupting its structure and function. Amongst the plethora of available bioorthogonal functional groups available, the "clickable", non-canonical amino acid L-azidohomoalanine (Aha) has been shown to function as an excellent surrogate for L-methionine in protein synthesis.[34,35] Compared to other azide-bearing amino acids, Aha has been shown to possess the highest rate of activation by methionyl-tRNA-synthetase.[34] Furthermore, the applicability of Aha as a noteworthy bioorthogonal tool has also been evidenced in proteome and secretome studies.[20,21,24] While most platforms used in these studies employed copper-catalyzed azide-alkyne cycloaddition, a catalyst-free approach through strain-promoted azide-alkyne cycloaddition (SPAAC) would not only lead to a "green chemistry" approach but would also lead to less protein modifications permitting facile and confident mass spectrometric identification.

To facilitate the catalyst-free capturing of azide-functionalized proteins, agarose resin was functionalized with a ring-strained alkyne such as dibenzocyclooctynes or cyclooctynes. Cyclooctynes and dibenzocyclooctynes possess favorable characteristics such as high azide-alkyne cycloaddition reaction kinetics.[36,37] Performing kinetics experiments of the cyclooctyne BCN-amine **1** with Aha in deuterated PBS (10 mM, pD 7.8) or in solution containing 8 M urea proceeded rapidly and reached complete conversion within 30–45 minutes (Figure S1). However, dibenzocyclooctynes have a higher lipophilicity than cyclooctynes that could promote the coupling towards lipophilic azide-containing moieties and may also lead to issues including non-specific interactions with lipophilic components in the cell media, e.g. denatured peptides, proteins and lipids. Dibenzocyclooctyne-functionalized agarose was therefore anticipated to lead to an inaccurate profile and quantitation of secreted proteins. To this end, the development of an agarose resin functionalized with cyclooctyne for the protein capturing process was pursued.

As shown in Scheme 1, the agarose resin is functionalized through a single step in a $CDCl_3$/DMF mixture (2/1 v/v) by addition of cyclooctyne-amine **1** to the *N*-hydroxysuccinimidyl (NHS) ester-functionalized agarose resin in the presence of Et_3N. Residual NHS esters were removed by the subsequent addition of an excess of ethanolamine rendering a hydrophilic, cyclooctyne-functionalized agarose resin (**2**). The degree of modification of the NHS-agarose was determined through the difference of ^{1}H-NMR integrals of the multiplets at 1.35 and 1.60 ppm of **1** relative to the DMF signal at 8.03 ppm before and after the addition to the NHS-agarose resin. This led to a BCN-on-resin conversion of 88% and a cyclooctyne-on-agarose resin loading of 0.265 mmol/g resin. It must be noted that modification of the NHS-agarose resin with **1** yielded lower conversions (~50%) and, correspondingly, lower cyclooctyne-on-agarose loading (0.148 mmol/g resin) when performed in $CDCl_3$. These lower yields were attributed to poor swelling of the NHS-agarose resin in $CDCl_3$.

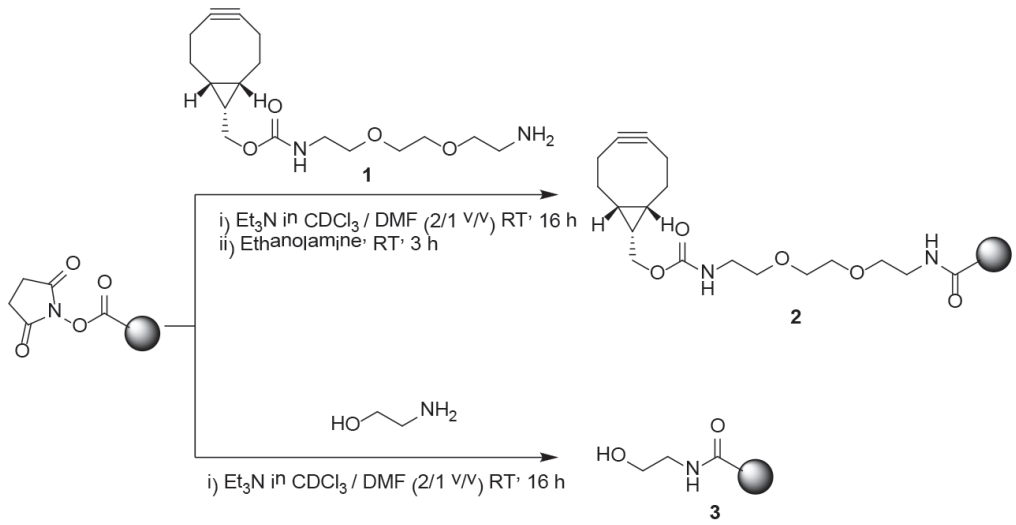

Scheme 1. ***Synthesis of cyclooctyne (BCN)-functionalized and Inactivated Agarose Resin.***
Capturing Azide-Functionalized Moieties

In addition to agarose resin **2**, an inactivated agarose resin (**3**) was generated through the reaction of ethanolamine with the NHS-agarose resin (Scheme 1). Resin **3** serves as an independent control to verify the specificity of the azide-functionalized peptide and proteins towards the BCN-functionalized resin **2** (*vide infra*).

The coupling efficiency of the BCN-functionalized agarose resin (**2**) was determined through an incubation with the amino acid Aha, a peptide (**4**) containing Aha and proteins modified with an azido-containing linker (*vide infra*). As depicted in Figure 1a, the reaction of an azide-functionalized compound with the BCN-functionalized agarose resin results in a resin bound triazole species. ^{1}H-NMR was employed to determine the amount of the Aha and peptide **4** present in the supernatant before and after the incubation with resin **2** relative to the 3-(trimethylsilyl)propionic-2,2,3,3-d_4 acid sodium salt (TMSP-d_4) internal standard. The difference in ^{1}H-NMR signal intensity was determined to be the amount coupled to the resin **2**. Figure 1b and c represents the efficiency of the incubation reactions consisting of Aha or peptide **4** in aqueous solutions consisting of deuterated PBS buffer or 4 M urea. An incubation of 4 μmol Aha resulted in 2.7 μmol coupled to the resin **2**. Conversely, an incubation with 3.6 μmol peptide **4** resulted in 1.3 mmol coupled to resin **2**. These results indicated that steric hindrance may play a role in reactivity with BCN-functionalized resin. Control experiments, where Aha was incubated with inactivated agarose resin **3** revealed no residual Aha or peptide **4** and therefore demonstrated that the cyclooctyne moiety was the sole functionality that enabled the capture of azide containing compounds.

In order to detect and verify the identity of the peptide and proteins by mass spectrometry, the captured proteins need to be digested to peptide fragments from which MS/MS spectra can be derived. Due to the general high abundance of lysine residues in

proteins,[38] LysC was selected to enzymatically digest the proteins that were captured by the resin. As shown in Figure 2a, LysC cleaves peptide **4** at the C-terminus of the Lys-4 residue of the peptide. This results in a peptide fragment attached to the agarose resin and peptide fragment that served as a reporter peptide (Figure 2b). Using LC-MS/MS, the presence of the reporter peptide was verified. As a control, peptide **4** was incubated with LysC (10% mass of peptide **4**) as determined from the peptide **4** bound to the agarose resin. The ratio of the chromatography signal obtained between the reporter peptide derived from the agarose captured experiment and from peptide **4** proteolyzed in solution yielded a near-quantitative (100%) recovery (Figure 2c and d). Further proof for the high recovery was demonstrated by the presence of mass spectral peak at m/z = 518.79, attributed to the reporter peptide (Figure 2c and d).

Further verification of protein recovery after SPAAC-enabled agarose capturing was demonstrated with a small protein (lysozyme, 14.3 kDa) and a large protein (lactoperoxidase, 77.5 kDa). Since these proteins do not naturally consist of an azide-containing amino acid, a modification with an azido-PEG_3-maleimide linker was carried at the cysteine residues. As shown in Scheme 2, the azido-PEG_3-maleimide linker was generated *in situ* from maleimido NHS-ester and an azido-PEG_3-amine according the specifications laid out by the manufacturer, whilst the disulfide bridges of lysozyme and lactoperoxidase were reduced using tris(carboxyethyl) phosphine (TCEP). TCEP was removed via ultrafiltration prior to the addition of the azido-PEG_3-maleimide so as to prevent any reduction of the maleimide[39] or azide[40] moieties. Coupling the azido-PEG_3-maleimide linker to the cysteines on the proteins resulted in a thioether succinimide azide-PEG_3 linker. To verify the presence and sequence position of this PEG_3 linker, the modified proteins were subjected to LysC proteolysis and subsequently verified with LC-MS/MS. Both protein samples **5** and **6** contained azido-PEG_3 linkers attached to the protein. The molar mass of the peptide fragment of the linker revealed that hydrolysis had occurred, which was attributed to the ring opening of the thioether succinimide moiety yielding a free carboxylic acid. The hydrolysis of thioether succinimide moieties has been observed before and has been associated with improved stability of the conjugated species.[41,42] As shown in Table S2, there was excellent agreement between the theoretical and found mass spectral values, which verifies the presence of the azide-PEG_3 linker attached to the peptide fragments. For lysozyme, complete conversion of the azide-PEG_3 linkers to Cys-6 and Cys-127 was observed. Despite adding an excess of azido-PEG_3 maleimide relative to cysteine residues, only 3 peptides containing the linker for lysozyme and 2 peptides containing the linker for lactoperoxidase were identified by MS. This was attributed to incomplete reduction leading to inefficient conjugation to the azido-PEG_3-maleimide linker or steric hindrance of the cysteine thiols. In addition, lactoperoxidase is glycosylated with mono-, di- and trisaccharides on a number of asparagine residues,[43] which complicates complete elucidation by mass analysis. Nevertheless, both azide-modified proteins **5** and **6** serve as excellent candidates for assessing the feasibility of the BCN-functionalized agarose resin to capture a small and large protein, respectively.

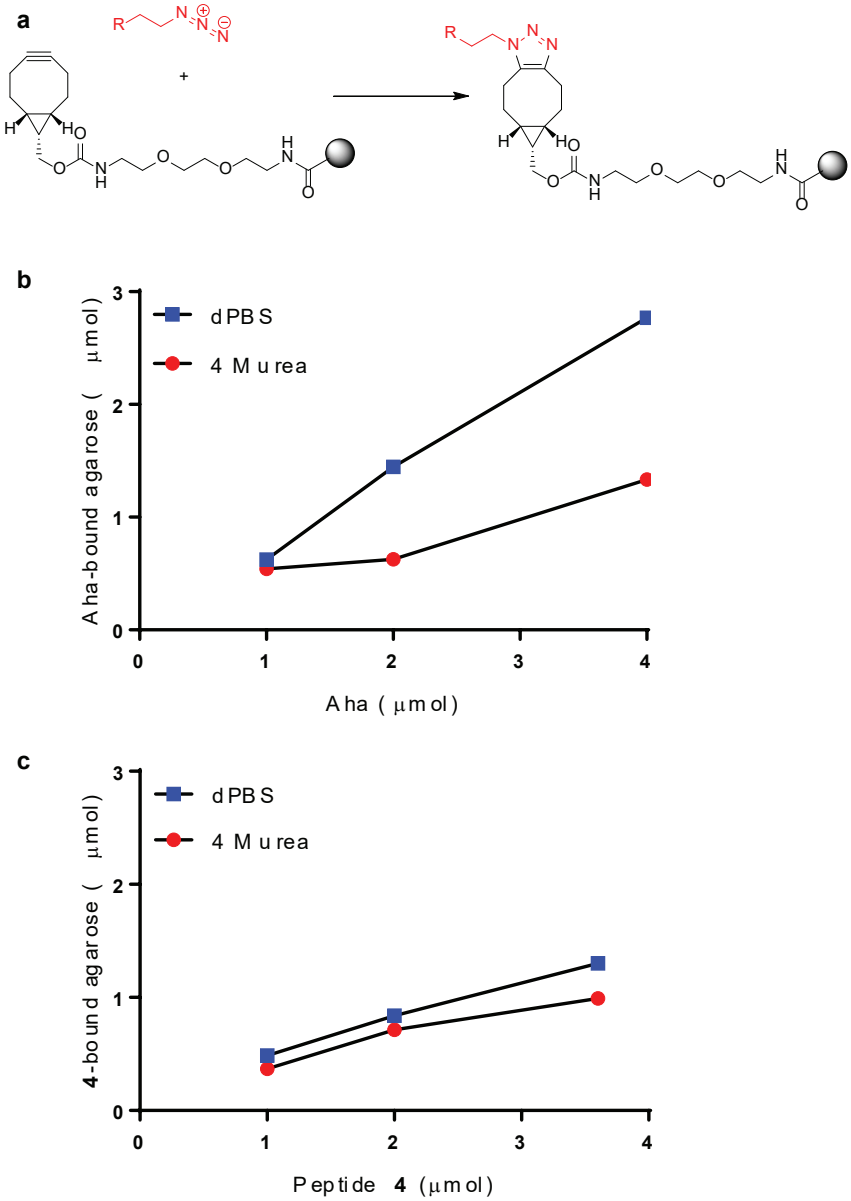

Figure 1. ***Capturing of azido containing compounds with BCN-functionalized agarose resin.***

(a) General reaction scheme between an azide-containing compound and the BCN-functionalized agarose resin. The amounts of (b) Aha and (c) peptide **4** *captured by BCN-functionalized agarose resin (***2***, 20 mg) performed in deuterated PBS solution (10 mM, pD 7.8) and 4 M urea in* D_2O.

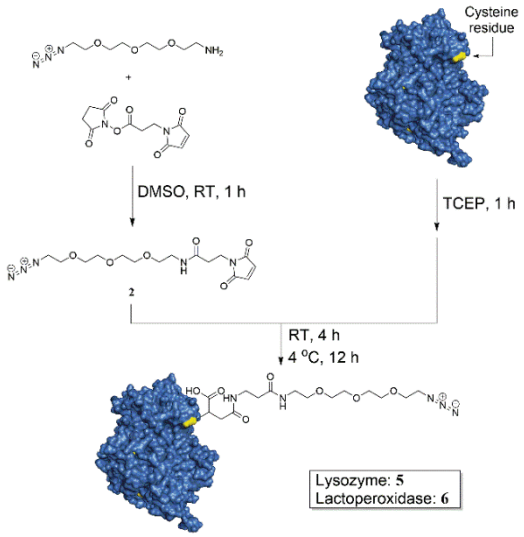

Scheme 2. *Synthesis of Model Azido-Functionalized Proteins.*

The azide-modified lysozyme (**5**) and the azide-modified lactoperoxidase (**6**) were then incubated with agarose resin **2** in three independent conditions including in PBS (pH 7.2), a 4 M urea solution and a 4 M-urea solution in a 10 % FCS containing culture medium. These experiments simulate binding under non-denaturing, denaturing as well as denaturing conditions in the presence of relevant culture media, respectively. Following incubation and subsequent washing, these resins were subjected to a LysC digestion from which the resulting peptide fragments were analyzed by LC-MS/MS. Overall, the MS results obtained from resins incubated with azide-modified lysozyme **5** revealed larger peptides than the results obtained with azide-modified lactoperoxidase **6**. It was evident that consistent miscleavage of the Lys116 residue in lysozyme occurred in the samples extracted from the resins incubated in PBS, 4 M urea or in 4 M urea containing FCS (Table S3 – Table S8). While larger peptides are typically less reliable when analyzed in MS/MS set up, the results obtained here indicated that even large peptide fragments, e.g. ranging from residues 34 – 97, could be analyzed and identified consistently. Another common modification in capturing experiments performed in aqueous solutions containing urea was carbamylation of the azide-modified lysozyme and azide-modified lactoperoxidase samples. Urea forms isocyanic acid in aqueous solutions, which acts as a nucleophile and can lead to the modification of primary amines and thiols. Despite efforts to reduce the modification of proteins by urea using ammonium bicarbonate,[44] carbamylation was still observed. Furthermore, capturing and proteolysis experiments with azide-modified lactoperoxidase **6** resulted in smaller peptides, which could also be analyzed efficiently (Table S9 – Table S14).

The specificity of the agarose resin capturing reaction was also assessed by performing control incubations involving lysozyme and lactoperoxidase with blocked resin **3**, lysozyme and lactoperoxidase with BCN-functionalized resin **2** and azide-modified lysozyme with blocked resin **3**. Following washing steps that were applied to remove

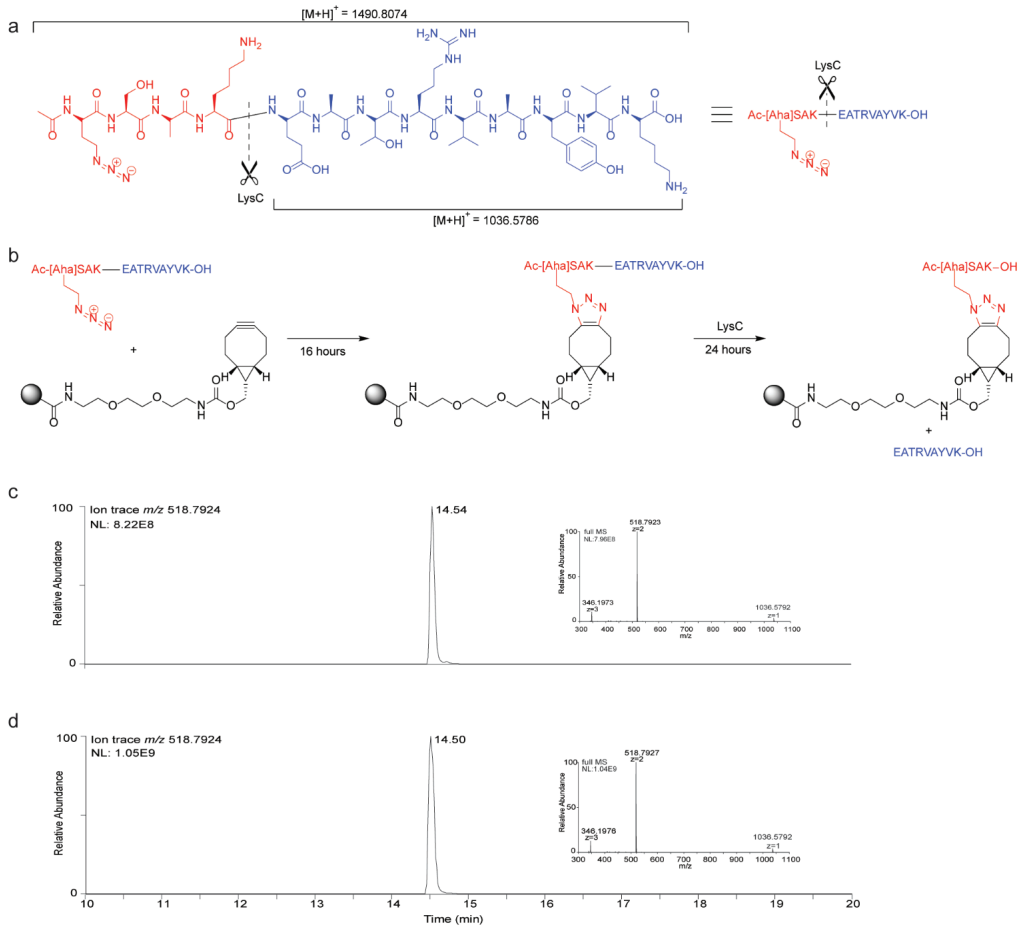

Figure 2. ***Proof of concept of Aha-functionalized peptide 4 capture by BCN-functionalized agarose resin.***

(a) Peptide **4** *structure and location of the LysC enzymatic cleavage site. (b) Reaction of the peptide with the BCN-functionalized agarose resin and LysC incubation resulting in a cleaved peptide EATRVAYVK-OH. (c) ion trace of the non-coupled peptide incubated with LysC resulting in a cleaved peptide (insert). (d) ion trace of the BCN-functionalized resin-coupled peptide obtained after incubation with LysC (10 ng injection). The inserts in (c) and (d) show the mass spectrum of the cleaved peptide EATRVAYVK-OH derived from the BCN-functionalized agarose resin incubated with LysC.*

the unconjugated protein, the agarose resins were subjected to LysC proteolysis. The resulting proteolyzed supernatant was then analyzed by MS. The samples that contained lactoperoxidase with blocked agarose resin **3** or with BCN-functionalized resin **2** did not reveal any peptides from lactoperoxidase, which indicated that non-specific adsorption of lactoperoxidase did not occur on functionalized or non-functionalized agarose resin. The experiments that involved incubation of lysozyme, however, did reveal lysozyme-derived peptide sequences, indicating non-specific adsorption on the

agarose resin (Table S15 – Table S18). The non-specific adsorption of the lysozyme-derived peptides were attributed to high affinity of lysozyme to agarose.[45]

Enrichment and analysis of cell-secreted proteins

To ascertain the application of the BCN-functionalized agarose resin for the determination of secreted proteins, a capturing, enrichment and analysis methodology was adopted as depicted in Figure 3. Human monocytic THP-1 cells were seeded and passaged in culture media deprived of L-methionine and L-leucine for 1 hour. A "pulse" then took place whereby the THP-1 cells were incubated with culture media containing Aha and the isotopically labelled L-leucine-$^{13}C_6$. This "pulse" permits the incorporation of these non-canonical amino acids into proteins instead of L-methionine and L-leucine. The incorporation of these amino acids serves two purposes. The Aha enables the capture of newly synthesized proteins through the reactivity of the azide moiety towards the BCN-functionalized resin **2**. The L-leucine-$^{13}C_6$ enables the mass spectrometry methodology to distinguish newly synthesized proteins from pre-existing proteins and bovine proteins in the serum being non-selectively bound to the BCN-functionalized resin **2** and not present in the exclusion list.

To demonstrate the capability and sensitivity of the catalyst–free capturing methodology, THP-1 cells were either stimulated with LPS for 24 hours, or allowed to remain in culture media in the absence of LPS. As such, the LPS-induced secreted protein profile relative to unstimulated THP-1 cells could be determined upon cell stimulation for 24 hours. Stimulation of the THP-1 cells with LPS is a well-described model that is commonly used in the analysis of innate immune responses.[46] In addition, the level of gene expression and cell surface marker expression in response to LPS stimulation in THP-1 cells is well-described[47] permitting comparison of secreted protein profiles.

The secreted proteins of the THP-1 cells contained in the culture supernatants were harvested 24 hours post LPS stimulation (Figure 3). Proteinase inhibitors were added to the supernatant to prevent proteolytic activity in the samples. Following filtration of the supernatant to remove residual Aha and L-leucine-$^{13}C_6$, an aqueous solution containing 4 M urea with ammonium bicarbonate was added to the samples. To capture the newly secreted proteins present in the samples, BCN-functionalized agarose resin was added to the filtered supernatant samples and incubated for 16 hours. The agarose resins were then washed and subjected to proteolytic digestion using the endoproteinase LysC. After enzymatic proteolysis, samples were labeled with TMTduplex™ to allow direct comparison of protein expression between stimulated and non-stimulated THP-1 cells by mass spectrometry. Samples were analyzed using quantitative MS^3 methods as described previously,[33] with the addition of a bovine protein exclusion list to filter out the most abundant peptides derived from the FCS containing medium.

Data analysis using Proteome Discoverer v2.1 revealed that after 24 hours, 113 proteins contained L-leucine-$^{13}C_6$ in lieu of L-leucine. The identified protein sequences also possessed additional methionine residues beyond the N-terminal signal peptide region. Through incorporation of Aha in lieu of Met at these amino acid positions thereby provides evidence that the proteins identified were specifically captured and enriched by the BCN-functionalized resin. Further evidence that supports capture of secreted proteins is that these proteins also contained the descriptors "extracellular" or "secreted" in the Gene Ontology Description. As shown in Figure 4, fold change analysis of the

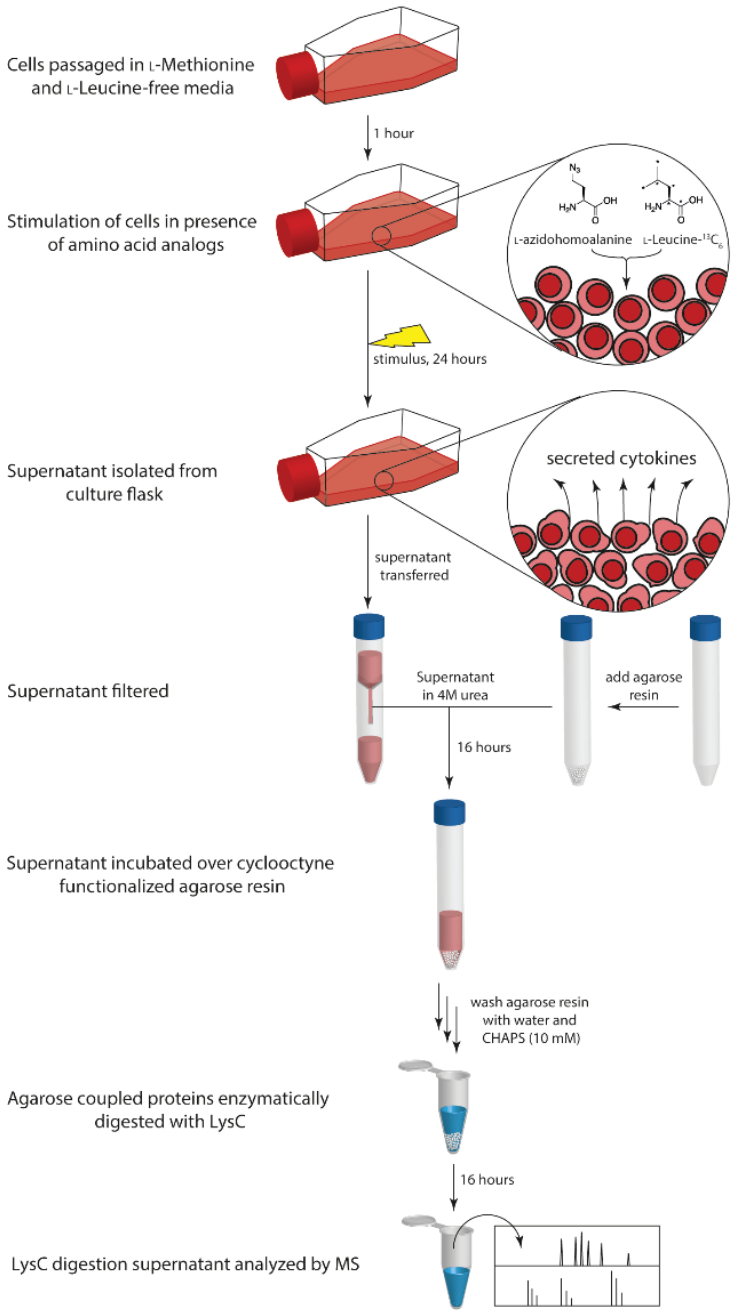

Figure 3. ***Process for stimulating and assessing secreted proteins from THP-1 cells using media modified with amino acid surrogates l-azidohomoalanine and l-leucine-13C$_6$ in lieu of l-methionine and l-leucine, respectively.***
The supernatant of the cell culture flasks is concentrated from which newly synthesized cytokines are captured by BCN-functionalized agarose resin via copper-free click chemistry.

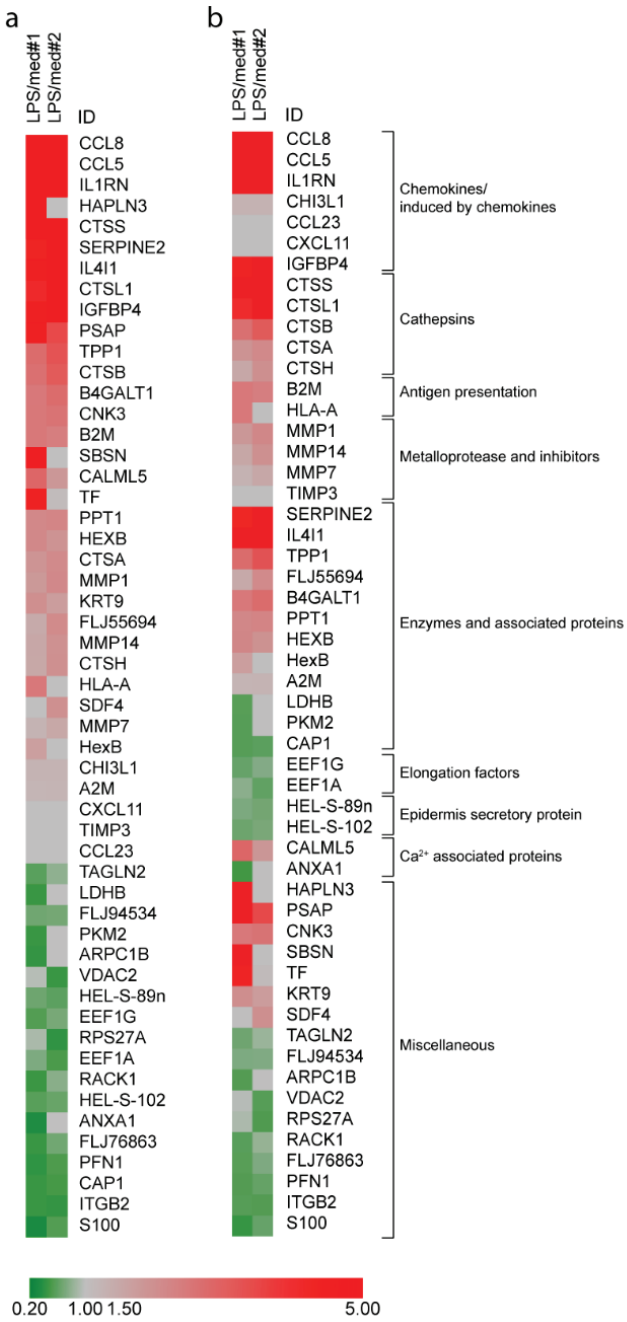

Figure 4. ***Heat map of secreted protein ratios obtained from two independent experiments comparing LPS-stimulated to non-stimulated THP-1 cells.***

The results are laid out in (a) order of factor of up- or downregulation and alternatively as (b) specific protein groups. The color scale indicates the upregulation (red) or downregulation (green) of the secreted proteins. Gray color indicated that there was no difference in the expression levels detected.

LPS-stimulated THP-1 cell secretome revealed 32 upregulated proteins and 12 downregulated proteins when compared to the non-stimulated cells. For a complete overview of all 113 proteins, see Table S19. The most notable difference in upregulation upon LPS stimulation was evident with CCL8,[48] a chemoattractant, as well as cathepsin B, cathepsin L and cathepsin S (collectively referred to as cysteine cathepsins).[49] The cathepsins are known to be essential in the LPS-induced NF-κB-dependent inflammatory response in macrophages.[49] In addition, upregulation of these cathepsins in response to LPS have been described to be TNF-α and IL-1β dependent.[50] In addition, CCL23, CCL27 and CXCL11 were identified in the supernatant, even though there was no TMT ratio available, it could still be stated that these proteins were newly secreted due to the incorporation of the non-canonical amino acids L-leucine-$^{13}C_6$ or Aha in these proteins. Other chemokines, such as CCL27 and CXCL11, have previously been associated with LPS responses.[51,52] IL-1β was not detected in the analysis, which implies that the concentration of IL-1β may be very low and could therefore not be detected.[53] The low levels of secreted IL-1β may also be attributed to the low level of expression in response to LPS.[33,54,55] Furthermore, the induction of cathepsins upon LPS stimulation may be caused by IL-1β and TNF-α.[50,56] Although TNF-α is associated with the immune response to LPS, it was not detected in the capture platform presented here. Closer inspection of the primary sequence of TNF-α, revealed the absence of methionine residues in the extracellular peptide region.[57] This implies that secreted TNF-α does not contain any Aha residues and can therefore not be captured and enriched by the BCN-functionalized resin. While IL-6 is also a cytokine expected to be found upon LPS stimulus it was not identified in this data set. This was attributed to variable expression kinetics. For example, Eichelbaum et.al., identified IL-6 between 6 and 8 hours but not at later time points following LPS stimulation.[24] As such, the results obtained after 24 hours incubation described here therefore agree with the results obtained by Eichelbaum et al.[24]

Other upregulated secreted proteins associated with LPS responses include IL-1 receptor antagonist,[58] CCL5 (RANTES), a chemoattractant for memory T cells,[59] IL4I1, a protein induced by LPS in M0 macrophages and involved in macrophage M2 differentiation[60] and β2M,[61] which is involved in HLA class I antigen presentation. In addition, integrin β_2, involved in cell migration and extravasation, was downregulated in LPS-stimulated cells, which is a previously described effect resulting from exposure to LPS.[62] As such, the results obtained here demonstrate a secreted protein profile consistent with LPS-stimulated macrophages. These data imply that by using this approach in an optimized model, the stimuli-induced secretome can be analyzed in an unbiased way, resulting in new insights about the mechanisms involved in the immune response.

Conclusions

In this paper, a new catalyst–free capture and enrichment platform was devised and applied to analysis of the THP-1 cell secretome. The devised BCN-functionalized agarose resins have demonstrated excellent applicability to capture large and small biomolecules that could easily be identified by mass spectrometry. The robustness of the catalyst-free enrichment technique as well as the stability of the agarose resin in aqueous solutions containing chaotropes such as urea, demonstrate the versatility and applicability of the approach. Furthermore, the BCN-functionalized agarose resin provides an excellent solid-state support that can be easily prepared and facilitates removal of proteins contained in the cell culture media. The method presented here showed selective enrichment of newly secreted proteins from which approximately 100 proteins have been identified in a single assay of LPS-stimulated THP-1 cells and suggests to be a viable alternative to conventional antibody-based multiplex assays.

Associated content

Supporting Information

The Supporting Information (PDF) contains the synthesis method to obtain the azide-modified lysozyme **5** and lactoperoxidase **6** and the NMR data that was employed to characterize the capturing capacity of the BCN-functionalized resin. Additional tables containing peptides identified from the model Aha-peptide, lysozyme and lactoperoxidase capture and enrichment procedure are also presented. A comprehensive overview of all 113 upregulated, downregulated and unchanged proteins as a result of LPS-stimulated THP-1 cells are compiled in an additional table. The Supporting Information is available free of charge on the ACS Publications website.

Author information

Corresponding Authors

* Hugo Meiring (Hugo.Meiring@intravacc.nl) * Maarten Danial (Maarten.Danial@intravacc.nl)

Author Contributions

The manuscript was written through contributions of all authors. All authors have given approval to the final version of the manuscript.

Acknowledgment

Rimko ten Have is acknowledged for help with freeze drying the azido-modified lysozyme and lactoperoxidase products. This work was performed within the Vac2Vac project supported by the Innovative Medicines Initiative 2 Joint Undertaking under grant agreement N-115924.

References

1 Lietzén, N.; Öhman, T.; Rintahaka, J.; Julkunen, I.; Aittokallio, T.; Matikainen, S.; Nyman, T. A. *PLoS Pathog.* 2011, *7*, e1001340.
2 Kaffamik, F. A. R.; Jones, A. M. E.; Rathjen, J. P.; Peck, S. C. *Mol. Cell. Proteomics* 2009, *8*, 145-156.
3 Hecker, M.; Becher, D.; Fuchs, S.; Engelmann, S. *Int. J. Med. Microbiol.* 2010, *300*, 76-87.
4 Eichelbaum, K.; Krijgsveld, J. *Mol. Cell. Proteomics* 2014, *13*, 792-810.
5 Koppenol-Raab, M.; Nita-Lazar, A. *Methods Mol. Biol.* 2017, *1636*, 301-312.
6 Oh, D.Y.; Dowling, D. J.; Ahmed, S.; Choi, H.; Brightman, S.; Bergelson, I.; Berger, S. T.; Sauld, J. F.; Pettengill, M.; Kho, A. T.; Pollack, H. J.; Steen, H.; Levy, O. *Mol. Cell. Proteomics* 2016, *15*, 1877-1894.
7 Meissner, F.; Scheltema, R. A.; Mollenkopf, H. J.; Mann, M. *Science* 2013, *340*, 475-478.
8 Kashyap, M. K.; Harsha, H. C.; Renuse, S.; Pawar, H.; Sahasrabuddhe, N. A.; Kim, M. S.; Marimuthu, A.; Keerthikumar, S.; Muthusamy, B.; Kandasamy, K.; Subbannayya, Y.; Prasad, T. S.; Mahmood, R.; Chaerkady, R.; Meltzer, S. J.; Kumar, R.V.; Rustgi, A. K.; Pandey, A. *Cancer Biol. Ther.* 2010, *10*, 796-810.
9 Makridakis, M.; Vlahou, A. *J. Proteomics* 2010, *73*, 2291-2305.
10 Debroy, S.; Dao, J.; Söderberg, M.; Rossier, O.; Cianciotto, N. P. *Proc. Natl. Acad. Sci. USA* 2006, *103*, 19146-19151.
11 Pasztor, L.; Ziebandt, A. K.; Nega, M.; Schlag, M.; Haase, S.; Franz-Wachtel, M.; Madlung, J.; Nordheim, A.; Heinrichs, D. E.; Götz, F. *J. Biol. Chem.* 2010, *285*, 36794-36803.
12 Deng, W.; De Hoog, C. L.; Yu, H. B.; Li, Y.; Croxen, M. A.; Thomas, N. A.; Puente, J. L.; Foster, L. J.; Finlay, B. B. *J. Biol. Chem.* 2010, *285*, 6790-6800.
13 Beer, L.; Zimmermann, M.; Mitterbauer, A.; Ellinger, A.; Gruber, F.; Narzt, M.-S.; Zellner, M.; Gyöngyösi, M.; Madlener, S.; Simader, E.; Gabriel, C.; Mildner, M.; Ankersmit, H. J. 2015, *5*, 16662.
14 Lavoie, J. R.; Rosu-Myles, M. *Biochimie* 2013, *95*, 2212-2221.
15 Mukherjee, P.; Mani, S. *Biochim. Biophys. Acta* 2013, *1834*, 2226-2232.
16 Berardis, S.; Lombard, C.; Evraerts, J.; El Taghdouini, A.; Rosseels, V.; Sancho-Bru, P.; Lozano, J. J.; van Grunsven, L.; Sokal, E.; Najimi, M. *PLoS One* 2014, *9*, e86137.
17 Thompson, A.; Schäfer, J.; Kuhn, K.; Kienle, S.; Schwarz, J.; Schmidt, G.; Neumann, T.; Hamon, C. *Anal. Chem.* 2003, *75*, 1895-1904.
18 Wiese, S.; Reidegeld, K. A.; Meyer, H. E.; Warscheid, B. *Proteomics* 2007, *7*, 340-350.
19 Mann, M. *Nat. Rev. Mol. Cell Biol.* 2006, *7*, 952-958.
20 Dieterich, D. C.; Link, A. J.; Graumann, J.; Tirrell, D. A.; Schuman, E. M. *Proc. Natl. Acad. Sci. USA* 2006, *103*, 9482-9487.
21 Dieterich, D. C.; Lee, J. J.; Link, A. J.; Graumann, J.; Tirrell, D. A.; Schuman, E. M. *Nat. Protocols* 2007, *2*, 532-540.
22 Rostovtsev, V.V.; Green, L. G.; Fokin, V.V.; Sharpless, K. B. *Angew. Chem., Int. Ed.* 2002, *41*, 2596-2599.
23 Tornøe, C. W.; Christensen, C.; Meldal, M. *J. Org. Chem.* 2002, *67*, 3057-3064.
24 Eichelbaum, K.; Winter, M.; Diaz, M. B.; Herzig, S.; Krijgsveld, J. *Nat. Biotechnol.* 2012, *30*, 984-990.
25 Stadtman, E. R. *Free Radicals Biol. Med.* 1990, *9*, 315-325.
26 Galaverna, G.; Corradini, R.; de Munari, E.; Dossena, A.; Marchelli, R. *J. Chromatogr. A* 1993, *657*, 43-54.
27 Sigel, H.; Martin, R. B. *Chem. Rev.* 1982, *82*, 385-426.
28 Bal, W.; Dyba, M.; Kasprzykowski, F.; Kozłowski, H.; Latajka, R.; Łankiewicz, L.; Małkiewicz, Z.; Pettit, L. D. *Inorg. Chim. Acta* 1998, *283*, 1-11.
29 Agard, N. J.; Prescher, J. A.; Bertozzi, C. R. *J. Am. Chem. Soc.* 2004, *126*, 15046-15047.
30 Agard, N. J.; Baskin, J. M.; Prescher, J. A.; Lo, A.; Bertozzi, C. R. *ACS Chem. Biol.* 2006, *1*, 644-648.
31 Debets, M. F.; Van Berkel, S. S.; Schoffelen, S.; Rutjes, F. P. J. T.; Van Hest, J. C. M.; Van Delft, F. L. *Chem. Commun.* 2010, *46*, 97-99.

32 Dommerholt, J.; Van Rooijen, O.; Borrmann, A.; Guerra, C. F.; Bickelhaupt, F. M.; Van Delft, F. L. Nat. Commun. **2014,** 5.

33 Kooijman, S.; Brummelman, J.; van Els, C.; Marino, F.; Heck, A. J. R.; Mommen, G. P. M.; Metz, B.; Kersten, G. F. A.; Pennings, J. L. A.; Meiring, H. D. *J. Proteomics* 2018.

34 Kiick, K. L.; Saxon, E.; Tirrell, D. A.; Bertozzi, C. R. *Proc. Natl. Acad. Sci. USA* **2002,** *99*, 19-24.

35 Link, A. J.; Tirrell, D. A. *J. Am. Chem. Soc.* **2003,** *125*, 11164-11165.

36 Dommerholt, J.; Rutjes, F. P. J. T.; van Delft, F. L. *Top. Curr. Chem.* **2016,** *374*, 16.

37 Chen, X.; Wu, Y.-W. *Org. Biomol. Chem.* **2016,** *14*, 5417-5439.

38 Kozlowski, L. P. *Nucleic Acids Res.* **2017,** *45*, D1112-D1116.

39 Kantner, T.; Watts, A. G. *Bioconjugate Chem.* **2016,** *27*, 2400-2406.

40 Faucher, A.-M.; Grand-Maître, C. *Synth. Commun.* **2003,** *33*, 3503-3511.

41 Tumey, L. N.; Charati, M.; He, T.; Sousa, E.; Ma, D.; Han, X.; Clark, T.; Casavant, J.; Loganzo, F.; Barletta, F.; Lucas, J.; Graziani, E. I. *Bioconjugate Chem.* **2014,** *25*, 1871-1880.

42 Lyon, R. P.; Setter, J. R.; Bovee, T. D.; Doronina, S. O.; Hunter, J. H.; Anderson, M. E.; Balasubramanian, C. L.; Duniho, S. M.; Leiske, C. I.; Li, F.; Senter, P. D. *Nat. Biotechnol.* **2014,** *32*, 1059-1062.

43 http://www.uniprot.org/uniprot/P80025 Accessed March 2017.

44 Sun, S.; Zhou, J.-Y.; Yang, W.; Zhang, H. *Anal. Biochem.* **2014,** *446*, 76-81.

45 Fernández-Sousa, J. M.; Rodriguez, R. *Biochem. Biophys. Res. Commun.* **1977,** *74*, 1426-1431.

46 Chanput, W.; Mes, J. J.; Wichers, H. J. *Int. Immunopharmacol.* **2014,** *23*, 37-45.

47 Guha, M.; Mackman, N. *Cell. Signal.* **2001,** *13*, 85-94.

48 Sharif, O.; Bolshakov, V. N.; Raines, S.; Newham, P.; Perkins, N. D. *BMC Immunol.* **2007,** *8*, 1.

49 de Mingo, A.; de Gregorio, E.; Moles, A.; Tarrats, N.; Tutusaus, A.; Colell, A.; Fernandez-Checa, J. C.; Morales, A.; Mari, M. *Cell Death Dis.* **2016,** *7*, e2464.

50 Creasy, B. M.; McCoy, K. L. *Cell Immunol.* **2011,** *267*, 56-66.

51 Zou, G. M.; Hu, W.Y.; Wu, W. *Cell. Signal.* **2007,** *19*, 87-92.

52 Widney, D. P.; Xia, Y. R.; Lusis, A. J.; Smith, J. B. *J. Immunol.* **2000,** *164*, 6322-31.

53 Cullen, S. P.; Kearney, C. J.; Clancy, D. M.; Martin, S. J. *Cell Rep* **2015,** *11*, 1535-48.

54 Bosshart, H.; Heinzelmann, M. *Ann. Transl. Med.* **2016,** *4*, 438.

55 Schmid-Burgk, J. L.; Gaidt, M. M.; Schmidt, T.; Ebert, T. S.; Bartok, E.; Hornung, V. *Eur. J. Immunol.* **2015,** *45*, 2911-7.

56 Hannaford, J.; Guo, H.; Chen, X. *Obesity* **2013,** *21*, 1586-95.

57 https://www.uniprot.org/uniprot/P01375 Accessed March 2017.

58 Arend, W. P.; Smith, M. F., Jr.; Janson, R. W.; Joslin, F. G. *J. Immunol.* **1991,** *147*, 1530-6.

59 Harrison, L. M.; van den Hoogen, C.; van Haaften, W. C.; Tesh, V. L. *Infect. Immun.* **2005,** *73*, 403-12.

60 Yue, Y.; Huang, W.; Liang, J.; Guo, J.; Ji, J.; Yao, Y.; Zheng, M.; Cai, Z.; Lu, L.; Wang, J. *PLoS One* **2015,** *10*, e0142979.

61 Cinar, M. U.; Islam, M. A.; Uddin, M. J.; Tholen, E.; Tesfaye, D.; Looft, C.; Schellander, K. *BMC Res. Notes* **2012,** *5*, 107.

62 Griffiths, K. L.; Tan, J. K.; O'Neill, H. C. *J. Cell Mol. Med.* **2014,** *18*, 1908-12.

Table of Contents Graphic

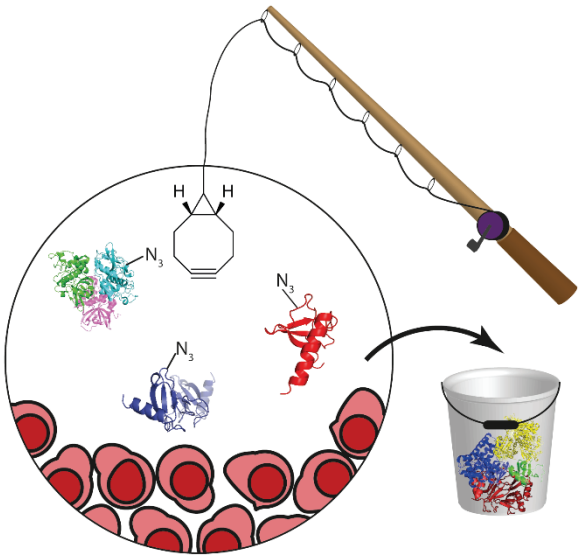

Supporting Information Chapter 6

Design of a Catalyst-free Enrichment Method for the Capture and Analysis of Cell-Secreted Proteins

Sietske Kooijman[1,2], Joost P. Uittenbogaard[1], Marieke Hoonakker[1], Hugo D. Meiring[1], Gideon F. A. Kersten[1,3], Bernard Metz[1] and Maarten Danial[1],*

1 Intravacc (Institute for Translational Vaccinology), Bilthoven, The Netherlands.
2 Biomolecular Mass Spectrometry and proteomics, Bijvoet center for Biomolecular Research and Utrecht Institute for Pharmaceutical sciences, Science faculty, Utrecht University, The Netherlands.
3 Division of Drug Delivery Technology, Leiden Academic Centre for Drug Research, Leiden, The Netherlands.

Synthesis of azido-modified lysozyme and lactoperoxidase

Lysozyme (4 mg, 2.23 mmol cysteine residues) was added to PBS (3 mL, pH 7.2) in a 15-mL polypropylene tube. TCEP (89.4 µL of 0.5 M stock) was added to the solution containing lysozyme. The solution was gently shaken at room temperature for 1.5 hours, which results in a slightly cloudy suspension. The TCEP and oxidized TCEP is removed from the protein solution by Amicon centrifuge filters (15 mL, 3.5 kDa MWCO). Meanwhile, the azido-PEG3-maleimide was prepared. DMSO (1 mL) was added to the azido-PEG3-maleimide (vial 2 of kit), which was then added dropwise to the maleimide NHS-ester (vial 1 of kit). This mixture was allowed to stir at room temperature for 1 hour after which the solution containing the azido-PEG3-maleimide (3, 274.9 µL, 74.5 µmol, 100 equiv) was added to 1 mL of the prepared lysozyme solution (0.744 mmol Cys) described above. The solution was gently stirred for 4 hours at room temperature followed by 12 hours at 4°C. The final lysozyme-azido conjugate (4) was purified using an Amicon centrifuge filter (15 ml, 3.5 kDa MWCO) and used directly in experiments with BCN-functionalized agarose resin or freeze-dried and stored at -20°C until future use.

Similarly, lactoperoxidase (15 mg, 2.23 µmol cysteine residues) was added to PBS (3 mL, pH 7.2) in a 15-mL polypropylene tube. TCEP (89.4 µL of 0.5 M stock) was added to the solution containing lactoperoxidase. After reduction, the residual TCEP and oxidized TCEP is removed using an Amicon centrifuge filter (3.5 kDa MWCO). The protein solution is concentrated and the volume is topped up to result in a total 3-mL volume. Azido-PEG3-maleimide (274.9 µL, 74.5 µmol, 100 equiv) prepared as described above was added to 1 mL of the lactoperoxidase solution (0.744 mmol Cys). The solution was gently stirred for 4 hours at room temperature followed by 12 hours at 4 °C. The lactoperoxidase-azide conjugate (5) was purified using an Amicon centrifuge filter (15 mL, 3.5 kDa MWCO) and used directly in experiments with BCN-functionalized agarose resin or freeze-dried and stored at -20°C until future use.

Table S1. ***Mass exclusion list used during the LC-MS runs with the THP-1 cell supernatant captured proteins.***

m/z	*z*[a]	*accession no*[b]
457.60	3	P02769
475.59	3	P02769
481.91	5	P02769
513.32	3	P01966
531.68	3	P02769
532.66	3	P02769
538.65	3	P02769
549.09	4	P02769
562.37	2	P01966
564.31	5	P01966
586.01	3	P02769
587.60	4	P02769
602.14	4	P02769
614.37	2	P02769
617.34	3	P02769
620.36	4	P02769
620.39	2	P02769
620.40	2	P02769
620.61	4	P02769
668.87	2	P02769
684.79	5	P01966
686.90	2	P02769
694.90	2	P02769
700.91	2	P02070
702.61	4	P01966
705.13	4	P01966
708.08	3	P02769
712.89	2	P02769
721.46	3	P02070
732.97	2	P02769
751.76	3	P02769
758.90	4	P01966
765.94	2	P02769
783.13	3	P02769
790.14	3	P02769
797.02	2	P02769
798.48	2	P02769
807.47	2	P02769
807.97	2	P02769
826.81	3	P02769
827.14	3	P02769
865.52	2	P01966
878.52	2	P02769
879.01	2	P02769
918.97	2	P02769
925.51	2	P02769
926.00	2	P02769
937.02	2	P02070
939.84	3	P01966
1011.53	3	P01966
1174.20	2	P02769

a z = charge. b P02769 – bovine serum albumin; P01966 – bovine hemoglobin subunit α; P02070 – bovine hemoglobin subunit β.

Table S2. ***Identification of lysC-proteolyzed sequences modified with azide-PEG3-maleimide linker.***

protein–linker sample	*protein (positions)*	*sequence*[a]	*conv.*[b] *(%)*	*theoretical m/z*[c]	*found m/z*[c]
5	Lysozyme (2-13)	[K].VFGRCELAAAMK.[R]	99	841.9213 (z=2) 561.6166 (z=3)	841.9217 (z=2) 561.6166 (z=3)
	Lysozyme (14-33)	[K].RHGLDNYRGYSLGN-WVCAAK.[F]	78	889.7664 (z=3) 667.5766 (z=4)	889.7671 (z=3) 667.5771 (z=4)
	Lysozyme (117-129)	[K].GTDVQAWIRGCRL.[-]	100	931.4710 (z=2) 621.3164 (z=3)	931.4716 (z=2) 621.3163 (z=3)
6	Lactoperoxidase (642-656)	[K].VSFSRLICDNTHITK.[V]	18	707.6968 (z=3) 531.0244 (z=4)	707.6964 (z=3) 531.0237 (z=4)
	Lactoperoxidase (657-679)	[K].VPLHAFQANNYPHDF-VDCSTVDK.[L]	50	1002.1350 (z=3) 751.8528 (z=4)	1002.1345 (z=3) 751.8525 (z=4)

a Peptide sequence derived from uniprot.org where lysozyme (P00698) or lactoperoxidase (P80025) was modified at the cysteine residues (bold, underlined) with a hydrolyzed azide-PEG3-maleimide linker (m/z = 389.19105). bConversion was calculated from the chromatographic base peak trace area of the azide-PEG3-thiosuccinimide linker containing peptides divided by the sum of the base peak areas for the native and azide-PEG3-thiosuccinimide linker containing peptides. cTheoretical and found m/z of the peptide–azide-PEG3-thioether succinimide linker fragments, where z=2, z=3 and/or z=4.

Table S3. ***Proteolysis summary of azido-modified Lysozyme[a] 5 after incubation with 10 mg cyclooctyne modified agarose resin 2 performed in 10 mM PBS.***

Accession	*Description*	*Coverage (%)*	*# Peptides*	*# PSMs*	*# Unique Peptides*	*# Protein Groups*	*# AAs*	*MW [kDa]*	*calc. pI*	*Modifications*	*Area: F3: Sample*	*emPAI*	*Score Sequest HT*
P00698	Lysozyme C | 19-147	51.1627907	4	45	4	1	129	14.3	9.04		1.09E+08	158488.3	60.7

Table S4. ***Peptides identified from incubation of azido-modified Lysozyme[a] 5 with 10 mg cyclooctyne modified agarose resin 2 performed in 10 mM PBS.***

Confidence	*Annotated Sequence*	*Modifications*	*# PSMs*	*Positions in Proteins*	*# Missed Cleavages*	*Theo. [M+H]⁺ [Da]*	*Area: F3: Sample*	*XCorr Sequest HT*
High	[K].IVSDGNGM-NAWVAWRNRCKGT-DVQAWIRGCRL.[-]	1xOxidation [M8]; 1x Deamidated [N16]	5	98-129	1	3649.769	15502406	3.81
High	[K].KIVSDGNGM-NAWVAWRNRCKGT-DVQAWIRGCRL.[-]	1xDeamidated [N]	6	97-129	2	3761.869	72848139	3.77
High	[K].IVSDGNGM-NAWVAWRNRCKGT-DVQAWIRGCRL.[-]	2xDeamidated [N9; N]	3	98-129	1	3634.758		3.4
High	[K].IVSDGNGM-NAWVAWRNRCKGT-DVQAWIRGCRL.[-]	1xDeamidated [N]	4	98-129	1	3633.774	2.42E+08	3.35
High	[K].IVSDGNGM-NAWVAWRNRCKGT-DVQAWIRGCRL.[-]	1xOxidation [M8]; 2x Deamidated [N9; N16]	3	98-129	1	3650.753	2953906	3.05
Medium	[K].IVSDGNGM-NAWVAWRNRCKGT-DVQAWIRGCRL.[-]	1xOxidation [M8]	1	98-129	1	3648.785	5352650	1.43

a Lysozyme accession number utilized: P00698.
Only well-annotated peptide-to-spectrum matches are tabulated.

Table S5. ***Proteolysis summary of azido-modified Lysozyme[a] 5 after incubation with 10 mg cyclooctyne modified agarose resin 2 performed in 4 M urea and 5 mM PBS.***

Accession	*Description*	*Coverage (%)*	*# Peptides*	*# PSMs*	*# Unique Peptides*	*# Protein Groups*	*# AAs*	*MW [kDa]*	*calc. pI*	*Modifications*	*Area: F3: Sample*	*emPAI*	*Score Sequest HT*
P00698	Lysozyme C |19-147	100	6	49	6	1	129	14.3	9.04	Carbamyl [K1; K13]	2.37E+08	999999	80.41

Table S6. ***Peptides identified from incubation of azido-modified Lysozyme[a] 5 with 10 mg cyclooctyne modified agarose resin 2 performed in 4 M urea and 5 mM PBS.***

Confidence	*Annotated Sequence*	*Modifications*	*# PSMs*	*Positions in Proteins*	*# Missed Cleavages*	*Theo. [M+H]+ [Da]*	*Area: F3: Sample*	*XCorr Sequest HT*
High	[-].KVFGRCELAAAMKRHGLDNYRGYSLGNWVCAAK.[F]	1xOxidation [M12]; Carbamyl [K]	4	1-33	2	3786.853	19161173	5.28
High	[K].FESNFNTQATNRNTDGSTDYGILQINSRWWCNDGRTPGSRNLCNIPCSALLSSDITASVNCAKK.[I]	2xDeamidated [N6; N26]	3	34-97	1	7027.253	684945.8	4.53
High	[K].FESNFNTQATNRNTDGSTDYGILQINSRWWCNDGRTPGSRNLCNIPCSALLSSDITASVNCAKK.[I]		4	34-97	1	7025.285	4446127	3.75
Medium	[K].KIVSDGNGMNAWVAWRNRCKGTDVQAWIRGCRL.[-]	2xDeamidated [N10; N]; 1xOxidation [M9]	5	97-129	2	3778.848	1904940	2.36
Medium	[K].IVSDGNGMNAWVAWRNRCKGTDVQAWIRGCRL.[-]	1xDeamidated [N6]; 1xOxidation [M8]; 1xCarbamyl [N-Term]	1	98-129	1	3692.774	348405.1	2.35
Medium	[K].FESNFNTQATNRNTDGSTDYGILQINSRWWCNDGRTPGSRNLCNIPCSALLSSDITASVNCAK.[K]	2xDeamidated [N6; N11]	1	34-96	0	6899.158	436978.2	2.26
Medium	[K].IVSDGNGMNAWVAWRNRCKGTDVQAWIRGCRL.[-]	1xOxidation [M8]	2	98-129	1	3648.785	24460850	1.81

Confidence	*Annotated Sequence*	*Modifications*	*# PSMs*	*Positions in Proteins*	*# Missed Cleavages*	*Theo. $[M+H]^+$ [Da]*	*Area: F3: Sample*	*XCorr Sequest HT*
Medium	[K].FESNFNTQATNRNTDGSTDYGILQINSRWWCNDGRTPGSRNLCNIPCSALLSSDITASVNCAKK.[I]	1xDeamidated [N4]	1	34-97	1	7026.269		1.65
Medium	[K].IVSDGNGMNAWVAWRNRCKGTDVQAWIRGCRL.[-]	3xDeamidated [N6; N9; N16]; 1xCarbamyl [K19]	1	98-129	1	3678.747	16218898	1.61

a Lysozyme accession number utilized: P00698. Only well-annotated peptide-to-spectrum matches are tabulated.

Table S7. ***Proteolysis summary of azido-modified Lysozyme[a] 5 after incubation with 10 mg cyclooctyne modified agarose resin 2 performed in 4 M urea in 10 % FCS medium.***

Accession	*Description*	*Coverage (%)*	*# Peptides*	*# PSMs*	*# Unique Peptides*	*# Protein Groups*	*# AAs*	*MW [kDa]*	*calc. pI*	*Modifications*	*Area: F3: Sample*	*emPAI*	*Score Sequest HT*
P00698	Lysozyme C | 19-147	100	7	57	7	1	129	14.3	9.04	Carbamyl [K97]	2.37E+08	398106.2	68.11

Table S8. ***Peptides identified from incubation of azido-modified Lysozyme[a] 5 with 10 mg cyclooctyne modified agarose resin 2 performed in 4 M urea in 10 % FCS medium.***

Confidence	*Annotated Sequence*	*Modifications*	*# PSMs*	*Positions in Proteins*	*# Missed Cleavages*	*Theo. [M+H]+ [Da]*	*Area: F3: Sample*	*XCorr Sequest HT*
High	*[K].FESNFNTQATNRNTDGSTDYGILQINSRWWCNDGRTPGSRNLCNIPCSALLSSDITASVNCAKK.[I]*	*2xDeamidated [N]*	*8*	*97-129*	*2*	*7027.253*	*13377686*	*4.01*
High	[K].FESNFNTQATNRNTDGSTDYGILQINSRWWCNDGRTPGSRNLCNIPCSALLSSDITASVNCAKK.[I]	3xDeamidated [N26; N32; N41]	2	34-97	1	7028.237	9139819	3.18
High	[K].KIVSDGNGMNAWVAWRNRCKGTDVQAWIRGCRL.[-]	1xDeamidated [N17]; 1xCarbamyl [K]	2	34-97	1	3804.874	2079227	3.14
High	[K].IVSDGNGMNAWVAWRNRCKGTDVQAWIRGCRL.[-]	1xDeamidated [N16]	11	97-129	2	3633.774	4.38E+08	3.03
Medium	[K].KIVSDGNGMNAWVAWRNRCKGTDVQAWIRGCRL.[-]	1xDeamidated [N6]	5	98-129	1	3761.869	1.69E+08	4.24
Medium	[K].FESNFNTQATNRNTDGSTDYGILQINSRWWCNDGRTPGSRNLCNIPCSALLSSDITASVNCAKK.[I]	1xDeamidated [N11]	2	34-97	1	7026.269	15759958	2.68
Medium	[K].FESNFNTQATNRNTDGSTDYGILQINSRWWCNDGRTPGSRNLCNIPCSALLSSDITASVNCAKK.[I]		4	34-97	1	7025.285	71710568	2.63
Medium	[K].IVSDGNGMNAWVAWRNRCKGTDVQAWIRGCRL.[-]	1xOxidation [M8]; 1xDeamidated [N16]	1	98-129	1	3649.769		2.09
Medium	[K].IVSDGNGMNAWVAWRNRCKGTDVQAWIRGCRL.[-]	1xOxidation [M8]	1	2-33	1	3648.785	12294555	1.73

Confidence	*Annotated Sequence*	*Modifications*	*# PSMs*	*Positions in Proteins*	*# Missed Cleavages*	*Theo. $[M+H]^+$ [Da]*	*Area: F3: Sample*	*XCorr Sequest HT*
Medium	[K].KIVSDGNGMNAWVAWRNRCKGTDVQAWIRGCRL.[-]	1xOxidation [M9]; 1xDeamidated [N]	2	98-129	2	3777.864	3853009	1.68
Medium	[K].GTDVQAWIRGCRL.[-]		3	98-129	0	1474.758	4545890	1.46
Medium	[K].IVSDGNGMNAWVAWRNRCK.[G]	1xOxidation [M8]	1	97-129	0	2193.044		1.28

a Lysozyme accession number utilized: P00698. Only well-annotated peptide-to-spectrum matches are tabulated.

Table S9. ***Proteolysis summary of azido-modified lactoperoxidase[a] 6 after incubation with 10 mg cyclooctyne modified agarose resin 2 performed in 10 mM PBS.***

Accession	*Description*	*Coverage (%)*	*# Peptides*	*# PSMs*	*# Unique Peptides*	*# Protein Groups*	*# AAs*	*MW [kDa]*	*calc. pI*	*Modifications*	*Area: F3: Sample*	*emPAI*	*Score Sequest HT*
P80025	PERL_BOVIN Lactoperoxidase 101-712 OS=Bos taurus GN=LPO PE=1 SV=1	19.60784314	12	52	12	1	612	69.4	7.99		89686281.48	19.153	69.05

Table S10. ***Peptides identified from incubation of azido-modified lactoperoxidase[a] 6 with 10 mg cyclooctyne modified agarose resin 2 performed in 10 mM PBS.***

Confidence	*Annotated Sequence*	*Modifications*	*# PSMs*	*Positions in Proteins*	*# Missed Cleavages*	*Theo. MH+ [Da]*	*Area: F3: Sample*	*XCorr Sequest HT*
High	[K].LMNQDKMVTSEL-RNK.[L]		5	423-437	1	1806.92006	1714767.461	3.45
High	[K].VSFSRLICDNTHIT-KVPLHAFQANNY-PHDFVDCST VDKLDLSPWASREN.[-]	1xDeamidat-ed [N25]	3	564-612	2	5601.69544	1993126.688	3.31
High	[K].LDLSPWASREN.[-]		2	602-612	0	1287.63279	163175882.9	3.19
High	[K].LMNQDKMVTSEL-RNK.[L]	1xOxidation [M7]	7	423-437	1	1822.91498	3584099.884	3.11
High	[K].LMNQDKMVTSEL-RNK.[L]	2xOxidation [M2; M7]	4	423-437	1	1838.90989	2244539.273	2.61
High	[K].GLQTVLKNK.[I]		2	483-491	1	1000.61496	2940056.313	2.49
High	[K].DGGIDPLVRGL-LAK.[K]		2	406-419	0	1423.82674	3073880.672	2.31
Medi-um	[K].VSFSRLICDNTHIT-KVPLHAFQANNY-PHDFVDCST VDKLDLSPWASREN.[-]		1	564-612	2	5600.71142	11106299.5	2.84
Medi-um	[K].VSFSRLICDNTHIT-KVPLHAFQANNY-PHDFVDCST VDKLDLSPWASREN.[-]	2xDeamidat-ed [N24; N]	2	564-612	2	5602.67945	4107386.625	2.83
Medi-um	[K].TRNG-FRVPLAREVSNK.[I]	1xDeamidat-ed [N3]	6	83-98	0	1845.00895	69890078.94	2.56
Medi-um	[K].KLNPHWNGEK.[L]	1xDeamidat-ed [N7]	2	299-308	1	1223.61675	682287.7813	2.23
Medi-um	[K].GLQTVLK.[N]		2	483-489	0	758.47707	17442360.38	1.96
Medi-um	[K].LNPHWNGEK.[L]	1xDeamidat-ed [N6]	3	300-308	0	1095.52178	2138961.668	1.94
Medi-um	[K].MVTSELRNK.[L]	1xOxidation [M1]	2	429-437	0	1093.56702	10817739.8	1.93
Medi-um	[K].VSFSRLICDNTHIT-KVPLHAFQANNY-PHDFVDCSTVDK.[L]	2xDeami-dated [N10; N24]	1	564-601	1	4334.0645		1.88
Medi-um	[K].LFQPTHK.[I]		2	438-444	0	870.48321	16931721.5	1.74

Confidence	*Annotated Sequence*	*Modifications*	*# PSMs*	*Positions in Proteins*	*# Missed Cleavages*	*Theo. MH+ [Da]*	*Area: F3: Sample*	*XCorr Sequest HT*
Medium	[K].VSFSRLICDNTHITKVPLHAFQANNYPHDFVDCSTVDK.[L]	1xDeamidated [N25]	1	564-601	1	4333.08049	5808621.875	1.61
Medium	[K].MVTSELRNK.[L]		3	429-437	0	1077.5721	35992882.62	1.49
Medium	[K].TRNGFRVPLAREVSNK.[I]	2xDeamidated [N3; N15]	1	83-98	0	1845.99297	296239.3672	1.4
Medium	[K].LNPHWNGEK.[L]		1	300-308	0	1094.53777	479858.4492	1.27

a Lactoperoxidase accession number utilized: P80025.

Table S11. ***Proteolysis summary of azido-modified Lactoperoxidase[a] 6 after incubation with 10 mg cyclooctyne modified agarose resin 2 performed in 4 M urea + 5 mM PBS.***

Accession	*Description*	*Coverage (%)*	*# Peptides*	*# PSMs*	*# Unique Peptides*	*# Protein Groups*	*# AAs*	*MW [kDa]*	*calc. pI*	*Modifications*	*Area: F3: Sample*	*emPAI*	*Score Sequest HT*
P80025	PERL_BOVIN Lactoperoxidase 101-712 OS=Bos taurus GN=LPO PE=1 SV=1	33.49673203	18	99	18	1	612	69.4	7.99	Carbamyl [K479; K482]	71292446	29.079	97.9

Table S12. ***Peptides identified from incubation of azido-modified Lactoperoxidase[a] 6 with 10 mg cyclooctyne modified agarose resin 2 performed in 4 M urea + 5 mM PBS.***

Confidence	*Annotated Sequence*	*Modifications*	*# PSMs*	*Positions in Proteins*	*# Missed Cleavages*	*Theo. MH+ [Da]*	*Area: F2: Sample*	*XCorr Sequest HT*
High	[K].LDLSPWASREN.[-]		8	602-612	0	1287.633	1.04E+08	3.76
High	[K].IHGFDLAAINLQR-CRDHGMPGYNSWRG-FCGLSQPKTLK.[G]	2xDeamidated [N10; N23]; 1xCarbamyl [K]	3	445-482	1	4332.101	16376243	3.74
High	[K].LMNQDKMVTSEL-RNK.[L]	1xOxidation [M7]	8	423-437	1	1822.915	2210092	3.63
High	[K].LMNQDKMVTSEL-RNK.[L]		2	423-437	1	1806.92	461135.5	3.48
High	[K].IVGYLDEEGVLD-QNRSLLFMQWGQI-VDHDLDFAPET ELGSNEHSK.[T]	1xDeamidated [N14]	1	99-143	0	5145.442	546950	3.28
High	[K].GLQTVLKNK.[I]		4	483-491	1	1000.615	3075131	2.72
High	[K].LMNQDKMVTSEL-RNK.[L]	2xOxidation [M2; M7]	8	423-437	1	1838.91	1616268	2.72
High	[K].MVTSELRNK.[L]		6	429-437	0	1077.572	44244057	2.42
High	[K].MVTSELRNK.[L]	1xOxidation [M1]	5	429-437	0	1093.567	8608565	2.26
High	[K].LNPHWNGEK.[L]		6	300-308	0	1094.538	933469.9	2.14
High	[K].LNPHWNGEK.[L]	1xDeamidated [N6]	6	300-308	0	1095.522	3090474	2.11
High	[K].GLQTVLK.[N]		2	483-489	0	758.4771	14545865	2.1
High	[K].LFQPTHK.[I]		3	438-444	0	870.4832	16220168	2.05
High	[K].QRDSLQK.[V]	1xGln->pyro-Glu [N-Term]	1	557-563	0	857.4476	1183384	2.05
Medi-um	[K].VSFSRLICDNTHIT-KVPLHAFQANNY-PHDFVDCSTVDK.[L]		1	564-601	1	4332.096	7919719	2.87
Medi-um	[K].VSFSRLICDNTHIT-KVPLHAFQANNY-PHDFVDCSTVDKL DLSPWASREN.[-]		4	564-612	2	5600.711	344015.4	2.81
Medi-um	[K].TRNG-FRVPLAREVSNK.[I]	1xDeamidated [N]	15	83-98	0	1845.009	65701139	2.67
Medi-um	[K].KLNPHWNGEK.[L]	1xDeamidated [N]	3	299-308	1	1223.617	1069951	2.45

Confidence	*Annotated Sequence*	*Modifications*	*# PSMs*	*Positions in Proteins*	*# Missed Cleavages*	*Theo. MH+ [Da]*	*Area: F2: Sample*	*XCorr Sequest HT*
Medium	[K].LYQEARK.[I]		4	309-315	0	907.4996	423355.6	1.85
Medium	[K].MVTSELRNKLFQPTHKIHGFDLAAINLQRCRDHGMPGY NSWRGFCGLSQPK.[T]	1xOxidation [M35]; 1xDeamidated [N]; 1xCarbamyl [K]; 1xAzido-linker-hydr [C]	2	429-479	2	6302.08	386940.4	1.83
Medium	[K].TRNGFRVPLAREVSNK.[I]		4	83-98	0	1844.025	1192960	1.64
Medium	[K].VSFSRLICDNTHITKVPLHAFQANNYPHDFVDCSTVDK.[L]	1xDeamidated [N24]	1	564-601	1	4333.08		1.63
Medium	[K].SKLMNQDKMVTSELRNK.[L]	2xOxidation [M4; M9]; 2xDeamidated [N5; N16]	1	421-437	2	2056.005		1.42
Medium	[K].VPLHAFQANNYPHDFVDCSTVDK.[L]		1	579-601	0	2617.214	1141583	1.01

a Lactoperoxidase accession number utilized: P80025.

Table S13. ***Proteolysis summary of azido-modified lactoperoxidase[a] 6 after incubation with 10 mg cyclooctyne modified agarose resin 2 performed in 4 M urea + 10 % FCS medium.***

Accession	*Description*	*Coverage (%)*	*# Peptides*	*# PSMs*	*# Unique Peptides*	*# Protein Groups*	*# AAs*	*MW [kDa]*	*calc. pI*	*Modifications*	*Area: F3: Sample*	*emPAI*	*Score Sequest HT*
P80025	PERL_BOVIN Lactoperoxidase 101-712 OS=Bos taurus GN=LPO PE=1 SV=1	26.30718954	19	123	19	1	612	69.4	7.99	Carbamyl [K479; K482]	89686281	121.168	129.55

Table S14. ***Peptides identified from incubation of azido-modified lactoperoxidase[a] 6 with 10 mg cyclooctyne modified agarose resin 2 performed in 4 M urea + 10 % FCS medium.***

Confidence	*Annotated Sequence*	*Modifications*	*# PSMs*	*Positions in Proteins*	*# Missed Cleavages*	*Theo. MH+ [Da]*	*Area: F1: Sample*	*XCorr Sequest HT*
High	[K].LDLSPWASREN.[-]		6	602-612	0	1287.633	50865057	3.67
High	[K].LMNQDKMVTSELRNK.[L]	1xOxidation [M7]	7	423-437	1	1822.915	576465.7	3.35
High	[K].VSFSRLICDNTHITKVPLHAFQANNYPHDFVDCSTVDKLDLSPWASREN.[-]	1xDeamidated [N]	8	564-612	2	5601.695	1730627	3.33
High	[K].TRNGFRVPLAREVSNK.[I]	1xDeamidated [N3]	17	83-98	0	1845.009	22722205	3.2
High	[K].LMNQDKMVTSELRNK.[L]	2xOxidation [M2; M7]	8	423-437	1	1838.91	899038.8	2.88
High	[K].DGGIDPLVRGLLAK.[K]		4	406-419	0	1423.827	1369670	2.79
High	[K].MVTSELRNK.[L]		4	429-437	0	1077.572	2523096	2.58
High	[K].GLQTVLKNK.[I]		2	483-491	1	1000.615	333398.2	2.38
High	[K].GLQTVLK.[N]		2	483-489	0	758.4771	10103629	2.05
High	[K].LFQPTHK.[I]		2	438-444	0	870.4832	3528631	2
Medium	[K].IVGYLDEEGVLDQNRSLLFMQWGQIVDHDLDFAPETELGSNEHSK.[T]		1	99-143	0	5144.458		2.79
Medium	[K].VSFSRLICDNTHITKVPLHAFQANNYPHDFVDCSTVDK.[L]	1xDeamidated [N]	4	564-601	1	4333.08	35746551	2.77
Medium	[K].MVTSELRNKLFQPTHKIHGFDLAAINLQRCRDHGMPGY NSWRGFCGLSQPK.[T]	1xOxidation [M]; 1xDeamidated [N]; 1xCarbamyl [K]; 1xAzido-linker-hydr [C]	3	429-479	2	6302.08	1365785	2.66
Medium	[K].IHGFDLAAINLQRCRDHGMPGYNSWRGFCGLSQPK.[T]		2	445-479	0	3944.901	629006.1	2.66

Confidence	*Annotated Sequence*	*Modifications*	*# PSMs*	*Positions in Proteins*	*# Missed Cleavages*	*Theo. MH+ [Da]*	*Area: F1: Sample*	*XCorr Sequest HT*
Medium	[K].VSFSRLICDNTHITKVPLHAFQANNYPHDFVDCSTVDK.[L]	2xDeamidated [N24; N]	4	564-601	1	4334.065	1187628	2.54
Medium	[K].VSFSRLICDNTHITKVPLHAFQANNYPHDFVDCSTVDKLDLSPWASREN.[-]		2	564-612	2	5600.711	3243407	2.5
Medium	[K].MVTSELRNK.[L]	1xOxidation [M1]	6	429-437	0	1093.567	1997126	1.98
Medium	[K].LNPHWNGEK.[L]	1xDeamidated [N6]	1	300-308	0	1095.522	656582.3	1.88
Medium	[K].KLNPHWNGEKLYQEARK.[I]	Carbamyl [K]	2	299-315	2	2197.126	767030.1	1.65
Medium	[K].IHGFDLAAINLQRCRDHGMPGYNSWRGFCGLSQPK.[T]	1xOxidation [M19]; 1xAzido-linker-hydr [C29]	1	445-479	0	4348.071		1.58
Medium	[K].QRDSLQKVSFSRLICDNTHITK.[V]	1xCarbamyl [K22]; 1xGln->pyro-Glu [N-Term]	1	557-578	1	2615.336	688298.4	1.21
Medium	[K].LDLSPWASREN.[-]	1xDeamidated [N11]	1	602-612	0	1288.617	1769223	0.93

a Lactoperoxidase accession number utilized: P80025.

Table S15. ***Proteolysis summary of unmodified lysozyme after incubation with 10 mg cyclooctyne modified agarose resin 2 performed in 10 mM PBS.***

Accession	*Description*	*Coverage (%)*	*# Peptides*	*# PSMs*	*# Unique Peptides*	*# Protein Groups*	*# AAs*	*MW [kDa]*	*calc. pI*	*Modifications*	*Area: F3: Sample*	*emPAI*	*Score Sequest HT*
P00698	Lysozyme C | 19-147	84.49612	6	42	1	1	129	14.3	9.04		7849932	250.189	74.5

Table S16. ***Peptides identified from incubation of unmodified lysozyme with 10 mg cyclooctyne modified ag[a]rose resin 2 performed in 10 mM PBS.***

Confidence	*Annotated Sequence*	*Modifications*	*# PSMs*	*Positions in Proteins*	*# Missed Cleavages*	*Theo. MH+ [Da]*	*Area: F4: Sample*	*XCorr Sequest HT*
High	[K].IVSDGNGMNAWVAW-RNRCKGTDVQAWIRG-CRL.[-]	2xDeamidated [N9; N]	4	98-129	1	3634.758	15915490	4.09
High	[K].KIVSDGNGM-NAWVAWRNRCKGTD-VQAWIRGCRL.[-]	1xDeamidated [N7]	1	97-129	2	3761.869	376369.5	3.97
High	[-].KVFGRCELAAAMK.[R]		10	1-13	1	1423.755	3482565	3.77
High	[-].KVFGRCELAAAMK.[R]	1xOxidation [M12]	16	1-13	1	1439.75	838747.8	2.91
High	[K].IVSDGNGMNAWVAW-RNRCKGTDVQAWIRG-CRL.[-]	1xDeamidated [N16]	5	98-129	1	3633.774	4934889	2.66
High	[K].GTDVQAWIRGCRL.[-]		4	117-129	0	1474.758	2369696	2.05
Medium	[K].VFGRCELAAAMK.[R]		1	2-13	0	1295.66	4151742	2.15
Medium	[K].FESNFNTQATNRNT-DGSTDYGILQINSRW-WCNDGRT PGSRNLCNIPCSALLSSDI-TASVNCAK.[K]		1	34-96	0	6897.19	1358157	1.77

Table S17. ***Proteolysis summary of azido-modified lysozyme 5 after incubation with 10 mg inactivated agarose resin 3 performed in 10 mM PBS.***

Accession	*Description*	*Coverage (%)*	*# Peptides*	*# PSMs*	*# Unique Peptides*	*# Protein Groups*	*# AAs*	*MW [kDa]*	*calc. pI*	*Modifications*	*Area: F3: Sample*	*emPAI*	*Score Sequest HT*
P00698	Lysozyme C | 19-147	35.65891	4	20	4	1	129	14.3	9.04		4107974	250.189	28.35

Table S18. ***Peptides identified from incubation of azido-modified lysozyme 5 with 10 mg inactivated agarose resin 3 performed in 10 mM PBS.***

Confidence	*Annotated Sequence*	*Modifications*	*# PSMs*	*Master Protein Accessions*	*Positions in Proteins*	*# Missed Cleavages*	*Theo. MH+ [Da]*	*Area: F3: Sample*	*XCorr Sequest HT*
High	[K].KIVSDGNGM-NAWVAWRNRCKGT-DVQAWIRGCRL.[-]	1xDeamidated [N7]	1	P00698	97-129	2	3761.869	2411230	4.48
High	[K].KIVSDGNGM-NAWVAWRNRCKGT-DVQAWIRGCRL.[-]	2xDeamidated [N7; N10]	1	P00698	97-129	2	3762.853		4.27
High	[K].IVSDGNGM-NAWVAWRNRCKGT-DVQAWIRGCRL.[-]	1xDeamidated [N]	4	P00698	98-129	1	3633.774	3184366	3.82
Medium	[K].IVSDGNGM-NAWVAWRNRCKGT-DVQAWIRGCRL.[-]	2xDeamidated [N9; N]	5	P00698	98-129	1	3634.758	3690928	2.99
Medium	[-].KVFGRCELAAAMK.[R]	1xAzido-linker-hydr [C6]	8	P00698	1-13	1	1810.93	6221765	1.74
Medium	[K].VFGRCELAAAMK.[R]	1xAzido-linker-hydr [C5]	1	P00698	2-13	0	1682.835	221240.4	1.42

Table S19. ***Comprehensive list of all secreted proteins identified by the capture, enrichment and MS analysis methodology.***

Accession no.	*Description*	*Symbol*	*LPS/ med#1*	*LPS/ med#2*
H0UIC7	C-C motif chemokine OS=Homo sapiens GN=CCL8 PE=3 SV=1	CCL8	58.765	86.133
A0A075B7C5	C-C motif chemokine 5 (Fragment) OS=Homo sapiens GN=CCL5 PE=1 SV=1	CCL5	99.800	12.969
P18510	Interleukin-1 receptor antagonist protein OS=Homo sapiens GN=IL1RN PE=1 SV=1	IL1RN	9.651	10.472
H3BTH8	Hyaluronan and proteoglycan link protein 3 OS=Homo sapiens GN=HAPLN3 PE=1 SV=1	HAPLN3	99.800	
P25774	Cathepsin S OS=Homo sapiens GN=CTSS PE=1 SV=3	CTSS	5.924	6.359
A0A024R451	Serpin peptidase inhibitor, clade E (Nexin, plasminogen activator inhibitor type 1), member 2, isoform CRA_a OS=Homo sapiens GN=SERPINE2 PE=3 SV=1	SERPINE2	4.324	8.686
A2RRH1	Amine oxidase OS=Homo sapiens GN=IL4I1 PE=2 SV=1	IL4I1	4.584	6.293
A5PLM9	Cathepsin L1 OS=Homo sapiens GN=CTSL1 PE=2 SV=1	CTSL1	4.099	5.809
P22692	Insulin-like growth factor-binding protein 4 OS=Homo sapiens GN=IGFBP4 PE=1 SV=2	IGFBP4	4.429	5.183
Q59EN5	Prosaposin variant (Fragment) OS=Homo sapiens PE=2 SV=1	PSAP	4.620	3.463
B4DIV8	cDNA FLJ56402, highly similar to Tripeptidyl-peptidase 1 (EC 3.4.14.9) OS=Homo sapiens PE=2 SV=1	TPP1	2.726	3.243
A0A024R374	Cathepsin B, isoform CRA_a OS=Homo sapiens GN=CTSB PE=3 SV=1	CTSB	2.643	3.097
P15291	Beta-1,4-galactosyltransferase 1 OS=Homo sapiens GN=B4GALT1 PE=1 SV=5	B4GALT1	2.485	2.732
G9CGD6	CNK3/IPCEF1 fusion protein long isoform OS=Homo sapiens PE=1 SV=1	CNK3	2.497	2.584
A6XMH4	Beta-2-microglobulin OS=Homo sapiens PE=2 SV=1	B2M	2.492	2.378
Q6UWP8	Suprabasin OS=Homo sapiens GN=SBSN PE=1 SV=2	SBSN	5.902	
Q9NZT1	Calmodulin-like protein 5 OS=Homo sapiens GN=CALML5 PE=1 SV=2	CALML5	2.859	1.832
B4DHZ6	Transferrin, isoform CRA_c OS=Homo sapiens GN=TF PE=2 SV=1	TF	4.466	1.091
P50897	Palmitoyl-protein thioesterase 1 OS=Homo sapiens GN=PPT1 PE=1 SV=1	PPT1	2.175	2.225

Accession no.	*Description*	*Symbol*	*LPS/ med#1*	*LPS/ med#2*
P07686	Beta-hexosaminidase subunit beta OS=Homo sapiens GN=HEXB PE=1 SV=3	HEXB	2.160	1.909
A0A1B0GU03	Uncharacterized protein OS=Homo sapiens PE=1 SV=1	_	1.949	2.077
X6R8A1	Carboxypeptidase OS=Homo sapiens GN=CTSA PE=1 SV=1	CTSA	1.887	2.120
P03956	Interstitial collagenase OS=Homo sapiens GN=MMP1 PE=1 SV=3	MMP1	1.820	2.149
P35527	Keratin, type I cytoskeletal 9 OS=Homo sapiens GN=KRT9 PE=1 SV=3	KRT9	2.027	1.729
B4DJQ8	cDNA FLJ55694, highly similar to Dipeptidyl-peptidase 1 (EC 3.4.14.1) OS=Homo sapiens PE=2 SV=1	FLJ55694	1.468	2.113
B2R6P3	cDNA, FLJ93047, highly similar to Homo sapiens matrix metallopeptidase 14 (membrane-inserted) (MMP14), mRNA OS=Homo sapiens PE=2 SV=1	MMP14	1.523	1.970
P09668	Pro-cathepsin H OS=Homo sapiens GN=CTSH PE=1 SV=4	CTSH	1.499	1.993
A0A0G2JPD3	HLA class I histocompatibility antigen, A-3 alpha chain OS=Homo sapiens GN=HLA-A PE=1 SV=1	HLA-A	2.489	
Q9BRK5	45 kDa calcium-binding protein OS=Homo sapiens GN=SDF4 PE=1 SV=1	SDF4		1.996
P09237	Matrilysin OS=Homo sapiens GN=MMP7 PE=1 SV=1	MMP7	1.276	1.500
B4DVA7	Beta-hexosaminidase OS=Homo sapiens PE=2 SV=1	HexB	1.682	
P36222	Chitinase-3-like protein 1 OS=Homo sapiens GN=CHI3L1 PE=1 SV=2	CHI3L1	1.267	1.279
P01023	Alpha-2-macroglobulin OS=Homo sapiens GN=A2M PE=1 SV=3	A2M	1.226	1.253
Q92608	Dedicator of cytokinesis protein 2 OS=Homo sapiens GN=DOCK2 PE=1 SV=2	DOCK2	1.495	
K7ER74	APOC4-APOC2 readthrough (NMD candidate) OS=Homo sapiens GN=APOC4-APOC2 PE=1 SV=1	APOC4-APOC2	1.260	1.183
P08253	72 kDa type IV collagenase OS=Homo sapiens GN=MMP2 PE=1 SV=2	MMP2	1.430	
D3DSQ1	N-acylsphingosine amidohydrolase (Acid ceramidase) 1, isoform CRA_c OS=Homo sapiens GN=ASAH1 PE=4 SV=1	ASAH1		1.367

Accession no.	*Description*	*Symbol*	*LPS/ med#1*	*LPS/ med#2*
V9HWA9	Epididymis secretory sperm binding protein Li 62p OS=Homo sapiens GN=HEL-S-62p PE=2 SV=1	HEL-S-62p	1.120	1.188
A0A024QZI2	HCG1998059, isoform CRA_a OS=Homo sapiens GN=hCG_1998059 PE=4 SV=1	hCG_1998059	1.393	0.941
Q6H3X3	Retinoic acid early transcript 1G protein OS=Homo sapiens GN=RAET1G PE=1 SV=1	RAET1G	1.134	1.151
V9HW12	Epididymis secretory sperm binding protein Li 2a OS=Homo sapiens GN=HEL-S-2a PE=2 SV=1	HEL-S-2a	1.252	
P16035	Metalloproteinase inhibitor 2 OS=Homo sapiens GN=TIMP2 PE=1 SV=2	TIMP2	1.105	1.100
A0A024R3D4	Uncharacterized protein OS=Homo sapiens GN=DKFZp547C195 PE=4 SV=1	DKFZ-p547C195		1.209
P06396	Gelsolin OS=Homo sapiens GN=GSN PE=1 SV=1	GSN	1.100	1.069
K7EPF9	Apolipoprotein C-I OS=Homo sapiens GN=APOC1 PE=1 SV=1	APOC1	1.061	
P15309	Prostatic acid phosphatase OS=Homo sapiens GN=ACPP PE=1 SV=3	ACPP		1.034
O94985	Calsyntenin-1 OS=Homo sapiens GN=CLSTN1 PE=1 SV=1	CLSTN1	0.955	1.071
J3KPS3	Fructose-bisphosphate aldolase OS=Homo sapiens GN=ALDOA PE=1 SV=1	ALDOA	0.763	1.319
A0A024R4H0	Procollagen-lysine 1, 2-oxoglutarate 5-dioxygenase 1, isoform CRA_a OS=Homo sapiens GN=PLOD1 PE=4 SV=1	PLOD1		
A0A024R8G3	Prostaglandin D2 synthase 21kDa (Brain), isoform CRA_a OS=Homo sapiens GN=PTGDS PE=2 SV=1	PTGDS		
A0A024RDS1	Heat shock 105kDa/110kDa protein 1, isoform CRA_c OS=Homo sapiens GN=HSPH1 PE=3 SV=1	HSPH1		
A0A0S2Z455	Serpin peptidase inhibitor clade I member 1 isoform 1 (Fragment) OS=Homo sapiens GN=SERPINI1 PE=2 SV=1	SERPINI1		
A0A140VJP2	Testicular tissue protein Li 118 OS=Homo sapiens PE=2 SV=1	MAT2B		
B3KUY2	Prostaglandin E synthase 3 (Cytosolic), isoform CRA_c OS=Homo sapiens GN=PTGES3 PE=2 SV=1	PTGES3		
B4DTP0	cDNA FLJ51087, highly similar to Cadherin-5 OS=Homo sapiens PE=2 SV=1	CDH5		

Accession no.	*Description*	*Symbol*	*LPS/ med#1*	*LPS/ med#2*
B7Z765	cDNA FLJ56258, highly similar to Squamous cell carcinoma antigen recognized by T-cells 2 OS-=Homo sapiens PE=2 SV=1	DSE		
D3DV26	S100 calcium binding protein A10 (Annexin II ligand, calpactin I, light polypeptide (P11)), isoform CRA_b (Fragment) OS=Homo sapiens GN=S100A10 PE=4 SV=1	S100A10		
G1AUC5	Protein phosphatase inhibitor 2-like protein OS-=Homo sapiens GN=PPP1R2P3 PE=1 SV=1	PPP1R2P3		
O14625	C-X-C motif chemokine 11 OS=Homo sapiens GN=CXCL11 PE=1 SV=1	CXCL11		
P35625	Metalloproteinase inhibitor 3 OS=Homo sapiens GN=TIMP3 PE=1 SV=2	TIMP3		
P55773	C-C motif chemokine 23 OS=Homo sapiens GN=CCL23 PE=1 SV=3	CCL23		
P63104	14-3-3 protein zeta/delta OS=Homo sapiens GN=YWHAZ PE=1 SV=1	YWHAZ		
P63261	Actin, cytoplasmic 2 OS=Homo sapiens GN=ACTG1 PE=1 SV=1	ACTG1		
Q15075	Early endosome antigen 1 OS=Homo sapiens GN=EEA1 PE=1 SV=2	EEA1		
Q4W4Y1	Dopamine receptor interacting protein 4 OS-=Homo sapiens GN=DRIP4 PE=2 SV=1	DRIP4		
Q59F66	DEAD box polypeptide 17 isoform p82 variant (Fragment) OS=Homo sapiens PE=2 SV=1	DDX17		
Q6MZW2	Follistatin-related protein 4 OS=Homo sapiens GN=FSTL4 PE=2 SV=3	FSTL4		
Q6ZQQ2	Spermatogenesis-associated protein 31D1 OS-=Homo sapiens GN=SPATA31D1 PE=2 SV=1	SPATA31D1		
Q7Z5P9	Mucin-19 OS=Homo sapiens GN=MUC19 PE=1 SV=3	MUC19		
Q9HB40	Retinoid-inducible serine carboxypeptidase OS-=Homo sapiens GN=SCPEP1 PE=1 SV=1	SCPEP1		
Q9UHL4	Dipeptidyl peptidase 2 OS=Homo sapiens GN=DPP7 PE=1 SV=3	DPP7		
Q9UNF0	Protein kinase C and casein kinase substrate in neurons protein 2 OS=Homo sapiens GN=PAC-SIN2 PE=1 SV=2	PACSIN2		
A0A1B1RVA9	Lipoprotein lipase OS=Homo sapiens GN=LPL PE=3 SV=1	LPL	1.000	0.966
A0A140VKF3	Testis tissue sperm-binding protein Li 70n OS-=Homo sapiens PE=2 SV=1	Li 70n	0.965	
P00338	L-lactate dehydrogenase A chain OS=Homo sapiens GN=LDHA PE=1 SV=2	LDHA	0.913	

Accession no.	Description	Symbol	LPS/ med#1	LPS/ med#2
B8ZWD9	Diazepam binding inhibitor, splice form 1D(2) OS=Homo sapiens GN=DBI PE=2 SV=1	DBI	1.406	0.638
P06733	Alpha-enolase OS=Homo sapiens GN=ENO1 PE=1 SV=2	ENO1	0.538	1.643
Q9BTY2	Plasma alpha-L-fucosidase OS=Homo sapiens GN=FUCA2 PE=1 SV=2	FUCA2	0.884	0.979
A8K7Q1	cDNA FLJ77770, highly similar to Homo sapiens nucleobindin 1 (NUCB1), mRNA OS=Homo sapiens PE=2 SV=1	FLJ77770		0.826
B2R5H0	Protein S100 OS=Homo sapiens PE=2 SV=1	S100	0.769	1.000
Q14CN4	Keratin, type II cytoskeletal 72 OS=Homo sapiens GN=KRT72 PE=1 SV=2	KRT72	0.768	
P14625	Endoplasmin OS=Homo sapiens GN=HSP90B1 PE=1 SV=1	HSP90B1	1.138	0.661
P09382	Galectin-1 OS=Homo sapiens GN=LGALS1 PE=1 SV=2	LGALS1		0.749
A0A024RDT4	Lymphocyte cytosolic protein 1 (L-plastin), isoform CRA_a OS=Homo sapiens GN=LCP1 PE=4 SV=1	LCP1		0.727
Q0P5N8	TMSB4X protein (Fragment) OS=Homo sapiens GN=TMSB4X PE=2 SV=1	TMSB4X	0.711	0.968
P54920	Alpha-soluble NSF attachment protein OS=Homo sapiens GN=NAPA PE=1 SV=3	NAPA	0.690	0.997
P52209	6-phosphogluconate dehydrogenase, decarboxylating OS=Homo sapiens GN=PGD PE=1 SV=3	PGD	0.649	1.034
Q15582	Transforming growth factor-beta-induced protein ig-h3 OS=Homo sapiens GN=TGFBI PE=1 SV=1	TGFBI	0.764	0.761
P00558	Phosphoglycerate kinase 1 OS=Homo sapiens GN=PGK1 PE=1 SV=3	PGK1	0.580	
A0A024R5Z7	Annexin OS=Homo sapiens GN=ANXA2 PE=3 SV=1	ANXA2	0.680	0.853
P08238	Heat shock protein HSP 90-beta OS=Homo sapiens GN=HSP90AB1 PE=1 SV=4	HSP90AB1	0.708	0.783
Q53GZ6	Heat shock 70kDa protein 8 isoform 1 variant (Fragment) OS=Homo sapiens PE=2 SV=1	HSC70	0.759	0.680
Q15084	Protein disulfide-isomerase A6 OS=Homo sapiens GN=PDIA6 PE=1 SV=1	PDIA6	0.752	0.648
P62736	Actin, aortic smooth muscle OS=Homo sapiens GN=ACTA2 PE=1 SV=1	ACTA2	0.637	0.761
P37802	Transgelin-2 OS=Homo sapiens GN=TAGLN2 PE=1 SV=3	TAGLN2	0.584	0.802
P07195	L-lactate dehydrogenase B chain OS=Homo sapiens GN=LDHB PE=1 SV=2	LDHB	0.465	

Accession no.	*Description*	*Symbol*	*LPS/ med#1*	*LPS/ med#2*
B2R9S4	cDNA, FLJ94534, highly similar to Homo sapiens capping protein (actin filament), gelsolin-like(CAPG), mRNA OS=Homo sapiens PE=2 SV=1	FLJ94534	0.670	0.687
A0A024R5Z9	Pyruvate kinase OS=Homo sapiens GN=PKM2 PE=3 SV=1	PKM2	0.458	
Q5EC54	Heterogeneous nuclear ribonucleoprotein K transcript variant OS=Homo sapiens GN=HNRPK PE=2 SV=1	HNRPK	0.712	0.643
O15143	Actin-related protein 2/3 complex subunit 1B OS=Homo sapiens GN=ARPC1B PE=1 SV=3	ARPC1B	0.442	
A0A024QZN9	Voltage-dependent anion channel 2, isoform CRA_a OS=Homo sapiens GN=VDAC2 PE=4 SV=1	VDAC2	0.960	0.458
V9HWB4	Epididymis secretory sperm binding protein Li 89n OS=Homo sapiens GN=HEL-S-89n PE=2 SV=1	HEL-S-89n	0.662	0.600
P26641	Elongation factor 1-gamma OS=Homo sapiens GN=EEF1G PE=1 SV=3	EEF1G	0.546	0.702
P62979	Ubiquitin-40S ribosomal protein S27a OS=Homo sapiens GN=RPS27A PE=1 SV=2	RPS27A	0.908	0.419
A8K9C4	Elongation factor 1-alpha OS=Homo sapiens PE=2 SV=1	EEF1A	0.735	0.516
D6REE5	Receptor of-activated protein C kinase 1 (Fragment) OS=Homo sapiens GN=RACK1 PE=1 SV=1	RACK1	0.474	0.776
V9HW43	Epididymis secretory protein Li 102 OS=Homo sapiens GN=HEL-S-102 PE=2 SV=1	HEL-S-102	0.573	0.633
B5BU38	Annexin OS=Homo sapiens GN=ANXA1 PE=2 SV=1	ANXA1	0.353	
A8K690	cDNA FLJ76863, highly similar to Homo sapiens stress-induced-phosphoprotein 1 (Hsp70/Hsp90-organizing protein) (STIP1), mRNA OS=Homo sapiens PE=2 SV=1	FLJ76863	0.461	0.675
P07737	Profilin-1 OS=Homo sapiens GN=PFN1 PE=1 SV=2	PFN1	0.433	0.530
B2RDY9	Adenylyl cyclase-associated protein OS=Homo sapiens PE=2 SV=1	CAP1	0.459	0.495
D3DSM0	Integrin beta OS=Homo sapiens GN=ITGB2 PE=1 SV=1	ITGB2	0.457	0.440
B2R577	Protein S100 OS=Homo sapiens PE=2 SV=1	S100	0.318	0.545

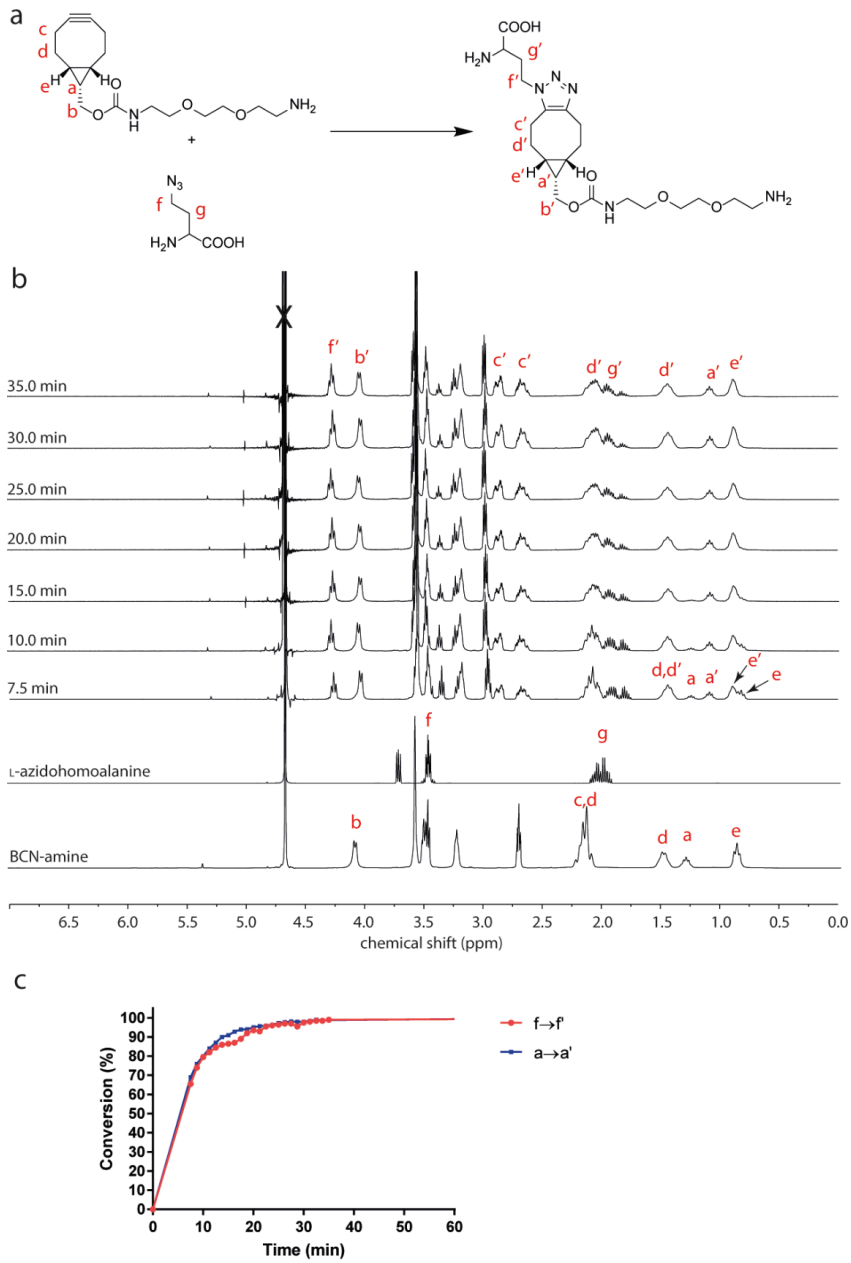

Figure S1. ***Kinetics of cyclooctyne-amine 1 with Aha reaction in deuterated PBS (10 mM, pD 7.8).***

(a) Reaction scheme with structural assignments. (b) 1H-NMR spectra of the reaction between Aha and cyclooctyne-amine 1 and structural assignments of SPAAC reactants and products. (c) Graph showing conversion of the SPAAC reaction where f→f' depicts the shift peak from 3.45 to 4.26 ppm derived from Aha and a→a' depicts the peak shift from 1.30 to 1.05 ppm. X marks the solvent peak.

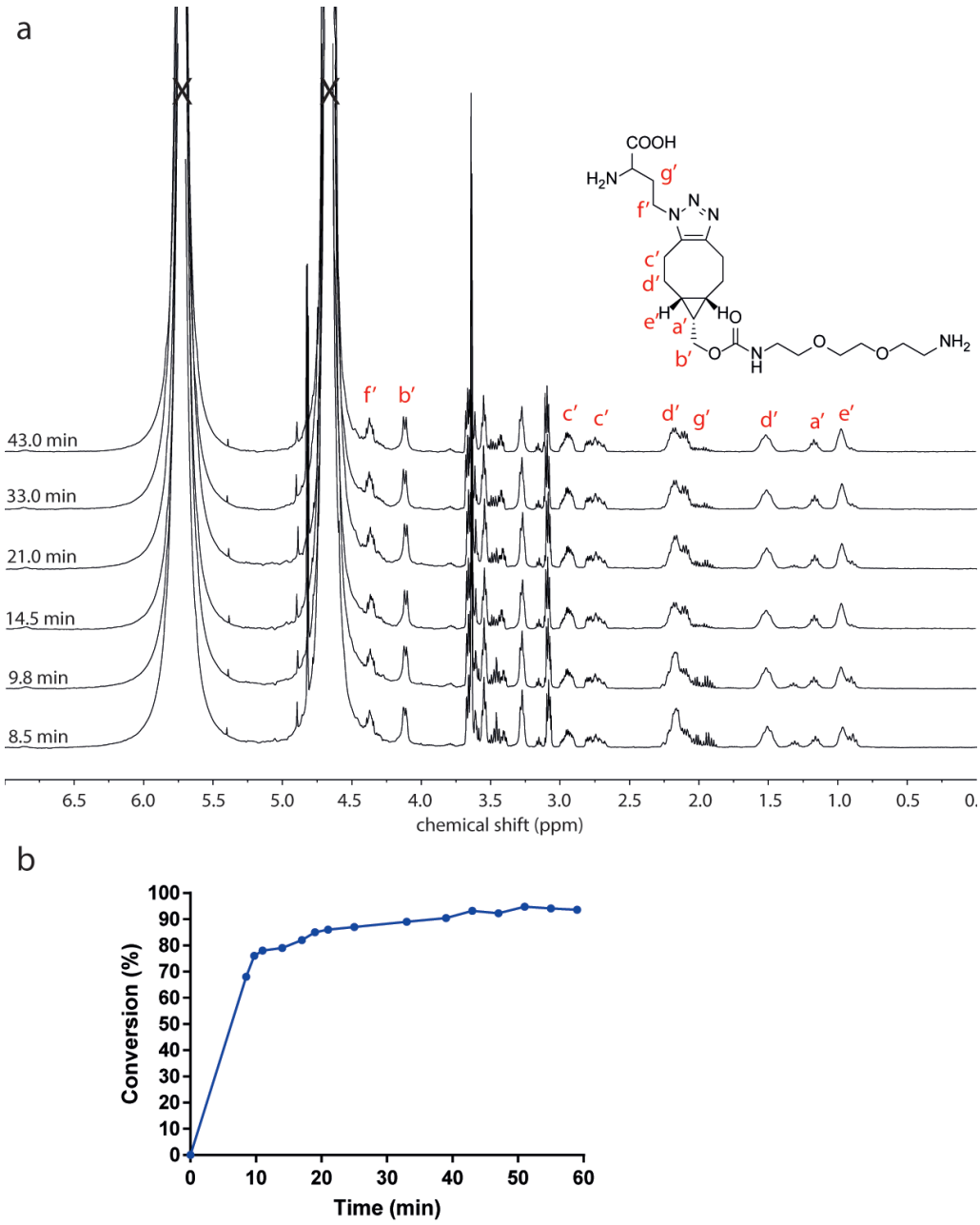

Figure S2. *Kinetics of cyclooctyne-amine 1 with Aha reaction in 8 M urea (in D2O).* *(a) 1H-NMR spectra of the reaction between Aha and cyclooctyne-amine 1 and structural assignments of SPAAC reactants and products. (b) Graph showing conversion of the SPAAC reaction where the conversion is calculated from the peak shift a→a′ from 1.30 to 1.05 ppm. X marks the 4 M urea solvent peaks.*

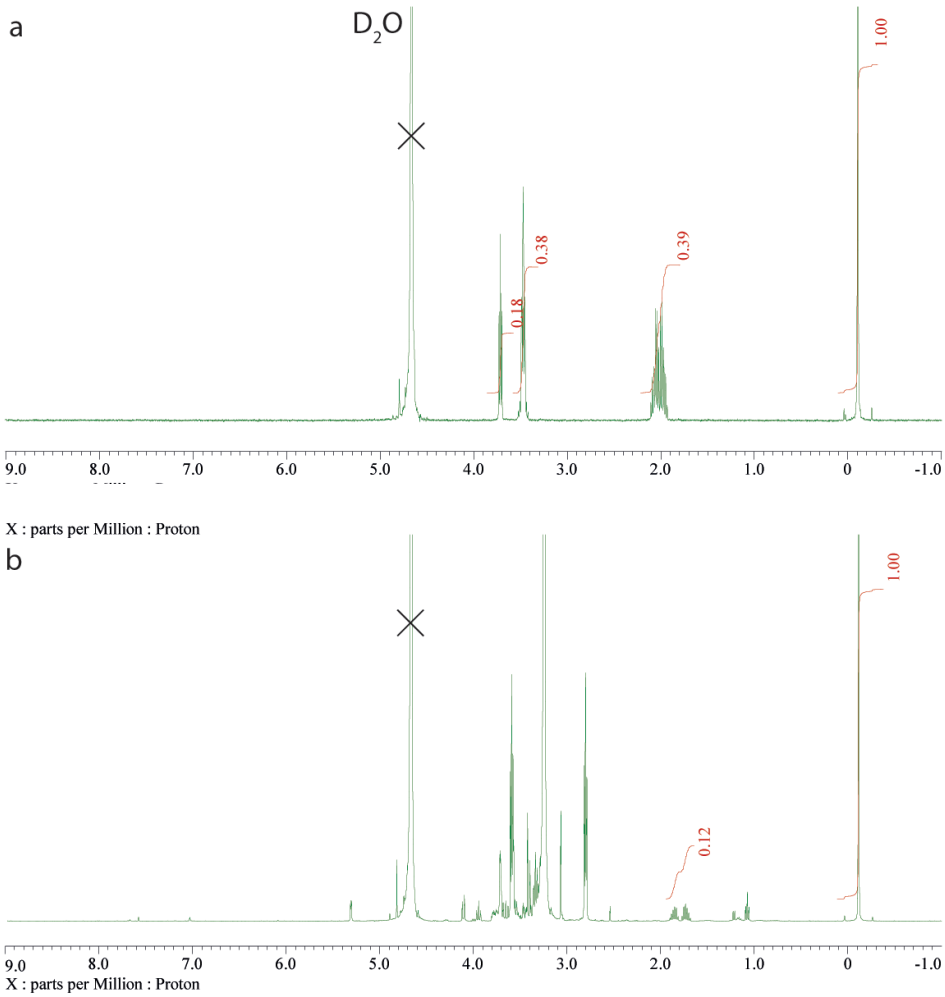

Figure S3. *1H-NMR (400 MHz) of 4 mmol Aha (a) before and (b) after incubation with 20 mg agarose resin 2 in deuterated PBS (pD 7.8) containing 0.075 vol. % 3-(trimethylsilyl)propionic-2,2,3,3-d4 acid sodium salt (TMSP-d4).*

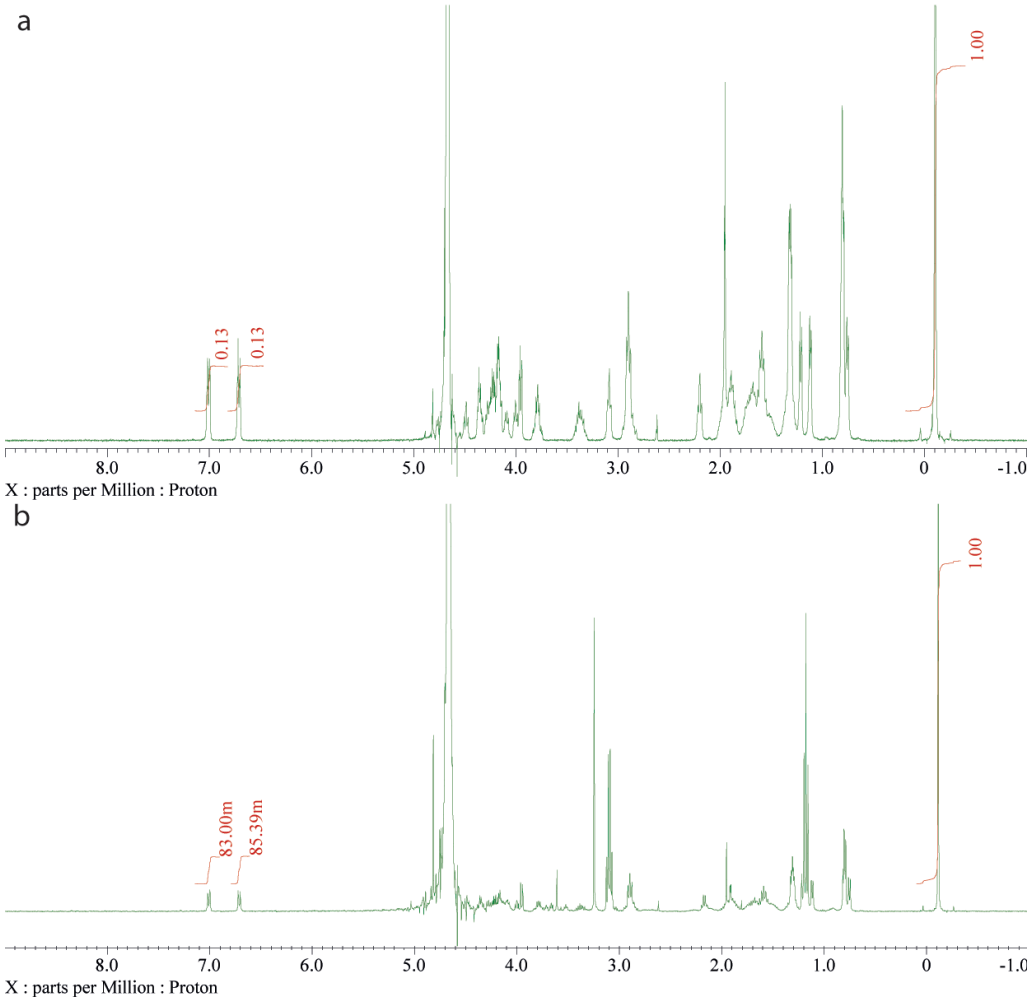

Figure S4. *1H-NMR (400 MHz) of 3.6 mmol peptide 4 (a) before and (b) after incubation with 20 mg agarose resin 2 in deuterated PBS (pD 7.8) containing 0.075 vol. % TMSP-d4.*

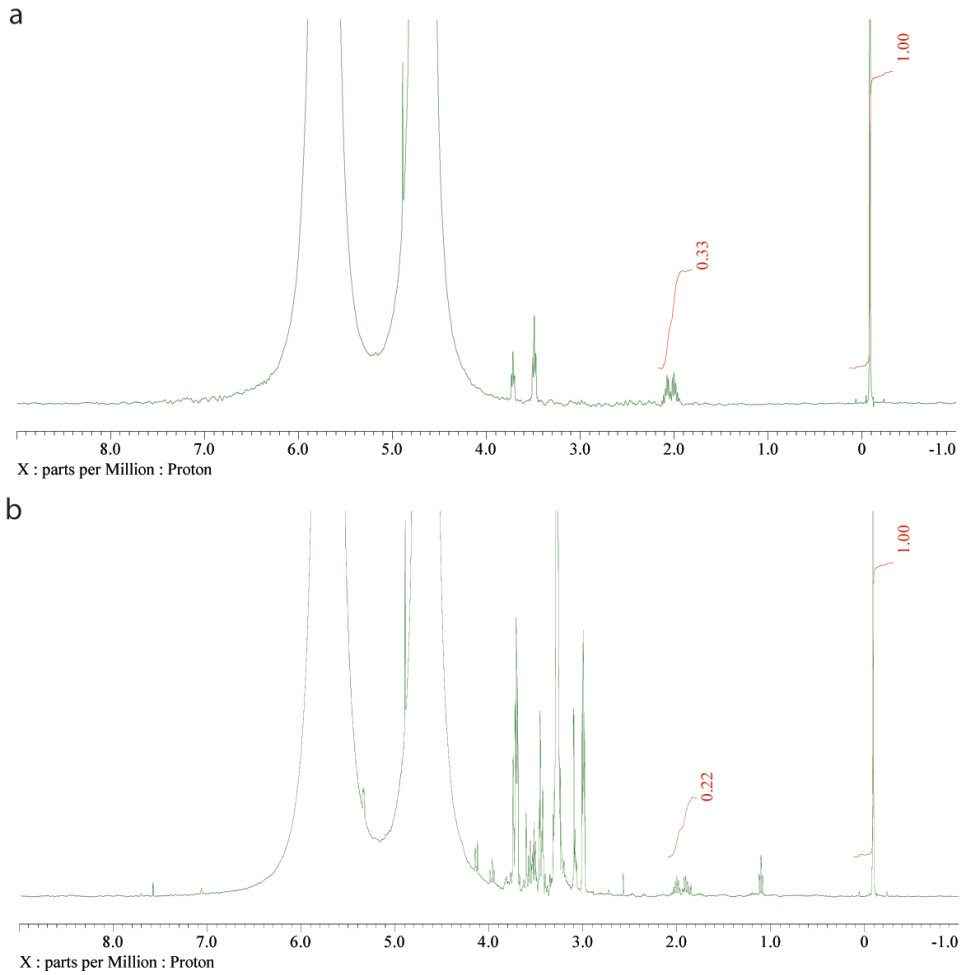

Figure S5. *1H-NMR (400 MHz) of Aha (a) before and (b) after incubation with 20 mg agarose resin 2 in 4M urea with 10 vol. % D2O and 0.075 vol. % TMSP-d4.*

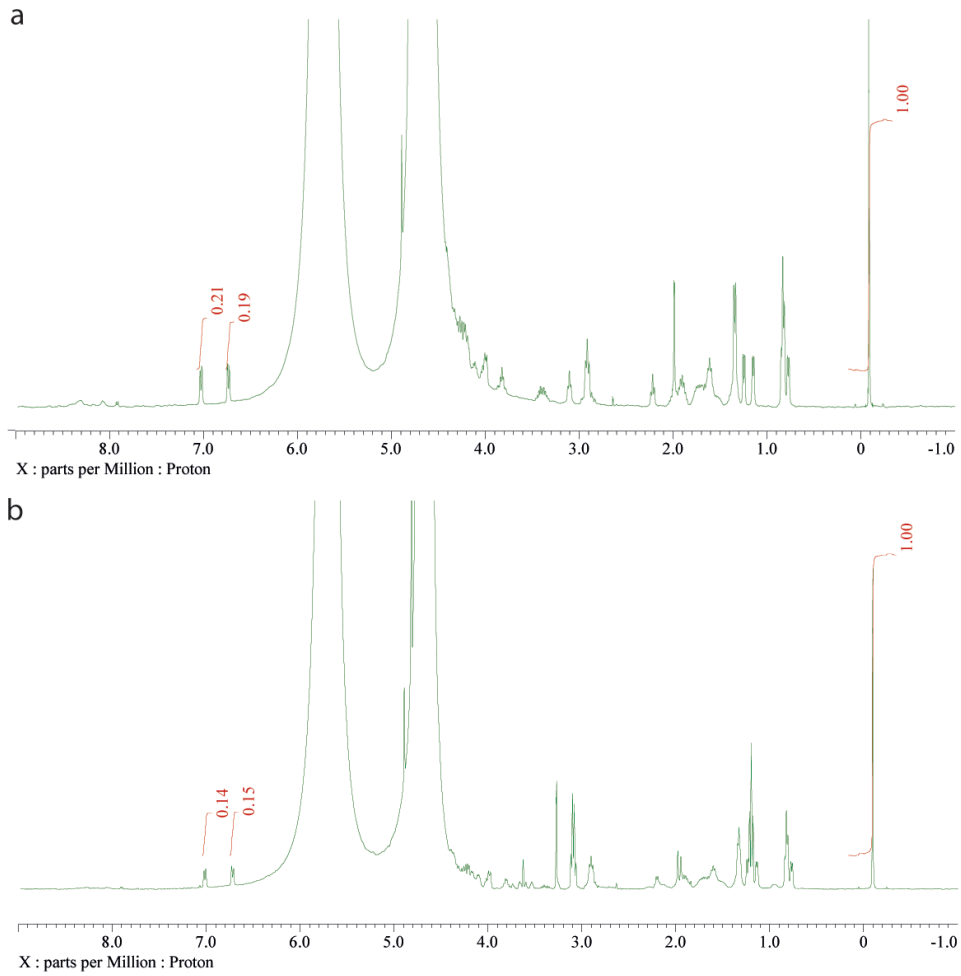

Figure S6. *1H-NMR (400 MHz) of peptide 4 (a) before and (b) after incubation with agarose resin 2 in 4 M urea with 10 vol% D2O and 0.075 vol. % TMSP-d4.*

Chapter 7

Summarizing Discussion

Summarizing Discussion

Aluminum-based adjuvants are being used since the 1920s in many vaccines such as widely used pediatric combination vaccines consisting of inactivated antigens. Although they work very well, the mechanism of action of these adjuvants is not completely understood. In this thesis, the molecular mechanisms of aluminum-based adjuvants, vaccines containing these aluminum-based adjuvants and nano-sized aluminum-based adjuvants were investigated, both *in vitro* and *in vivo*, utilizing a comprehensive approach.

This approach comprised on the one hand on two acknowledged immunological techniques: flow cytometry (for the analysis of cell types *in vitro* and *in vivo*) and ELISA (for the cytokine analysis in culture supernatants). On the other hand, systems biology-related techniques were utilized to target the transcriptome of 89 innate and adaptive immune system-related genes by qPCR and to quantitatively assess the proteome in an *unbiased* way using mass spectrometry, employing Tandem Mass Tag (TMT) stable isotope labeling. These relative quantitative methods enable reliable analysis of cell responses relative to control, which provides insight in the changes in gene transcription and protein expression, upon stimulation[1]. By combining all these techniques, a wide ranging overview of the molecular mechanism(s) involved in the adjuvant activity of aluminum-based adjuvants could be obtained.

The innate immune response towards $Al(OH)_3$

The aim of the research described in **chapter 2** of this thesis was to unravel the molecular mechanism of action of $Al(OH)_3$ *in vitro*. $Al(OH)_3$ is a frequently used aluminum-based adjuvant. This adjuvant is often described as a T helper (Th) cell type 2 polarizing adjuvant, which (*i*) activates the inflammasome, (*ii*) induces Danger Associated Molecular Patterns (DAMPs), (*iii*) attracts immune cells to the site of injection and (*iv*) activates complement-related pathways[2-18]. Applying the multi-tier approach, described above the analysis of the innate immune response induced by $Al(OH)_3$ in primary monocytes revealed novel molecular pathways involved in the innate immune response. For example, several complement pathways became activated in parallel. Complement C3 is at the initiation state of the complement cascade and C3 can activate multiple pathways. By identifying the other complement actors at the protein level, it was clear that more than one pathway of the complement cascade became activated: C4 is related to the classical and lectin pathway, C5aR is involved in the classical pathway, while C8 is involved in the alternative pathway[4].

We were able to identify novel mechanisms by combining transcriptome and proteome data. For example, IFNβ and IFNγ-induced signaling could be confirmed by combining data from these techniques. Antigen processing and presentation pathways were also identified, both with transcriptome and proteome data. Although it is assumed that mRNA will at some point be translated into protein, the amount of mRNA is not directly indicative for the amount of protein produced since the one-to-one correlation between mRNA transcript and protein expression is low[19-21]. Thus, by combining mRNA with protein analysis, more components of a pathway can be identified. This low correlation between mRNA levels and protein expression levels is most likely due to differences in kinetics of the transcription of the genes and the expression and

degradation of the proteins (*i.e.* turnover rate). The combination of our transcriptome and proteome data provided evidence that combining genomics data and proteomics experiments is very useful in identifying molecular mechanisms underlying adjuvant responses.

Comparison of the innate immune response towards $Al(OH)_3$ and the $Al(OH)_3$-containing vaccine DTaP

In **chapter 3** of this thesis, the innate immune response induced by $Al(OH)_3$ was compared with the innate immune response induced by the $Al(OH)_3$-containing vaccine DTaP (Infanrix®). The DTaP vaccine is a licensed vaccine for infants and children, against diphtheria, tetanus and pertussis and comprises diphtheria toxoid, tetanus toxoid and *Bordetella pertussis*-derived filamentous hemagglutinin (FHA), pertussis toxoid (Ptx) and pertactin P.69 (Prn). We analyzed whether the antigens in the vaccine alter the immune response towards a vaccine adjuvant and whether the Th2 response, often associated with $Al(OH)_3$ and $Al(OH)_3$-containing vaccines, was indeed observed for DTaP[22-24]. Gene expression analysis revealed that *IL-4*, the main Th2-associated gene, was induced by DTaP stimulation of monocytes. However, the induction of *IL-4* was stronger in $Al(OH)_3$-stimulated monocytes as compared to the expression in DTaP stimulated monocytes. The gene expression of *IL-5*, another Th2-related cytokine[25-26], was upregulated by both $Al(OH)_3$ and DTaP. In addition, IL-10, associated with the induction of a Th2 response by repressing a Th1 response[27-35], was induced by DTaP and by FHA, one of the *Bordetella pertussis* antigens in DTaP, but not by $Al(OH)_3$. DTaP indeed induced Th2 polarization, as described previously[22, 36-37] and the antigens in the vaccine clearly alter the innate immune response induced by the plain adjuvant. Besides the previously described effects of IL-10, the induction of IL-10 by DTaP and FHA potentially has additional effects: IL-10 inhibits the induction of HLA/MHC protein complexes on the cell surface and the secretion of the pro-inflammatory cytokines, such as IL-2 and IL17A and IFNγ[29-35]. This inhibition of pro-inflammatory cytokines was indeed observed our current study. This indicates that there are components in DTaP that induce an anti-inflammatory response. For bacteria, the induction of anti-inflammatory cytokines could be a very useful property since this possibly allows them to evade the human immune system. However, for the vaccine response this might not be desired. With the knowledge obtained in this study and previous studies regarding the induction of the anti-inflammatory cytokine IL-10 by FHA, it might be interesting to consider analyzing the immune response towards DTaP without FHA present. Due to its Th2-polarizing activity, $Al(OH)_3$ might not be the most suitable adjuvant because a Th1 response is an important component in the protective immunity against pertussis[22, 37-39] since memory Th1 and Th17 cells are involved in effective immunity against pertussis[39]. Thus, it might be interesting to analyze the immune response to DTaP without $Al(OH)_3$ or in the presence of other adjuvants such as MF59 or AS04.

In this study, we could confirm the Th2 profile often assigned to $Al(OH)_3$ and $Al(OH)_3$-adjuvanted vaccines. DTaP appears to induce a less inflammatory response as compared to $Al(OH)_3$ alone, most likely due to the induction of the Th1-inhibiting and anti-inflammatory cytokine IL-10. The data provide evidence that the antigens in a vaccine clearly qualitatively and quantitatively alter the adjuvant-induced innate immune and that the combination of antigen and adjuvant determine the innate response to a vaccine.

Differences in the innate immune response between $Al(OH)_3$ and $AlPO_4$

In **chapter 4**, the commercial adjuvants $Al(OH)_3$ and $AlPO_4$ were compared with respect to their characteristics and effects on the innate immune response both *in vitro* and *in vivo*. When selecting an alum-based adjuvant for a vaccine, the choice for $AlPO_4$ or $Al(OH)_3$ is often made based on the adsorption capacity of the antigen to the adjuvant. This adsorption capacity is related to the charge state of the antigen, as $Al(OH)_3$ and $AlPO_4$ are of opposite charge at physiological pH. $Al(OH)_3$ is positively charged, while $AlPO_4$ is slightly negative. Quite often however, the degree of adsorption of the antigen to the adjuvant is not correlated to the induced immune response[40]. To determine, whether a more rational choice for the use of $Al(OH)_3$ *versus* $AlPO_4$ can be made, we analyzed the innate immune response towards $Al(OH)_3$ and $AlPO_4$. This was done *in vitro* on primary monocytes with a quantitative proteome analysis and *in vivo*, with flow cytometry and quantitative proteomics. Our data show the that antigen processing and presentation pathways were strongly upregulated by $Al(OH)_3$ and much less $AlPO_4$. This may be related to the previously observed enhanced cellular uptake of $Al(OH)_3$ compared to the uptake of $AlPO_4$[41]. This enhanced uptake is probably related to the physicochemical properties of the adjuvants. $Al(OH)_3$ is more positively charged at physiological pH even though this charge may be partly shielded by proteins and salts in the culture medium[41]. This positive charge of $Al(OH)_3$ allows for stronger interactions with the negatively charged cell membrane, compared to the negatively charged $AlPO_4$[41-42], resulting in different signaling. In addition, the $Al(OH)_3$ particle size might be more suitable for phagocytosis as compared to the particle size of $AlPO_4$, allowing for relatively more uptake of $Al(OH)_3$[41], which was also observed in our study. In addition to this difference in primary monocytes, one main difference was observed *in vivo*: the influx of neutrophils at 96 hours induced by $Al(OH)_3$ and not by $AlPO_4$. This influx, uniquely induced by $Al(OH)_3$, is possibly related to the induction of hemostasis and Neutrophil Extracellular Trap formation. The process of hemostasis is often related to the formation of extracellular traps (ETs) and also neutrophil extracellular traps (NETs)[43]. Based on the data in **chapter 4**, it was concluded that after 96 hours of $Al(OH)_3$ stimulation NET formation could possibly occur as described previously[44]. The formation of NETs has previously been described to play a significant role in the adjuvant activity of $Al(OH)_3$ by inducing antigen specific T cells, B cell maturation and increased IgG1 titers[44]. NET induction is important in the immune response to bacteria[45-46], however the role of NETs during vaccination is less clear. NETs may retain particular vaccine antigens at the site of injection, thus changing the kinetics of antigen clearance. This may affect the immunogenicity of a vaccine. In addition, the systemic adaptive response is indeed influenced by the presence of NETs, since the IgG1 antibody titers (upon vaccination, with an $Al(OH)_3$-containing vaccine) were higher in mice capable of NET formation, compared to mice that had impaired NET formation[44]. Purified antigens in a vaccine might not induce NET formation *without* adjuvant present. It has been shown that $Al(OH)_3$-induced NET formation attributes to the adaptive immune response towards an $Al(OH)_3$-adsorbed antigen in a positive way. Hence, it might be stated that when neutrophils are involved in the immune response to the pathogen, $Al(OH)_3$ might be the more suitable adjuvant compared to $AlPO_4$: NET formation can still occur in response to adjuvant while this is most likely not the case when $AlPO_4$ is used. However, the effects of an antigen being trapped in the NETs, changing their ex-

posure to antigen presenting cells, needs to be assessed further. Besides their beneficial effects on the immune response, neutrophils do also contain high amounts of cytotoxic molecules which can result for instance in local inflammation[47]. Perhaps, $AlPO_4$ would be more suitable as an adjuvant when neutrophils are not required to elicit the desired immune response, since than there are most likely less side effects.

Molecular mechanisms involved in the adjuvant effect of nanoparticulate aluminum-based adjuvants

In **chapter 5**, the innate immune response towards two differently shaped $Al(OH)_3$ nanoparticles were compared with the innate immune response induced by the conventional $Al(OH)_3$ adjuvant. Aluminum-based adjuvants are already used for decades in human vaccines, but are not always considered optimal adjuvants, because the adjuvant response is not as desired. This is probably related to the rather large particle size, which makes the uptake of alum-based adjuvants by cells difficult. Also their surface area is rather small making the adsorption capacity smaller compared to small particles[5]. In addition, the structure/shape of these classical products have been weakly characterized thus harder to reproduce between manufactures.

One way to solve these problems is to standardize the size and use of $Al(OH)_3$ nanoparticles as an adjuvant. The idea behind using nanoparticles is that smaller particles might enter the cells more easily and have an increased adsorption capacity compared to the conventional adjuvants. Previously, it was observed that $Al(OH)_3$ nanoparticles induce more IL-1β secretion by THP-1 cells as compared to conventional $Al(OH)_3$ particles[48], indicating that these particles activate the inflammasome more strongly. This pronounced inflammasome activation was directly correlated to the crystallinity, surface hydroxyl display and the size of the particles[48]. When comparing the specific antibody responses of antigens adsorbed to standard antigens adsorbed to $Al(OH)_3$ (Alhydrogel, size 9.3 micometer) with those induced by antigens adsorbed to aluminum hydroxide nanoparticles (df≈110 nm), the responses were higher in the nanoparticle-immunized groups as compared to the $Al(OH)_3$-stimulated groups[49]. In addition, adverse effects at the site of injection (in mice) were milder in the nanoparticle-stimulated group as compared to the reaction induced by $Al(OH)_3$ micro particles. This indicates that nanoparticles might be of interest as a vaccine adjuvant.

Two types of $Al(OH)_3$-based nanoparticles were investigated by us. One type (Gibbsite) was shaped like a disk, while the other (Boehmite) was needle-shaped. At both the gene expression and the proteome level, the measured innate immune response towards the nanoparticles was substantially lower compared to the traditional $Al(OH)_3$. Gibbsite hardly induced immunological pathways, while Boehmite did induce an immune response, albeit less strong compared to $Al(OH)_3$. Our data are contradictory to the data from Li *et al.*[49] Which could be explained by the fact that no antigen was used in our study whereas Li *et al.* did. As shown in **chapter 3**, antigens can affect the innate response. Moreover, the study from Li *et al.* was performed *in vivo*, while our study was performed *in vitro*. Another contradiction with literature was observed when we analyzed inflammasome activation in THP-1 cells: Boehmite induced less IL-1β compared to $Al(OH)_3$, while the reverse was observed by Li *et al.* although they used another alum-based adjuvant (*i.e.* Imject alum) as control[50]. Imject alum is a mixture of $Al(OH)_3$ and magnesium hydroxide and is of completely different composition as compared to the $Al(OH)_3$ used in our study (Alhydrogel®)[50]. In addition, it cannot be

excluded that the nanoparticles used in the current study differed from the nanoparticles in the study of Li *et al*. The needle-shaped nanoparticle Boehmite, but not the disc-shaped nanoparticle Gibbsite, activated various immune system-related pathways less strong than $Al(OH)_3$. In addition, much less stress response-related pathways were induced by Boehmite compared to $Al(OH)_3$. Moreover, the pathway associated with an allergic response was not induced by Boehmite but was only induced by $Al(OH)_3$. This difference in stress response-related pathways and allergic response could explain why it was observed previously that the local side effects in mice caused by the nanoparticles are milder[49] as compared to conventional $Al(OH)_3$-based adjuvants: cellular stress might be related to side effects, as is an allergic response. In summary, our data imply that Boehmite is capable of inducing an innate immune response which, however, is weaker than the immune response to $Al(OH)_3$. Boehmite, on the other hand, might induce less adverse effects since the processes associated with these effects were much less or even completely not induced by Boehmite.

We demonstrated that the particle size and shape clearly affect the *in vitro* innate immune response towards a vaccine adjuvant. Boehmite (being a needle-shaped nanoparticle) might be an interesting adjuvant concept, because it is capable of eliciting an immune response without activating the pathways associated with the side effects of $Al(OH)_3$.

Improved secretome analysis

Chapter 6 of this thesis describes an improved method to analyze the secretome of stimulated cells. Secreted proteins such as cytokines, hormones and enzymes are essential in the communication processes between cells. Analyzing these molecules in a cell culture supernatant can provide valuable knowledge about the understanding of intercellular communication. Targeted antibody-based assays, *e.g*. Mutliplex Immuno Assays (MIAs) and ELISAs, are popular methods for the analysis of secreted proteins, because they are sensitive and relatively easy to perform. However, the disadvantage of these techniques is that only preselected analytes can be quantified based on the panel of antibodies available, thus potentially missing novel messengers involved in the *cell-to-cell* communication. A mass spectrometry-based approach for the analysis of the secretome does not have this disadvantage. However, because of the generally low concentration of secreted proteins enrichment strategies are mandatory. Also, the high abundance of serum albumin in culture medium interferes with an unbiased proteomics approach. Culturing cells in serum free medium is sometimes possible but can induce cell stress. Therefore, enrichment procedures for secreted proteins have been developed. This was achieved by pulse labeling newly formed proteins with a methionine analogue, L-azidohomoalanine (Aha)[51]. Aha-containing proteins in the culture medium are covalently *clicked* to an alkyne-functionalized resin based on a copper-catalyzed azide-alkyne cycloaddition. The beads with the newly synthesized proteins are isolated and the covalently bound proteins are further processed using general proteomics-based approached (*i.e.* digestion and mass spectrometric analysis). A drawback of this method, however, is the use of a copper catalyst. The copper(I) catalyst induces unwanted oxidative side reactions on proteins, complicating the identification and quantification of these proteins. Additionally, the copper(II) precursor used in these *click* reactions often chelates to the amine groups of amino acids[52], as well as the amide peptide bonds, which hampers the efficiency of the click reaction[53].

We therefore developed a novel resin, based on cyclooctyne-functionalized beads, that does not require any catalysts for the click chemistry. Cyclooctyne functionalization has proven to be an efficient chemistry tool in biological click conjugation[54-55]. In addition to the methionine analogue L-azidohomoalanine, $^{13}C_6$-Leucine was incorporated as a stable isotopically labeled amino acid at the start of the pulse, to further discriminate between *de novo*-synthesized proteins and proteins nonspecifically adsorbed to the beads. As a proof of principle, THP-1 cells in combination with an LPS stimulus where initially investigated whereby, 116 secreted proteins could be identified. The expression of proteins known to be associated with LPS was increased, *e.g.* CCL5, CCL8, IL1R1 and Cathepsin S[56-61]. Thus, we indeed could confirm the induction of proteins known to be related to the response towards LPS. It must be noted that it is a prerequisite that the secreted proteins must contain methionine residue(s) to enable the click chemistry. An important LPS-related protein in THP-1 cells, TNFα, was not identified in the culture medium, due to the fact that the excreted version of the protein does not contain a methionine. With a prevalence of only 2.3% for methionine in particular small proteins might lack this amino acid. Adding additional or other analogues might result in identifying more secreted proteins. Our data provide evidence that secretome analysis utilizing the newly developed cyclooctyne-functionalized beads significantly improves the analysis of messenger proteins involved in immune responses upon a stimulus.

Summarizing conclusions and future perspectives

By analyzing the proteome in an unbiased manner, a comprehensive insight in the molecular mechanisms involved in different *stimuli* can be obtained. Due to the multiplexing abilities of the TMT labeling reagent, a direct quantitative comparison between sample and control is possible. By using pathway analysis with (up)regulated proteins as input, processes in the cell, affected by the *stimuli* can be identified. In this thesis, this approach was applied for the analysis of molecular mechanisms underlying the immune response affected by aluminum-based adjuvants and vaccines. The main conclusions are:

1. By using a comprehensive approach we were able to perform pathway analysis, resulting in novel insights into molecular mechanism of alum-based adjuvants.

2. Antigens in a vaccine qualitatively and quantitatively alter the immune response induced by the adjuvant and the combination of the antigen and adjuvant determines the innate immune response induced.

3. The different chemical and physicochemical characteristics of commercial adjuvants $Al(OH)_3$ and $AlPO_4$ result in different capabilities to stimulate the immune system. Based on both *in vitro* and *in vivo* profiling of the innate immune response, $Al(OH)_3$ is perhaps the more potent adjuvant.

4. The size and shape of alum-based adjuvants clearly influence the strength of the innate immune response. Aluminum-based nanoparticles induce a weaker immune response compared to the microparticle $Al(OH)_3$ adjuvant. When the nanoparticles are needle-shaped, the immune response is stronger than when the nanoparticles are shaped like a disc. Based on these findings and the fact

that it potentially induces less adverse effects, the needle-shaped nanoparticulate (Boehmite) might be an interesting candidate as future adjuvant.

5. Mass spectrometry-based analysis of the secretome is possible without the use of a copper catalyst, which may interfere with the downstream processing.

Future perspectives

Adjuvants play an important role in inducing effective immunity against subunit vaccines. Currently however, there is only a limited number of adjuvants that is licensed for use in human vaccines. Thus, a quest for novel and better adjuvants is ongoing. These novel adjuvants need to be safe and efficacious. The comprehensive approach described in this thesis facilitates the screening of adjuvants and improves understanding of the molecular mechanisms underlying the innate immune response induced them. By comparing responses of plain adjuvant and different antigen-adjuvant combinations, synergistic or antagonistic effects of the adjuvants/antigens on the innate immune response can be compared aiming at the optimal formulation of combinations.

By applying this approach both *in vitro* and *in vivo*, a better understanding of the molecular mechanism underlying the immune response towards an adjuvant/adjuvant-antigen combination will be obtained. This is important, because this allows for determining the optimal antigen-adjuvant combination in evoking an immune response that is similar to the immune response against the causative pathogen, thus often inducing the best protection[39]. Mass spectrometry-based proteomics has proven to be an essential component of this comprehensive approach. Quantitative experiments can now be multiplexed up until 25 different conditions in one run[62], making it very suitable in comparing several responses and kinetics towards multiple adjuvants in one experiment. Mass spectrometry-based proteomics also allows for analyzing *de novo*-secreted proteins *without* the use of pre-selected antibodies. Although limited to *in vitro* studies only, mass spectrometry-based proteomics also allows for analyzing *de novo*-secreted proteins without prior selection of analytes of interest.

It is obvious that the MS-based proteomics tools, as applied in this thesis, require a significant investment in technical facilities (*e.g.* instrumentation, dedicated software applications) and skilled personnel. It is therefore most likely that the contribution of this technique predominantly will occur during the research and development phase of a vaccine, both in lead finding and vaccine formulation. The combination of proteomics technique with other molecular and immunological techniques (systems vaccinology approach) is essential in several aspects of modern vaccine development. For instance, lead finding for identifying the optimal adjuvant-antigen combinations in an early stage and reduce the risk of late stage failure by improving understanding of the mechanisms of action of a vaccine as stated by Sunasara *et al.*[63]. Vaccine development will never be based solely on proteomics approaches, but it is a mutual reinforcement of immunoassays and modern 'omics'-based approaches (*e.g.* transcriptomics, proteomics, metabolomics, secretomics, and lipidomics). It is expected that, due to accelerating technical developments, additional approaches will be embedded in the vaccine development chain in the near future, for example profiling protein-protein interaction (interactome) and mapping protein degradation kinetics (degradome).

References

1. Altelaar, A. F.; Frese, C. K.; Preisinger, C.; Hennrich, M. L.; Schram, A. W.; Timmers, H. T.; Heck, A. J.; Mohammed, S., Benchmarking stable isotope labeling based quantitative proteomics. *J Proteomics* 2013, *88*, 14-26.
2. Brewer, J. M., (How) do aluminium adjuvants work? *Immunol Lett* 2006, *102* (1), 10-5.
3. Eisenbarth, S. C.; Colegio, O. R.; O'Connor, W.; Sutterwala, F. S.; Flavell, R. A., Crucial role for the Nalp3 inflammasome in the immunostimulatory properties of aluminium adjuvants. *Nature* 2008, *453* (7198), 1122-6.
4. Guven, E.; Duus, K.; Laursen, I.; Hojrup, P.; Houen, G., Aluminum hydroxide adjuvant differentially activates the three complement pathways with major involvement of the alternative pathway. *PLoS One* 2013, *8* (9), e74445.
5. He, P.; Zou, Y.; Hu, Z., Advances in aluminum hydroxide-based adjuvant research and its mechanism. *Hum Vaccin Immunother* 2015, *11* (2), 477-88.
6. Hogenesch, H., Mechanism of immunopotentiation and safety of aluminum adjuvants. *Front Immunol* 2012, *3*, 406.
7. Kool, M.; Petrilli, V.; De Smedt, T.; Rolaz, A.; Hammad, H.; van Nimwegen, M.; Bergen, I. M.; Castillo, R.; Lambrecht, B. N.; Tschopp, J., Cutting edge: alum adjuvant stimulates inflammatory dendritic cells through activation of the NALP3 inflammasome. *J Immunol* 2008, *181* (6), 3755-9.
8. Kool, M.; Soullie, T.; van Nimwegen, M.; Willart, M. A.; Muskens, F.; Jung, S.; Hoogsteden, H. C.; Hammad, H.; Lambrecht, B. N., Alum adjuvant boosts adaptive immunity by inducing uric acid and activating inflammatory dendritic cells. *J Exp Med* 2008, *205* (4), 869-82.
9. Kool, M.; Fierens, K.; Lambrecht, B. N., Alum adjuvant: some of the tricks of the oldest adjuvant. *J Med Microbiol* 2012, *61* (Pt 7), 927-34.
10. Lambrecht, B. N.; Kool, M.; Willart, M. A.; Hammad, H., Mechanism of action of clinically approved adjuvants. *Curr Opin Immunol* 2009, *21* (1), 23-9.
11. Lindblad, E. B., Aluminium adjuvants--in retrospect and prospect. *Vaccine* 2004, *22* (27-28), 3658-68.
12. Marichal, T.; Ohata, K.; Bedoret, D.; Mesnil, C.; Sabatel, C.; Kobiyama, K.; Lekeux, P.; Coban, C.; Akira, S.; Ishii, K. J.; Bureau, F.; Desmet, C. J., DNA released from dying host cells mediates aluminum adjuvant activity. *Nat Med* 2011, *17* (8), 996-1002.
13. McKee, A. S.; MacLeod, M. K.; Kappler, J. W.; Marrack, P., Immune mechanisms of protection: can adjuvants rise to the challenge? *BMC Biol* 2010, *8*, 37.
14. O'Hagan, D. T.; Ott, G. S.; De Gregorio, E.; Seubert, A., The mechanism of action of MF59 - an innately attractive adjuvant formulation. *Vaccine* 2012, *30* (29), 4341-8.
15. Seubert, A.; Calabro, S.; Santini, L.; Galli, B.; Genovese, A.; Valentini, S.; Aprea, S.; Colaprico, A.; D'Oro, U.; Giuliani, M. M.; Pallaoro, M.; Pizza, M.; O'Hagan, D. T.; Wack, A.; Rappuoli, R.; De Gregorio, E., Adjuvanticity of the oil-in-water emulsion MF59 is independent of Nlrp3 inflammasome but requires the adaptor protein MyD88. *Proc Natl Acad Sci U S A* 2011, *108* (27), 11169-74.
16. Ulanova, M.; Tarkowski, A.; Hahn-Zoric, M.; Hanson, L. A., The Common vaccine adjuvant aluminum hydroxide up-regulates accessory properties of human monocytes via an interleukin-4-dependent mechanism. *Infect Immun* 2001, *69* (2), 1151-9.
17. Brewer, J. M.; Conacher, M.; Satoskar, A.; Bluethmann, H.; Alexander, J., In interleukin-4-deficient mice, alum not only generates T helper 1 responses equivalent to freund's complete adjuvant, but continues to induce T helper 2 cytokine production. *Eur J Immunol* 1996, *26* (9), 2062-6.
18. Calabro, S.; Tortoli, M.; Baudner, B. C.; Pacitto, A.; Cortese, M.; O'Hagan, D. T.; De Gregorio, E.; Seubert, A.; Wack, A., Vaccine adjuvants alum and MF59 induce rapid recruitment of neutrophils and monocytes that participate in antigen transport to draining lymph nodes. *Vaccine* 2011, *29* (9), 1812-23.

19. Ghazalpour, A.; Bennett, B.; Petyuk, V. A.; Orozco, L.; Hagopian, R.; Mungrue, I. N.; Farber, C. R.; Sinsheimer, J.; Kang, H. M.; Furlotte, N.; Park, C. C.; Wen, P. Z.; Brewer, H.; Weitz, K.; Camp, D. G., 2nd; Pan, C.; Yordanova, R.; Neuhaus, I.; Tilford, C.; Siemers, N.; Gargalovic, P.; Eskin, E.; Kirchgessner, T.; Smith, D. J.; Smith, R. D.; Lusis, A. J., Comparative analysis of proteome and transcriptome variation in mouse. *PLoS Genet* 2011, *7* (6), e1001393.

20. Gygi, S. P.; Rochon, Y.; Franza, B. R.; Aebersold, R., Correlation between protein and mRNA abundance in yeast. *Mol Cell Biol* 1999, *19* (3), 1720-30.

21. Guo, Y.; Xiao, P.; Lei, S.; Deng, F.; Xiao, G. G.; Liu, Y.; Chen, X.; Li, L.; Wu, S.; Chen, Y.; Jiang, H.; Tan, L.; Xie, J.; Zhu, X.; Liang, S.; Deng, H., How is mRNA expression predictive for protein expression? A correlation study on human circulating monocytes. *Acta Biochim Biophys Sin (Shanghai)* 2008, *40* (5), 426-36.

22. Brummelman, J.; Helm, K.; Hamstra, H. J.; van der Ley, P.; Boog, C. J.; Han, W. G.; van Els, C. A., Modulation of the CD4(+) T cell response after acellular pertussis vaccination in the presence of TLR4 ligation. *Vaccine* 2015, *33* (12), 1483-91.

23. Brummelman, J.; Raeven, R. H.; Helm, K.; Pennings, J. L.; Metz, B.; van Eden, W.; van Els, C. A.; Han, W. G., Transcriptome signature for dampened Th2 dominance in acellular pertussis vaccine-induced CD4(+) T cell responses through TLR4 ligation. *Sci Rep* 2016, *6*, 25064.

24. Morefield, G. L.; Sokolovska, A.; Jiang, D.; HogenEsch, H.; Robinson, J. P.; Hem, S. L., Role of aluminum-containing adjuvants in antigen internalization by dendritic cells in vitro. *Vaccine* 2005, *23* (13), 1588-95.

25. Koyasu, S.; Moro, K., Type 2 innate immune responses and the natural helper cell. *Immunology* 2011, *132* (4), 475-81.

26. Na, H.; Cho, M.; Chung, Y., Regulation of Th2 Cell Immunity by Dendritic Cells. *Immune Netw* 2016, *16* (1), 1-12.

27. Chomarat, P.; Rissoan, M. C.; Banchereau, J.; Miossec, P., Interferon gamma inhibits interleukin 10 production by monocytes. *J Exp Med* 1993, *177* (2), 523-7.

28. Fiorentino, D. F.; Zlotnik, A.; Mosmann, T. R.; Howard, M.; O'Garra, A., IL-10 inhibits cytokine production by activated macrophages. *J Immunol* 1991, *147* (11), 3815-22.

29. Fiorentino, D. F.; Zlotnik, A.; Vieira, P.; Mosmann, T. R.; Howard, M.; Moore, K. W.; O'Garra, A., IL-10 acts on the antigen-presenting cell to inhibit cytokine production by Th1 cells. *J Immunol* 1991, *146* (10), 3444-51.

30. Gu, Y.; Yang, J.; Ouyang, X.; Liu, W.; Li, H.; Yang, J.; Bromberg, J.; Chen, S. H.; Mayer, L.; Unkeless, J. C.; Xiong, H., Interleukin 10 suppresses Th17 cytokines secreted by macrophages and T cells. *Eur J Immunol* 2008, *38* (7), 1807-13.

31. Redford, P. S.; Murray, P. J.; O'Garra, A., The role of IL-10 in immune regulation during M. tuberculosis infection. *Mucosal Immunol* 2011, *4* (3), 261-70.

32. Saraiva, M.; O'Garra, A., The regulation of IL-10 production by immune cells. *Nat Rev Immunol* 2010, *10* (3), 170-81.

33. Taga, K.; Tosato, G., IL-10 inhibits human T cell proliferation and IL-2 production. *J Immunol* 1992, *148* (4), 1143-8.

34. Ma, X.; Yan, W.; Zheng, H.; Du, Q.; Zhang, L.; Ban, Y.; Li, N.; Wei, F., Regulation of IL-10 and IL-12 production and function in macrophages and dendritic cells. *F1000Res* 2015, *4*.

35. Maynard, C. L.; Weaver, C. T., Diversity in the contribution of interleukin-10 to T-cell-mediated immune regulation. *Immunol Rev* 2008, *226*, 219-33.

36. Mascart, F.; Hainaut, M.; Peltier, A.; Verscheure, V.; Levy, J.; Locht, C., Modulation of the infant immune responses by the first pertussis vaccine administrations. *Vaccine* 2007, *25* (2), 391-8.

37. Redhead, K.; Watkins, J.; Barnard, A.; Mills, K. H., Effective immunization against Bordetella pertussis respiratory infection in mice is dependent on induction of cell-mediated immunity. *Infect Immun* 1993, *61* (8), 3190-8.

38. Ross, P. J.; Sutton, C. E.; Higgins, S.; Allen, A. C.; Walsh, K.; Misiak, A.; Lavelle, E. C.; McLoughlin, R. M.; Mills, K. H., Relative contribution of Th1 and Th17 cells in adaptive immunity to Bordetella pertussis: towards the rational design of an improved acellular pertussis vaccine. *PLoS Pathog* 2013, *9* (4), e1003264.

39. Raeven, R. H.; Brummelman, J.; van der Maas, L.; Tilstra, W.; Pennings, J. L.; Han, W. G.; van Els, C. A.; van Riet, E.; Kersten, G. F.; Metz, B., Immunological Signatures after Bordetella pertussis Infection Demonstrate Importance of Pulmonary Innate Immune Cells. *PLoS One* 2016, *11* (10), e0164027.

40. Clapp, T.; Siebert, P.; Chen, D.; Jones Braun, L., Vaccines with aluminum-containing adjuvants: optimizing vaccine efficacy and thermal stability. *J Pharm Sci* 2011, *100* (2), 388-401.

41. Mold, M.; Shardlow, E.; Exley, C., Insight into the cellular fate and toxicity of aluminium adjuvants used in clinically approved human vaccinations. *Sci Rep* 2016, *6*, 31578.

42. Caulfield, M. J.; Shi, L.; Wang, S.; Wang, B.; Tobery, T. W.; Mach, H.; Ahl, P. L.; Cannon, J. L.; Cook, J. C.; Heinrichs, J. H.; Sitrin, R. D., Effect of alternative aluminum adjuvants on the absorption and immunogenicity of HPV16 L1 VLPs in mice. *Hum Vaccin* 2007, *3* (4), 139-45.

43. Munks, M. W.; McKee, A. S.; Macleod, M. K.; Powell, R. L.; Degen, J. L.; Reisdorph, N. A.; Kappler, J. W.; Marrack, P., Aluminum adjuvants elicit fibrin-dependent extracellular traps in vivo. *Blood* 2010, *116* (24), 5191-9.

44. Stephen, J.; Scales, H. E.; Benson, R. A.; Erben, D.; Garside, P.; Brewer, J. M., Neutrophil swarming and extracellular trap formation play a significant role in Alum adjuvant activity. *NPJ Vaccines* 2017, *2*, 1.

45. Brinkmann, V.; Reichard, U.; Goosmann, C.; Fauler, B.; Uhlemann, Y.; Weiss, D. S.; Weinrauch, Y.; Zychlinsky, A., Neutrophil extracellular traps kill bacteria. *Science* 2004, *303* (5663), 1532-5.

46. Yipp, B. G.; Petri, B.; Salina, D.; Jenne, C. N.; Scott, B. N.; Zbytnuik, L. D.; Pittman, K.; Asaduzzaman, M.; Wu, K.; Meijndert, H. C.; Malawista, S. E.; de Boisfleury Chevance, A.; Zhang, K.; Conly, J.; Kubes, P., Infection-induced NETosis is a dynamic process involving neutrophil multitasking in vivo. *Nat Med* 2012, *18* (9), 1386-93.

47. Kobayashi, S. D.; DeLeo, F. R., Role of neutrophils in innate immunity: a systems biology-level approach. *Wiley Interdiscip Rev Syst Biol Med* 2009, *1* (3), 309-33.

48. Sun, B.; Ji, Z.; Liao, Y. P.; Wang, M.; Wang, X.; Dong, J.; Chang, C. H.; Li, R.; Zhang, H.; Nel, A. E.; Xia, T., Engineering an effective immune adjuvant by designed control of shape and crystallinity of aluminum oxyhydroxide nanoparticles. *ACS Nano* 2013, *7* (12), 10834-49.

49. Li, X.; Aldayel, A. M.; Cui, Z., Aluminum hydroxide nanoparticles show a stronger vaccine adjuvant activity than traditional aluminum hydroxide microparticles. *J Control Release* 2014, *173*, 148-57.

50. Hem, S. L.; Johnston, C. T.; HogenEsch, H., Imject Alum is not aluminum hydroxide adjuvant or aluminum phosphate adjuvant. *Vaccine* 2007, *25* (27), 4985-6.

51. Eichelbaum, K.; Winter, M.; Berriel Diaz, M.; Herzig, S.; Krijgsveld, J., Selective enrichment of newly synthesized proteins for quantitative secretome analysis. *Nat Biotechnol* 2012, *30* (10), 984-90.

52. Sigel, H.; Martin, R. B., Coordinating properties of the amide bond. Stability and structure of metal ion complexes of peptides and related ligands. *Chemical Reviews* 1982, *82* (4), 385-426.

53. Bal, W.; Dyba, M.; Kasprzykowski, F.; Kozłowski, H.; Latajka, R.; Łankiewicz, L.; Małkiewicz, Z.; Pettit, L. D., How non-bonding amino acid side-chains may enormously increase the stability of a Cu(II)—peptide complex. *Inorganica Chimica Acta* 1998, *283* (1), 1-11.

54. Agard, N. J.; Baskin, J. M.; Prescher, J. A.; Lo, A.; Bertozzi, C. R., A comparative study of bioorthogonal reactions with azides. *ACS Chem Biol* 2006, *1* (10), 644-8.

55. Dommerholt, J.; van Rooijen, O.; Borrmann, A.; Guerra, C. F.; Bickelhaupt, F. M.; van Delft, F. L., Highly accelerated inverse electron-demand cycloaddition of electron-deficient azides with aliphatic cyclooctynes. *Nat Commun* 2014, *5*, 5378.

56. Sharif, O.; Bolshakov, V. N.; Raines, S.; Newham, P.; Perkins, N. D., Transcriptional profiling of the LPS induced NF-kappaB response in macrophages. *BMC Immunol.* 2007, *8*, 1.

57. de Mingo, A.; de Gregorio, E.; Moles, A.; Tarrats, N.; Tutusaus, A.; Colell, A.; Fernandez-Checa, J. C.; Morales, A.; Mari, M., Cysteine cathepsins control hepatic NF-kappaB-dependent inflammation via sirtuin-1 regulation. *Cell Death Dis.* 2016, *7* (11), e2464.

58. Creasy, B. M.; McCoy, K. L., Cytokines regulate cysteine cathepsins during TLR responses. *Cell Immunol.* 2011, *267* (1), 56-66.

59. Harrison, L. M.; van den Hoogen, C.; van Haaften, W. C.; Tesh, V. L., Chemokine expression in the monocytic cell line THP-1 in response to purified shiga toxin 1 and/or lipopolysaccharides. *Infect. Immun.* 2005, *73* (1), 403-12.

60. Yue, Y.; Huang, W.; Liang, J.; Guo, J.; Ji, J.; Yao, Y.; Zheng, M.; Cai, Z.; Lu, L.; Wang, J., IL4I1 Is a Novel Regulator of M2 Macrophage Polarization That Can Inhibit T Cell Activation via L-Tryptophan and Arginine Depletion and IL-10 Production. *PLoS One* 2015, *10* (11), e0142979.

61. Cinar, M. U.; Islam, M. A.; Uddin, M. J.; Tholen, E.; Tesfaye, D.; Looft, C.; Schellander, K., Evaluation of suitable reference genes for gene expression studies in porcine alveolar macrophages in response to LPS and LTA. *BMC Res. Notes* 2012, *5*, 107.

62. Potts, G. K.; Voigt, E. A.; Bailey, D. J.; Rose, C. M.; Westphall, M. S.; Hebert, A. S.; Yin, J.; Coon, J. J., Neucode Labels for Multiplexed, Absolute Protein Quantification. *Anal Chem* 2016, *88* (6), 3295-303.

63. Sunasara, K.; Cundy, J.; Srinivasan, S.; Evans, B.; Sun, W.; Cook, S.; Bortell, E.; Farley, J.; Griffin, D.; Bailey Piatchek, M.; Arch-Douglas, K., Bivalent rLP2086 (Trumenba(R)): Development of a well-characterized vaccine through commercialization. *Vaccine* 2017.

Apendices

Nederlandse samenvatting

Dankwoord

Curriculum Vitae

List of Publications

Nederlandse samenvatting

Samen met schoon drinkwater is vaccineren één van de meeste belangrijke middelen in de bestrijding van infectieziekten. Vanaf het moment dat vaccineren geïntroduceerd werd, is de dood van 2.5 miljoen kinderen per jaar voorkomen[1]. Het vaccineren is bedacht door Edward Jenner, een huisarts in de 18e eeuw. Het Variola Virus (een virus dat pokken veroorzaakte) was in die tijd een dodelijk virus, waaraan 10-20% van de bevolking overleed. Het viel Edward Jenner op dat door veelvuldig contact met koeien, de melkmeisjes de koeienpokken kregen, maar niet de dodelijke variant van pokken. In 1796 injecteerde hij een jongeman met het koeienpokken-materiaal van de handen van één van deze melkmeisjes. Deze jongen kreeg hele milde symptomen van de ziekte. Na het herstel, injecteerde hij dezelfde jongen met het dodelijke pokkenvirus. Deze jongen werd niet ziek en bleek dus immuun voor deze ziekte. Deze door Edward Jenner geïntroduceerde behandeling werd de 'inoculatie met vaccinia' genoemd; later veranderde deze naam in 'vaccinatie'[2].

Vanaf dat moment ging het snel met de ontwikkeling van vaccins, voornamelijk als gevolg van nieuwe ontdekkingen. Een van de belangrijkste ontdekkingen was die van Robert Koch: hij ontdekte dat micro-organismen (bacteriën, virussen en schimmels) de veroorzakers zijn van infectieziekten. Hierdoor wist men wat er bestreden moest worden. Een andere hele belangrijke ontdekking was het feit dat als componenten van de ziekteverwekker gecombineerd werden met een andere stof, bv. 'aluminiumzouten', de vaccinatie betere bescherming gaf[3, 4]. Deze toevoegingen aan vaccins werden 'adjuvantia' genoemd.

Het woord 'adjuvare' betekent "om te helpen" in het Latijn. Deze stoffen zijn er dus voor bedoeld om te helpen je immuunsysteem te activeren en te reageren op de ziekteverwekker in het vaccin. Dit zodat degene die het vaccin ontvangt in de toekomst niet meer ziek wordt van deze ziekteverwekker. Deze adjuvantia worden steeds belangrijker. Vroeger zat er een hele, verzwakte bacterie of virus in een vaccin. Deze virussen/bacteriën bevatten van nature stoffen die het immuunsysteem activeren. Het is echter gebleken dat hele virussen/bacteriën in vaccines soms nog wel onveilig was. Daarom is er voor veel vaccins inmiddels de keuze gemaakt om eiwitten (de bouwstenen van de virussen/bacteriën), die verantwoordelijk zijn voor de immuunrespons tegen de betreffende bacterie of virus (immunogene eiwitten/antigenen), te gebruiken in vaccins. Deze eiwitten/antigenen bleken wel de hulp nodig te hebben van adjuvantia om ervoor te zorgen dat de ontvanger van het vaccin inderdaad beschermd is.

Het menselijk immuunsysteem bestaat uit twee componenten: het *aangeboren* immuunsysteem en het *adaptieve* immuunsysteem. Het adaptieve immuunsysteem is uiteindelijk verantwoordelijk voor het opwekken van 'geheugen' tegen de ziekteverwekker, waardoor men beschermd is tegen de gevolgen van toekomstige infecties van dezelfde ziekteverwekker. Geheugen opwekken kan alleen gebeuren door blootstelling aan (componenten van) de ziekteverwekker, ofwel via vaccineren, ofwel ziek worden als gevolg van een natuurlijke infectie. Door deze bloostellingen gaan bepaalde immuun cellen antistoffen vormen. Deze antistoffen ruimen de ziekteverwekker op. Een deel van de cel populatie die blootgesteld wordt aan de ziekteverwekker zal niet direct reageren maar wordt een geheugen cel. Deze cellen kunnen bij een volgende blootstelling heel snel delen en reageren. Hierdoor zal de ziekteverwekker snel worden opge-

ruimd en wordt men niet ziek. Het adaptieve immuunsysteem wordt geactiveerd door het aangeboren immuunsysteem. Het idee achter adjuvantia is dat deze stoffen het *aangeboren* immuunsysteem activeren en dat de componenten van de ziekteverwekker resulteren in de activatie van het *adaptieve* immuunsysteem. Binnen het adaptieve immuunsysteem zijn globaal gezien twee stromingen: een 'humorale' en een 'cellulaire' respons, of een 'Th2' en een 'Th1' response. Voor optimale bescherming is het wenselijk dat de respons tegen het vaccin lijkt op de respons die de ziekteverwekker induceert. De richting van deze respons wordt gedeeltelijk bepaald door het aanwezig 'adjuvans'.

Er is maar een beperkt aantal stoffen beschikbaar als 'adjuvans' voor vaccins die aan mensen gegeven worden: 1) aluminium zouten, b.v. aluminium hydroxide ($Al(OH)_3$) en aluminium fosfaat ($AlPO_4$), 2) olie-in-water emulsies (oliedruppeltjes verdeeld in water) b.v. MF59® of 3) Lipopolysacharide (LPS) derivaten. LPS zit aan de membranen (de buiten rand) van bacteriën en geeft een sterke immuunrespons maar is ook toxisch (giftig). Monophosphoryl lipide A (MPLA) is een component van LPS en is minder extreem immuun stimulerend en veel veiliger. Om een goede combinatie te kiezen van de ziekteverwekker en 'adjuvans' is het noodzakelijk om te weten hoe het 'adjuvans' het immuunsysteem activeert.

In dit proefschrift is het werkingsmechanisme van het meest gebruikte type 'adjuvans' (namelijk de aluminium-gebaseerde adjuvantia) onderzocht, in verschillende vormen: alleen als $Al(OH)_3$ of als $AlPO_4$, of gecombineerd in een vaccin, of juist in kleinere deeltjes. Deze analyses werden gedaan op cellen uit het aangeboren immuunsysteem (monocyten) omdat dit de cellen zijn waarvan verwacht werd (op basis van literatuur) dat het adjuvans daar zijn immuun stimulerende effect op heeft. Er werd gekeken naar activatie/differentiatie status van de cellen (als aangeboren immuun cellen geactiveerd worden of transformeren in een meer volwassen celtype, kunnen ze makkelijker het adaptieve immuunsysteem activeren). Dit hebben we gedaan door te kijken naar de boodschappermoleculen (cytokines) die cellen uitscheiden als gevolg van stimulatie met het adjuvans. Er is ook gekeken naar de richting van de signalen die de aangeboren immuunrespons geeft naar de adaptieve immuunrespons (humoraal, cellulair of beide). Dit is gedaan door te kijken naar mRNA (de werkkopie van DNA). In het mRNA is te zien welke boodschappermoleculen er mogelijk gevormd gaan worden. Tot slot is er gekeken naar de eiwitten (de uiteindelijk functionele moleculen) in de cel. Van de eiwitten is bepaald of ze meer of minder aanwezig waren t.o.v. van de niet-gestimuleerde groep en of ze samenhangen met processen die horen bij een immuunrespons. Dit laatste is gedaan met massaspectrometrie; deze methode is in het vaccinonderzoek nog niet heel veel gebruikt maar heeft in dit proefschrift wel heel duidelijk zijn toegevoegde waarde aangetoond.

In **hoofdstuk 2** van dit proefschrift is er gekeken naar het effect van een op aluminium gebaseerd adjuvans (Al(OH)3) op cellen van het aangeboren immuunsysteem. Door de verschillende methoden hierboven beschreven te combineren, was het mogelijk om een aantal al eerder geïdentificeerde mechanismen te verifiëren; bijvoorbeeld het sturen van de adaptieve response naar een 'humorale/Th2 type' respons en het activeren van het inflammasome (een groep eiwitten die in ontstekingsreactie activeert). Het was ook mogelijk om mechanismen die nog niet eerder waren beschreven te zien: bijvoorbeeld het verhogen van de expressie van mRNA horend bij een ontstekingsreactie (type I interferonen). De eiwitten die horen bij deze type I interferonen kwamen

ook verhoogd tot expressie en we hebben aan kunnen tonen dat deze reactie inderdaad plaatsvond. Er waren ook moleculen te zien die samenhingen met een cellulaire/Th1 type adaptieve respons (type II interferonen). Cellen die gestimuleerd worden met $Al(OH)_3$ verhoogden ook de aanwezigheid van moleculen die horen bij 'antigeen-presenterende routes'. Deze routes zorgen ervoor dat de cellen van het aangeboren immuunsysteem componenten van de ziekteverwekker effectief kunnen 'presenteren' aan het adaptieve immuunsysteem waardoor dit gaat reageren. Er werd altijd gedacht dat cellen die waren gestimuleerd met $Al(OH)_3$ dit via één van beide soorten routes deden (HLA II) maar in deze data was te zien dat het ook via de andere route (HLA I) gebeurt.

Dit hoofdstuk zien dat $Al(OH)_3$ een heel aantal verschillende mechanismen activeert in het aangeboren immuunsysteem. Maar ook, dat we door het combineren van de verschillende methoden nieuwe informatie hebben kunnen verkrijgen over deze mechanismen.

In **hoofdstuk 3** van dit proefschrift werd gekeken naar de verschillen in reactie van de cellen tegen $Al(OH)_3$ en tegen een vaccin dat zowel $Al(OH)_3$ bevat alsook eiwitten van kinkhoest, tetanus en difterie. Van dit vaccin is bekend dat het vooral een 'humorale/Th2' response opwekt en dat de bescherming tegen kinkhoest mogelijk niet optimaal is (niet levenslang). Vaak wordt gedacht dat dit aan het adjuvans ligt. Uit de analyses in dit hoofdstuk kwam naar voren dat inderdaad $Al(OH)_3$ humoraal/Th2 sturend is: na stimulatie met het vaccin (dat ook $Al(OH)_3$ bevat) zijn de markers voor deze respons ook naar voren gekomen. Ook bleek dat het mRNA van een molecuul dat gerelateerd is aan het remmen van een cellulaire/Th1 response duidelijk verhoogd was, als gevolg van het vaccin in vergelijking met het adjuvans alleen. Het eiwit was ook duidelijk verhoogd aanwezig in de cellen waar vaccin bij was gedaan. Dit eiwit remt niet alleen de ontwikkeling van een cellulaire/Th1 response maar ook remt dit eiwit het ontwikkelen van een ontstekingsreactie (een ontstekingsreactie is noodzakelijk voor het starten van een immuunrespons). We hebben kunnen zien dat een eiwit afkomstig van de kinkhoestbacterie naar alle waarschijnlijkheid verantwoordelijk is voor de verhoogde expressie van dit eiwit. Het mogelijke gevolg van de aanwezigheid van dit kinkhoesteiwit zou kunnen zijn dat de bescherming niet optimaal is.

De algemene conclusie van deze studie was dat antigenen/immunogene in vaccins, waarvan verwacht werd dat ze vooral de adaptieve immuunrespons activeren, ook een zeer duidelijke invloed hebben op de aangeboren immuunrespons tegen het adjuvans en deze zelfs mogelijk remt.

In **hoofdstuk 4** van dit proefschrift werden de responsen tegen twee verschillende aluminium-bevattende adjuvantia, $Al(OH)_3$ en $AlPO_4$, met elkaar vergeleken. Dit zijn beide 'adjuvantia' die in vaccins gebruikt worden, maar er was nog nooit gekeken naar mogelijke verschillen in de immuunrespons tegen deze adjuvantia. Deze responsen werden gemeten in cellen van het aangeboren immuunsysteem maar ook in de spier van een muis. er werd in de spier gemeten omdat vaccins bij mensen ook in de spier geprikt wordt; op deze manier lijkt de respons dus het meest op de respons in de mens. Als gevolg van de lichaamsvreemde stof worden er cellen van het immuunsysteem aangetrokken naar de plaats van injectie. In deze studie werd gezien dat de verschillende adjuvantia ervoor zorgen dat er verschillende soorten immuun cellen werden aangetrokken naar de spier van de muis. Het soort immuun cellen dat aangetrokken

werd naar de spier door $Al(OH)_3$ is een celtype dat een soort van netten (een soort web) kan vormen waar het bacteriën mee kan vangen en doden. Eiwitten die samenhangen met de vorming van deze netten werden ook gevonden. Van deze netten is bekend dat ze bijdragen aan een sterkere adaptieve immuunrespons. De cellen die deze netten vormen, werden niet gezien als gevolg van een $AlPO_4$ injectie.

In cellen werd gezien dat er een groot verschil was in het aanzetten van antigeen-presenterende routes (routes die nodig zijn om de adaptieve immuunrespons te activeren): $Al(OH)_3$ deed dit wel maar $AlPO_4$ niet.

De combinatie van deze gegevens leidde tot de volgende conclusies: ondanks dat $Al(OH)_3$ en $AlPO_4$ beide op aluminium-gebaseerde adjuvantia zijn, wekken ze toch een zeer verschillende immuunrespons op in zowel cellen als muizen. Bovendien is $Al(OH)_3$ mogelijk een sterker adjuvans vergeleken met $AlPO_4$

In **hoofdstuk 5** van dit proefschrift is gekeken naar de mogelijkheid om aluminium-bevattende adjuvantia te verbeteren door de deeltjes kleiner te maken naar nanometer-grootte (nm). De hypothese is, dat door het verkleinen van de deeltjes ze misschien makkelijker de cel in kunnen. Er is al onderzoek gedaan naar nanodeeltjes waaruit blijkt dat het goede vaccinadjuvantia zouden zijn en een immuunrespons induceren die ten minste vergelijkbaar is met de huidige aluminium adjuvantia. In deze studie werd wederom gekeken naar verschillen in expressie van eiwitten en mRNA. Er werden twee soorten nanodeeltjes gebruikt: één in de vorm van een zeshoek en één in de vorm van een naaldje en deze zijn vergeleken met $Al(OH)_3$. Uit deze analyse kwam naar voren dat de immuunrespons tegen de kleine deeltjes in stuk minder sterk was dan de immuunrespons tegen $Al(OH)_3$. Dit kwam terug in zowel de mRNA data als de eiwit data. Daarnaast kwam eruit dat het nanodeeltje in de vorm van een naaldje wel een redelijke reactie opwekte maar het nanodeeltje in de vorm van een zeshoek juist niet.

De conclusies hier waren dat het huidige 'grote' deeltje een veel sterkere respons opwekte. Mogelijk geeft $Al(OH)_3$ ook meer bijwerkingen, omdat processen die niets met het immuunsysteem te maken hebben ook veranderden. Deze processen zouden gerelateerd kunnen zijn aan bijwerkingen. Daarentegen, wekte het nanodeeltje in de vorm van een naaldje een subtiele immuunrespons op. Hierdoor geeft het mogelijk minder bijwerkingen, omdat processen die niet met de immuunrespons te maken hebben veel minder geactiveerd werden.

In **hoofdstuk 6** van dit proefschrift is er een nieuw protocol opgesteld voor het meten van boodschappermoleculen/eiwitten in kweekmedium. De boodschappermoleculen in het kweekmedium zijn belangrijke parameters voor het monitoren van de status van de ontstekingsreactie en voor de sturing van het adaptieve immuunsysteem. Deze worden normaal gesproken gemeten met immunologische technieken waarmee je vooraf kiest welke componenten je gaat meten. Het onbekende wordt dus vaak niet opgepikt. De nieuwe methode is een protocol met massaspectometrie waarmee we alle nieuw-gevormde eiwitten in het kweekmedium kunnen meten die na een bepaald moment door de cel worden gemaakt en uitgescheiden. Dit protocol is opgesteld ter verbetering van een bestaand protocol. In het bestaande protocol, worden componenten gebruikt een interactie aangaan met eiwitten en die storend kunnen zijn voor de metingen met de massaspectrometer; deze componenten zijn in het nieuwe protocol

niet nodig De conclusie in dit hoofdstuk is dat de methode werkt maar dat er nog wel optimalisatie-mogelijkheden zijn.

In **hoofdstuk 7** staat alle data nog een keer samengevat en zijn de belangrijkste conclusies van dit proefschrift geformuleerd. Deze zijn:

Door het combineren van de verschillende technieken was het mogelijk om nieuwe inzichten te verkrijgen en de werkingsmechanismen van adjuvantia

Antigenen (immunogene eiwitten) in een vaccin beïnvloeden de aangeboren immuunrespons die geïnduceerd wordt door het adjuvans, zowel kwalitatief als kwantitatief.

De verschillende chemische karakteristieken van $Al(OH)_3$ en $AlPO_4$ resulteren erin dat ze een verschillende immuunrespons induceren en dat $Al(OH)_3$ mogelijk een sterker adjuvans is.

De vorm en de grootte van de aluminiumdeeltjes beïnvloeden de sterkte van de immuunrespons. De grotere deeltjes induceren sterkere responsen maar geven mogelijk ook meer bijwerkingen. Het kleine deeltje in de vorm van een naald zou een interessante kandidaat kunnen zijn als vaccin adjuvans.

Analyse van de boodschappermoleculen in het kweekmedium is mogelijk met massaspectrometrie zonder het gebruik van storende stoffen.

Blik op de toekomst: het gebruik van de massaspectrometrische methode draagt onmiskenbaar bij aan het ontwikkelen van nieuwe vaccins en in de keuze van de optimale combinatie van componenten van de ziekteverwekker en het adjuvans. Dit door vast te stellen welke combinatie de respons geeft die het meest lijkt op de respons die het ziek worden zelf opwekt. In het onderzoek dat beschreven is in dit proefschrift, speelde massaspectrometrie een essentiële rol. Met massaspectrometrie is het nu mogelijk om hele grote experimenten met veel vergelijkingen in een keer te meten, zodat er kwantitatief bepaald kan worden of er verschillen zijn tussen de groepen die gestimuleerd worden en de controlegroepen. Ook zijn er op het gebied van massaspectrometrie en de toepassingen ervan nog veel ontwikkelingen gaande. Een massaspectrometer en de bijbehorende mensen zijn echter een behoorlijke investering, daarom zal deze methode vooral in de vroege onderzoekfase toegepast kunnen worden. Het zal echter nooit alleen met massaspectrometrie kunnen, maar juist een combinatie zijn van veel verschillende technieken.

Referenties:

1 R. Rappuoli, M. Pizza, G. Del Giudice, E. De Gregorio, Vaccines, new opportunities for a new society, Proc Natl Acad Sci U S A 111(34) (2014) 12288-93.
2 S. Riedel, Edward Jenner and the history of smallpox and vaccination, Proc (Bayl Univ Med Cent) 18(1) (2005) 21-5.
3 A.T. Glenny, C.G. Pope, H. Waddington, U. Wallace, Immunological notes. XVII–XXIV, The Journal of Pathology and Bacteriology 29(1) (1926) 31-40.
4 F.R. Vogel, Improving vaccine performance with adjuvants, Clin Infect Dis 30 Suppl 3 (2000) S266-70.

Dankwoord

Het is zover! Mijn proefschrift is af! Maar geen proefschrift is compleet zonder een echt dankwoord, een stukje waarin ik mijn dank mag uitspreken aan iedereen die een bijdrage heeft geleverd aan de totstandkoming ervan!

Allereerst wil ik **Hugo** als copromotor en projectleider bedanken. Hugo, ik had me geen betere projectleider/copromotor kunnen wensen! Dank je wel voor het opzetten van dit project en voor het aan mij toevertrouwen van de uitvoering. Dank voor je inhoudelijke bijdragen. Met name op de gebieden van massaspectrometrie en het schrijven van manuscripten heb ik enorm veel van je geleerd. Ook dank voor je persoonlijke steun, het feit dat je deur altijd open stond en je vertrouwen in mij en dit project.

Mijn promotor **Gideon**, dank je wel voor je enorme inhoudelijke bijdrage aan dit project. Op het gebied van vaccins en adjuvantia heb ik enorm veel van je geleerd! Je kritische blik op manuscripten en je hulp en steun bij het schrijven ervan hebben mij goed gedaan. De wijze lessen neem ik mee naar de toekomst.

Mijn promotor **Albert**, de 3-maandelijkse gesprekken waren altijd erg prettig en goed voor het creëren van overzicht. Je wist in deze gesprekken een helikopterview te creëren, waardoor we de grote lijnen van het project weer zagen, prioriteiten (weer) helder werden en we niet in details verzandden. Dank je wel hiervoor. Ook dank voor de ondersteuning, sturing van het project en het delen van je kennis op het gebied van massaspectrometrie. **Bernard**: het was fijn om je in het projectteam te hebben, dank je wel voor je inhoudelijke bijdragen aan dit project, je kritische blik op mijn manuscripten en de data en je steun als het even niet mee zat. Het was prettig te weten dat je deur altijd open stond. **Elly**, Ik heb erg veel gehad aan je immunologische bijdragen, maar ook aan je enthousiasme over de data, je enthousiasme over het gebruik van massa spectrometrie in immunologisch onderzoek en je heldere kijk op de mansucripten. Ik vond het ook erg prettig om met jou over de betekenis van de data te kunnen discussiëren en even langs te lopen als er wat was. Dank je wel hiervoor. Ook wil ik **Cécile** bedanken. Dank voor je kritische blik op mijn manuscripten, je immunologische bijdrage aan dit project, de leuke discussies over de data die was gegenereerd en je enthousiasme over dit project en de data. **Jeroen**, zonder jou was dit project toch echt een stuk ingewikkelder geworden en was ik verzand in de proteomics data. Bedankt voor je enorme hulp met de bio-informatica, de pathway analyses en het maken van de figuren voor de manuscripten. Dank je wel voor de fijne samenwerking en alle hulp.

Hilde, onze beide projecten raken elkaar nauw, vandaar de "logische" keuze om samen te werken aan een aantal onderdelen, deze samenwerking liep in het begin niet al te soepel. Echter, we hebben onze weg hierin gevonden en het is een prima samenwerking geworden met als resultaat een samen geschreven manuscript! Dank je wel hiervoor en voor alle fijne gesprekken over afronden/stress van een proefschrift en al het andere. Succes met het afronden van jouw proefschrift. **Jolanda**, binnen onze projecten was er verwantschap en hoewel deze niet in jouw proefschrift terecht zijn gekomen, zijn er uit onze samenwerking toch 2 manuscripten ontstaan. Dank je wel voor je steun en het leren van de celkweek en de FACS, maar vooral bedankt voor de fijne samenwerking! **Fabio**, thank you so much for all your effort to run all the samples in Utrecht, sometimes it was a real struggle for you with the machines or the columns, but

it was never too much for you. Ik heb tijdens mij AIO periode één stagiaire mogen begeleiden. **Lisette**, het begin van je stage periode was niet altijd even soepel. Ik heb echt moeten leren om los te laten, daarna werd het voor beiden beter. Je stage is dan ook uitgemond in een mooi verslag en veel kennis over het gebruik van THP-1 cellen. Dank je wel hiervoor en dank je wel voor de prettige tijd, ik heb er veel van geleerd! **Joost**, zonder jou zou het in het mass spec lab heel anders zijn geweest, dank je wel voor alle hulp met de mass specs en alle lessen hoe er mee te werken Dank je wel voor je steun en de leuke gesprekken over vakantie bestemmingen! **Geert,** dank je wel je voor je hulp met het aanleren van de mass spec, de gezelligheid en je ideeën voor dit project. **Maarten Danial**, dank je wel voor de prettige samenwerking tijdens het opzetten van de secretoom analyse. Het was heel fijn om hierover met jou te kunnen sparren. Er ligt een heel mooi manuscript! **Peter**, dank je wel voor je bijdrage aan de samenwerking tussen **Hilde** en mij en de totstandkoming van hoofdstuk 5.

Alle collega's binnen Intravacc, bedankt omdat de deuren open stonden! Bijzondere dank aan **Dedeke** en **Lisa** voor alle hulp met de celkweek, dierproef en de FACS, **Justin** voor alle hulp met de PCRs en het verwerken van de dierproef samples, **Alex** en **Sven U**, voor jullie hulp tijdens de dierproef, **Dionne** voor je hulp met de celkweek, **Larissa** voor de goeie adviezen op het gebied van stage begeleiding en je hulp op het lab. **Andreja**, **Arjan**, **Marieke** en **Diana** voor jullie bijdragen aan het secretoom project. **Wichard** voor alle lab-gerelateerde zaken en bestellingen kon ik bij jou terecht. Bedankt hiervoor! **Janny**, bedankt voor de fijne gesprekken. **Gaurav**, thanks for the advice in the last couple of months. It was nice to talk to someone in the same situation.

Thomas en **Hilde** succes met het jullie promotie project, **Heleen** succes op de dag van je promotie. Ik wil alle mensen van het ARC bedanken voor de fijne samenwerking en in het bijzonder **Hans** en **Karin**. De intramusculaire toediening die ik wilde tijdens mijn proeven was nog even een uitdaging, maar door goede voorbereidende testen van jullie, zijn het goed gelukte proeven geworden! Ik wil ook graag de mensen van de IvD en de WTC bedanken voor de adviezen tijdens het schrijven van dierproef protocollen! **Mireille** en **Sanne** bedankt voor het regelen van de reizen naar congressen en alle andere administratieve hulp. I would like to thank the group in Utrecht for their kindness and support when I was there and wish all the AIOs the best in finishing their PhD. Specifiek wil ik **Corine** ontzettend bedanken voor alle hulp tijdens het afronden: je bewaakte de tijdslijnen zorgde voor de juiste formulieren en je beantwoordde al mijn vragen! Dank je wel. Door mijn samenwerking met **Jolanda** heb ik ook met andere mensen van het RIVM mogen samen werken, **Jacqueline, Ronald** en **Jeroen**, bedankt voor jullie hulp met de FACS en de qPCR.

Tijdens mijn AIO periode heb ik het kantoor mogen delen met een aantal mensen. Bedankt **Afshin, Yara, Sigrid, Debbie, René** en **Berdine** voor de gesprekken, de sushi lunches, de steun en de gezelligheid! **René** en **Afshin**, bedankt voor jullie steun en advies bij het afronden van een proefschrift en alle zaken die er bij komen kijken. **Debbie** bedankt voor de gezelligheid en de fijne gesprekken. Het was fijn om ook met andere dingen bezig te zijn dan promoveren. **Sigrid** dank voor je adviezen, je hoeft inderdaad niet alles zelf te doen! **Yara**, bedankt voor de gezelligheid. **Berdine**, 3,5 jaar hebben we een kantoor gedeeld, dank voor je steun je gezelligheid, de fijne gesprekken en al je hulp! Ik ben blij dat jij mij als paranimf wilt bijstaan!

Hoewel een AIO periode gerelateerd is aan veel met werk bezig zijn, zijn er buiten de werkomgeving ook een aantal mensen die ik wil bedanken: Mijn nieuwe collega's

voor hun warme ontvangst en interesse in de laatste maanden van dit proefschrift. **Rob** dank je wel voor alle hulp en werk aan de opmaak van mijn boekje en het ontwerp van de bijzondere kaft! Ik ben er heel erg blij mee! **Gerda**, dank je wel voor je adviezen. **Karlijne,** dank je wel voor de hulp aan de quilt die nu de omslag van boekje siert. **Suzanne J**, dank je wel voor een hele lange, bijzondere en waardevolle vriendschap. We kennen elkaar al en hele tijd en hebben veel samen meegemaakt. Dank je wel voor alle steun, leuke uitjes, ontspannende middagen en samen met **Maikel** voor de gezellige etentjes! **Suzanne de B**, vanaf het moment dat wij begonnen met onze studie was er een klik: allebei farmacie studerend, maar niet om apotheker te worden. Sindsdien is een waardevolle vriendschap ontstaan. Het was fijn om met jou te kunnen praten over het afronden van een proefschrift! Dank je wel voor de hulp, gezelligheid en samen met **Steef** voor de gezellige etentjes.

Tjeerd en Sandra, dank jullie wel voor de gezelligheid en de spelletjesavonden. **Lieve Vrienden**, dank jullie wel voor jullie steun, gezelligheid en broodnodige afleiding! **Badmintonteamgenootjes** dank jullie wel voor de sportieve afleiding en gezellige avonden met lekker eten, gelach en geborrel!

Lieve Familie en Schoonfamilie, dank jullie wel voor alle gezelligheid, afleiding en oprechte interesse in waar ik mee bezig was en hoe dat ging. **Ooms** en **tantes, neefjes** en **nichtjes**: we zijn een hechte familie waarin iedereen voor elkaar klaar staat. Dank jullie wel hiervoor! **Ben** en **Margriet**, dank jullie wel dat ik bij jullie altijd welkom ben en jullie belangstelling in mij en mijn werk! **Daan** en **Kirstin**, dank jullie wel voor de fijne gedeelde Oostenrijk vakanties en de spelletjes avonden, mijn hoofd was er niet altijd bij, dat is vanaf nu hopelijk anders! **Bram** en **Sue** dank jullie wel voor de gezelligheid en de aanmoediging om nog even vol te houden! **Opa** en **Oma Piet** en **Oma Hannie.** Dank jullie wel voor alle gezelligheid en jullie liefde. Lieve **Oma Piet** en **Peter:** ik had jullie zo graag dit boekje overhandigd, helaas mag dit niet zo zijn.

Govert, ik ben trots op je, broertje! Afgestudeerd als meester in de rechten. Ondanks dat we dicht bij elkaar wonen zagen we elkaar niet altijd even veel, als er wat was kon ik echter altijd op je rekenen! Dank je wel en samen met **Emily** dank voor alle gezelligheid! Ik ben blij dat je als paranimf naast me wil staan op deze bijzondere dag!

Lieve **Pap** en **Mam**, dankzij jullie ben ik geworden wie ik ben: ik kreeg alle vrijheid om keuzes te maken en mijn eigen weg te vinden. Dank voor jullie onvoorwaardelijke steun en liefde! Een zeer fijne thuishaven! Ik hou van jullie! Mam: bijna gelijktijdig met de start van mijn promotie traject ben jij gestart met een quilt. De echte quilt is je cadeau aan mij, de foto siert nu de prachtige omslag van mijn boek. Dank je wel!

Lieve, lieve **Bart**: het is niet makkelijk, samenleven met een promovendus. We hebben samen een hectische tijd achter de rug en soms was het lachen en soms was het huilen. Altijd was daar echter weer jouw schouder en jouw geloof in mij. Je maakt me aan het lachen en je steunt me onvoorwaardelijk! Ik hou van je! Op naar een prachtige toekomst samen!

Sietske

Curriculum Vitae

Sietske Kooijman was born in Arnhem on the 29th of November 1988. She attended her pre-university education at the Lorentz Lyceum (bilingual VWO) in Arnhem and graduated in June 2007. After graduating, she started with her study Pharmacy at Utrecht University. She obtained a Bachelor's degree in February 2011 and continued her studies at Utrecht University with a combination of the two masters Drug innovation and Toxicology and environmental health. During her first internship at the research department of pathology and immunology, she investigated Hen's egg allergy models and genetic imprinting via dietary intervention in mother mice, influencing the susceptibility to allergy in the pups. She performed her second internship at Pamgene in 's-Hertogenbosch were she analyzed a method to replace the rat uterotrophic assay in endocrine toxicology testing. In February 2013 she obtained her Master's degree in Drug Innovation and a certificate stating that the demands for toxicology and environmental health were met. In the same year, she started her PhD project at Intravacc under the supervision of Prof. Albert Heck, (Utrecht University) Prof. Gideon Kersten (Intravacc and Leiden University) and Dr. Hugo Meiring (Intravacc), investigating the molecular mechanisms underlying the immunological activity of vaccine adjuvants. This resulted in this thesis. Currently, Sietske is working as a senior scientist at MSD animal health.

List of publications

Sietske Kooijman, Jolanda,Brummelman, Cécile A.C.M.van Els, Fabio Marino, Albert J.R.Heck, Geert P.M.Mommen, Bernard Metz, Gideon F.A.Kersten, Jeroen L.A.Pennings, Hugo D.Meiring. Novel identified aluminum hydroxide-induced pathways prove monocyte activation and pro-inflammatory preparedness. Journal of Proteomics 175(2018) 144-155. https://doi.org/10.1016/j.jprot.2017.12.021

Sietske Kooijman, Jolanda Brummelman, Cécile A.C.M. van Els, Fabio Marino, Albert J.R. Heck, Elly van Riet, Bernard Metz, Gideon F.A. Kersten, Jeroen L.A. Pennings, Hugo D. Meiring. Vaccine antigens modulate the innate response of monocytes to $Al(OH)_3$. PLoS ONE 13 (5): e0197885. https://doi.org/10.1371/journal.pone.0197885

Sietske Kooijman, Joost P. Uittenbogaard, Marieke Hoonakker, Hugo D. Meiring, Gideon F. A. Kersten, Bernard Metz and Maarten Danial. Design of a Catalyst-free Enrichment Method for the Capture and Analysis of Cell-Secreted Proteins. Manuscript submitted to analytical chemisty